Influence of disulfide-bonds on structural and functional properties of peptides and proteins – Case studies on FXIIIa inhibitor tridegin and μ-conotoxin PIIIA

Dissertation

zur

Erlangung des Doktorgrades (*Dr. rer. nat.*)

der

Mathematisch-Naturwissenschaftlichen Fakultät

der

Rheinischen Friedrich-Wilhelms-Universität Bonn

vorgelegt von

Thomas Schmitz

aus

Bad Neuenahr-Ahrweiler

Bonn, Februar 2021

Angefertigt mit Genehmigung der Mathematisch-Naturwissenschaftlichen Fakultät der Rheinischen Friedrich-Wilhelms-Universität Bonn.

Die vorliegende Arbeit wurde in der Zeit vom Oktober 2017 bis Februar 2021 am Pharmazeutischen Institut der Rheinischen Friedrich-Wilhelms-Universität Bonn unter der Leitung von Prof. Dr. Diana Imhof angefertigt.

Erstgutachterin: Prof. Dr. Diana Imhof

Zweitgutachter: PD Dr. Arijit Biswas

Tag der Promotion: 22.04.2021

Erscheinungsjahr: 2021

Die Straße ist nicht immer eben, und grad‘ deswegen: Auf das Leben!

– *Jupiter Jones*

Abstract

Disulfide-bonded peptides have been studied for many decades serving as tools to investigate various biochemical pathways as well as lead structures for drug development for numerous diseases. Among these, the most fatal are cardiovascular diseases, triggered by dysregulated haemostasis. An essential component of the haemostasis is the blood coagulation cascade, involving the formation of a fibrin network, thereby stabilizing the blood clot. In addition to the central enzyme thrombin, the blood coagulation factor FXIII has a decisive role, as it cross-links the fibrin network and hence stabilizes it. FXIII is thus an attractive target for the development of therapeutically relevant anticoagulants. One of the most promising compounds for inhibiting FXIII activity is the 66mer leech-derived peptide tridegin, which is structurally stabilized by three disulfide bonds. Recent studies focused on the impact of these three disulfide bonds on the structure and function of tridegin. Similar investigations have been carried out earlier for the 15 3-disulfide-bonded μ-conotoxin PIIIA (μ-PIIIA) isomers, that displayed different biological activity towards voltage-gated sodium ion channels. Both studies revealed a significant influence of the disulfide bond connectivity on the functional effectiveness of these peptides encouraging further investigations.

The present dissertation focuses on both these topics providing deeper insights into chemosynthetic, bioanalytical, and biological aspects of the differentially disulfide-linked tridegin and μ-PIIIA variants. First, all 2-disulfide-bonded tridegin analogs deficient in the bond between Cys19 and Cys25 of the native lead structures were synthesized as well as chemically and biologically analyzed. These investigations revealed that the aforementioned disulfide bond is not as crucial for the inhibitory potential towards FXIIIa as supposed. In addition, one of the 2-disulfide-bonded tridegin variants was examined structurally via experimental and computer-based analyses. In this context, the structure of a tridegin analog was determined by NMR-based structural analysis for the first time. The drastic reduction of the synthesis complexity, compounded by the marked retention of inhibitory activity of the disulfide-deficient isomers poise them as attractive candidates as lead structures for therapeutic anticoagulant development.

In a second study of this dissertation, the applicability of LC-TIMS-MS for the discrimination of isomers with different disulfide bond connectivities was examined using ten different μ-PIIIA isomers and analogs. Therefore, the LC and TIMS profiles of pure peptide samples as well as mixtures of three 2- and seven 3-disulfide-bonded variants were compared. This analysis demonstrated that LC-TIMS-MS is a valuable supplement to the commonly used methods HPLC and MS to distinguish different 2- and 3-disulfide-bonded peptide isomers.

In summary, this dissertation provides new insights into the structure-activity relationships of tridegin and serves as a basis for the development of new anticoagulants. Furthermore, it uncovers a methodologically underexplored territory, presenting the suitability of LC-TIMS-MS for the differentiation of peptide isomers with distinct disulfide bond connectivities.

Zusammenfassung

Disulfidverbrückte Peptide werden schon seit vielen Jahrzehnten untersucht und dienen als chemisches Werkzeug in der Erforschung verschiedener biochemischer Abläufe und als Leitstruktur für die Entwicklung von Medikamenten in zahlreichen Krankheiten. Die am häufigsten zum Tode führenden Krankheiten sind dabei die kardiovaskulären Erkrankungen, die durch eine dysregulierte Hämostase ausgelöst werden können. Ein wesentlicher Bestandteil der Hämostase ist die Blutgerinnungskaskade, die zur Ausbildung eines Fibrinnetzwerkes führt und darüber das Blutgerinnsel stabilisiert. Neben dem zentralen Enzym Thrombin, spielt der Blutgerinnungsfaktor FXIII eine entscheidende Rolle, da dieser das Fibrinnetzwerk quervernetzt und zusätzlich stabilisiert. FXIII ist daher eine interessante Zielstruktur für die Entwicklung von therapeutisch relevanten Antikoagulantien. Eines der vielversprechendsten Substanzen zur Hemmung der FXIII-Aktivität ist das 66 Aminosäure lange Peptid Tridegin, welches strukturell durch drei Disulfidbrücken stabilisiert wird. Jüngste Tridegin-Studien untersuchten dabei den Einfluss dieser drei Disulfidbrücken auf die Struktur und Funktion dieses Peptides. Dasselbe wurde bereits für die 15 dreifach disulfid-verbrückten Isomere des μ-Conotoxin PIIIA (μ-PIIIA) durchgeführt, wobei die Isomere unterschiedliche biologische Aktivitäten gegenüber spannungsgesteuerter Natriumionenkanäle zeigten. Beide Studien offenbarten einen wesentlichen Einfluss der Disulfidverbrückung auf die funktionellen Eigenschaften dieser Peptide, was zu weiteren Untersuchungen anregte.

Die vorliegende Dissertation beschäftigt sich mit den beschriebenen Themen, um weitere Einblicke in die chemosynthetischen, bioanalytischen und biologischen Aspekte unterschiedlicher disulfidverbrückter Tridegin- bzw. μ-PIIIA-Analoga zu erhalten. Dabei sollten im ersten Teil dieser Arbeit alle zweifach disulfidverbrückten Tridegin-Analoga, ohne die in den nativen Leitstrukturen enthaltende Bindung zwischen Cys19 und Cys25, hergestellt und chemisch sowie biologisch analysiert werden. Die entsprechenden Untersuchungen ergaben, dass die erwähnte Disulfidbrücke nicht so entscheidend für das inhibitorische Potential gegenüber FXIIIa ist. Darüber hinaus wurde eine zweifach disulfidverbrückte Trideginvariante mit Hilfe von experimentellen und computerbasierten Analysen strukturell untersucht. In diesem Zusammenhang konnte erstmals über NMR-basierte Strukturaufklärung die Struktur eines Tridegin-Analogons experimentell ermittelt werden. Aufgrund der vereinfachten Synthese der disulfidreduzierten Isomere, die zeitgleich eine gleichbleibende inhibitorische Aktivität gegenüber FXIIIa beibehielten, dürfte die neue Leitstruktur von Tridegin für die zukünftige Entwicklung von Antikoagulantien sehr geeignet sein.

In einer zweiten Studie dieser Dissertation wurde die Anwendbarkeit von LC-TIMS-MS zur Unterscheidung von Isomeren mit unterschiedlicher Disulfidverbrückung anhand von 10 verschiedenen μ-PIIIA-Varianten untersucht. Dafür wurden die LC- und TIMS-Profile der reinen Peptidproben sowie der Mischungsexperimente von 3 zweifach und 7 dreifach disulfid-verbrückten Varianten verglichen. Mittels dieser Analyse konnte gezeigt werden, dass LC-TIMS-MS eine wertvolle Ergänzung zu den üblicherweise verwendeten Methoden HPLC und MS zur Unterscheidung verschiedener disulfidverbrückter Peptidisomere darstellt.

Zusammenfassend bietet diese Dissertation neue Einblicke in die Struktur-Aktivitäts-Beziehungen von Tridegin und dient als Grundlage für die Entwicklung neuer Antikoagulanzien. Darüber hinaus liefert sie einen ersten Hinweis auf die nützliche Anwendbarkeit von LC-TIMS-MS zur Differenzierung von Peptidisomeren mit unterschiedlicher Disulfidverbrückung.

Content

1 Introduction

Peptides are biomacromolecules that often play an important role in various processes in nature. They are defined as compounds containing fewer than 100 amino acids that are classified as middle space molecules between small molecules and proteins.[1,2] In addition to the large variety of different functions, peptides can combine the advantageous properties of small molecules with those of proteins, which also leads to their use as drugs and in drug development.[3] Some of these peptides are “cysteine-rich” and thus capable of forming intramolecular disulfide bonds. The latter is a covalent linkage between the sulfur atoms of two cysteines.[4] Such disulfide bonds are usually of great importance for the structural integrity of these peptides, as they define and stabilize the corresponding peptide structures. This, in turn, affects the biological activity of the peptides, making the disulfide bonds not only structurally but also functionally relevant.[3] However, despite the numerous achievements in peptide synthesis, the preparation of disulfide-bonded peptides is still a complex task and often leads to very low yields and quality of the product.[3,5,6] For this reason, several studies have investigated disulfide bonds for their functional significance on the biological activity employing disulfide-deficient analogs. Essentially, the number of intramolecular disulfide bonds of the lead molecule is reduced in order to determine the impact of the missing disulfide bond(s) on the structure and activity of the parent.[7–10]

In the same vein, the 3-disulfide bonded 66mer peptide tridegin from the Amazon giant leech *Haementeria ghilianii* (*H. ghilianii*)[11] is poised as a promising tool for medical research concerning cardiovascular diseases. However, as mentioned earlier, its synthesis is still a formidable challenge.[12,13] Tridegin is a potent and specific inhibitor of the blood coagulation factor FXIIIa, an enzyme that catalyzes the final step of the blood coagulation cascade, the cross-linking and thereby stabilization of the fibrin network within a blood clot.[14–16] In this context, the present dissertation focuses on the relevance of disulfide bonds, more precisely the disulfide bond between Cys19-Cys25 residues in the amino acid sequence, for the functional and structural properties of tridegin. Thereby, the approach of exploring disulfide-deficient tridegin variants was chosen as a means to simplify the synthesis of tridegin and to optimize the lead structure for the development of new therapeutically relevant anticoagulants.[17] Beyond that, an approach to provide the first experimentally-derived structural insights into tridegins 3D-architecture was undertaken employing solution NMR spectroscopy augmented by molecular modeling approaches, serving as foundational work for future investigations into the structure-activity relationships of potential analogs in more detail.[18] Finally, an analytical strategy was implemented based on the application of liquid chromatography-trapped ion mobility spectrometry-mass spectrometry (LC-TIMS-MS) in order to develop alternative protocols for the successful and unequivocal differentiation of peptide and protein isomers with different disulfide bond connectivities. Therefore, a selection of 2- and 3-disulfide-bonded isomers of the μ-conotoxin PIIIA was analyzed.[19]

2 Theoretical background

Peptides play a myriad of roles in nature, for example as messenger substances or hormones, and are increasingly used in medical applications.[20–22] Peptides adopt a wide variety of conformations, since they are more flexible than the structures of proteins.[3] Primarily, secondary structure elements are crucial for the functional properties of peptides. These are stabilized by a plethora of intramolecular (or intrachain) or intermolecular (or interchain) hydrogen bonds.[23] In addition, post-translational modifications are frequently found in peptides and proteins, one of which is the disulfide bond occurring as either inter- or intramolecular bond between two cysteine side chains.[24] Cysteine-rich peptides and proteins characterized by the presence of more than two cysteine residues are often found in organisms such as snakes, scorpions, spiders, cone snails[25,26], leeches[27] and plants[28,29].

2.1 Cysteine-rich peptides

Disulfide bonds are established by oxidation of the thiol functions of two cysteine side chains followed by the covalent bonding of their respective sulfur atoms.[30] The advantage of this covalent linkage is the increased structural rigidity leading to a more stable peptide structure.[3,4] A high number of cysteines found in these cysteine-rich peptides lead to the potential formation of multiple disulfide bonds. Due to the underlying therapeutic potential of these peptides, including antimicrobial defensin peptides[31–33], knottins[34], plant-derived cyclotides[35,36], heat-stable enterotoxins[37], venom-derived peptides[38–40] such as conotoxins from marine cone snail venom[41–43], and leech-derived peptides such as tridegin[27,44], their synthesis is of great interest. However, the synthesis of the cysteine-rich peptides is still considered to be a demanding endeavor, especially owing to the fact that the selective formation of disulfide bonds is not trivial.[3] Advances in this field have been achieved by the work of G. Barany, L. Moroder, and F. Albericio in recent years.[3,4,45–49] Disulfide bonds can be generated in a self-folding experiment in one step, or can be obtained selectively and sequentially via specific protecting group strategies.[48] The problems with the selective synthesis of multiple disulfide bonds within a peptide is that undesired disulfide-bonded isomers can emerge due to various rearrangements.[4] In this context, the two extreme folding pathways BPTI-folding (Bovine pancreatic trypsin inhibitor) and hirudin-like folding are described for disulfide-bonded peptides.[50] The BPTI-folding exclusively proceeds via intermediates that only comprise disulfide bonds also appearing in the native isomer, whereas during the hirudin-like folding as many different disulfide-bonded intermediates (native and non-native) as possible emerge.[50] A mixture of these two extreme folding pathways is also referred to as the BPTI/hirudin-like model.[50] Thus, for cysteine-rich peptides with six cysteines it is possible to form 15 different 3-disulfide-bonded isomers, whereas 4 disulfide bonds (8 cysteines) can already lead to 105 isomers.[51,52] In addition to the desired, biologically active isomer, further undesired isomers may be structurally altered due to their changed disulfide bond connectivity, which at the same time may affect the overall biological activity expected of these isomers. With increasing number of these “less active” isomers formed during such a synthesis, a consequent lower yield of the desired product is obtained detrimentally influencing the biological activity. Furthermore, these isomers cannot always be separated from each other via reversed-phase high-performance liquid chromatography (RP-HPLC) due to similar physical properties.[6,12] As previously described for tridegin by Böhm *et al*.[12] (more information in section 2.3.2), this results in mixtures of different disulfide isomers, in which structure and function of each individual isomer cannot be studied independently of the other isomers.

Due to the challenges described above, the strategy of disulfide-deficient peptide variants has been developed and increasingly pursued over time.[7–10,53] Disulfide-deficient peptides are variants of the naturally occurring (and often the biologically active) peptide in which one or more disulfide bonds are removed by specific point mutations of the respective cysteines (e.g. to serine or alanine), thereby decreasing the number of bridges. However, removal of disulfide bonds often results in more flexible and structurally altered peptide structures. This can lead to a significant loss of activity, which has already been demonstrated in the case of the μ-conotoxins PIIIA[54] and GIIIA[55]. Indeed, not in all peptides each of the different disulfide bonds are equally important for their structural features and their biological activity, which is why in some cases certain disulfide bonds can be removed without major loss of activity.[7–10,53] A clear advantage of reducing the number of disulfide bonds is the dramatically simplified synthesis within a protecting group strategy and the number of possible undesired isomers is minimized. In this regard, upon reduction from 3 to 2 disulfide bonds, the number of undesired disulfide-bonded isomers is decreased from 14 to only 2 isomers. While maintaining the same activity and improving synthesizability, an optimization of the lead structure can be forseen in these cases. The μ-conotoxin KIIIA[8,56] and the scorpion toxin leiurotoxin I[7] can be notably mentioned as examples of successful disulfide-deficient optimization strategies.

2.1.1 Peptides as drugs

Peptidic and peptidomimetic drugs are currently used in a variety of therapeutic areas. These include, for example, diabetes, cancer, hormone therapies, cardiovascular diseases, and many other areas of application.[57,58] The first developed peptide drug is the hormone insulin, that has been used for diabetic medications since the 1920s.[21] During the last two decades, an increasing number of peptides have been approved due to the improved synthetic accessibility as well as novel analytical techniques and methods for structure elucidation.[59,60] Solid-phase peptide synthesis (SPPS), introduced by B. Merrifield in 1963[61], and many other innovations in the field of native chemical ligations and recombinant expression,[62,63] led to the availability of more than 60 peptide-based drugs in the market (as of May 2017) and more than 150 peptides being investigated in clinical trials.[64] The latest peptides approved by the U.S. Food and Drug Administration (FDA) in 2020/21 are the cyclic peptides voclosporin (Lupkynis™, Figure 1, **1**), a calcineurin inhibitor used for the treatment of lupus nephritis[65], setmelanotide (Imcivree™, **2**) for the treatment of obesity[66], and the ^{64}Cu-dotatate (Detectnet™, **3**) with the peptide Tyr3-octreotate as a radioactive diagnostic agent for the localization of somatostatin receptor positive neuroendocrine tumors[67].

Table 1: Non-insulin peptide-based drugs approved by the U.S. Food Drug and Administration (FDA) between 2010-2021.[20,68–73] The marked amino acids are D-amino acids (red), N-methylated amino acids (blue) and cysteines (bold) that form disulfide bonds.

Year	Name	Indication	Sequence	Features
2021	Voclosporin (Lupkynis™)[65]	Lupus nephritis	(Pmt)(Abu)GLVLAALLV	Cyclic, D-aa N-methylation Non-standard aa
2020	Setmelanotide (Imcivree™)[66]	Obesity	Ac-R**C**AHFRW**C**-NH_2	D-aa Disulfide bond
2020	^{64}Cu-dotatate (Detectnet™)[67]	Neuroendocrine tumors, diagnostic	H-F**C**YWKT**C**T-OH	Attached to DOTA D-aa disulfide bond
2019	Bremelanotide (Vyleesi™)[74]	Hypoactive sexual desire disorder	Ac-(Nle)DHFRWL-OH	Cyclic D-aa
2019	Afamelanotide (Scenesse®)[75]	Skin damage and pain	Ac-SYS(Nle)EHFRWGKPV-NH_2	D-aa Non-standard aa
2019	^{68}Ga-dotatoc[76]	Neuroendocrine tumors, diagnostic	H-F**C**YWKT**C**T-(ol)	Attached to DOTA D-aa disulfide bond
2018	^{177}Lu dotatate (Lutathera®)[77]	Neuroendocrine tumors, theranostic	H-F**C**YWKT**C**T-OH	Attached to DOTA D-aa disulfide bond
2017	Semaglutide (Ozempic®)[78]	Diabetes	H-H(Aib)EGTFTSDVSSYL EGQAAKEFIAWLVRGRG-OH	Attached to PEG Non-standard aa
2017	Plecanatide (Trulance®)[79]	Chronic idiopathic constipation	H-NDE**C**EL**C**VNVA**C**TG**C**L-OH	Disulfide bonds (C4-C12, C7-C15)
2017	Macimorelin (Macrilen™)[80]	Growth hormone deficiency	Tripeptide with non-standard aa	D-aa Non-standard aa
2017	Etelcalcetide (Parsabiv®)[81]	Hyperpara-thyroidism	Ac-**C**ARRRAR-NH_2	Attached to Cys Disulfide bond
2017	Angiotensin II (Giapreza™)[82]	Hypotension	H-DRVYIHPF-OH	
2017	Abaloparatide (Tymlos®)[83]	Osteoporosis	H-AVSEHQLLHDKGKSIQDLR RRELLEKLL(Aib)KLHTA-NH_2	Non-standard aa
2016	Lixisenatide (Adlyxin®)[84]	Diabetes	H-HGEGTFTSDLSKQMEEEAVRF IEWLKNGGPSSGAPPSKKKKKK-NH_2	
2015	Ixazomib (Ninlaro®)[85]	Multiple myeloma	Dipeptide with a C-terminal boronic acid	
2014	Oritavancin (Orbactiv®)[86]	Acute bacterial skin infections	Glycopeptide with non-standard aa	D-aa Non-standard aa
2012	Sinapultide (Surfaxin®)[87]	Respiratory distress syndrome	H-KLLLLKLLLLKLLLLKLLLLK-OH	
2012	Peginesatide (Omontys®)[88]	Anemia	Ac-GGLYACHMGPIT($_1$Nal)VC QPLRGK-NH_2	Attached to PEG N-metylation
2012	Carfilzomib (Kyprolis®)[85]	Multiple myeloma	Tetrapeptide with non-standard aa	Non-standard aa
2012	Linaclotide (Linzess®)[89,90]	Irritable bowel syndrome	H-**CC**EY**CC**NPA**C**TG**C**Y-OH	Disulfide bonds (C1-C6, C2-C10, C5-C13)
2011	Icatibant (Firazyr®)[91]	Hereditary angioedema	H-RRP(Hyp)G(Thi)S(Tic)(Oic)R-OH	D-aa Non-standard aa
2010	Tesamorelin (Egrifta®)[92]	HIV-associated lipodystrophy	H-YADAIFTNSYRKVLGQLSAR KLLQDIMSRQQGESNQERGARA RL-NH_2	

Pmt: (4R)-4-[(E)-penta-2,4-dienyl]-4,N-dimethyl-threonine; Abu: α-aminobutanoic acid; DOTA: 1,4,7,10-tetra-azacyclododecane-1,4,7,10-tetraacetic acid; Nle: norleucine; -(ol): C-terminal carboxylic acid function is reduced to alcohol function; Aib: α-aminoisobutyric acid; PEG: polyethylene glycol; $_1$Nal: 1-naphthylalanine; Hyp: hydroxyproline; Thi: β-2-thienylalanine; Tic: 1,2,3,4-tetrahydroisoquinoline-3-carboxylic acid; Oic: octahydroindole-2-carboxylic acid.

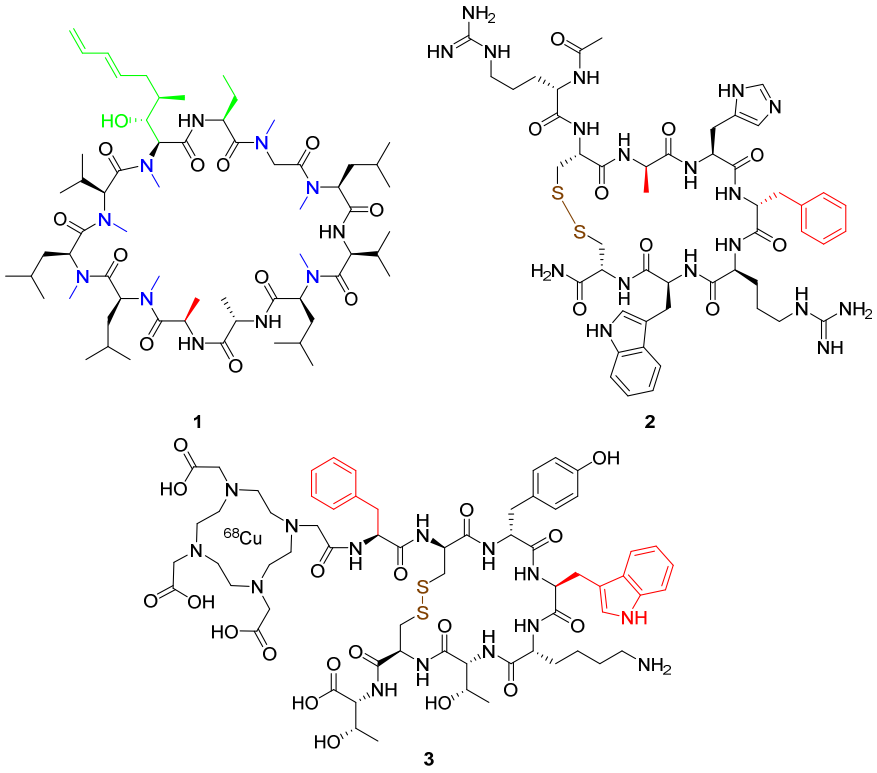

Figure 1: Structures of the three peptides-based drugs Voclosporin (**1**)[93], Setmelanotide (**2**)[66] and ^{64}Cu dotatate (**3**)[77] that were approved by the FDA in 2020/2021. The modifications within the peptides, such as disulfide bonds (brown), *N*-methylation (blue) and incorporation of D-amino acids (red) as well as non-standard amino acids (green) are marked in different colors.

Similar to proteins, peptides may exhibit an increased potency, affinity, and selectivity towards therapeutic targets with only few side effects as opposed to small molecules.[1,3,57] Additionally, peptides are synthetically more accessible than proteins. Today, the synthesis of a peptide length of up to 100 amino acid is technically possible, however, it strongly depends on the primary sequence.[1,3] All these aspects resulted in an increased importance of peptides in drug development and today's medical care.[57] That said, it is often the case that peptides exhibit poor oral bioavailability, low cell permeability, and low stability towards proteolytic enzymes leading to short plasma half-lives.[3,57] To circumvent these drawbacks, alternative strategies, such as various forms of injection (subcutaneous, intravenous or intrathecal) or modifications within the peptide chain, are often employed. These include, for example, the incorporation of D-amino acids, non-proteinogenic (also called non-standard) amino acids, PEGylation or Nα-methylation to improve the stability and cell permeability among others (Table 1).[59,94] In addition, peptide cyclization is also another technique often used to improve the stability or cell permeability. For this reason, many new peptide-based drugs (Table 1) exhibit cyclic structures through head-to-tail cyclizations, like the aforementioned voclosporin (Figure 1, **1**), or side-chain-to-side-chain cyclizations with the aid of disulfide bonds. Currently there are several of these disulfide-bonded peptides available on the market and since 2010 7 of the 22 peptid drugs approved by the FDA containing disulfide bonds (Table 1). These include the octreotide derived analogs ^{177}Lu-dotatate, ^{68}Ga-dotatoc and ^{64}Cu-dotatate,[69,72] containing one disulfide bond and D-amino acids that are used for imaging applications. In addition, also with one disulfide bond and D-amino acids, the aforementioned setmelanotide[66] and etelcalcetide[70] for the treatment of hyperparathyroidism[81] are FDA-approved peptides drugs. Regarding peptides with multiple disulfide bonds, the FDA has approved the orally administered peptide

linaclotide, a 3-disulfide-bonded peptide used in irritable bowel syndrome with constipation[89,90] and the 2-disulfide-bonded plecanatide[79], a peptide used for the treatment of chronic idiopathic constipation, in the last 12 years (Table 1).[20,68]

2.1.2 Conotoxins as drug candidates

As mentioned earlier in section 2.1, a large pool of different disulfide-rich peptides can be found in toxins of several organisms.[95,96] In this context, a wide variety of marine cone snail venoms have been investigated for their components over many years. These neurotoxins serve as self-protection for these snails as well as hunting tools, injecting their venom into the enemy or prey via a harpoon-like radular tooth.[97] However, the interesting aspect of these venom mixtures is that they can contain a huge number of peptides (100-200 per species), all of which address a wide variety of biological targets and exert different biological activities.[98] One class of such venom-derived peptides represent the so-called conotoxins, i.e. multiply disulfide-bonded peptides, derived from marine cone snails. These conotoxins can be utilized as neurotoxins due to their inhibitory potential towards a wide range of ion channels (e.g. voltage-gated sodium (VGSC) and potassium (VGPC) channels) and receptors (e.g. G protein-coupled receptors (GPCRs), nicotinic acetylcholine receptors (nAChRs)).[5,99,100] In this regard, low doses of conotoxins have a great potential for medical applications, especially in pain therapy, as the dose usually determines the toxicity.[5] It is estimated that there are roughly 1,000,000 different conotoxins in various cone snails, that are grouped in different classes according to their pharmacological target proteins (Table 2).[41,98] For example, μ-conotoxins selectively engage and inhibit voltage-gated sodium channels, whereas ω-conotoxins block voltage-gated calcium channels and thus impede the electrical conduction in nerves.[41] The best-known representative of the ω-conotoxins is MVIIA, also known as ziconotide (Table 2) isolated from the cone snail *Conus magus*, which is approved under the trade name Prialt® and is applied in the treatment of severe chronic pain associated with cancer and neuropathies.[101,102] Currently, ziconotide is the only venom-derived peptide targeting voltage-gated ion channels ($Ca_v2.2$) employed in therapy.[43,102] This peptide exemplifies the high potential of conotoxins as tools for drug discovery.

***Table 2*:** Representatives of the major conotoxin classes defined by their target proteins. Cysteines are marked in bold.

Class	Target proteins	Conotoxin	Sequence
ω	$Ca_v2.2$ inhibitor	MVIIA[101]	**C**KGKGAK**C**SRLMYD**CC**TGS**C**RSGK**C**-NH_2
μ	Na_v inhibitor	PIIIA[6]	ZRL**CC**GFOKS**C**RSRQ**C**KOHR**CC**-NH_2
μO	$Na_v1.8$ inhibitor	MrVIB[103]	A**C**SKKWEY**C**IVPILGFVY**CC**PGLI**C**GPFV**C**V
χ	NET inhibitor	MrIA[104]	NGV**CC**GYKL**C**YHO**C**
α	nAChR inhibitor	Vc1.1[105]	G**CC**SDPR**C**NYDHPEI**C**-NH_2

NET: norepinephrine transporter; nAChR: nicotinic acetylcholine receptor

To date, various conotoxins and the impact of their disulfide bonds on structure and activity have been investigated.[41] Earlier studies on μ-conotoxin PIIIA (Table 2) from *Conus purpurascens* showed that not only the disulfide bonds alone but also their precise connectivity is of great importance for its inhibitory potential towards the skeletal voltage-gated sodium ion channel $Na_v1.4$.[54] This was accomplished by synthesizing all 15 possible disulfide-bonded isomers as well as select disulfide-deficient variants of μ-PIIIA.[6,54,106] The significance of the

presence of all three disulfide bonds was demonstrated by the loss of activity observed for the disulfide-deficient variants, whereas several 3-disulfide-bonded isomers still exhibited reduced bioactivities.[54] The study by Heimer *et al.*[6] also provided important insights into the analytical characterization of disulfide-bonded peptides.[6] It was observed that it was not possible to distinguish all 15 disulfide-bonded isomers by conventional methods such as HPLC and MS. The reason for this was that some peptides coeluted in the HPLC due to very similar physicochemical properties. Unambiguous differentiation of these isomers was only possible by elaborate MS- and NMR-based methodologies.[6] These results indicate that there is still a need for optimization of analytical methods in the field of disulfide-bonded peptides. More detailed information on the analytical characterization of disulfide-bonded peptides is given in section 2.4.

2.1.3 Leech-derived peptides as drug candidates

The occurrence of a high number of cysteine-rich peptides is not exclusive to marine organisms (see section 2.1.2). These peptides are also abundant in the saliva of bloodsucking animals like ticks and leeches. Usually, the peptides found in these organisms have an anticoagulant activity, which is supposed to avoid blood clotting during the ingestion of blood.[107,108] These representatives are mostly stabilized by disulfide bonds and can be often divided into antistatin (10 cysteines (C), connectivity: Cys1-Cys3, Cys2-Cys4, Cys5-Cys8, Cys6-Cys9, Cys7-Cys10) and leech antihemostatic protein types (6 cysteines, connectivtiy:Cys1-Cys2, Cys3-Cys5, Cys4-Cys6) according to their intramolecular disulfide bonds.[109–113] Detailed information concerning these peptides from the salvia of bloodsucking leeches and their influence on the blood coagulation can be found within the review article provided in section 4.1 (in Table 1 of the review article).[27] Due to their anticoagulant activity, these substances are another naturally occurring group considered to be of great interest for medical applications in the field of cardiovascular diseases.[114] According to the World Health Organization (WHO), cardiovascular diseases are the most common cause of death worldwide.[115] In most cases, an imbalance in the regulation of the blood coagulation is the initial cause, which can lead either to excessive bleeding or to undesirable clot formation (hypercoagulation), i.e. thrombosis. As a consequence, these vascular occlusions can trigger myocardial infarction, stroke, pulmonary embolism (PE) or deep vein thrombosis (DVT), leading to death in the worst scenario. Thus, the development of anticoagulant agents is essential for the treatment and prevention of these diseases. Hirudin, a peptide originating from the medicinal leech *Hirudo medicinalis* is probably the best-known representative of anticoagulants isolated from leeches.[44] It is a 65mer peptide containing 3 disulfide bonds (Cys6-Cys14, Cys16-Cys28, Cys22-Cys39, antistatin type) formed as a result of the 6 cysteines within the sequence.[109] Hirudin exhibits an anticoagulant activity due to its inhibitory potential on the blood coagulation factor thrombin (factor II), a serine protease, which is essential for the stabilization of blood clots by indirectly supporting the formation of fibrin polymers.[112] In addition to these direct thrombin inhibitors, which include various hirudin derivatives (bivalirudin and argatroban), there are also indirect thrombin inhibitors available with clinical applications.[113,116–118] These indirect inhibitors act either through interaction with other blood coagulation factors, such as FX, or through systems that show an effect on blood coagulation, such as vitamin K antagonists.[119,120] All these anticoagulants, directly or indirectly inhibit thrombin, share the disadvantage of possible unwanted bleeding.[120,121] In order to not affect fibrin clot formation, and thereby potentially avoiding such side effects, anticoagulants capable of acting in a thrombin-independent manner are beneficial. In this regard, another blood clotting factor, FXIIIa, that catalyzes the final step of the blood coagulation cascade, namely the cross-linking

of fibrin clots, could serve as an alternative target structure. The inhibition of this factor would preserve thrombin activity and thus fibrin clot formation. However, the impaired cross-linking of the fibrin clots would result in a reduced stability of the blood clot and the unwanted thrombus, leading to an easier degradation of the clot.[122,123] Consequently, FXIIIa is a potential target for the development of further anticoagulant drugs. FXIIIa and its importance for the blood coagulation cascade will be presented in more detail in the following sections.

2.2 Blood coagulation factor XIIIa

Haemostasis is a complex system broadly divided into primary and secondary haemostasis.[124,125] Within the primary haemostasis, platelet aggregation occurs during damage of the blood vessel wall, leading to wound closure by the interaction of platelets with each other and with the extravascular tissue.[124,125] The secondary haemostasis happens simultaneously and triggers the generation of insoluble fibrin that forms a covalent network around the thrombus of primary haemostasis and stabilizes it from an early fibrinolysis.[124,125] The impact of the blood coagulation factor XIII, which is in the prime focus of this work, resides in the generation of the fibrin network and thus in the secondary haemostasis. The secondary haemostasis (Figure 2), also known as the blood coagulation cascade, is a network of different factors that, through a multistep sequence of activations, initially aims to generate a high amount of thrombin, the activated factor IIa.[124,125]

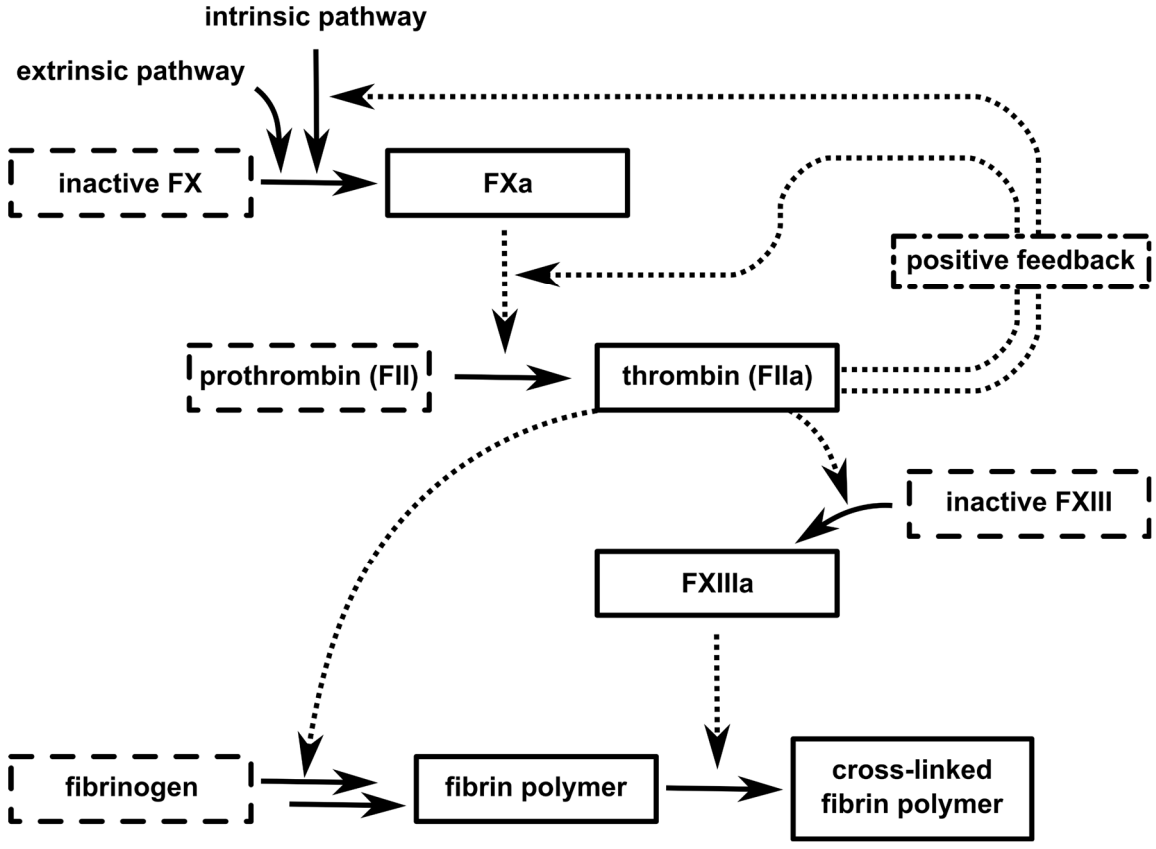

Figure 2: Schematic illustration of the blood coagulation cascade with the focus on thrombin and fibrin formation. The dashed arrows indicate a stimulation of the depicted reactions. The positive feedback describes the thrombin-catalyzed activation of blood coagulation factors, such as FVa, FVIIIa and FXIa, which in turn enhance the generation of thrombin. Dashed boxes: inactive states of the blood coagulation factors; normal boxes: active states of the blood coagulation factors.

Originating from prothrombin, activated thrombin induces platelet adhesion and the activation of various factors of the coagulation cascade (FVa, FVIIIa, FXIa, FXIIIa), which, except FXIIIa, in turn contribute through the cascade to generate further amounts of thrombin and enhance the coagulation process.[126–130] Many of these blood coagulation factors and the complexes formed from these factors, such as tenase (FVIIIa/FIXa) and prothrombinase (FXa/FVa) complexes, interact in their activated states with the surface of aggregating platelets. Thus, haemostasis can occure specifically at the site of injury.[131–133] Additionally, as explained later (in section 2.2.3), thrombin cleaves fibrinogen to fibrin. The latter can subsequently polymerize via noncovalent interactions and form an initial haemostatic fibrin clot.[125,131] However, this fibrin clot is not very stable due to the lack of covalent linkages between the individual fibrin monomers, resulting in a smaller size of the blood clot per se and can be more easily dissolved by fibrinolysis.[123,134,135] The fibrin-stabilizing factor FXIII, catalytically activated by thrombin and Ca^{2+}-ions to form FXIIIa, plays a crucial role in stabilizing the fibrin clot.[136] FXIIIa is a transglutaminase that covalently cross-links and thus stabilizes fibrin monomers within the fibrin network via the formation of isopeptide bonds.[128,137] Furthermore, FXIIIa catalyzes additional bond formations of the fibrin monomers to proteins of the extracellular space as well as the platelet surface, which enhance the biomechanical stabilization of the entire clot.[131] These covalent interactions, along with the attachment of α_2-antiplasmin to fibrin (catalyzed by FXIIIa), further protect the formed clot from early fibrinolysis by plasmin.[122] The stabilizing properties of FXIIIa for the fibrin clot were first described by Kálmán Laki and László Lóránd in 1948, when they observed that fibrin clots could not be dissolved from urea with the help of FXIIIa and Ca^{2+}-ions.[138,139] Moreover, they showed that the viscosity of fibrin (without cross-linking) was comparable to fibrinogen in 30% urea solution, which was an important indication of the reversibility of fibrin polymerization.[139,140] This demonstrates the importance of FXIIIa in the stabilization and preservation of the blood clot without exerting any influence on thrombin generation and concomitant fibrin polymerization.

2.2.1 Localization and activation of FXIII

The transglutaminase FXIII exists in two different forms in the human body: the plasmatic FXIII (pFXIII) and the cellular FXIII (cFXIII). These two forms differ mainly in their localization in the human body, their structural composition and their mode of activation, which exposes the active site with the catalytic triad (Cys314, His373, Asp396).[141]

Cellular FXIII occurs in the cytoplasm of various cell types, for instance platelets[142], and is composed of two inactive FXIII-A subunits. These subunits are usually converted non-proteolytically by conformational changes into an active, activation peptide-bound form (XIIIa°, Figure 3) by the influence of Ca^{2+}-ions.[141,143,144] If thrombin is also present, cFXIII can be proteolytically activated by the cleavage of the activation peptide and thus can be converted to the functionally more active FXIIIa.[144–148]

In comparison to cFXIII, the plasmatic FXIII exists as an A_2B_2 heterotetramer, with two FXIII-A subunits, important for the transglutaminase activity, and two FXIII-B subunits, which are non-covalently bound to the FXIII-A_2 dimer.[149] The two FXIII-B subunits protect the FXIII located in the blood plasma from proteolytic degradation by plasmatic proteases and from spontaneous activations via Ca^{2+}-ions.[150–152] In a structural perspective, the FXIII-B subunit has not been well characterized, due to the lack of crystal structures of the protein or the plasmatic FXIII. However, it is known that the FXIII-B subunit consists of 10 so-called “sushi domains”, each structurally stabilized with two disulfide bonds, and occurs as a dimer in solution.[153–157] Moreover, the first two sushi domains of the FXIII-B subunits are each thought to interact with the FXIII-A subunits to stabilize the FXIII-A_2B_2 complex.[158] Currently, the

FXIII-A subunits that form a homodimer (FXIII-A_2) in complex with the FXIII-B subunits, are structurally better characterized due to existing crystal structures (Protein Data Bank (PDB) ID: 1GGT[159], 1GGU[160], 1QRK[160], 1GGY[160], 1F13[148], 4KTY[148], 1FIE[161]). The FXIII-A subunits are composed of four main domains (Figure 3), e.g., the N-terminal β-sandwich domain (1-184) with the activation peptide (1-37), the catalytic core domain (185-515) and two β-barrel domains (β-barrel 1: 516-628, β-barrel 2: 629-731).[141,159,162]

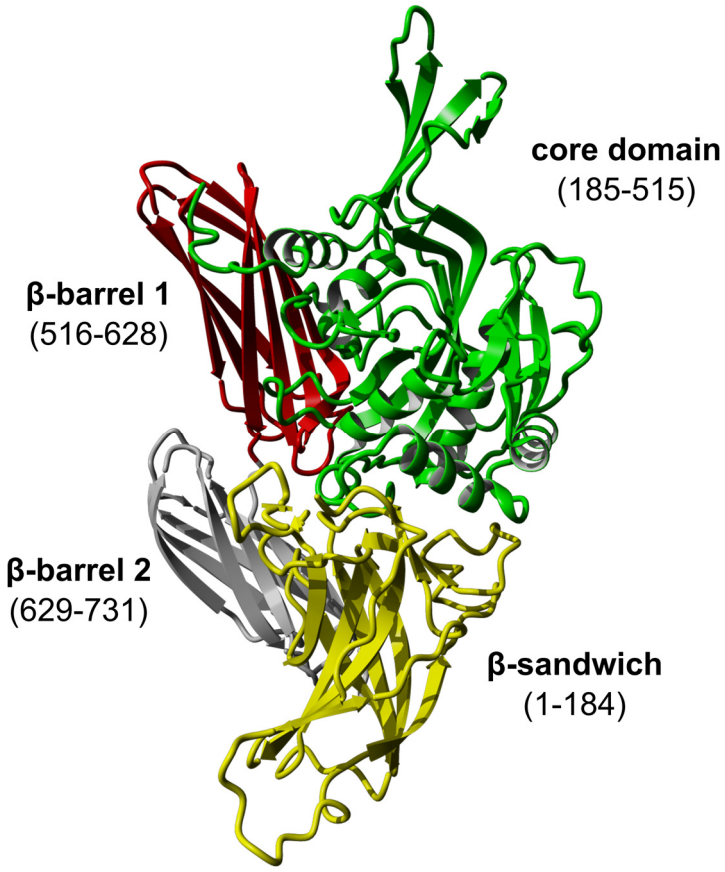

Figure 3: Crystal structure of FXIIIa° (PDB ID: 4KTY[148]). The domains are shown in different colors. Yellow: B-sandwich; green: core domain; red: β-barrel 1; grey: β-barrel 2.

In the inactive state of FXIII, the active site comprising the catalytic triad Cys314, His373 and Asp396 is inaccessible to substrates due to several intramolecular interactions. On the one hand, the active site is blocked by the activation peptide of the second FXIII-A subunit via an ionic bond between Asp343 located in the active site and Arg11 of the activation peptide. On the other hand, hydrogen bonding between Tyr560 and the catalytically significant Cys314 results in a blockage of the catalytic center via the β-barrel 1 domain which leads to an inhibition of the transglutaminase activity.[148,159] Activation and simultaneous exposure of the active site initially occurs via proteolytic cleavage of the N-terminal activation peptide by thrombin (Figure 4). This step removes the ionic bond between Asp343 and Arg11, thereby weakening the interaction between FXIII-A and FXIII-B. In addition, the cleavage of the activation peptides results in the fact that even the presence of a small amount of Ca^{2+}-ions are sufficient to release the FXIII-B subunits. In this context, the coordination of Ca^{2+}-ions at three different binding sites induces a conformational change making the active site accessible

to substrates and is therefore crucial for the transglutaminase activity and the generation of the active FXIIIa conformation.[163,164] Interestingly, the cleavage of the activation peptide and the dissociation of the FXIII-B subunits within the FXIII activation process is also activated by fibrinogen and fibrin.[164–167]

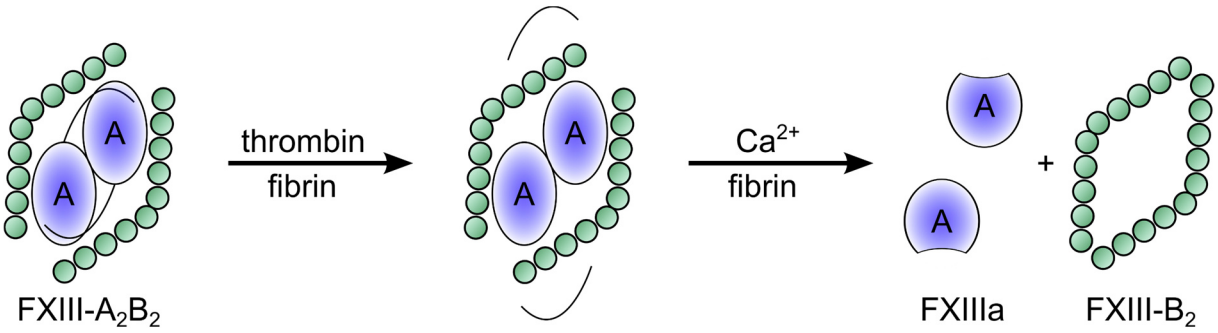

Figure 4: Proteolytic activation of plasmatic FXIII via thrombin and Ca^{2+}-ions. The first, thrombin-catalyzed step leads to the proteolytic cleavage of the activation peptide, whereas the second, Ca^{2+}-mediated step separates the subunits of FXIII and changes the conformation within the FXIII-A subunit to active FXIIIa.[27]

2.2.2 Structure of FXIIIa

FXIIIa belongs to the enzyme class of transglutaminases (TGase, EC2.3.2.13).[168] Transglutaminases catalyze isopeptide bond formation between the γ-carboxy-amine group (γ-$CONH_2$) of glutamine (amine acceptor) and the ε-amino group (ε-NH_2) of lysine (amine donor) via an acyltransferase reaction.[140,169] Among the transglutaminases, nine human genes are known, with six of these transglutaminases (TGase 1-5, FXIIIa) characterized in more detail while the function of TGase 6 and 7 are still undefined.[170,171] The most well characterized representative is the tissue transglutaminase (TGase 2), which is present in various tissues and cell types.[172] Due to its multifunctional properties (transamidation, deamidation, protein disulfide isomerase, kinase activity, ability to act as a G-protein[173]), TGase 2 serves as a promising pharmaceutical target for various diseases such as celiac disease, Alzheimer's disease and cancer.[174–177] On account of the structural similarity within the active site of FXIIIa and TGase 2, many FXIIIa inhibitors known in the literature lack specificity, which may induce side effects due to interaction with TGase 2.[148,178–180]

Many recent studies already indicate that FXIIIa is present as a monomer[144,145,148,181–183] and not as a dimer[184,185], as initially assumed. The active site consists of a catalytic triad, a catalytic diad and a hydrophobic tunnel, which surrounds the active site. In this context, Cys314 is mainly responsible for the transglutaminase reaction within the catalytic triad consisting of Cys314, His373, and Asp396 (Figure 5).[186] The catalytic diad, composed of His342 and Glu401, is formed only after the conformational change induced by Ca^{2+} coordination, and is responsible for the deprotonation of the amine function of the co-substrate lysine.[148] The hydrophobic tunnel is established by two tryptophans, Trp279 and Trp370, and is also formed by a conformational change after Ca^{2+} coordination. The interaction of the two tryptophans during the transglutaminase reaction protects the substrate glutamine from unwanted hydrolysis. This tunnel has also been found to be similar in TGase 2.[159,187,188]

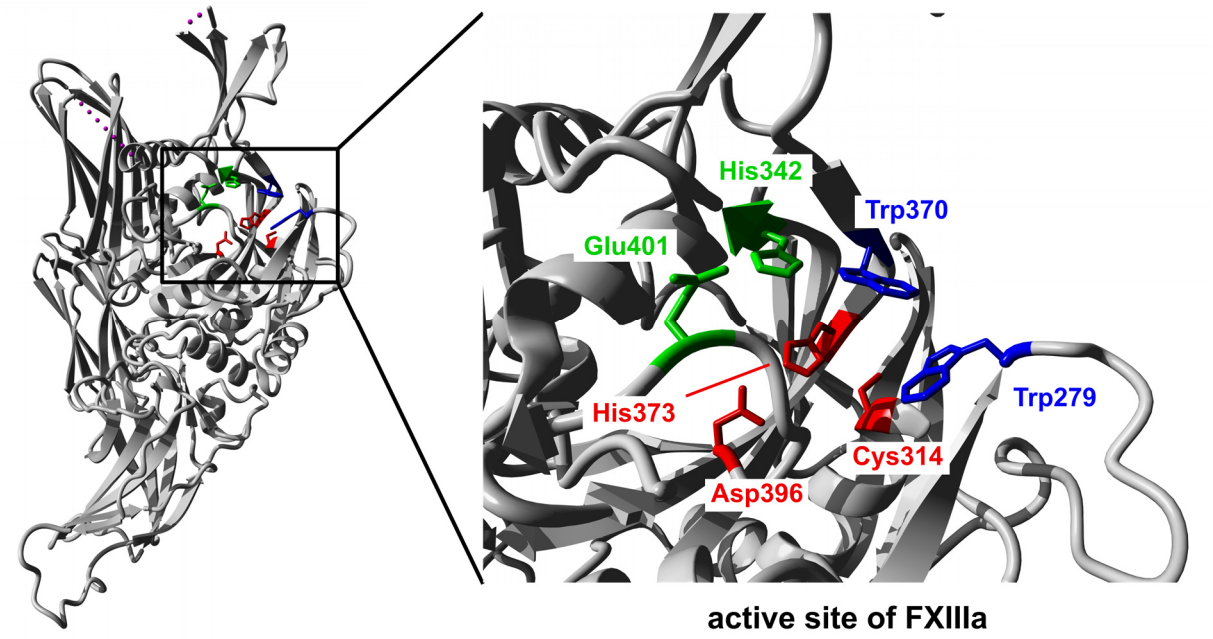

Figure 5: The active site of FXIIIa° (PDB ID: 4KTY [148]). The active site of FXIIIa is located in the core domain and is composed of the catalytic triad (red), the catalytic diad (green), and a hydrophobic tunnel (blue).

The transglutaminase reaction is initiated by the introduction of a glutamine side chain into the active site (Figure 6, **II**).[189] The thiol function of Cys314, which is activated via the triad, then nucleophilically attacks the glutamine at the carbonyl carbon atom of the side chain. In this process, a thioester bond is formed after cleavage of ammonia between FXIIIa and glutamine (**IV**) via a tetrahedral transition state stabilized by various hydrogen bonds (**III**). The subsequent insertion of the second substrate (**V**), the lysine side chain, then occurs from the other side of the hydrophobic tunnel.[148,189] For the nucleophilic attack of the amine function on the carbon atom of the thioester function, the lysine is first activated via the catalytic diad and the catalytic triad. In this process, the catalytic diad is responsible for deprotonating the positively charged amine function of the lysine side chain, resulting in the loss of the positive charge and allowing the lysine side chain to enter the hydrophobic tunnel. After the nucleophilic attack of the lysine side chain, the new generated tetrahedral intermediate is again stabilized via hydrogen bonds (**VI**). Subsequent transfer of the acyl group to the amino function of lysine and regeneration of the free thiol function of Cys314 (**I**), leads to the generation of the isopeptide bond between the glutamine and lysine side chains. As a result, the free thiol function of Cys314 of FXIIIa is again available for a renewed catalytic mechanism.[148,189–191] Without the hydrophobic tunnel of FXIIIa, water would be able to enter as a second substrate in the catalytic mechanism, which would finally lead to deamidation and conversion of glutamine to glutamic acid.[148,189] This shows the importance of the hydrophobic tunnel in addition to the catalytic triad and diad for the catalytic transglutaminase function of FXIIIa.

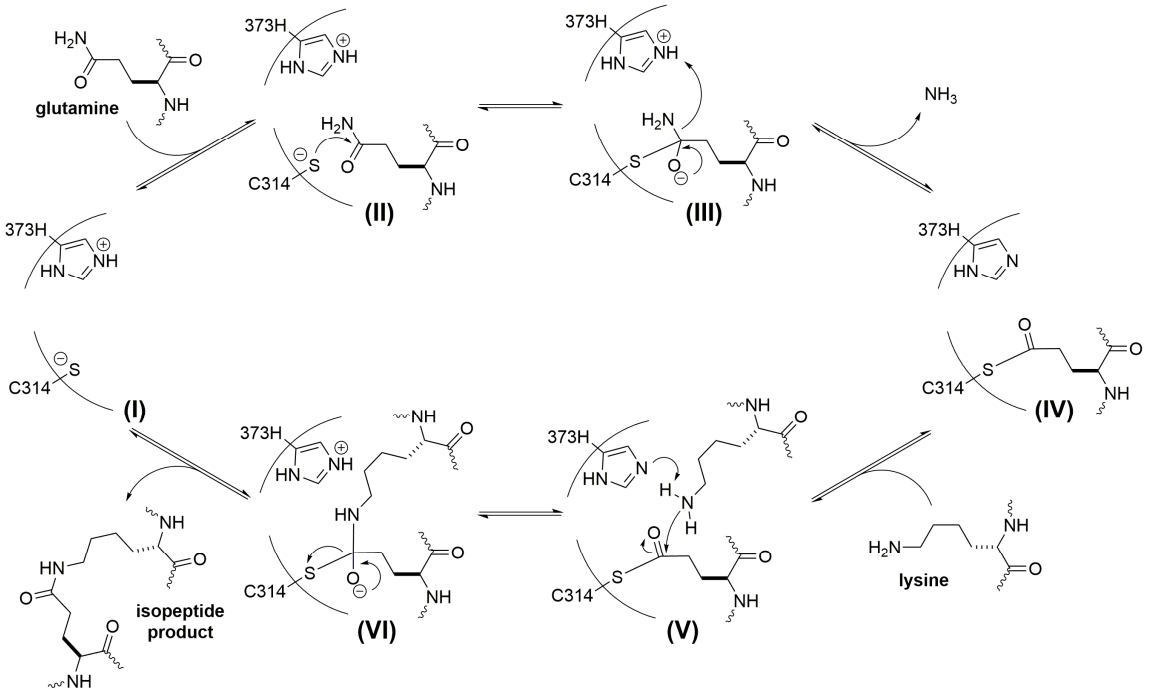

Figure 6: Catalytic mechanism of FXIIIa with involvement of Cys314 and His373 of the catalytic triad. Image derived from Keillor *et al*.[189]

2.2.3 FXIIIa in haemostasis and fibrinolysis

The transglutaminase function of FXIIIa (section 2.2.2) contributes tremendously to haemostasis and fibrinolysis. FXIIIa not only cross-links and stabilizes fibrin polymers via covalent isopeptide bonds, it also covalently links these fibrin molecules to extracellular proteins and structural proteins of the platelet membrane.[122,131] The resulting fibrin network secures platelets aggregated in primary haemostasis, and biochemically stabilizes the entire blood clot.[131] Consequently, the conversion of fibrinogen to the fibrin clot structure cross-linked by FXIIIa is a central step in haemostasis and will be described in more detail in the following section.

Fibrinogen is a hexamer consisting of three different polypeptide chains, the Aα-chain, the Bβ-chain and the γ-chain, each of which occurs twice (Figure 7).[16,192] The individual chains form two identical halves (the AαBβγ trimer) and are held together by 5 different disulfide bonds across their N termini in the central E domain.[16,192,193] In total, fibrin/fibrinogen contains 58 cysteines that comprise the possibility, in addition to the 5 already mentioned, to form 24 further disulfide bonds, stabilizing the structure of fibrinogen and fibrin.[194] In this context, 12 of the 24 remaining disulfide bonds constitute intramolecular bonds within the chains (1 per Aα-chain, 3 per Bβ-chain, and 2 per γ-chain), whereas the other 12 disulfide bonds stabilize the coiled-coil regions connecting the central E-domain to the D-domains via ring structures consisting of 3 intermolecular bonds.[195,196] The D domains are composed of the C termini of the Bβ- and γ-chain (β-node and γ-node) and contain interaction sites that are crucial for polymerization and subsequent cross-linking of the fibrin molecules.[192] In addition, fibrinogen includes further building blocks like the very flexible portion of the two Aα-chains, as well as the fibrinopeptides A and B, which are exclusive to fibrinogen, at the N termini of the Aα-chains and Bβ-chains.[197] The seminal contribution to the structural analysis of human fibrinogen was made by the first crystal structure in 2009[198], along with computational work, transmission electron microscopy, and atomic force microscopy, which illustrated flexible and thus structurally only slightly

elucidated regions in addition to the insights obtained from the crystal structure.[196,199,200] Apart from the structural features originating from the polypeptide chains within fibrin/fibrinogen, the Bβ- and γ-subunits are concomitantly N-glycosylated.[192] Moreover, fibrin/fibrinogen has multiple binding sites for Ca^{2+}-ions[201–204] providing protection against proteolytic cleavage[205,206] as well as, being significant for fibrin polymerization similar to the glycosylations[207–210].

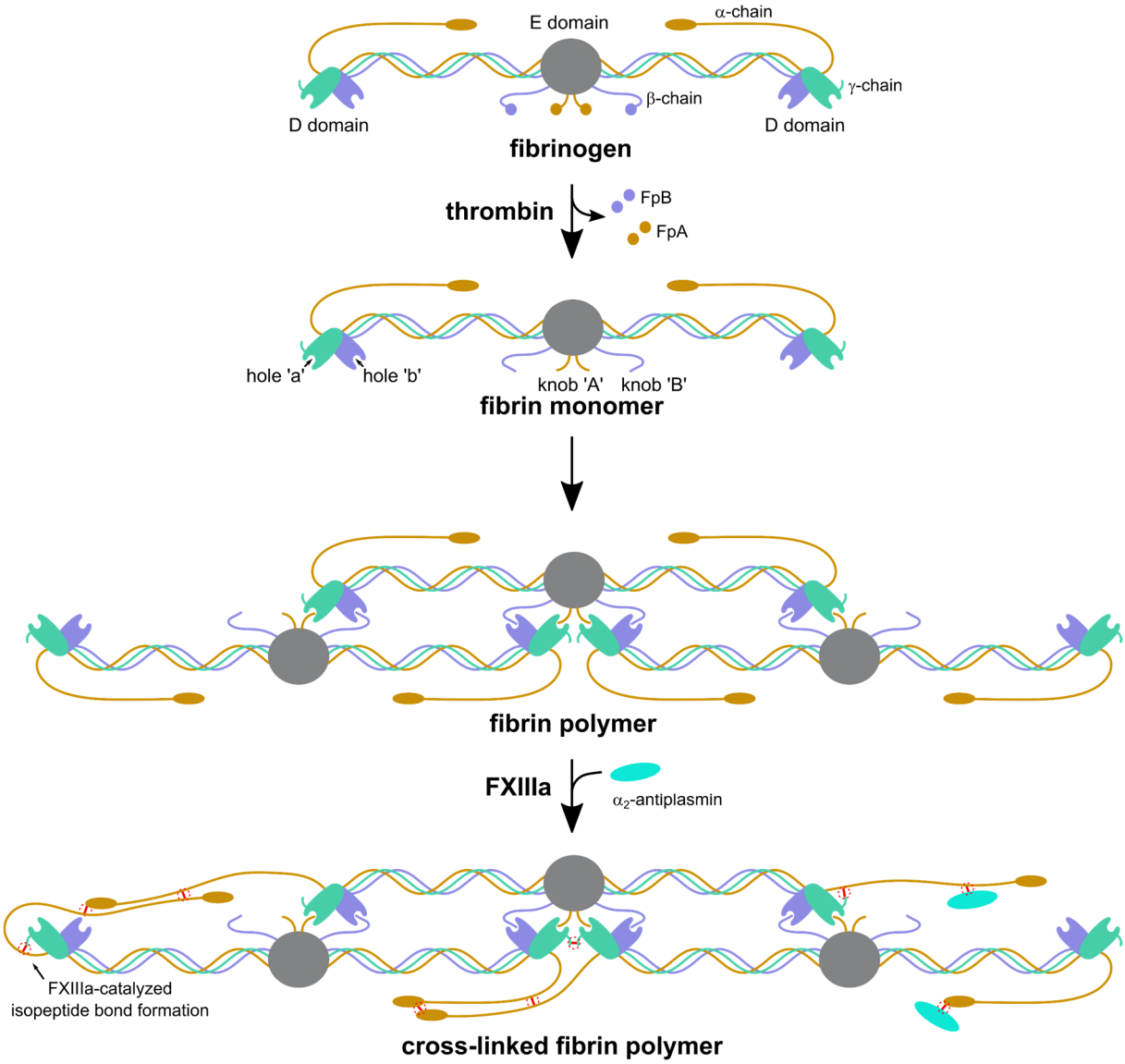

Figure 7: Activation mechanism to form cross-linked fibrin polymers. Step 1: Cleavage of the activation peptides (FpA, FpB) and generation of fibrin monomers catalyzed by thrombin. Step 2: Non-enzymatic polymerization of the fibrin monomers to protofibrils by non-covalent interactions. Step 3: Cross-linking of the fibrin clot as well as incorporation of α_2-antiplasmin catalyzed by FXIIIa. The isopeptide bonds are marked in red.[15,211]

Fibrin polymerization takes place in various enzymatic and non-enzymatic steps (Figure 7). Initially, the serine protease thrombin detaches the fibrinopeptides FpA and FpB, exposing so-called 'A' and 'B' knobs on the central E-domain.[192] These knobs subsequently interact with 'a' and 'b' holes of the D domains of other fibrin monomers and thus spontaneously form a two-stranded fibrin oligomer, a protofibril. These noncovalent interactions, as well as interactions between αC-regions of different fibrin monomers, result in lateral and longitudinal aggregation

of the protofibrils. Resulting from this fibrin polymerization, a fibrous gel-like network is formed, which, however, is held together exclusively by non-covalent interactions and is consequently rather unstable and easily degraded by fibrinolysis.[192] The importance of FXIIIa for the stability of the fibrin network and thus of the entire blood clot is clear from what has been described above, since covalent bonds between the individual fibrin monomers are only formed in the final step by FXIIIa-catalyzed cross-linking. On the one hand, FXIIIa is able to link two γ-chains of two E-domains of adjacent fibrin monomers via end-to-end cross-linking. In this process, ε-(γ-glutamyl)-lysyl isopeptide bonds are formed between γGln398/399 and γLys406, which contribute to the stabilization of longitudinal spreading of protofibrils and increase fiber density and stiffness.[212–214] On the other hand, FXIIIa also catalyzes the covalent connection of α-chains to each other and α-γ linkages. Such stabilization occurs mostly in the αC-regions of fibrin monomers and, along with increasing the strength of fibrin polymers, it enhances fiber thickness and the incorporation of red blood cells into the clot.[135,213–218] As a consequence of the aforementioned covalent connections between the individual building blocks of the fibrin network, the previously reversible equilibrium of fibrin polymerization changes into an irreversible clot formation.[219] Furthermore, FXIIIa also catalyzes cross-linking to proteins, such as the plasmin inhibitor α_2-antiplasmin (α_2-AP), plasminogen activator inhibitor 2 (PAI-2), thrombin-activatable fibrinolysis inhibitor (TAFI), and fibronectin, that provide additional protection against fibrinolysis by plasmin or contribute to the wound healing process.[220–223]

All these FXIIIa-catalyzed cross-links within the fibrin networks play a significant role in the structure and biomechanical properties of the blood clots. In various mouse models as well as in human whole blood, it has been shown that lower levels of FXIII result in fewer erythrocytes depositing into the clot, leading to smaller thrombi.[123,134,135,224,225] The cross-links also increase the stiffness and elasticity of protofibrils and decrease their fiber extensibility.[218,224,226] Interestingly, these effects may be specifically associated with the formation of high molecular weight cross-linked fibrin species triggered primarily by α-chain cross-linking.[213,214,218]

cFXIII, that is present in platelets, stabilizes fibrin clots similarly to pFXIII by cross-linking γ-dimers and α-polymers and binding α_2-AP to fibrin.[227–231] However, cFXIII appears to have only a minor role in FXIIIa-mediated stabilization of blood clots and retention of erythrocytes, owing to the slower recruitment and exposure of the factor.[134,217,232,233] In contrast, cFXIII is considered to play an important role during thrombus retraction together with the pFXIII. While pFXIII stabilizes the condensed thrombus by binding to the fibrin network and promoting the spread of a platelet[14,234], cFXIII strengthens the platelet cytoskeleton during platelet activation.[235,236]

In summary, FXIIIa-catalyzed cross-linking within the fibrin network has a significant function in stabilizing and protecting blood clots but also in retaining erythrocytes in the thrombus, making FXIII a therapeutic target worth of investigation.[233]

2.2.4 (Patho-)physiology of FXIII

Besides its role in haemostasis, FXIII has also been reported to play an important role in the lung[237,238], eye and optic nerve[239–242], kidney[243] and hepatocyte regeneration[244]. Moreover, FXIII has been associated with other physiological functions (Figure 8), which, however, have only been briefly characterized to date.[14,233]

In the physiological context, the influence on wound healing[168,245,246] and angiogenesis[247] is noteworthy. FXIII-deficient humans and FXIII-knockout mice, for example, were found to have impaired wound healing[141,245], which could be restored by FXIII administration. In this regard, FXIII influences the wound healing process by FXIII-catalyzed cross-linking of extracellular

matrix proteins, by promoting angiogenesis through activation of macrophages, and by enhancing fibroblast migration.[141,248] Similarly, FXIII is essential for myocardial healing after myocardial infarction.[249,250] This is evidenced in both, FXIII knockout mice as well as myocardial infarction patients with low FXIII levels, showing significantly more post-infarction complication of cardiac rupture.[249,251] Therefore, FXIII has been suggested to be used as a prognostic biomarker and as a drug.[252] Likewise, FXIII plays a critical role in pregnancy.[253,254] Untreated pregnancies of FXIII-deficient women resulted in very high miscarriage rates (>91%), whereas prophylactic FXIII substitution during pregnancy massively reduced the number of miscarriages (approximately 11%).[255,256] The exact function of FXIII has not been fully elucidated but several studies suggest a role in the implantation of the blastocyst into the placenta.[253,257] In this context, the development of a functional cytotrophoblast shell is thought to be dependent on the formation of fibrin-fibronectin cross-links catalyzed by FXIII.[257,258] Moreover, embryonic FXIII regulates vascular density and permeability during maternal angiogenesis.[259]

Furthermore, FXIII is involved in inflammation and in immune response.[260,261] FXIII is capable of covalently binding pathogens to the fibrin fibers, thereby significantly controlling pathogen entrapment in the fibrin clot. The process of early immune response has already been confirmed in mouse models as well as patients with necrotizing fasciitis.[262] In addition, an influence of FXIII on immune cells of the innate immune system has been described. These include M2 macrophages and granulocytes, that show increased FXIII expression and whose recruitment has been significantly reduced in FXIII-A knockout mice.[263–266] Apart from the function of FXIII on wound healing and immune response, an effect on bone biology has also been reported.[267,268] *In vitro* studies showed that FXIII-A can contribute to the formation and stabilization of bone connective tissue by cross-linking various components of the extracellular matrix.[143,269–272] Moreover, FXIII regulates osteoclast formation at various steps, which is related to its role in rheumatoid arthritis.[268,273] Nevertheless, the role of FXIII in bone biology has not yet been defined *in vivo*, as knockout of FXIII-A did not alter bone apposition processes.[14,274]

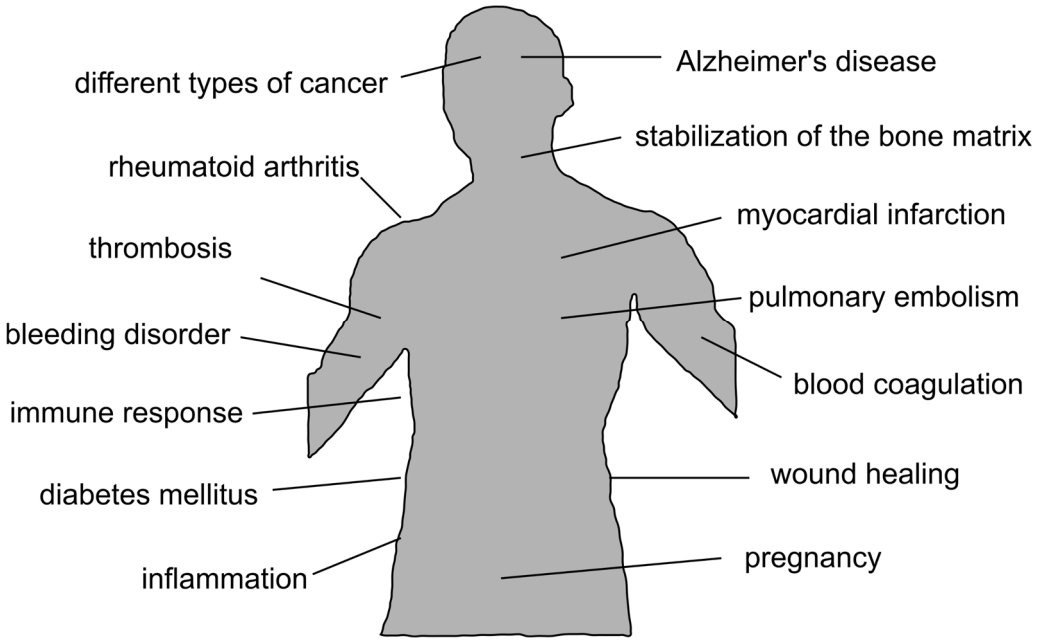

Figure 8: (Patho-)physiological functions of FXIII in the human body.

Due to the various physiological processes, FXIII is also involved in some pathophysiological conditions (Figure 8). Among these, the FXIII deficiency diseases represent a major emerging field.[275] This deficiency causes a rare bleeding disorder that can only be diagnosed by a fibrin solubility assay or a functional FXIII assay, as all standard coagulation tests result to be normal.[141,275–278] The origin of FXIII deficiency can be genetic (hereditary) or acquired, and depending on which subunit is affected, FXIII-A deficiency and FXIII-B deficiency can be distinguished.[279] Genetically caused FXIII-A deficiency is divided into type I (quantitative deficiency) and type II (qualitative deficiency), with quantitative deficiency caused by the synthesis of truncated or misfolded FXIII-A subunits while qualitative deficiency occurs due to a mutation, for example, in the active site, which impairs the functionality of FXIII.[277] FXIII-B deficiency is usually not as severe as FXIII-A deficiency since functional FXIII-A subunits can still be generated. Consequently, in these cases, cFXIII is not affected, whereas plasmatic FXIII-A is degraded more rapidly (only 10% of the normal amount of FXIII-A detectable) due to the lack of FXIII-B subunit in plasma.[150] In contrast to genetic FXIII deficiency, acquired FXIII deficiency can be induced by increased FXIII depletion in various pathologies such as leukemia, pulmonary embolism, stroke, and sepsis or by major chirurgical intervention.[280,281] Similarly, acquired FXIII deficiency may be caused by impaired FXIII-B synthesis in the liver [281]. In clinical terms, FXIII deficiency is divided into three classes: mild (FXIII activity: >30%, asymptomatic), moderate (FXIII activity: <30%, spontaneous mild bleeding), and severe (FXIII activity: 0%/non-detectable, spontaneous severe bleeding).[280,282] The latter affects wound healing and pregnancies and can lead to cerebral hemorrhage, which is the most common cause of death in this context.[277] The treatment of FXIII deficiency is usually performed by FXIII supplementation. Solely the FXIII deficiency due to endogenous autoantibodies against FXIII subunits prevents the therapy via FXIII substitution, as there is only a temporary relief of symptoms possible.[283] In this case, the goal of the treatment is to eliminate the FXIII antibody.[283]

Cardiovascular diseases may be caused by dysfunctionality of haemostasis, and, therefore, misregulation of FXIII may indirectly trigger such diseases. In this regard, FXIII may be involved in the development of numerous cardiovascular diseases through its influence on the clot structure and its stabilization against fibrinolysis.[15,217,233,284–290] In addition, there is evidence that FXIII plays a role in pulmonary embolism and myocardial infarction[291,292], and has an impact on abnormal thrombus structures with recurrent venous thrombosis and other thromboembolic events.[16] All in all, due to the various contributions of other factors in the occurrence of cardiovascular diseases, the precise influence of FXIII has not been yet fully elucidated, and further studies in this area are required.

Apart from cardiovascular diseases, FXIII is also correlated with tumor pathologies. Indeed, accumulations of fibrin and FXIII have been observed in brain tumors[293] and a positive effect of FXIII on tumor progression and metastasis has been observed in various forms of lung cancer.[294,295] Furthermore, evidence on the role of FXIII in various types of acute leukemia[296–299], breast cancer[300], ovarian cancer[301] colorectal cancer[302] and hepatocellular carcinoma exist.[303] Due to the diverse links of FXIII to tumor-related diseases, FXIII has been proposed as a potential biomarker in cancer therapy.[304]

Since FXIII-A is produced in pancreatic β-cells, it is thought to be involved in insulin regulation.[305] In this regard, a link between type II diabetes mellitus and FXIII in pancreatic islets has been found.[306] FXIII-A also serves as a regulator of preadipocyte differentiation and influences insulin signaling via fibronectin cross-linking to the extracellular matrix of preadipocytes.[307] FXIII thus plays a role in adiposity, which was also confirmed by FXIII-

deficient mice that showed significantly healthier fatness than normal mice on a very high-fat diet.[308]

Finally, in addition to the previously described disease pathologies, an influence of FXIII on rheumatoid arthritis[273], inflammatory bowel diseases such as Crohn's disease[309–312], and on the development of Alzheimer's disease[313–315] has been reported.

2.3 Inhibition of FXIIIa

Considering the various functions of FXIII in the human body, it represents an attractive target protein for the development of therapeutically relevant compounds. The focus of current research is concentrated mainly on the development of FXIII(a) inhibitors that effect clot formation and can be classified as anticoagulants.[316] The advantage of these specific FXIII(a) inhibitors compared to commonly used anticoagulants is that they do not interfere with thrombin production or fibrin formation, potentially providing a reduced risk of bleeding. Indeed, conventionally used blood thinners, in addition to their ability to reduce the number of venous thromboses, usually have a bleeding risk that should not be underestimated.[121] Accordingly, a specific FXIII(a) inhibitor could be distinguished from conventional anticoagulants by its broad therapeutic potential.[233]

2.3.1 FXIIIa inhibitors

To date, only a few agents have been described affecting the activity of FXIII(a). These can be divided into three different classes based on their inhibitory behavior towards FXIII: 1) inhibitors influencing the mechanism of FXIII-activation, 2) inhibitors that serve as co-substrates and thus prevent fibrin cross-linking and 3) molecules that block the active site of FXIIIa. Since only few studies of the first two classes are available so far and limitations are known that exclude these inhibitors for application in pharmacological research, the focus nowadays centers on inhibitors that directly block the active site of FXIIIa.[12,12,178–180,317,318] Currently, peptidic as well as allosteric inhibitors are being investigated, which should solve two problems compared to the already known small molecule inhibitors.[148,319,320] Firstly, most small molecule inhibitors lack specificity, especially between FXIII and TGase 2, and secondly, they have very short plasma half-lives.[179,180,318] Small molecule inhibitors among these are cerulenin (**4**) from *Cephalosporium caerulens* and alutacenoic acid A (**5**) and B (**6**) from *Eupenicilium alutaceum* (Figure 9).[321,322] In recent years, the most promising peptidic and allosteric inhibitors, in addition to the tridegin studied in this work, are the allosteric inhibitor non-saccharide sulfated glucosaminoglycan 13 (NSGM 13, **7**) as well as the peptidomimetics ZED1301 (**8**) and ZED3197 (**9**).[148,319,320] With the latter, the structure of FXIIIa could be elucidated via co-crystallization with ZED1301 (**8**), whereas ZED3197 (**9**) revealed potential for medical use in initial *in vitro* and *in vivo* studies.[148,319] For more information on the individual FXIII inhibitors and how they function against FXIII, please refer to the following review article[27] on FXIII inhibitors in section 4.1.

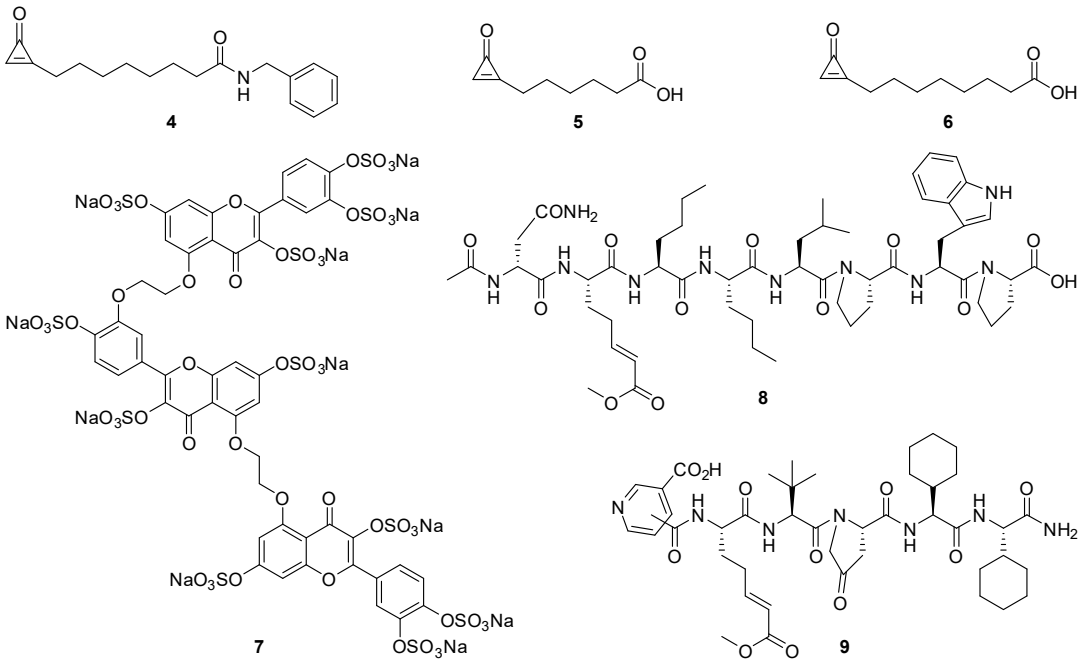

Figure 9: Structures of cerulenin (**4**)[180], alutacenoic acid A (**5**) and B (**6**)[322], NSGM 13 (**7**)[320], ZED1301 (**8**)[148], and ZED3197 (**9**)[319].

2.3.2 Tridegin

Tridegin is one of the best studied and to date the only naturally occurring peptidic FXIIIa inhibitor. It is a 66mer polypeptide (7.6 kDa, Figure 10) from the saliva of the Amazon giant leech *H. ghillianii* which was first isolated and characterized from the leech saliva in 1997 by Finney *et al*.[11] This isolated tridegin showed an initial IC_{50} value of 9.2 nM with respect to inhibition of FXIIIa. Moreover, no inhibitory potential of tridegin on other factors of the blood coagulation cascade (thrombin, factor FXa) and several cysteine proteases (bromelain, papain, cathepsin C) was observed.[11] Only TGase 2 was inhibited by tridegin with 23-fold lesser effect, which is why tridegin can be considered as a very potent and specific FXIII inhibitor.[11] In addition to its functional characterization, Edman degradation was applied to analyze the amino acid sequence of tridegin. Unfortunately, the sequence of the 66mer peptide could not be fully elucidated.[11] Subsequent studies concerning tridegin were able to complement the tridegin sequence and to examine further structural features, which are important for its bioactivity.[12,323,324] The chronological course of these studies can be found in detail in the review article[27] in section 4.1. Therefore, in the following the status of tridegin research before the start of this project and the relevant information for the work presented herein will be exclusively illustrate.

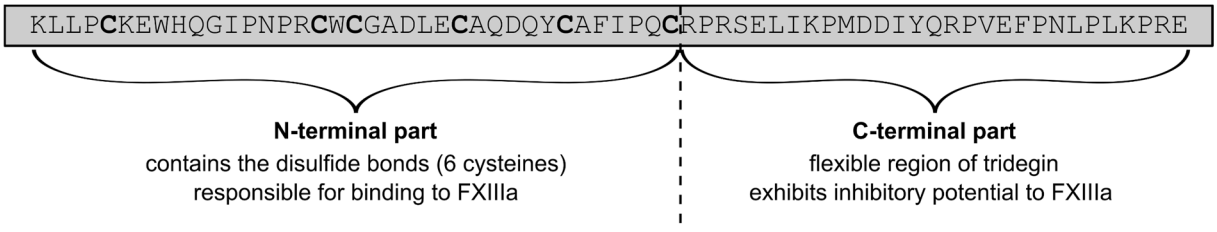

Figure 10: Amino acid sequence of the 66mer peptide tridegin. Tridegin is divided into an N- and C-terminal region, due to different structural and functional properties of these fragments.

For the further discussion, the peptide sequence of tridegin is divided into two regions due to the different properties of the N- and the C-terminal part (Figure 10). The C-terminal fragment (aa 38-66) is a flexible and intrinsically disordered region contributing mainly to the inhibitory potential of tridegin. The N-terminal part (aa 1-37), which is thought to have a large impact in binding to FXIIIa, is a well ordered segment containing six cysteines linked by three disulfide bonds, thus conferring structural stability.[12,324] However, due to the scarcity of the endangered *H. ghilianii*, the exact disulfide bond connectivity in the native tridegin is still unknown. This uncertainty renders it possible that the tridegin variants recombinantly or chemosynthetically produced in recent studies may differ in their disulfide bond connectivity as well as their amino acid sequence from the naturally occurring tridegin. In order to investigate which of the 15 theoretically possible 3-disulfide-bonded tridegin isomers are preferentially formed from the primary sequence of tridegin, a self-folding experiment was conducted in 2014.[12] The resulting oxidatively produced tridegin did not comprise only one preferred tridegin isomer, but three different isomers could be identified by mass spectrometric analysis of a chymotryptic digest. These isomers, which exhibited activity towards FXIIIa as a mixture, featured a common disulfide bond between Cys19 and Cys25. The bridging Cys05-Cys17, Cys19-Cys25, Cys31-Cys37 was defined at that time as isomer A, whereas the linkage, Cys05-Cys37, Cys17-Cys31, Cys19-Cys25 was referred to isomer B and Cys05-Cys31, Cys17-Cys37, Cys19-Cys25 was designated as isomer C (Figure 11).[12]

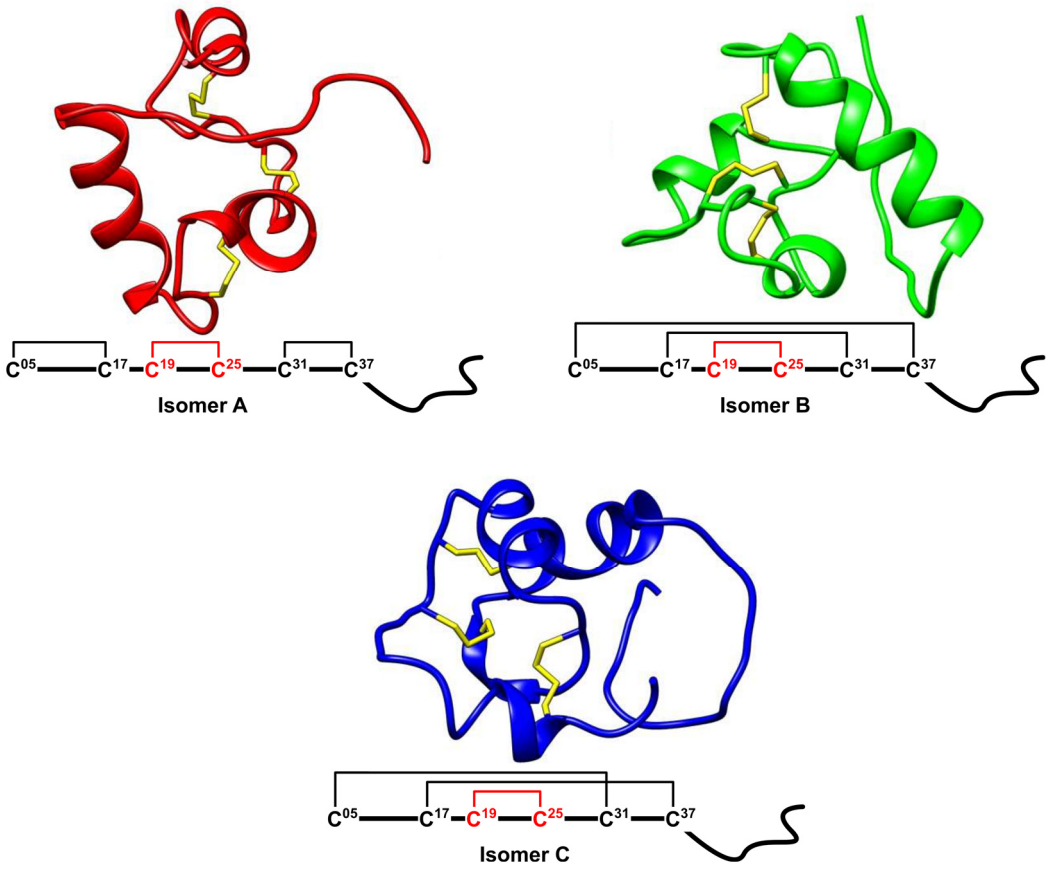

Figure 11: Computationally-generated model structures and disulfide bond connectivities of the 3-disulfide-bonded tridegin isomers, identified by Böhm *et al.*[12] in a self-folding approach. In the structures depicted the disulfide bonds are marked in yellow. Interestingly, all isomers share a common disulfide bond between Cys19 and Cys25 (marked in red).

However, compared to the naturally occurring tridegin, the mixture displayed a significant loss of activity.[12] One reason for this may be the fact that the IC_{50} values vary due to the use of different assays and thus cannot be properly compared. Alternative, it may be possible that the disulfide bond connectivity in the native variant is distinct or that exclusively one of the three formed isomers of the mixture is responsible for the inhibitory potential towards FXIIIa. Unfortunately, however, separation of the isomers by RP-HPLC has not been possible, and therefore structural and functional studies of the individual isomers could not be conducted.[12] Nevertheless, in parallel to the work performed within this thesis, Dr. Charlotte A. Bäuml selectively synthesized and characterized the 3-disulfide-bonded isomers A-C as part of her doctoral thesis. The results of this work and the relation to the work done in this thesis are shown in the publication[13] in section 4.3. In summary, the synthesis of the 3-disulfide-bonded tridegin isomers (Figure 11) is very complex, which is why no experimental structural analysis of the corresponding isomers by NMR or crystallography has been performed to date. Therefore, their structural analysis has so far been restricted to computer-based molecular modeling and simulation-derived structures.

2.4 Analysis of multiple disulfide-bonded peptides

Both the synthesis of cysteine-rich peptides and the appropriate analytical methods for their structural characterization and identification have been improved significantly over the last decades. Among these methods NMR spectroscopy and X-ray crystallography are used to elucidate the three-dimensional structures of the peptides, while mass spectrometry facilitates the determination of the primary sequence or the disulfide bond connectivity.[325–327] As evidence of the importance of these methods for the analysis of peptides, Kurt Wüthrich, John B. Fenn and Koichi Tanaka received the Nobel prize in chemistry in 2002 for the development of NMR- and MS-based techniques for the study of biological macromolecules.[326]

In this respect, there are several advantages and disadvantages for the different methods. X-ray crystallography, which provides a 3D structure of proteins or peptides, is encumbered by the fact that the optimal conditions first need to be determined upon preparation of the peptide crystals. This might be very time and material consuming, as the growth of the peptide crystals critically depends on various factors, such as the used buffer, the pH, and additives including salts and cryogenic protectants, and thus occurs only under optimal conditions.[325,328] An additional aspect is, that the acquired peptide structures are determined in solid phase and therefore might differ from the naturally occurring structure of the peptides in solution.[327]

Solution NMR spectroscopy is thus an advantageous alternative also enabling the elucidation of 3D peptide structures with the benefit of detecting structures in solution.[327] Indeed, NMR is the most commonly used method for the elucidation of peptide structures, with over 80% of the available peptide structures within the PDB obtained via NMR.[329] However, a disadvantage of this non-destructive method for disulfide-bonded peptides is that the final disulfide bond connectivity cannot always be unambiguously identified, potentially resulting in incorrect structures.[329] In addition, NMR spectroscopy, like X-ray crystallography, requires high amounts of starting material that cannot always be achieved, despite the improvements in peptide synthesis.[330]

Due to the difficulties during the synthesis of disulfide-bonded peptides, such as scrambling and the generation of non-desired isomers, the elucidation of the disulfide bond connectivity of these peptides and the differentiation of the individual isomers is of high importance.[331] In this context, the simplest and fastest way to identify the isomers is via a combination of HPLC

(via retention time) and MS (via molecular weight). Nevertheless, there is a possibility that isomers with different disulfide bond connectivities may coelute in HPLC due to similar physical properties, making it impossible to distinguish them in this regard.[6,12] For the assessment of the disulfide bond connectivity, the soft ionization methods ESI- and MALDI-MS are mainly used within mass spectrometry analyses of peptides (see section 2.5.2). Thereby, top-down proteonomics (tandem mass spectrometry (MS/MS) analysis of the entire peptide sequence) and bottom-up proteonomics (MS/MS analysis of previously digested peptide fragments), are applied for the sequencing of peptides.[332,333] At the same time, various methods are employed to reliably elucidate the disulfide bond connectivity of the peptides.[334,335] Unfortunately, these methods are usually very time-consuming and the analysis of the acquired MS data is complex. Accordingly, a certain expertise in data evaluation is needed to ensure the accuracy of results and to avoid misinterpretation of the data.[336–338]

2.4.1 Two-dimensional NMR spectroscopy

The NMR spectroscopic analysis of biomacromolecules has advanced tremendously since the first NMR structural elucidation from ribonuclease, owing to technical innovations such as superconducting magnets and progressive computational power for instrumental control.[326,339] Moreover nowadays, a wide variety of homonuclear and heteronuclear couplings can be registered via NMR, providing a wide variety of structural information, thus facilitating the structural elucidation of molecules such as peptides.[326,327,340] The focus of this section is the structure determination of peptides using 2D NMR spectroscopy, which will be discussed in more detail below.

The most relevant and commonly used experiments for peptide structure elucidation are correlation spectroscopy (COSY), total correlation spectroscopy (TOCSY), and nuclear Overhauser enhancement spectroscopy (NOESY).[327,340] COSY and TOCSY, revealing correlations exclusively within a spin center, are most commonly utilized to assign signals to a spin system, allowing a bundle of signals to be constrained to one amino acid based on characteristic cross peaks.[327,340] The NOESY experiment displays correlations across space (dipole-dipole coupling), i.e. interactions between two neighboring amino acids can be detected despite belonging to different spin systems. In addition, correlations can also be observed between amino acids that are far away from each other within the sequence but are spatially close due to the structure of the peptide.[327,340] By examining the NH-Hα regions within the TOCSY and NOESY spectra, the so-called 'sequential walk' can be performed. By assigning the NH and Hα signals, the signals within the spectra can be attributed exactly to the correct amino acids within the peptide sequence. The sequential walk is limited by the presence of prolines within the sequence, since the missing NH atom causes the walk across the backbone of the peptide chain to be aborted.[326,327] Accordingly, a new starting point for the sequential walk has to be identified for each proline, which renders the assignment of the signals more complex with increasing numbers of prolines. Besides the number of prolines, the length of the peptide chain also affects the complexity of the evaluation, since a higher number of amino acids results in more signals in the NMR spectrum. Thus, a higher number of signals increases the likelihood of overlapping signals in the spectrum, which can lead to incorrect assignments of the NMR signals. For proteins and long peptide chains, this superposition of signals is usually prevented by using 3D NMR spectra, which, as a result of the third dimension, simplify the assignment of signals compared to 2D NMR spectra of the same molecules.[326,327] For sufficient resolution of the three-dimensional NMR spectra, ^{13}C and ^{15}N labeled peptides and proteins are generally required, which could be an expensive procedure. Following signal assignment, distance constraints and dihedral angles between

residues are extracted from detected NOESY correlations, which are used in the structural calculation and define the resulting peptide structure.[326,327]

Overall, the evaluation of NMR spectra of peptides and proteins (whether 2D or 3D) is challenging and time-consuming, but provides a more detailed insight into the structural features which are important for the function of the peptide (insights into structure-activity relationships).[100]

2.4.2 Mass spectrometry

As described above, MS-based techniques are used to analyze the sequence and disulfide bond connectivity of peptides, mostly employing ESI- and MALDI-MS.[341–343] In addition to the chosen MS technique itself, sample preparation is also decisive.[334,336] In bottom-up sequencing, the peptide is cleaved into enzyme-specific fragments via enzymatic digestion and subsequently, these fragments are analyzed by MS/MS.[12] In this context, the disulfide bond connectivity can also be analyzed by digesting the peptide via proteases, like trypsin and chymotrypsin, in such a way that the cysteines responsible for the disulfide bonds are present in different fragments. Under non-reduced conditions, the MS-based analysis shows fragments that are connected to each other by a disulfide bond. These linked fragments can then be assigned to a position within the actual peptide sequence, thus confirming the presence of the disulfide bond in the peptide. Additional MS analysis of the disulfide-bonded fragments under reducing conditions is expected to show a loss of the corresponding mass compared to non-reducing conditions, thus confirming further the presence of the particular disulfide bond in the peptide.[12,334] However, if no suitable cleavage sites for proteases are available (i.e. cysteines cannot be separated), a top-down sequencing methodology can be applied to elucidate the disulfide bond connectivity. In this approach, the disulfide-bonded peptides are first partially reduced and the thiol functions of the cysteines, which are free due to occasionally opened disulfide bonds, are derivatized.[335] Subsequently, the peptide is completely reduced and sequenced by MS/MS, analyzing the cysteines regarding whether they had been derivatized or not. The presence of different partially reduced fractions with a wide variety of cysteine derivatization patterns allows to deduce the disulfide bond connectivity within the peptide.[331,335,344] Nevertheless, during sample preparation as well as upon the measurement itself, it is essential to ensure that conditions are set in such a way that disulfide scrambling, a phenomenon that can potentially bias results, does not occur.[331,345,346] Therefore, different independent methods are often performed for the analysis of the peptides to ensure reproducibility of the obtained results.[345,347]

Electrospray ionization (ESI) is a method based on the evaporation of solvent droplets with a high positive charge, allows the peptides contained in the droplets to be charged and detected after complete evaporation.[336,341] As a result of this soft ionization method, proteins and peptides tend to have a high charge and can be identified in different charge states[341], a fact that can partly impede the evaluation of the corresponding MS/MS spectra for sequence analysis. Sequencing of peptides via MS/MS methods, which would allow differentiation of isomers, is usually performed by ESI-MS via collision-induced dissociation (CID), during which peptide ions are fragmented and isolated in a collision cell by collision with inert gas particles such as N_2.[348] The differentiation of peptide isomers via the MS/MS methodologies may be very time- and material-consuming. An advantage of this technique is, however, that the MS can be directly equipped with an upstream liquid chromatography (LC). Thus, even impure samples can be analyzed in the MS via pre-separation by the LC.[39] In the case of disulfide-bonded peptide isomers as already shown for the μ-conotoxin PIIIA and the FXIIIa inhibitor tridegin, separation and differentiation via LC and MS alone is not always possible.[6,12] In this

regard, a more straightforward option is to incorporate a third separation dimension into the LC-ESI-MS system. One possibility is the use of ion mobility technologies, in which the ions of the individual isomers can be separated via different collision cross section (CCS) values defined by the size and the shape of the molecules.[345] During this separation method, the molecules to be separated interact with an inert gas. The molecules having a larger CCS value collide more frequently with the gas particles, causing them to accelerate or decelerate, depending on the measurement principle. For disulfide-rich peptides, the discrimination of isomers via ion mobility-MS has already been described in a few studies, and consequently separation problems as described above can be solved by combining ion mobility with LC-MS.[349,350] A further development of ion mobility-MS is trapped ion mobility spectrometry-mass spectrometry (TIMS-MS), which provides increased resolution and better baseline separation of ions.[351,352]

In comparison to ESI-MS, for matrix-assisted laser desorption ionization (MALDI)-MS the peptide is first co-crystallized with a specific matrix.[346] Ionization is then performed using a laser power suitable for the matrix. The matrix is thereby vaporized together with the peptide, and, as a result, the peptide is ionized and can subsequently be detected.[346] On the one hand, this is a softer ionization method than ESI-MS, which results in less complex MALDI spectra, since mostly single- or double-charged peptide ions are generated.[344,346] On the other hand, MALDI-MS can be used to detect molecules with higher molecular weights.[346] In addition to the advantages due to the ionization methodology, the whole setup is more robust against contamination.[8,343] Regarding peptide sequencing by MS/MS, there are mainly two different techniques for MALDI-MS. Firstly, in-source decay (ISD) and secondly, post-source decay (PSD), the latter allowing preselection of the desired parent ion (peptide ion) and its selective fragmentation.[353,354]

3 Thesis outline

The aim of the present thesis is to investigate the potential usage of disulfide-deficient tridegin analogs to reduce the synthesis complexity of the 66mer peptide without significant loss of activity against FXIIIa, thereby improving the lead structure for the development of new specific FXIIIa inhibitors. Additionally, the unambiguous separation and identification of disulfide-bonded isomers should be investigated by LC-TIMS-MS using the 2- and 3-disufide-bonded μ-conotoxin PIIIA analogs.

Regarding the tridegin project, previous studies in the group of Prof. Dr. Diana Imhof revealed that a shortening of the amino acid sequence as well as the complete removal of all three disulfide bonds within the tridegin sequence caused a negative effect on the inhibitory potential towards FXIIIa.[12,324] Since the selective synthesis of three 3-disulfide-bonded tridegin analogs, performed as part of the dissertation of Dr. Charlotte A. Bäuml, proved to be acutely laborious and resulted in only low yields, the question arose on whether removing a single disulfide bond to yield 2-disulfide-bonded tridegin variants might be a possibility to structurally simplify tridegin without major loss of activity. Furthermore, all three tridegin isomers from the self-folding experiment published in 2014[12] interestingly featured a disulfide bond between Cys19 and Cys25, which thus should be investigated for its influence with respect to the inhibitory potential of tridegin towards FXIIIa. In this context, the corresponding 2-disulfide-bonded tridegin variants without the Cys19-Cys25 disulfide bond should be selectively synthesized via an Fmoc-based protecting group strategy. In addition, a self-folding experiment with the 2-disulfide-bonded tridegin variant should also be conducted. Subsequently, activity assays should provide information on how the arrangement of the remaining two disulfide bonds affects the activity toward FXIIIa and whether a loss of inhibitory potential arises compared to the 3-disulfide-bonded tridegin analogs. Positive results from these studies should pave the way to derive a new lead structure from the three disulfide-deficient tridegin variants. Finally, NMR-based structural elucidation of these variants should fill the missing pieces to the puzzle of the structure-activity relationship of these variants.

In addition, former studies in the group of Prof. Dr. Diana Imhof performed by Dr. Miriam Reuleaux (previously Böhm) and Dr. Pascal Heimer showed that disulfide-bonded isomers with the same number of disulfide bonds but different connectivities are in certain cases difficult to distinguish by conventional HPLC and MS methods alone.[6,12] The differentiation of the disulfide-bonded isomers always had to be analyzed with a combination of complex methods, such as MS/MS analysis of an enzymatic digest or a partial reduction, which is very time-consuming and requires a large amount of starting material. In order to improve differentiation of these peptides in routine RP-HPLC and MS analyses, the use of trapped-ion-mobility spectrometry (TIMS) as a supportive tool should be investigated. In this context, the distinguishability of different 2- and 3-disulfide-bonded variants of the μ-conotoxin PIIIA should be analyzed via LC-TIMS-MS. The μ-conotoxin PIIIA variants were selected for the applicability of this method, since various disulfide-bonded μ-PIIIa isomers were already available in the research group of Prof. Dr. Diana Imhof.

In summary, the present work serves as vital foundations for lead structure optimization of tridegin, a selective FXIIIa inhibitor, and may positively influence the development of new anticoagulants in the future. Furthermore, the applicability of LC-TIMS-MS for the differentiation of disulfide-bonded isomers should be evaluated, thus contributing to the analytical characterization of disulfide-bonded peptides.

This thesis is divided into 5 parts, with the first 4 chapters referring to the studies on tridegin and the last chapter representing the results of the LC-TIMS-MS investigations using μ-conotoxin PIIIA derivatives, based on the 5 publications included in this work. The publications are incorporated as such with the exception of the publication described in chapter II, which was transcribed, as it was featured in the dissertation of Dr. Ajay Abisheck Paul George, who performed the computer-based studies for this publication.

Chapter I (section 4.1) provides information on FXIII inhibitors already known from the literature. This review presents functionalities as well as advantages and disadvantages of the different FXIII inhibitors available so far. This compilation also includes tridegin, which was examined in detail in this work.

Chapter II (section 4.2) presents a manuscript that describes the synthesis and the analytical as well as the functional characterization of the three 2-disulfide-bonded tridegin analogs, which are deficient in the disulfide bond between Cys19 and Cys25. The inhibitory potential towards FXIIIa was investigated within an *in vitro* FXIIIa assay and in human whole blood samples using a whole blood contraction assay.

Chapter III (section 4.3) addresses the synthesis and characterization of the 3-disulfide-bonded tridegin analogs prepared by Dr. Charlotte A. Bäuml (Dissertation, University of Bonn, February 2020). These compounds were compared with the 2-disulfide-bonded variants, prepared in the present work, in particular concerning their functional characterization towards FXIIIa. In addition, the FXIIIa specificity of two different tridegin variants, namely Isomer B and the mixture of the 2-disulfide-bonded analogs from the self-folding experiment, Isomer $ABC_{[C19S,C25S]}$ (prepared in the present work) towards TGase 2 was investigated.

Chapter IV (section 4.4) covers the NMR-based structure elucidation of two fragments of the 2-disulfide-bonded tridegin variant $B_{[C19S,C25S]}$ (Cys05-Cys37, Cys17-Cys31). Both structures were then combined to yield the first structure-based model of the 66mer tridegin analog determined from experimentally obtained data, further refined by molecular simulations. This structure was used in computer-based docking studies with FXIIIa, thereby providing novel insight into the structure-activity relationships of this specific tridegin analog.

Chapter V (section 4.5) presents the results of the LC-TIMS-MS measurements of different 2- and 3-disulfide-bonded variants of the μ-conotoxin PIIIA. The aim was to investigate whether all disulfide-bonded variants can be distinguished using this system. Additionally, the goal was to examine if the determined CCS values of the individual molecules are in agreement with the structural findings of the μ-PIIIA variants obtained from NMR and computer-based studies.[6,54]

4 Manuscripts

4.1 Chapter I - Inhibitors of blood coagulation factor XIII (Review)

Authors*

Thomas Schmitz*, Charlotte A. Bäuml*, and Diana Imhof

This article was published in:
Analytical Biochemistry **2020**, 605, 113708.
DOI: 10.1016/j.ab.2020.113708

4.1.1 Introduction

FXIII is a blood coagulation factor that catalyzes the final step of the blood coagulation cascade, the cross-linking of fibrin clots. These covalent cross-links are generated via isopeptide bonds and play a crucial role in stabilizing the blood clot and protecting it from premature fibrinolysis.[122,131,192,219] Accordingly, FXIII serves as an interesting target for the therapeutic treatment of the most common fatal diseases in humans, namely cardiovascular diseases. While direct and indirect thrombin inhibitors are employed for the protection against unwanted blood clots (thrombosis), there are still no FXIII inhibitors applied in medical applications.[44,118,355–357] However, various preclinical FXIII inhibitors contributed to the current knowledge of FXIII and could serve as lead structures for future drug design.[17,316,320] The review presented in the following chapter discusses all available FXIII inhibitors in detail. Special attention is given on their mode of action, their ability to inhibit the transglutaminase activity and consequently the fibrin cross-linking. Advantages and disadvantages of these inhibitors are analyzed and placed in the context of future FXIII inhibitor drug development. A major focus of chapter I is tridegin, the only naturally occurring peptidic inhibitor of FXIII. The history of tridegin research from its discovery by Finney *et al*.[11] to the development of the 2-disulfide-bonded tridegin analogs is presented.

***Contributions:**

TS and CAB contributed equally. TS and CAB collected the literature. The manuscript draft was written by TS and proofread by DI and CAB. All authors contributed to the final manuscript and have given approval to the final version.

4.1.2 Article

On the following pages, the article is printed in its published form with permission of Elsevier Inc., Amsterdam, Netherlands.

Analytical Biochemistry 605 (2020) 113708

Contents lists available at ScienceDirect

Analytical Biochemistry

journal homepage: www.elsevier.com/locate/yabio

Inhibitors of blood coagulation factor XIII

Thomas Schmitz[1], Charlotte A. Bäuml[1], Diana Imhof*

Pharmaceutical Biochemistry and Bioanalytics, Pharmaceutical Institute, University of Bonn, An der Immenburg 4, D-53121, Bonn, Germany

ARTICLE INFO

Keywords:
FXIIIa
Transglutaminase
FXIIIa inhibitor
Tridegin
Blood coagulation cascade

ABSTRACT

The blood coagulation factor XIII (FXIII) plays an essential role in the stabilization of fibrin clots. This factor, belonging to the class of transglutaminases, catalyzes the final step of secondary hemostasis, i.e. the crosslinking of fibrin polymers. These crosslinks protect the clots against premature fibrinolysis. Consequently, FXIII is an interesting target for the therapeutic treatment of cardiovascular diseases. In this context, inhibitors can influence FXIII in the activation process of the enzyme itself or in its catalytic activity. To date, there is no FXIII inhibitor in medical application, but several studies have been conducted in the past. These studies provided a better understanding of FXIII and identified new lead structures for FXIII inhibitors. Next to small molecule inhibitors, the most promising candidates for the development of clinically applicable FXIII inhibitors are the peptide inhibitors tridegin and transglutaminase-inhibiting Michael acceptors (TIMAs) due to their selectivity towards activated FXIII (FXIIIa). In this review, select FXIII inhibitors and their pharmacological potential are discussed.

1. Introduction

Cardiovascular diseases are the world's leading mortality cause with 17.9 million (31% of total number) deaths in 2016 according to the World Health Organization (WHO) [1]. The origin of these diseases is the formation of undesired blood clots, i.e. thrombosis. Thrombosis is normally caused by a combination of dysregulated hemostasis, changes in vascular function and changes in blood flow velocity – the so-called Virchow triad [2,3]. Hemostasis is divided into primary and secondary hemostasis. Primary hemostasis leads to the formation of the “white thrombus” via platelet aggregation. During secondary hemostasis, an activation cascade of several enzymatic and non-enzymatic factors leads to the formation of insoluble fibrin clots which become attached to the thrombus in a net-like manner and stabilize the coagulate [4]. Many of these factors belong to the class of serine proteases, which are initially present as inactive proenzymes [4–6]. When vascular injury or an unregulated hemostasis occurs, the individual factors are successively converted into their active form by proteolytic cleavage [7]. A key enzyme of blood coagulation is the active form of prothrombin, i.e. thrombin, which activates coagulation factors V [8], VI [9], XI [10], and XIII [11,12] and initiates the formation of fibrin polymers [13,14]. Therein, thrombin converts fibrinogen to fibrin which then polymerizes and reticulates the white thrombus [6,15,16]. This leads to the formation of a first hemostatic fibrin clot that is subsequently stabilized and crosslinked by FXIIIa in the final step of the secondary hemostasis [13,16–18]. Due to the central role of thrombin and its great importance regarding the formation of stable blood clots, leeches have developed potent thrombin inhibitors to prevent blood coagulation during a blood meal. A well-known example is the anticoagulant hirudin, a 65mer peptide with three disulfide bridges, derived from the European medical leech *Hirudo medicinalis* [19,20]. Based on hirudin, highly specific thrombin inhibitors such as bivalirudin and argatroban were developed and used as anticoagulants in cardiovascular and thromboembolic diseases. Both compounds belong to the class of reversible direct thrombin inhibitors which are given as an intravenous infusion [19,21–24]. A drawback of these direct thrombin inhibitors is that they may increase the risk of bleeding, which excludes many patients from these treatments [25,26]. A unique way to influence the blood clot formation without causing thrombin inactivation is to intervene with the enzymatic reaction of the transglutaminase factor XIII [27–32]. FXIII exists in two distinct forms in the human body: the plasmatic and the cellular FXIII. Both types are subjected to an activation process that converts the enzyme into the active form of FXIIIa exposing the catalytic triad (Cys314, His373, Asp396) within the active site [33–36]. The cellular FXIII consists of two FXIII-A subunits in the inactive form and is activated mostly nonproteolytically by Ca^{2+} ions [33,37,38]. In contrast, the inactive plasmatic FXIII heterotetramer (FXIII-A_2B_2) is additionally stabilized by two FXIII-B units [33]. These

* Corresponding author.
E-mail address: dimhof@uni-bonn.de (D. Imhof).
[1] Equal contribution.

https://doi.org/10.1016/j.ab.2020.113708
Received 20 January 2020; Received in revised form 11 March 2020; Accepted 30 March 2020
Available online 23 April 2020

two FXIII-B subunits protect the plasmatic FXIII from proteolytic degradation by plasmatic proteases and spontaneous activation of the factor by Ca^{2+} ions [39–41]. During activation, the FXIII-B subunits dissociate from the tetrameric complex resulting in two active FXIII-A monomers, in which the catalytic triad is exposed. In comparison to cellular FXIII, plasmatic FXIII is - due to the higher participation in fibrin stabilization - a better target for pharmacological research concerning secondary hemostasis [2,33–36,39,40]. This review summarizes the fundamental developments concerning FXIII inhibitors, highlighting recent advances towards the understanding of the structure-activity relationships of the leech-derived peptide inhibitor tridegin.

2. Plasmatic FXIII

In the inactive state of the plasmatic FXIII, the catalytic triad comprised of Cys314, His373, and Asp396 of each of the FXIII-A subunits is blocked by the N-terminal region of the other FXIII-A subunit (aa 1-37), the so-called activation peptide, and additional intramolecular interactions within the FXIII-A subunit [34,42–44]. The activation of the heterotetramer FXIII-A_2B_2 is physiologically mediated by a proteolytic cleavage catalyzed by thrombin and Ca^{2+} ions (Fig. 1A). At first, thrombin cleaves FXIII between Arg37 and Gly38 to remove the activation peptide from each of the two FXIII-A subunits [33,45]. The following binding of Ca^{2+} cations to distinct calcium binding sites results in the dissociation of the FXIII-B_2 molecule from the FXIII-A subunits and conformational changes of the individual FXIII-A subunits revealing the active center to substrates such as fibrin [35,36]. Then, the active enzyme FXIIIa can catalyze the crosslinking of fibrin molecules (Fig. 1B).

FXIIIa belongs to the enzyme class of transglutaminases which catalyze the formation of an isopeptide bond between the carbonyl function of a glutamine side chain (γ-$CONH_2$) and a lysine side chain amino group (ε-NH_2) [46]. Fig. 1C shows the catalytic reaction carried out by FXIIIa involving the aforementioned residues Cys314, His373, and Asp396 of its active site [42]. In addition, a catalytic diad comprised of a further histidine (His342) and a glutamic acid (Glu401) is important for the enzymatic function [47]. The reaction is initiated by the insertion of a glutamine side chain of fibrin into the active center and the nucleophilic attack of the cysteine thiol group to the carbonyl carbon atom of this glutamine side chain. The resulting tetrahedral intermediate is stabilized via hydrogen bonds to the cysteine backbone and to the indole function of a tryptophan side chain. The following cleavage of ammonia results in the thioester bond between FXIIIa and the glutamine residue. The subsequent insertion and activation of the amino function of a lysine side chain, e.g. of fibrin, for the nucleophilic attack on the carbon atom of the thioester function takes place via the catalytic triad and the catalytic diad. Thereby, the catalytic diad abstracts a proton of the protonated amine function (loss of its charge) to enable the lysine side chain to enter the hydrophobic tunnel of FXIIIa. The resulting tetrahedral transition state is stabilized again by hydrogen bonds. Afterwards, the acyl group of the thioester is transferred to the amino function of the lysine generating the isopeptide bond between the glutamine and the lysine side chain in the substrate. At the same time, the thiol function of Cys314 is reduced and available for the next catalytic cycle [46–48]. The FXIIIa-catalyzed fibrin crosslinking during clot formation leads to biomechanically and biophysically stabilized fibrin polymers rendering them less susceptible to dissolution

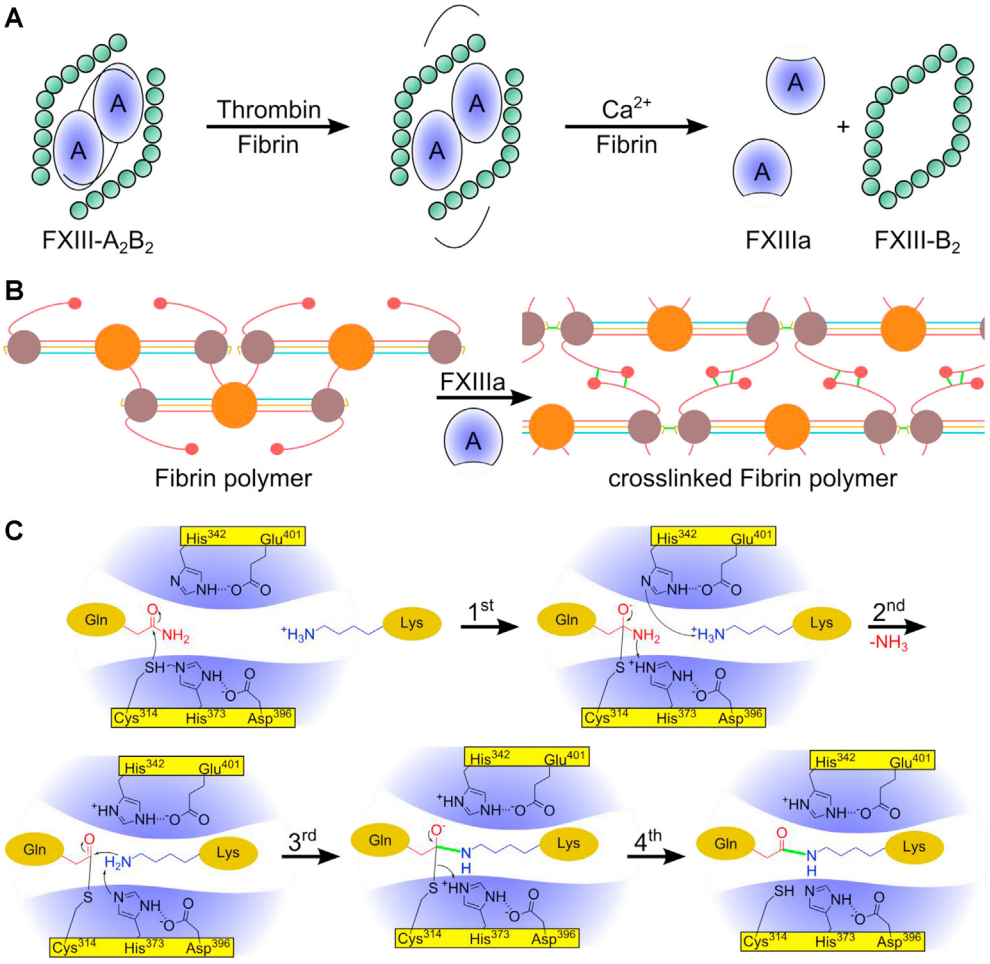

Fig. 1. FXIII activation (A) and the mechanism of fibrin crosslinking mediated by FXIIIa (B). **A**: Activation via thrombin (step 1: Proteolytical cleavage of the activation peptides) and Ca^{2+} ions (step 2: Separation of FXIII-B_2 and conformational changes within monomer FXIIIa). **B**: Isopeptide bond formation (bonds are depicted as green bars) between glutamine (Gln) and lysine (Lys) side chains in a fibrin polymer catalyzed by FXIIIa. **C**: Mechanism of the isopeptide bond formation within the active site of FXIIIa. 1st step: Nucleophilic attack of Cys314 to Gln (red); 2nd step: Formation of the thioester bond by release of ammonia and deprotonation of the lysine side chain (blue) by the catalytic diad of FXIIIa; 3rd step: Nucleophilic attack of the lysine side chain on the thioester carbonyl function; 4th step: Formation of the isopeptide bond resulting in the crosslinked fibrin polymer and regeneration of the catalytic triad; Cys314, His373, Asp396 correspond to the catalytic triad of FXIIIa. His342 and Glu401 form the catalytic diad of FXIIIa.

[13,17,18,30–32,49,50]. In addition to the crosslinking, FXIIIa also covalently links the fibrin molecules to extracellular proteins and structural proteins of the platelet membrane and incorporates e.g. α2-antiplasmin into the clot [13,51–55]. The latter also protects against early fibrinolysis by plasmin. Given the importance of FXIIIa for the composition and stability of the blood clot, FXIII is considered as an interesting therapeutic target [2,56–58]. In this regard, specific inhibition of the FXIIIa reaction influences only the last step within the blood coagulation cascade by maintaining the biological activity of the other blood coagulation factors.

3. Inhibitors of FXIII/a

The commonly-used anticoagulants, which limit the function of vitamin K-dependent proteins or directly inhibit factors within the secondary hemostasis, have been shown to reduce the frequency of venous thrombi, but are also associated with an increased risk of bleeding [26,59]. From this perspective, a pharmacological inhibition of the fibrin crosslinking, which has no effect on thrombin generation, could prove beneficial. Specific FXIIIa inhibitors come into account that may have an effect on clot size and stability in plasma [60,61]. Various compounds or substance classes with an inhibitory potential against FXIII have contributed significantly to the state of knowledge on FXIII due to their individual inhibitory properties. In the following chapter, the described inhibitors are divided into three different classes: 1) inhibitors, which influence the activation mechanism of FXIII; 2) substances, which serve as cosubstrates and thus prevent crosslinking within the clot; and 3) molecules that block the accessibility of the active site.

3.1. Indirect inhibition of FXIIIa by inhibition of FXIII activation

As aforementioned, FXIII is converted to the catalytically active FXIIIa by thrombin and Ca^{2+} ions [11,12]. Inhibition of this activation process leads to a reduction or absence of FXIIIa in the plasma and thereby prevents crosslinking of fibrin molecules. In this context, an inhibition of Ca^{2+} binding to the respective binding sites prevents dissociation of the FXIII-A and FXIII-B subunits and thereby impedes the conformational changes of the FXIII-A subunit required for FXIIIa activity [37,38]. Consequently, the catalytic triad within the active site is not accessible for substrates such as fibrin. In 1973, Lóránd et al. demonstrated that FXIII activation is impaired *in vitro* by addition of the Ca^{2+} chelating agent EDTA (ethylenediaminetetraacetic acid) [62]. It seems plausible that complexing agents such as EDTA cannot be employed *in vivo* as Ca^{2+} ions are involved in a plethora of essential signaling cascades.

Another approach to diminish FXIII activation is via the inhibition of thrombin or the prevention of the thrombin-catalyzed proteolytic cleavage of the activation peptide (amino acids 1-37) [45]. Since thrombin inhibition also affects other factors within the blood coagulation cascade, blocking the release of the activation peptide is the only specific way to prevent FXIII activation [23]. Antibodies bind to their respective targets with high affinity via multiple protein-protein interactions and can thus influence the activity of their target. Consequently, several antibodies have been developed as potential FXIII inhibitors [63,64]. For example, FXIII activation can be disrupted by binding of the monoclonal antibody MAb309 to a peptide sequence near the activation peptide cleavage site [63]. MAb309 was obtained from an experiment, in which mice were immunized with a peptide comprising the amino acid sequence G^{38}VNLQEF^{44} of the FXIII-A subunits. In a solid-phase radioimmunoassay and in immunoblotting using whole human platelets, the antibody MAb309 displayed substantial binding affinity to the FXIII-A subunit [63]. The inhibition is exclusively mediated via the blockade of thrombin-induced FXIII activation, which was verified by comparing the FXIII activation with and without MAb309 preincubation using SDS-PAGE analysis. The analysis of the MAb309 preincubated samples revealed only the inactive FXIII-A subunit at different activation times, whereas the control group indicated the cleavage of the activation peptide by thrombin. As expected, inhibition of FXIII activation by MAb309 also had an effect on FXIIIa-catalyzed reactions since the activated factor is composed of the FXIII-A subunit. For instance, the FXIIIa-mediated incorporation of putrescine into casein in the presence of MAb309 could be reduced by 99% [63]. Besides MAb309, the antibodies MAb9C11 and MAb10G10 are also found to be inhibitors of thrombin-mediated FXIII activation [64,65]. These antibodies were generated by immunizing mice directly with the FXIIIA dimer. Compared to MAb309, the more recently developed antibodies showed a higher inhibitory potential towards the thrombin-induced FXIII activation. Notably, the antibodies showed binding to different sites of the FXIII-A subunit, which suggests that either the thrombin binding site was blocked or a conformational change due to the attachment of MAb9C11 or MAb10G10 leads to the inhibition of FXIII activation [64,65]. Unfortunately, an excess of thrombin causes a displacement of the antibodies which limits their usage for pharmacological research [65].

Another approach towards the use of antibodies to interfere with FXIIIa activity is to employ the monoclonal antibody (5A2) introduced by Mitkevich et al. in 1996 [66]. Application of this antibody led to an inhibition of FXIIIa, which was more precisely suggested to be based on an uncompetitive inhibition in the case of the glutamine substrate and a competitive interaction in the case of the lysine amine [67]. Additionally, a comparison of the different inhibition modes gave the first indication as to which order the substrates are interacting within the active site of FXIIIa and showed that glutamine binding leads to a conformational change of FXIIIa, enabling amine substrates to enter the active site [67].

3.2. Inhibition of FXIIIa by competitive substrates

The prevention of fibrin crosslinking via competitive inhibition is another possibility to address FXIII activity. Competitive “inhibitors” act more precisely as alternative substrates for the FXIIIa-catalyzed reaction, thus inhibiting the crosslinking of fibrin and the covalent bond formation between fibrin and other proteins such as α2-antiplasmin.

In this context, specific amines play a decisive role in the aminolytic deacylation [68]. Within the active site, these amines compete with the ε-amino function of the lysine side chains. Thereby, they prevent the isopeptide bond formation within the fibrin clusters due to a nucleophilic attack on the acyl carbonyl function of the enzyme-substrate complex (Fig. 2A). As a result, these inhibitors form a carboxamide bond with the glutamine side chains of fibrin. This leads to the formation of less stable fibrin structures since the crosslinking of the fibrin polymers is interrupted. The resulting clot is therefore more susceptible to degradation [68].

Examples of such amine-containing FXIII inhibitors are 5-dansylamidopentamine (**1**) and glycine ethyl ester (**2**) (Fig. 2B) [68]. Regarding the amine incorporation into fibrin, the apparent K_M of 5-dansylamidopentamine (1; $K_{M,app}$ = 1.6*10^{-4} M) revealed a 20-fold stronger binding to fibrin than the glycine ethyl ester (2; $K_{M,app}$ = 3*10^{-3} M) in the same study [68]. It was suggested that the increased activity of the 5-dansylamidopentamine (**1**) is due to the apolar substituent. The analysis of modified analogues revealed that penta- or hexamethylene derivatives are beneficial for optimal inhibition. However, these competitive substrates do not only interact with FXIIIa but also “inhibit” other transglutaminases, such as TGase 2 [68]. Compounds that also serve as co-substrates for other transglutaminase reactions cannot be specific for FXIIIa. Consequently, selective interaction with FXIIIa to weaken or completely inhibit the catalytic function of this enzyme is required for a specific inhibition.

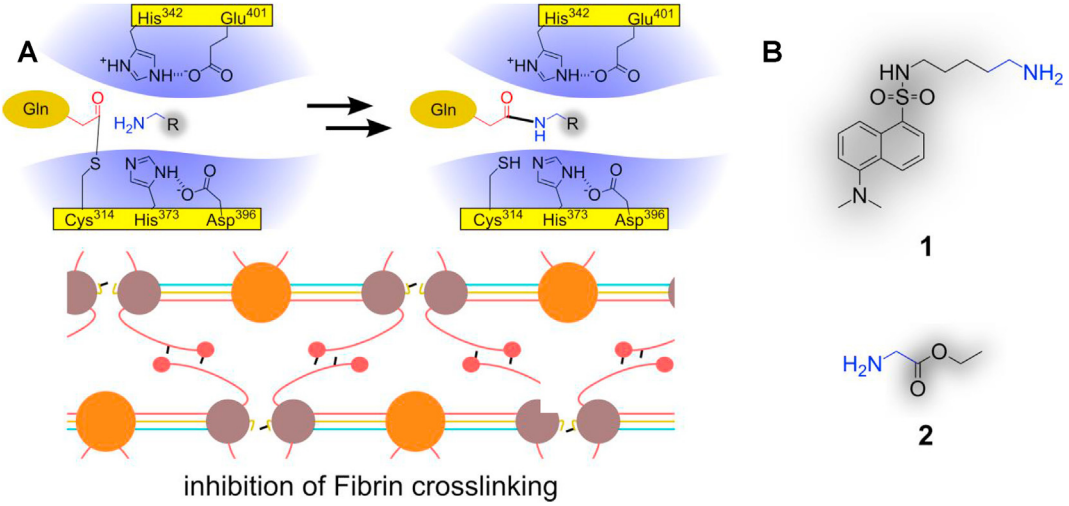

Fig. 2. Amine derivatives as competitive substrates for FXIIIa-mediated crosslinking of fibrin. **A**: Mechanism of amine derivatives binding to the glutamine side chains (carboxamide bonds are depicted as black bars) of the fibrin polymers resulting in inhibition of fibrin crosslinking; **B**: Two Examples of amine-based competitive substrates; **1** - 5-dansylcadaverine; **2** - glycine ethyl ester.

3.3. Direct inhibitors of FXIIIa activity

The inhibition of enzymes such as FXIIIa can be achieved by direct interaction of the inhibitor with the active site or via allosteric binding sites [69–78]. In the case of FXIIIa, the catalytic triad can be reversibly or irreversibly blocked, which limits the accessibility of the active site for substrates. A frequently addressed target of FXIIIa inhibitors is the catalytically active Cys314 which binds the acyl group of the glutamine side chain via a nucleophilic attack and is regenerated after subsequent reamidation of the acyl group (fibrin crosslinking with a lysine side chain) [46–48]. Structurally simplified examples for this strategy of FXIIIa inhibition are halomethylcarbonyl derivatives such as iodoacetamide [79], which serve as an alkylating agent for cysteines, e.g. in mass spectrometry, as well as nitric oxide donors [79]. Mechanistically, both compounds bind irreversibly to the catalytically active Cys314 and thus inactivate the function of FXIIIa. Iodoacetamide treatment results in carbamidomethylation of the cysteine thiol group, whereas nitric oxide donors are able to *S*-nitrosylate this residue [79,80]. However, the corresponding molecules cannot be used in therapeutic applications, as many other freely accessible cysteines would be modified as well. Thereby, the function of a considerable number of other important enzymes would be influenced. In addition, the activity of these non-specific alkylating agents can be decreased by the presence of high levels of thiols like glutathione (GSH) and dithiothreitol (DTT). For the development of specific FXIIIa inhibitors, a reduction of the intrinsic reactivity compared to nonspecific alkylation reagents is required. At the same time, it is important to increase the reactivity and specificity towards FXIIIa by favored orientation within the active site.

3.3.1. Small molecule inhibitors

Concerning the design of small molecules for active-site directed irreversible FXIIIa inhibition, the focus in research has been on three different substance classes: 1) 2-[(2-oxopropyl)thio]imidazolium derivatives, 2) cerulenin-derived compounds, and 3) alutacenoic acids A and B. In addition, section 3.3.1.4 also discusses the non-saccharide glucosaminoglycan mimetic 13 (NSGM 13), which - unlike the three classes of active site directed irreversible FXIIIa inhibitors - acts as an allosteric inhibitor.

3.3.1.1. 2-[(2-Oxopropyl)thio]imidazolium derivatives. Thioimidazolium derivatives, which were first described by Freund et al. in 1988 [69], are FXIIIa inhibitors that alkylate the active site thiol group of FXIIIa (Fig. 3A).

The inhibition occurs via acetonylation of Cys314 and simultaneous release of the corresponding thione (Fig. 3A). Thereby, the active site thiol group is activated and nucleophilically attacks the carbonyl carbon of the thioimidazolium, which results in a thiohemiketal. The subsequent stabilization of the 'oxyanion hole' and the thiol shift to the α-carbon atom lead to the release of the corresponding thione derivative and the generation of the acetonylated cysteine. The inhibitory potential of the thioimidazolium derivatives (Fig. 3B, **3**-**6**) against FXIIIa was specifically analyzed by the incorporation of ^{125}I-α2-antiplasmin into the fibrin chains. In this experiment, molecule **4** at 7 μM caused only 15% of the normal α2-antiplasmin incorporation, whereas 30 μM of the least potent inhibitor **5** resulted in only 20% of the total number of attachments. The different potencies of the thioimidazolium derivatives are affected by the substitution of the 2-thioimidazole moiety, forming a leaving group during inactivation. In a comparative experiment with iodoacetamide, it was also shown that thioimidazolium derivatives alkylate GSH to a lesser extent and are thus more selective for FXIII inhibition than iodoacetamide [70]. Moreover, certain interactions within the active site of FXIIIa, such as the stabilization of the tetrahedral transition state, lead to an enhanced reaction. In addition to its weak reactivity to GSH, the potent FXIIIa inhibitor **3** displayed a relatively low potency towards serine proteases of the blood coagulation cascade and other cysteine-containing enzymes such as papain, calpain, fatty acid synthetase, HMG-CoA (3-hydroxy-3-methylglutaryl-coenzyme A) synthetase and HMG-CoA reductase. The thioimidazolium derivatives possess a high selectivity towards FXIIIa within the secondary hemostasis and thus the impact of these inhibitors on blood coagulation can only be connected to the interaction with FXIIIa [70,71]. The inhibitors of this class, however, do not distinguish between the different transglutaminases [72] and have a plasma half-life of 5–10 min [73], which is why a therapeutic application has not been considered.

3.3.1.2. Cerulenin. The second class of small-molecule FXIIIa inhibitors was explored and further developed on the basis of the natural compound cerulenin. Cerulenin, an antifungal and antimicrobial substance, was the only potent FXIIIa inhibitor identified in the study of Tymiak et al. in 1993 [74]. Therein, 500 solid and liquid fermentation extracts in addition to various synthesized substances were screened for FXIIIa inhibition. The screening method for the identification of such inhibitors was based on clot stability tests in urea. Blood clots were formed in the presence of different potential FXIIIa inhibitors and their urea solubility was subsequently analyzed via

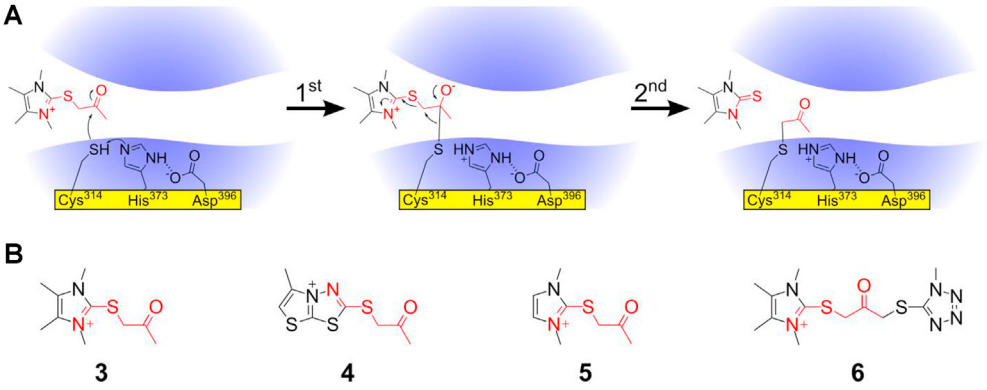

Fig. 3. FXIIIa inhibition mechanism (A) and different derivatives (B) of the thioimidazolium substance class. A: Postulated mechanism of the irreversible Cys314 acetonylation. 1st step: Nucleophilic attack of the Cys314 on the carbonyl function; 2nd step: Release of the thione leads to acetonylation of Cys314; **B**: **3**-**6** - different thioimidazolium derivatives with an inhibitory potential against FXIIIa.

turbidity of the corresponding urea solution. The presence of FXIIIa inhibitors such as cerulenin during the blood clot formation resulted in less crosslinked fibrin clots. In contrast to the regularly crosslinked clots, the less crosslinked ones are urea soluble leading to a weaker turbiditiy of the reaction mixtures. Mechanistically, cerulenin irreversibly inhibits FXIIIa by formation of a covalent bond with the active site Cys314 (Fig. 4A). The epoxide function in cerulenin (Fig. 4B, **7**) serves as an electrophilic center. This epoxide ring is opened by the nucleophilic attack of the thiol group of Cys314 (Fig. 4A), which results in a covalent binding to the enzyme [74].

In silico studies with a FXIIIa model developed from the FXIII crystal structure (PDB ID: 1GGT) [42] allowed more precise conclusions regarding the underlying inhibition mechanism [75]. Within this model, the epoxide oxygen points toward the NH function of the Cys314 backbone in the active center of FXIIIa. In addition, the α-carbon atom of the amide points toward the thiol group of the Cys314. The nucleophilic attack of **7** thus takes place on the epoxy carbon atom adjacent to the amide (Fig. 4A) [75]. In the transition state, the resulting oxyanion is stabilized by hydrogen bonding with NH functions of the backbone. Due to the moderate FXIIIa inhibition of cerulenin (**7**, IC_{50} value of 4 μM) the *in silico* study was additionally used to show further possible interaction sites for improved cerulenin-based FXIIIa inhibitors. Based on the newly acquired knowledge, improved FXIIIa inhibitors (**8**, **9**) were synthesized [75]. As shown in Fig. 4B, the 3-keto function of cerulenin (**7**) was replaced by an amide bond and the aliphatic function by an aromatic system resulting in compounds **8** and **9**. This led to an improvement of the IC_{50} value from 4 μM to about 4 nM for the derivatives (**8**, **9**). It was assumed that a hydrogen bond between the amide function and the backbone carbonyl group of Tyr372 as well as π-stacking interactions between the aromatic system and the side chain of Tyr372 are responsible for the increased inhibitory potential of inhibitors **8** and **9** [75]. Furthermore, analysis of other derivatives revealed that the absolute stereochemistry of the cerulenin analogues as well as the primary amide at the epoxide are very important for the inhibitory activity towards FXIIIa [75]. A further improvement of these analogues (**8**, **9**) compared to cerulenin (**7**) is that the activity of these molecules towards FXIIIa does not decrease in the presence of simple thiols such as reduced glutathione (GSH) [74,75]. As also described for thioimidazolium derivatives, the inhibitory potential of the molecules against TGase 2 is comparable to FXIIIa [75], making them suitable for research purposes but not for clinical applications.

3.3.1.3. Alutacenoic acids A and B. A further class of irreversible small molecule inhibitors is derived from the natural compounds alutacenoic acid A and B derived from the fungi *Eupenicillium alutaceum* [76]. These compounds contain a cyclopropenone ring which is the target for the nucleophilic attack of the FXIIIa Cys314. The ligand binding to the enzyme takes place via a Michael addition of the Cys314 thiolate to the unsubstituted carbon atom of the cyclopropenone ring (Fig. 5A). Based on docking experiments it is hypothesized that the transition state as well as the cyclopropanone product are stabilized by a hydrogen bond between the carbonyl oxygen of the ligand and the indole NH function of Trp279 [77].

Due to the fact that the structure of the cyclopropene ring resembles an epoxide, it was assumed that exchanging the cyclopropene ring with a cerulenin-derived epoxide could lead to a minor reduction of activity. However, the exchange resulted in a considerable loss of the inhibitory potential towards FXIIIa, which showed that the ring system is very important for inhibition. The natural compounds exhibited a FXIIIa inhibition with IC_{50} values of 1.9 μM for alutacenoic acid A (Fig. 5B, **10**) and 0.61 μM for B (**11**) in the assay used [77]. The extension of the cyclopropenone substituent to undecylic acid (**12**, IC_{50} = 0.31 μM) or an exchange of the acid function of alutacenoic acid B (**11**) with phenethyl amide (**13**, IC_{50} = 0.026 μM) led to an improved inhibitory potency towards FXIIIa [77]. Cyclopropenones with two substituents are unfavorable inhibitors because the ligand is incorrectly positioned

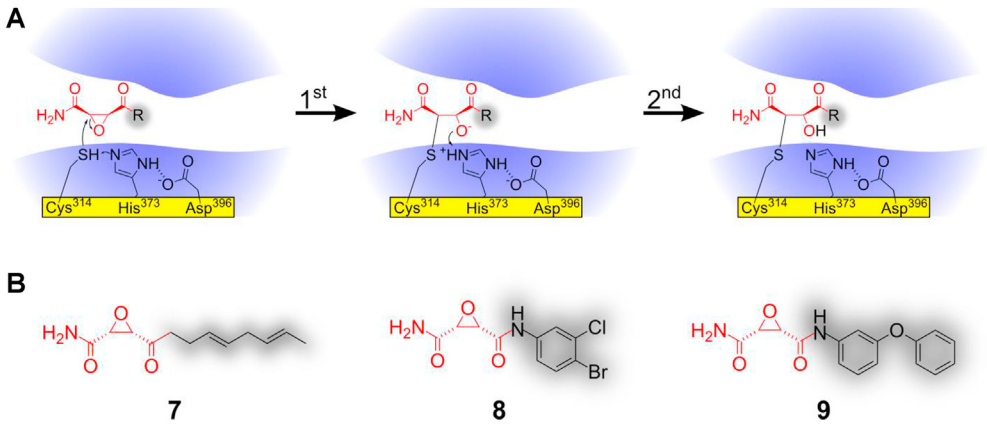

Fig. 4. FXIIIa inhibition mechanism (A) and structures (B) of cerulenin and corresponding derivatives. A: Postulated mechanism of Cys314 blockage. 1st step: Nucleophilic attack of the Cys314 to the epoxide function results in a ring opening of the epoxide; 2nd step: Protonation of the oxyanion to form the irreversible FXIIIa-inhibitor complex; **B**: Structures of the FXIIIa inhibitors; **7** - cerulenin; **8**, **9** - cerulenin derivatives with a high inhibitory potential toward FXIIIa.

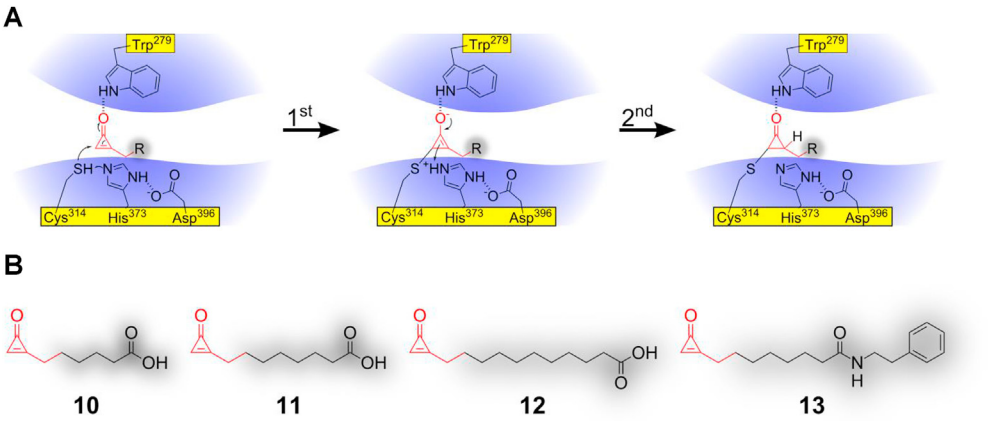

Fig. 5. FXIIIa inhibition mechanism (A) and structures of different alutacenoic acids (B) A: Stepwise mechanism of the irreversible binding of alutacenoic acids to the Cys314 of FXIIIa; 1st step: Michael addition of the Cys314 to the cyclopropenone ring system; 2nd step: Formation of the cyclopropanone system binding covalently to the Cys314 of FXIIIa; **B**: Structure of **10** - alutacenoic acid A; **11** - alutacenoic acid B; **12,13** - alutacenoic acid derivatives.

in the active site. All in all, the alutacenoic acid derivatives (**10**-**13**) are also potent FXIIIa inhibitors, which have not yet been sufficiently investigated with respect to other transglutaminases and their selectivity towards FXIIIa [77].

In conclusion, all three classes show a high inhibitory potential against FXIIIa. In terms of impaired clot formation, these molecules would therefore be perfectly suited for applications in anticoagulation therapy [2]. Such inhibitors could influence unwanted hemostasis, but at the same time represent a lower risk of bleeding. However, the problem of reduced selectivity of these small molecules leads to the fact that side reactions in therapeutic applications cannot be excluded. The targeting of other binding sites of FXIIIa via allosteric inhibitors, as well as the use of peptidic compounds are further possibilities to increase the selectivity.

3.3.1.4. Non-saccharide glucosaminoglycan mimetic 13 (NSGM 13). Beside active site inhibitors, allosteric interactions are capable of changing the conformation of enzymes and thereby of blocking the

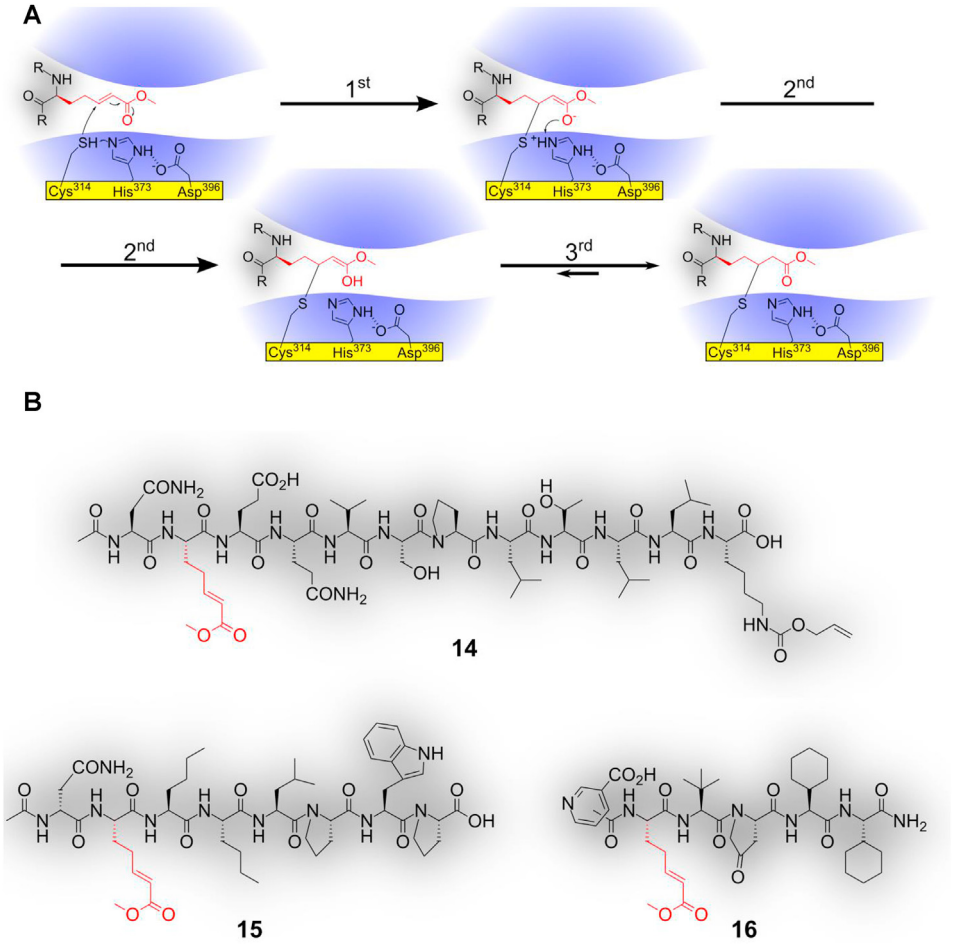

Fig. 6. FXIIIa inhibition mechanism (A) and structures (B) of peptidic and peptidomimetic Michael acceptors. A: Stepwise mechanism; 1st step: Michael addition of the Cys314 to the side chain with the Michael acceptor leads to the formation of an enolate; 2nd step: Protonation of the enolate results in an enol which is converted via keto-enol tautomerism in the 3rd step to the irreversible complex of FXIIIa and the inhibitor; **B**: Structures of **14** - ZED1251, **15** - ZED1301, and **16** - ZED3197 [47,81,82].

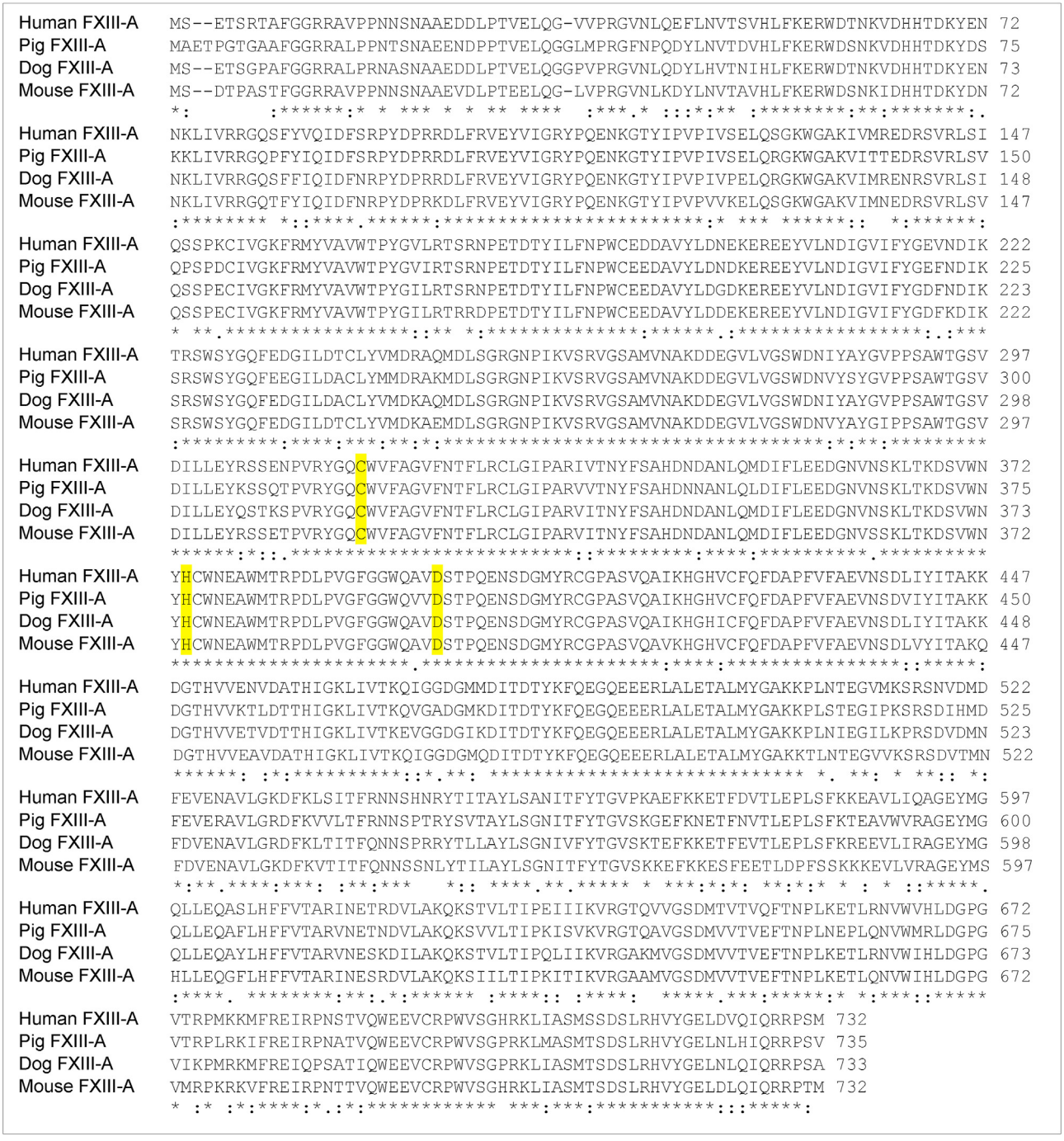

Fig. 7. Alignment of various FXIII-A variants from different species (human, pig, dog, and mouse). The catalytic triad is marked in yellow. Asterisk: Position with a single, fully conserved residue. Colon: Conservation between groups of strongly similar properties. Period: Conservation between groups of weakly similar properties.

active center for substrate conversion. Allosteric inhibitors for FXIIIa have not been well researched yet, but could have advantages compared to active side inhibitors. On the one hand, an increased FXIIIa specificity compared to other transglutaminases is possible. On the other hand, a conformational change of FXIIIa induced by allosteric inhibitors can sensitively regulate FXIIIa activity [83–89]. This could minimize side effects [29,90,91], such as an increased risk of bleeding which may occur upon complete FXIIIa inhibition [56,92,93]. For the development of allosteric FXIIIa inhibitors, the group of Al-Horani et al. investigated the surface of FXIIIa for the occurrence of clusters with a relatively high number of Lys and Arg residues. In this regard, a cluster of numerous Lys and Arg residues is located 16-24 Å from the catalytical site of FXIIIa. As already shown for other enzymes, such clusters have the possibility to interact with sulfated molecules such as sulfated glucosaminoglycans (GAGs) and non-saccharide GAG mimetics (NSGMs) and thereby serve as allosteric sites [94–100]. Based on these preliminary findings, Al-Horani et al. screened 22 variably GAGs and NSGMs against human FXIIIa [78]. In this study, NSGM 13 , an undecasulfated trimeric flavone, was identified as a potential allosteric inhibitor for FXIIIa. Further analyses on the inhibitory mechanism of NSGM 13 revealed its interaction with FXIIIa via ionic interactions between the inhibitor's sulfate groups and different arginines and lysines of FXIIIa leading to a slight conformational change in the active site of FXIIIa [78]. This eventually results in a

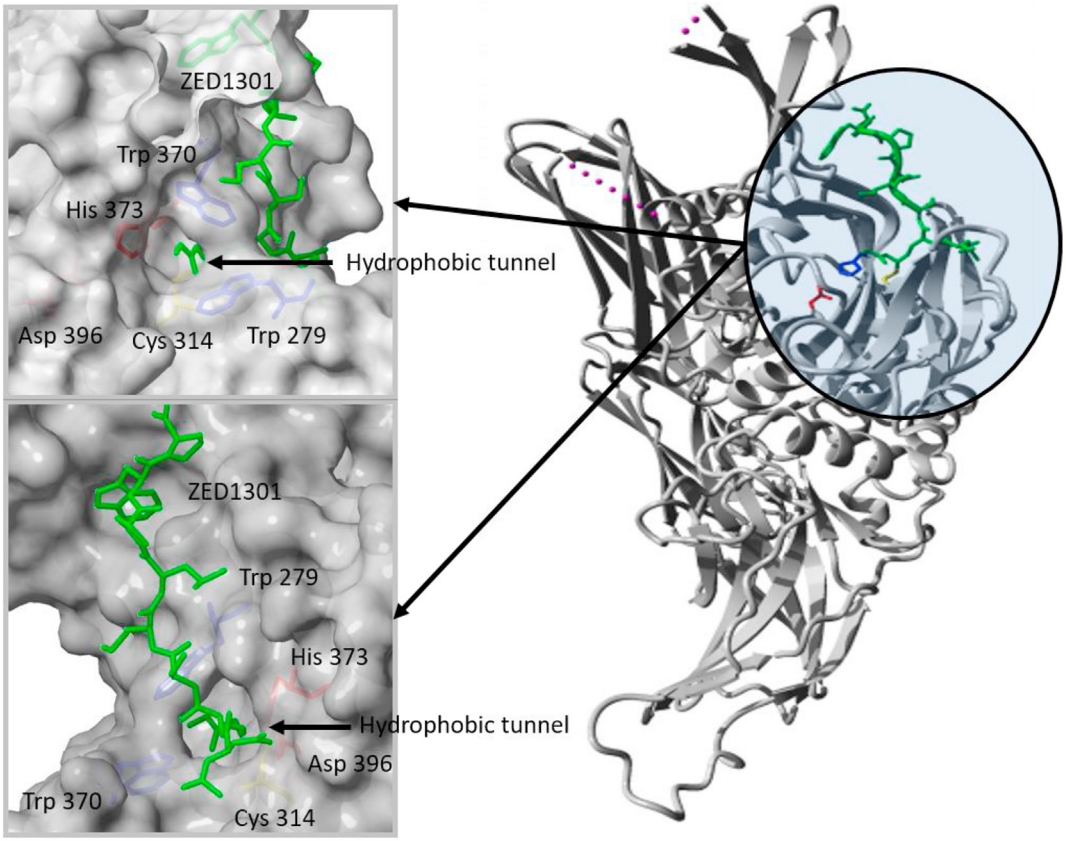

Fig. 8. Crystal structure of the calcium-activated FXIIIa monomer (PDB ID: 4KTY**) [47] complexed with the octapeptide ZED1301.** Grey: FXIIIa; green: ZED1301; yellow: Cys314; red: His373 and Asp396; blue: Trp279 and Trp370.

slower conversion of substrates by FXIIIa. Studies have shown that NSGM 13 has an effect on fibrin crosslinking and selectively inhibits FXIIIa (no inhibition of thrombin and FXa). The inhibitory effect of NSGM 13 on FXIIIa, however, is relatively low with an IC_{50} of 36.2 μM, as determined in this study [78]. In addition, the inhibitor is equally active toward guinea pig liver transglutaminase (IC_{50} = 23.5 μM), i.e. lacks specificity. In summary, the described study serves as 'proof of principle' for allosteric inhibition of FXIIIa, yet further investigations are required to come up with a potent and specific allosteric inhibitor.

3.3.2. Peptide inhibitors

In the last few years, several peptidic FXIIIa inhibitors have been developed to eliminate deficits of small molecule inhibitors including low specificity and low plasma half-life. The FXIIIa inhibitory potential of the naturally occurring peptide tridegin [101–107] and various transglutaminase-inhibiting Michael acceptors (TIMAs) [47,81,82] were reported and optimized in parallel. In addition to the differences in the FXIIIa inhibition of these peptides and the strategies for their optimization, the two approaches are derived from completely different origins. In the following sections, the TIMAs and tridegin are explained in more detail including the first successes in the development of clinically relevant FXIIIa inhibitors.

3.3.2.1. Peptidic transglutaminase-inhibiting Michael acceptors (TIMAs). Transglutaminase-inhibiting Michael acceptors are a group of transglutaminase inhibitors that combine peptidic or peptidomimetic backbones relevant for the specificity with a Michael acceptor function responsible for the inhibition of the catalytically active cysteine of the corresponding transglutaminase [47,81,82,108]. One of the first developed TIMAs for FXIIIa is the dodecapeptide ZED1251 which was derived from the sequence of the human α2-antiplasmin. The former substrate glutamine was replaced by a Michael acceptor. On the one hand, the peptide backbone generated from the FXIIIa substrate α2-antiplasmin leads to a high binding affinity and, simultaneously, selectivity towards FXIIIa [106]. On the other hand, the Michael acceptor mimics the FXIIIa substrate glutamine and is responsible for the inactivation. In addition, chloromethyl ketones [79] and 6-diazo-5-oxo-L-norleucines [109] also serve as glutamine substrate for covalent linking with the Cys314. This review focuses on the TIMAs since they are - due to their lower reactivity - more suitable for therapeutic applications. The successful usage of a peptidic Michael acceptor for transglutaminases can be seen in the case of the human transglutaminase 2 (TGase 2) inhibitor ZED1227, which has already reached phase 2a clinical trials for the treatment of celiac disease. The inactivation mechanism of the TIMAs is similar to the mode of action of the cyclopropenones (section 3.3.1.3) [77]. The thiol of the FXIIIa Cys314 side chain binds to the Michael acceptor (Fig. 6A). This leads to the formation of an enolate which is stabilized via hydrogen bonds to Trp279 and to the Cys314 backbone. Eventually, keto-enol tautomerism results in a stable inhibitor-enzyme complex and FXIIIa inactivation.

All representatives of the TIMAs for FXIIIa use the mechanism described for ZED1251 (Fig. 6B, **14**) to irreversibly inhibit FXIIIa. Only the peptide sequence and the corresponding structure of the molecules influence the inhibitory potential of these inhibitors against FXIIIa. At a concentration of 5 μM, ZED1251 (**14**) displays a complete inhibition of different FXIII variants, including human rFXIII-A (recombinant FXIII-A), rFXIII-A_2B_2, and animal rFXIII-A. In addition, the FXIII-A variants showed different second-order rate constants when using ZED1251 (**14**). In relation to human rFXIII-A, all animal variants, such as dog (4 times), pig (3 times), and mouse-rFXIII-A (2.5 times), were inhibited more strongly [81]. This can be explained by the fact that, despite of the high degree of sequence homology (Fig. 7), there are still small

differences in the amino acid sequence of the FXIII-A variants that could possibly influence structural diversity. This may lead to distinctions within the binding pocket, which is why FXIII-A activities vary.

Since ZED1251 (Fig. 6B, **14**) inactivates rFXIII-A faster than e.g. 5 (Fig. 3B), it was assumed that it has a higher binding affinity towards FXIIIa. Due to the high inhibitory potential and selectivity of **14** (Fig. 6B) to FXIIIa, further investigations on TIMAs were performed [81]. A structurally similar TIMA from Zedira, i.e. the octapeptide ZED1301 (**15**), was also identified as an irreversible binding ligand for Cys314 of FXIIIa. ZED1301 (**15**) was used in a crystallization experiment with activated FXIII, which led to the first high resolution crystal structure of FXIIIa (PDB ID: 4KTY) (Fig. 8) [47]. The comparison of this new FXIIIa crystal structure with the already existing FXIII crystal structures (PDB ID: 1GGU, 1GGT) [42,110] provided new insights into the activation process and the structural features of FXIIIa which are important for the transglutaminase reaction [47]. In detail, the catalytic diad (His342, Glu401) and several Ca^{2+} binding sites important for FXIII activation were identified. Moreover, it was suggested that FXIIIa acts as a monomer [47].

The novel insights obtained from the crystal structure also served as a basis for further FXIII studies [35–37]. One of these studies showed that the FXIII-A calcium binding sites may also be pharmacologically useful as targets for the development of FXIII inhibitors [36]. Apart from that, the structural analysis supported the development of compounds such as the hexamer peptidomimetic ZED3197 (Fig. 6B, **16**) derived from ZED1301 (**15**), which led to an optimized compound stability as well as a higher potency and selectivity towards FXIIIa [82]. In the corresponding study, ZED3197 (**16**) affected the transglutaminases TGase 1, TGase 2, TGase 3, and TGase 7 20- to 3000-times less than FXIIIa and achieved more than 95% inhibition of FXIIIa. Additionally, **16** had no effect on the bleeding time in a rabbit animal model, which qualified it as a potential drug candidate for further clinical studies on hypercoagulable patients. The only disadvantage of **16** is its short half-life of about 5–10 min as determined in *in vivo* studies using rabbits, which should lead to improved analogues in the course of further development. Currently, the short half-life is bypassed by continuous application [82]. In conclusion, the studies on TIMAs highlight the potential of peptide-based inhibitors over small molecule inhibitors for the progress of FXIII research. In contrast to the covalently binding synthetic TIMAs, the following section will focus on the natural reversible FXIIIa inhibitor tridegin.

3.3.2.2. Tridegin. As blood-sucking leeches need to prevent the formation of blood clots during food intake, many natural inhibitors of blood coagulation factors have been found in the salivary glands of leeches. Most of these leech-derived anticoagulants are cysteine-rich peptides or proteins that contain multiple disulfide bonds. These disulfide bonds increase the selectivity and stability of the peptide inhibitors. In Table 1, leech-derived cysteine-rich peptide anticoagulants are listed. Because of their specificity and selectivity towards different blood coagulation factors, these peptides are frequently investigated in pharmacological research. One of these disulfide-rich anticoagulants is the 66mer tridegin from the giant Amazon leech *Haementeria ghilianii*. Tridegin was first described by Finney et al. in 1997 and is the only known natural peptide inhibitor of FXIIIa [101]. The isolated peptide showed an IC_{50} of 9.2 nM in the original characterization. Inhibitory activity towards other enzymes of the blood coagulation cascade (FXa, thrombin) and cysteine proteases (bromelain, cathepsin C, papain) was not detected. In addition, guinea pig liver transglutaminase, which is related to human TGase 2, was inhibited to a much lower extent [101]. Therefore, the study of Finney et al. demonstrated that tridegin is a very potent and specific FXIIIa inhibitor.

In addition to the first results regarding the inhibitory potential of tridegin towards FXIIIa, Finney et al. revealed the amino acid sequence of tridegin almost completely (Fig. 9) [101]. Suggestions regarding possible amino acids for the uncertain positions were described subsequently [102–104]. In contrast to the original sequence reported in 1997 [101], the later version was extended by an additional N-terminal methionine and a C-terminal glutamate. Unfortunately, the authors did not publish how their sequence was determined [102–104].

The undefined positions in the original tridegin sequence of Finney et al. [101] were also analyzed by Böhm et al. performing an alignment of a tridegin-like cDNA sequence from the related leech *Haementeria depressa* and the incomplete sequence (Fig. 9) [105]. Interestingly, the homologous peptide could not be detected in *Haementeria depressa* [135]. The sequence of tridegin obtained from this alignment was identical to the tridegin sequence published in the above-mentioned studies [102–104], except for the two terminal amino acids methionine and glutamate and was therefore assumed to be the correct sequence (Fig. 9).

In addition to the sequence analysis, the first indications concerning the functional properties of tridegin have since been presented. Firstly, Giersiefen et al. localized the inhibitory potential of tridegin within the C-terminal part (Arg38-Glu66). Furthermore, an alanine scan identified Ile50 and Leu62 as essential amino acids for the inhibitory potential against FXIIIa [104,105]. Later studies using N-terminally truncated tridegin variants showed a deamidation or transamidation of the tridegin's Gln52 by FXIIIa. As a result, the shortened tridegin variants rather served as substrates, which lose their inhibitory activity over time in FXIIIa activity assays. Full-length reduced or oxidized tridegin, in turn, showed no substrate-like properties [105,106]. The N-terminal segment of tridegin (Lys1-Cys37) contains six cysteines (Cys5, Cys17, Cys19, Cys25, Cys31, Cys37) enabling the formation of three intramolecular disulfide bonds, which increase the inhibitory activity by a factor of 3–4 [106]. In further experiments, the disulfide-rich N-terminal segment (Lys1-Cys37) and the flexible C-terminal segment (Arg38-Glu66) were analyzed separately. Böhm et al. observed that the C-terminal part alone was able to inhibit FXIIIa, whereas the N-terminal segment showed no inhibitory potential. However, MST (Microscale Thermophoresis) binding studies revealed that the N-terminal part contributes to FXIIIa binding [106]. Due to the six cysteines within this segment, it is possible to obtain 15 different disulfide connectivities, which might have a strong impact on the tridegin structure. Unfortunately, the exact disulfide bond pattern of the naturally occurring tridegin is not known so far as tridegin has not been isolated since 1997 [101] due to a lack of the endangered *Haementeria ghilianii*. Thus, recombinant or chemosynthetic tridegin was used in recent studies, which might differ in the sequence and disulfide connectivity compared to the natural compound. To gain insight into the preferred folded structure, synthetically produced tridegin was analyzed by chymotryptic digestion and subsequent mass spectrometry. As a result, three disulfide isomers (isomers A, B and C, Fig. 10) were identified in the mixture of buffer-oxidized tridegin [106].

To date, it was not possible to elucidate the oxidative folding pathway of tridegin. Apparently, tridegin with its three conformational isomers does not behave like BPTI or the conotoxins μ-SIIIA and x-RIIIK, in which one major isomer is formed, nor like hirudin and the conotoxins μ-PIIIA and μ-SmIIIA, in which several different isomers are formed [107,136–141]. In addition, it is interesting that all three isomers contained a common disulfide bond between Cys19 and Cys25 (Fig. 10), which led to the assumption that this disulfide bond might be conserved in natural tridegin and may have an important role for structure, folding, and function of the peptide. In order to compare the inhibitory potential of the naturally occurring tridegin with the buffer-oxidized product, the synthetic isomer mixture ABC was tested for FXIIIa inhibition as well. A comparison of the resulting IC_{50} of the ABC mixture with the value of the naturally occurring tridegin revealed a significant difference in their activity [106], with the latter being the stronger inhibitor. Since IC_{50} values are always assay-dependent, it was not possible to draw a meaningful conclusion for these two tridegin samples. Nevertheless, native and synthetic tridegin could differ in their

Table 1
Cysteine-rich peptides derived from leeches which have an effect on clot formation. The peptides are subdivided into the specific target structures that are inhibited. [101, 111-134]

Peptide	Sequence
Thrombin	
Bufrudin [111] *(Hirudinaria manillensis)*	VSYTDCTESG QNYCLCVGSN VCGEGKNCQL SSSGNQCVHG EGTPKPKSQT EGDFEEIPDE XIK
Granulin [112] *(Hirudo nipponia)*	IDCPDKSKCK DDNTCCEVPS GKFACCDLPE AVCCADKMHC CPPKS
Hirudin [113] *(Hirudo medicinalis)*	VVYTDCTESG QNLCLCEGSN VCGQGNKCIL GSDGEKNQCV TGEGTPKPQS HNDGDFEEIP EEYLQ
Hirullin-P18 [111,114] *(Hirudinaria manillensis)*	VSYTDCTSGQ NYCLCGGNFC GDGKHCEMDG SENKCVDGEG TPKRQTSGPS DFEEFSLDDI EQ
Haemadin [115] *(Haemadipsa sylvestris)*	IRFGMGKVPC PDGEVGYTCD CGEKICLYGQ SCNDGQCSGD PKPSSEFEEF EIDEEEK
Theromin [116] *(Theromyzon Tessulatum)*	ECENTECPRA CPGEYEFDED GCNTCVCKGC DDAQCRCSSD ANGCESFCTC NTRCSAADEC NPRCTCK
FXa	
Antistasin [117] *(Haementeria officinalis)*	MIKLAILLLF TVAIVRCQGP FGPGCEEAGC PEGSACNIIT DRCTCSGVRC RMHCPHGFQR SRYGCEFCKC RLEPMKATCD ISECPEGMMC SRLTNKCDCK IDINCRKTCP NGLKRDKLGC EYCECRPKRK LIPRLS
Ghilanten [118,119] *(Haementeria ghilianii)*	QGPFGPGCEE AGCPEGSACN IITDRCTCPE VRCRVYCSHG FQRSRYGCEV CRCRTEPMKA TCDISECPEG MMCSRLTNKC DCKIDINCRK TCPNGLKRDK LGCEYCECKP KRKLVPRLS
Lefaxin [120] *(Haementeria depressa)*	FDVPEPFKWV DHFFYEKLDE QHKGLFFAFF DWGKGPDYWG KDTISLSQEQ VDAKFELDLE YGIFYGNGET IENPSENGDL QGIFFSWGSE
Therostasin [121] *(Theromyzon Tessulatum)*	MRGLAVLLLV ACFCSVAFGD CENTECPRAC PGEYEFDEDG CNTCLCKGCN DACCRIYCPL GFTTDANGCE SFCTCNTRET VCQNVVCSGK RVCNPRSGRC E
IIb/IIIa	
Decorsin [122] *(Macrobdella decora)*	APRLPQCQGD DQEKCLCNKD ECPPGQCRFP RGDADPYCE
Ornatin-A2 [123] *(Placobdella ornata)*	IPQCRDVKES GQPNDKCRCN GKPCTVGKCT IARGDDNDKC T
Ornatin-B [123] *(Placobdella ornata)*	IYVRPTNDEL NYCGDFRELG QPDKKCRCDG KPCTVGRCKF ARGDNDDKCI SA
Kallikrein	
Hirustasin [124] *(Hirudo medicinalis)*	TQGNTCGGET CSAAQVCLKG KCVCNEVHCR IRCKYGLKKD ENGCEYPCSC AKASQ
Piguamerin [125] *(Hirudo nipponia)*	TDCGGKTCSE AQVCKDGKCV CVIGQCRKYC PNGFKKDENG CTFPCTCA
Elastase	
Guamerin [126,127] *(Hirudo nipponia)*	VDENAEDTHG LCGEKTCSPA QVCLNNECAC TAIRCMIFCP NGFKVDENGC EYPCTCA
Fibrin	
Destabilase [128,129] (*Hirudo medicinalis*)	MIIAIYVSLA LLIASVEVNS QFTDSCLRCI CKVEGCDSQI GKCGMDVGSL SCGPYQIKKP YWIDCGKPGG GYESCTKNKA CSETCVRAYM KRYGTFCTGG RTPTCQDYAR IHNGGPRGCK SSATVGYWNK VQKCLR
Plasmin	
Bdellin B-3 [130,131] *(Hirudo medicinalis)*	DTECVCTKEL HRVCGSDGVT YDNECLATCH GASVAHDHAC EGHEEHHVDE HGEDHD
Carboxypeptidase B	
Carboxypeptidase Inhibitor [132,133] *(Hirudo medicinalis)*	SHTPDESFLC YQPDQVCCFI CRGAAPLPSE GECNPHPTAP WCREGAVEWV PYSTGQCRTT CIPYVE
vWF-collagen interaction	
Saratin [134,135] *(Hirudo medicinalis)*	EEREDCWTFY ANRKYTDFDK SFKKSSDLDE CKKTCFKTEY CYIVFEDTVN KECYYNVVDG EELDQEKFVV DENFTENYLT DCEGKDAGNA AGTGDESDEV DED
FXIIIa	
Tridegin [99] (*Haementeria ghilianii*)	KLLPCKEWHQ GIPNPRCWCG ADLECAQDQY CAFIPQCRPR SELIKPMDDI YQRPVEFPNL PLKPRE

```
A:  1 KLLPCKEXHQ GIPNPRCXCG ADLEXAQDQY CAFIPQC/E 37
B:  2 KLLPCKEWHQ GVPNPRCWCG ADLECAQDQY CAFIPQC   37
C:  3 KLLPCKEWHQ GIPNPRCWCG ADLECAQDQY CAFIPQC   37

A: 38 RPR SELIKPMDDI YQRPVC/EFPNL PLKPRC/E 66
B: 38 RPR SELIKPEDDI YQRPLE  FPKL PPKP     64
C: 38 RPR SELIKPMDDI YQRPVE  FPNL PLKPRE   66
```

Fig. 9. Sequence alignment of postulated tridegin sequences with a cDNA-derived sequence from *Haementeria depressa*. **A**: Tridegin sequence determined by Finney et al. [101]; **B**: Tridegin-like sequence derived from *Haementeria depressa* [105]; **C**: Postulated sequence by Böhm et al. [105]. The uncertainties of the tridegin sequence are highlighted in bold (modified from Böhm et al. 2012 [105]).

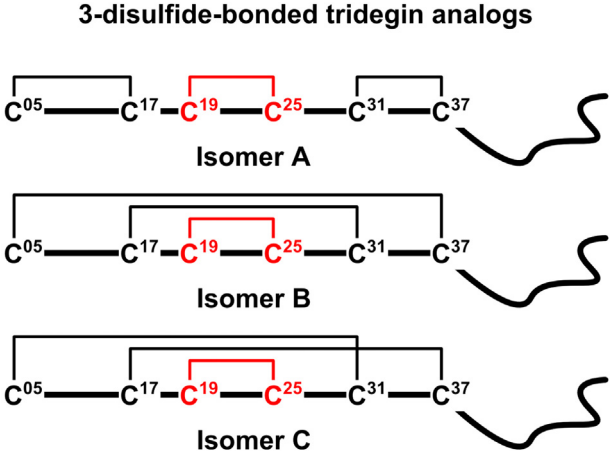

Fig. 10. Disulfide connectivities of tridegin isomers with three disulfide bonds. The common disulfide bond between Cys19-Cys25 is marked in red (modified from Bäuml et al., 2019 [107]).

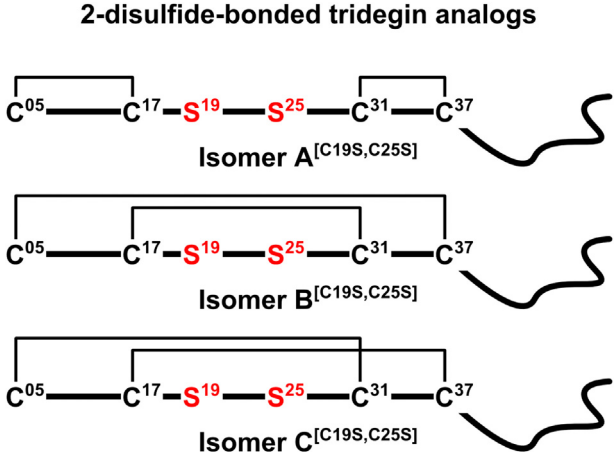

Fig. 11. Disulfide connectivity of the tridegin analogues with two disulfide bonds. Serine mutations of Cys19 and Cys25 are marked in red (modified from Bäuml et al., 2019 [107]).

disulfide connectivities and/or further post-translational modifications [106]. Another possibility is that only one of the three isomers A, B, and C, which is present to a very small extent in the mixture, is responsible for the inhibitory activity towards FXIIIa. In order to investigate the individual inhibitory potential of these three isomers, an attempt was made to separate the mixture ABC. However, the separation with standard HPLC methods was not possible so far. Therefore, a targeted protecting group strategy for the synthesis of the three isomers A, B, and C is required. Such a synthesis, however, is very challenging. Due to the high selectivity of tridegin for FXIIIa compared to other transglutaminases, such as guinea pig liver TGase (23-fold higher IC_{50} value), this peptide is very interesting for future medical application. In order to simplify the complex synthesis of the 3-disulfide-bonded tridegin isomers and to elucidate the role of disulfide bond Cys19-Cys25, analogues lacking this bond were synthesized (Fig. 11) [107].

In case of several cysteine-rich peptides described in the literature, the biological activity of their disulfide-reduced isomers compared to their fully-oxidized disulfide-bonded variants was either maintained or a loss of function was detected [142–146]. In our study, the three disulfide-reduced analogues lacking the common disulfide bond Cys19-Cys25 ($A_{[C19S,C25S]}$, $B_{[C19S,C25S]}$, $C_{[C19S,C25S]}$) were produced in a targeted way together with a product obtained from a self-folding experiment of the corresponding linear tridegin precursor according to Böhm et al. [106]. The latter approach was performed to investigate which 2-disulfide-bonded isomers are preferably formed. A fluorogenic isopeptidase activity assay revealed a similar inhibitory potential towards FXIIIa for all isomers and the mixture $ABC_{[C19S,C25S]}$, respectively. In addition, the 2-disulfide-bonded isomers showed a higher inhibitory potential than the linear all-serine mutant [107]. This confirmed the role of the disulfide bonds in tridegin for structural integrity in general. However, the finding also disclosed that the bond between Cys19-Cys25 does not have a large influence on the inhibitory potential of tridegin. Whole blood clotting assays based on the FXIIIa-mediated promotion of red blood cell retention in contracted whole blood clots were also performed in this study and confirmed the inhibitory potential of the isomers $A_{[C19S,C25S]}$, $B_{[C19S,C25S]}$, and $C_{[C19S,C25S]}$ [107]. The studies showed promising results for targeted FXIIIa inhibition and identified the three disulfide-deficient isomers as lead compounds for further development.

In order to gain insights into the structural properties of tridegin, CD-spectroscopic analyses were carried out which indicated small proportions of α-helices and β-sheets and larger proportions of β-loops and disordered structures [147]. Up to now, it was not possible to perform NMR structure analyses, as tridegin aggregates in higher concentrations. Also, attempts to crystallize tridegin alone or together with FXIIIa were unsuccessful – possibly due to the existence of different tridegin isomers in the used buffer-oxidized mixture [106]. However, computational studies including molecular modeling were performed to obtain structural information and insights into the mode of action of the 2-disulfide-bonded ($A_{[C19S,C25S]}$, $B_{[C19S,C25S]}$, $C_{[C19S,C25S]}$) as well as the 3-disulfide-bonded (A, B, C) isomers [106,107]. In comparative studies between the 3-disulfide- and the 2-disulfide-bonded isomers Molecular Dynamics (MD) simulations revealed that the removal of the disulfide bridge between Cys19-Cys25 strongly altered the structural conformation of the C-terminal part, but at the same time this disulfide bridge had no major impact on the structural integrity of the region comprised by the two remaining disulfide bonds [107]. The resulting MD simulated structures were docked to FXIIIa in a blind and a semi-flexible ensemble docking approach (Fig. 12, PDB ID: 4KTY [47]) [107].

The binding of all disulfide-deficient tridegin isomers $A_{[C19S,C25S]}$, $B_{[C19S,C25S]}$, and $C_{[C19S,C25S]}$ close to the active site is in line with the results of the activity studies [107]. It can be assumed that the disulfide-deficient isomers block the active site of FXIIIa and do not interact with individual residues of the active site. According to the aforementioned, it can be concluded that tridegin is a promising tool for the specific inhibition of FXIIIa and that simplified lead structures could be further developed for application in pharmacological research. Currently, *in vivo* testing in mice is being carried out and has revealed the first promising results (data not published).

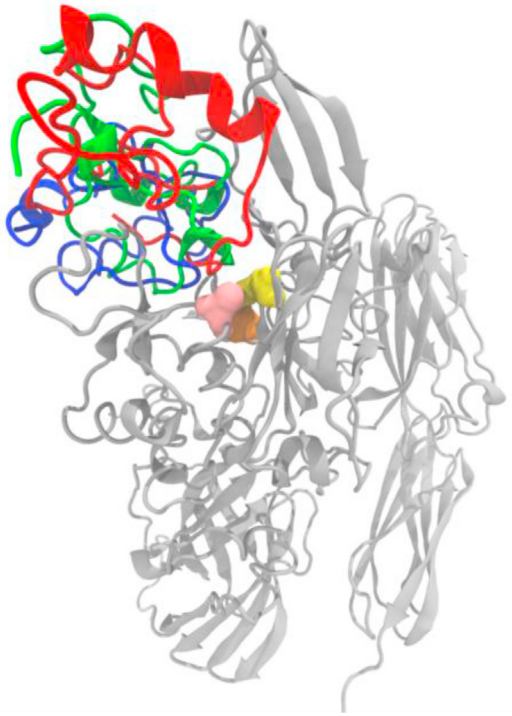

Fig. 12. Docking of the three tridegin variants with two disulfide bonds to the FXIIIa crystal structure (PDB ID: 4KTY). The crystal structure of FXIIIa with the catalytic triad Cys314 (pink), His373 (yellow) and Asp396 (orange) is shown in grey, while tridegin analogues are in blue ($A_{[C19S,C25S]}$), red ($B_{[C19S,C25S]}$), and green ($C_{[C19S,C25S]}$) (modified from Bäuml et al. 2019 [107]).

4. Conclusion

FXIIIa is an interesting pharmacological target molecule because it has an enormous importance for the biomechanical stability, size, and composition of the blood clot. In contrast to established anticoagulants which are vitamin K-mediated or address enzymes of the blood coagulation cascade, specific FXIIIa inhibition can reduce the risk of bleeding. This is due to the fact that a specific FXIIIa inhibitor does not affect thrombin or fibrin formation. To date, several compounds have been described that reduce the activity of FXIIIa. Among them are small molecules such as cerulenin and alutacenoic acids A and B, but also peptide-derived inhibitors such as tridegin and the TIMAs have been reported. These inhibitors have contributed significantly to the current state of knowledge concerning FXIIIa, but are not yet in medical use. For application, however, a higher specificity for FXIIIa compared to other transglutaminases, an increased plasma half-life, and better chemical accessibility is required. In recent years, promising peptide inhibitors such as tridegin and ZED3197 have therefore been developed and are still under discussion. The continuous development of these lead structures is essential for their exploitation in the direction of future biomedical applications.

Acknowledgements

Authors are grateful to Dr. A. Biswas (Institute of Experimental Haematology and Transfusion Medicine, University of Bonn) for technical support. Financial support by the German Foundation of Heart Research and by the University of Bonn (to D.I.) is gratefully acknowledged.

References

[1] World Health Organization, Global Health Estimates 2016: Deaths by Cause, Age, Sex, by Country and by Region. 2000-2016, (2018).
[2] A.S. Wolberg, Fibrinogen and factor XIII: newly recognized roles in venous thrombus formation and composition, Curr. Opin. Hematol. 25 (2018) 358–364.
[3] C.N. Bagot, R. Arya, Virchow and his triad: a question of attribution, Br. J. Haematol. 143 (2008) 180–190.
[4] A.J. Gale, Continuing education course #2: current understanding of hemostasis, Toxicol. Pathol. 39 (2011) 273–280.
[5] S. Palta, R. Saroa, A. Palta, Overview of the coagulation system, Indian J. Anaesth. 58 (2014) 515–523.
[6] M. Hoffman, D.M. Monroe, A cell-based model of hemostasis, Thromb. Haemost. 85 (2001) 958–965.
[7] A.P. Owens, N. Mackman, Tissue factor and thrombosis: the clot starts here, Thromb. Haemost. 104 (2010) 432–439.
[8] D.D. Monkovic, P.B. Tracy, Activation of human factor V by factor Xa and thrombin, Biochemistry 29 (1990) 1118–1128.
[9] M.B. Hultin, Modulation of thrombin-mediated activation of factor VIII:C by calcium ions, phospholipid, and platelets, Blood 66 (1985) 53–58.
[10] J.A. Oliver, D.M. Monroe, H.R. Roberts, M. Hoffman, Thrombin activates factor XI on activated platelets in the absence of factor XII, Arterioscler. Thromb. Vasc. Biol. 19 (1999) 170–177.
[11] L. Lóránd, K. Konishi, Activation of the fibrin stabilizing factor of plasma by thrombin, Arch. Biochem. Biophys. 105 (1964) 58–67.
[12] K. Konishi, L. Lóránd, Separation of activated fibrin-stabilizing factor from thrombin, BBA - Gen. Subj. 121 (1966) 177–180.
[13] J.W. Weisel, R.I. Litvinov, Fibrin formation, structure and properties, Subcell. Biochem. 82 (2017) 405–456.
[14] M. Pieters, A.S. Wolberg, Fibrinogen and fibrin: an illustrated review, Res. Pract. Thromb. Haemost. 3 (2019) 161–172.
[15] D.A. Lane, H. Philippou, J.A. Huntington, Directing thrombin, Blood 106 (2005) 2605–2612.
[16] K. Madlener, B. Pötzsch, Hämostasesystem, Hamostaseologie, 2010, pp. 7–12.
[17] S.R. Fraser, N.A. Booth, N.J. Mutch, The antifibrinolytic function of factor XIII is exclusively expressed through α2-antiplasmin cross-linking, Blood 117 (2011) 6371–6374.
[18] I.N. Chernysh, C. Nagaswami, P.K. Purohit, J.W. Weisel, Fibrin clots are equilibrium polymers that can be remodeled without proteolytic digestion, Sci. Rep. 2 (2012) 879.
[19] A. Greinacher, T.E. Warkentin, The direct thrombin inhibitor hirudin, Thromb. Haemost. 99 (2008) 819–829.
[20] F. Markwardt, Hirudin as alternative anticoagulant - a historical review, Semin. Thromb. Hemost. 28 (2002) 405–413.
[21] D.D. Callas, D. Hoppensteadt, J. Fareed, Comparative studies on the anticoagulant and protease generation inhibitory actions of newly developed site-directed thrombin inhibitor drugs. Efegatran®, argatroban, hirulog, and hirudin, Semin. Thromb. Hemost. 21 (1995) 177–183.
[22] A.C. Teger-Nilsson, R. Bylund, D. Gustafsson, E. Gyzander, U. Eriksson, In vitro effects of inogatran. A selective low molecular weight thrombin inhibitor, Thromb. Res. 85 (1997) 133–145.
[23] K.A. Arsenault, J. Hirsh, R.P. Whitlock, J.W. Eikelboom, Direct thrombin inhibitors in cardiovascular disease, Nat. Rev. Cardiol. 9 (2012) 402–414.
[24] C.J. Lee, J.E. Ansell, Direct thrombin inhibitors, Br. J. Clin. Pharmacol. 72 (2011) 581–592.
[25] J.H. Griffin, The thrombin paradox, Nature 378 (1995) 337–338.
[26] C.M. Shaw, D.M. O'Hanlon, G.P. McEntee, Venous thrombosis, Am. J. Surg. 186 (2003) 167–168.
[27] Y.V. Matsuka, L.V. Medved, M.M. Migliorini, K.C. Ingham, Factor XIIIA-catalyzed cross-linking of recombinant αC fragments of human fibrinogen, Biochemistry 35 (1996) 5810–5816.
[28] K.F. Standeven, A.M. Carter, P.J. Grant, J.W. Weisel, I. Chernysh, L. Masova, S.T. Lord, R.A.S. Ariëns, Functional analysis of fibrin γ-chain cross-linking by activated factor XIII: determination of a cross-linking pattern that maximizes clot stiffness, Blood 110 (2007) 902–907.
[29] M.M. Aleman, J.R. Byrnes, J.G. Wang, R. Tran, W.A. Lam, J. Di Paola, N. Mackman, J.L. Degen, M.J. Flick, A.S. Wolberg, Factor XIII activity mediates red blood cell retention in venous thrombi, J. Clin. Invest. 124 (2014) 3590–3600.
[30] J.R. Byrnes, C. Duval, Y. Wang, C.E. Hansen, B. Ahn, M.J. Mooberry, M.A. Clark, J.M. Johnsen, S.T. Lord, W.A. Lam, J.C.M. Meijers, H. Ni, R.A.S. Ariëns, A.S. Wolberg, Factor XIIIa-dependent retention of red blood cells in clots is mediated by fibrin α-chain crosslinking, Blood 126 (2015) 1940–1948.
[31] E.L. Hethershaw, A.L. Cilia La Corte, C. Duval, M. Ali, P.J. Grant, R.A.S. Ariëns, H. Philippou, The effect of blood coagulation factor XIII on fibrin clot structure and fibrinolysis, J. Thromb. Haemost. 12 (2014) 197–205.
[32] C.C. Helms, R.A.S. Ariëns, S. Uitte De Willige, K.F. Standeven, M. Guthold, α-α Cross-links increase fibrin fiber elasticity and stiffness, Biophys. J. 102 (2012) 168–175.
[33] L. Muszbek, Z. Bereczky, Z. Bagoly, I. Komáromi, É. Katona, Factor XIII: a coagulation factor with multiple plasmatic and cellular functions, Physiol. Rev. 91 (2011) 931–972.
[34] A.D. Protopopova, A. Ramirez, D.V. Klinov, R.I. Litvinov, J.W. Weisel, Factor XIII topology: organization of B subunits and changes with activation studied with single-molecule atomic force microscopy, J. Thromb. Haemost. 17 (2019) 737–748.
[35] S. Gupta, A. Biswas, M.S. Akhter, C. Krettler, C. Reinhart, J. Dodt, A. Reuter, H. Philippou, V. Ivaskevicius, J. Oldenburg, Revisiting the mechanism of coagulation factor XIII activation and regulation from a structure/functional perspective, Sci. Rep. 6 (2016) 30105.
[36] S. Singh, J. Dodt, P. Volkers, E. Hethershaw, H. Philippou, V. Ivaskevicius, D. Imhof, J. Oldenburg, A. Biswas, Structure functional insights into calcium binding during the activation of coagulation factor XIII A, Sci. Rep. 9 (2019) 1–18.
[37] B.A. Anokhin, W.L. Dean, K.A. Smith, M.J. Flick, R.A.S. Ariëns, H. Philippou, M.C. Maurer, Proteolytic and nonproteolytic activation mechanisms result in conformationally and functionally different forms of coagulation factor XIII A, FEBS J. 287 (2020) 452–464.
[38] B.A. Anokhin, V. Stribinskis, W.L. Dean, M.C. Maurer, Activation of factor XIII is accompanied by a change in oligomerization state, FEBS J. 284 (2017) 3849–3861.
[39] V. Schroeder, H.P. Kohler, Factor XIII deficiency: an update, Semin. Thromb. Hemost. 39 (2013) 632–641.
[40] S. Singh, M.S. Akhter, J. Dodt, A. Sharma, S. Kaniyappan, H. Yadegari, V. Ivaskevicius, J. Oldenburg, A. Biswas, Disruption of structural disulfides of coagulation FXIII-B subunit; functional implications for a rare bleeding disorder, Int. J. Mol. Sci. 20 (2019) 1956.
[41] S. Singh, M.S. Akhter, J. Dodt, P. Volkers, A. Reuter, C. Reinhart, C. Krettler, J. Oldenburg, A. Biswas, Identification of potential novel interacting partners for coagulation factor XIII B (FXIII-B) subunit, a protein associated with a rare bleeding disorder, Int. J. Mol. Sci. 20 (2019) 2682.
[42] V.C. Yee, L.C. Pedersen, I. Le Trong, P.D. Bishop, R.E. Stenkamp, D.C. Teller, Three-dimensional structure of a transglutaminase: human blood coagulation factor XIII, Proc. Natl. Acad. Sci. U.S.A. 91 (1994) 7296–7300.
[43] E.L. Hethershaw, P.J. Adamson, K.A. Smith, W.N. Goldsberry, R.J. Pease, S.E. Radford, P.J. Grant, R.A.S. Ariëns, M.C. Maurer, H. Philippou, The role of β-barrels 1 and 2 in the enzymatic activity of factor XIII A-subunit, J. Thromb. Haemost. 16 (2018) 1391–1401.
[44] É. Katona, K. Pénzes, A. Csapó, F. Fazakas, M.L. Udvardy, Z. Bagoly, Z.Z. Orosz, L. Muszbek, Interaction of factor XIII subunits, Blood 123 (2014) 1757–1763.
[45] T.A. Trumbo, M.C. Maurer, Examining thrombin hydrolysis of the Factor XIII activation peptide segment leads to a proposal for explaining the cardioprotective effects observed with the Factor XIII V34L mutation, J. Biol. Chem. 275 (2000) 20627–20631.
[46] M. Griffin, R. Casadio, C.M. Bergamini, Transglutaminases: nature's biological glues, Biochem. J. 368 (2002) 377–396.
[47] M. Stieler, J. Weber, M. Hils, P. Kolb, A. Heine, C. Büchold, R. Pasternack, G. Klebe, Structure of active coagulation factor XIII triggered by calcium binding: basis for the design of next-generation anticoagulants, Angew. Chem. Int. Ed. 52 (2013) 11930–11934.
[48] S.E. Iismaa, S. Holman, M.A. Wouters, L. Lóránd, R.M. Graham, A. Husain, Evolutionary specialization of a tryptophan indole group for transition-state stabilization by eukaryotic transglutaminases, Proc. Natl. Acad. Sci. U.S.A. 100 (2003) 12636–12641.
[49] T.J. Hornyak, J.A. Shafer, Interactions of factor XIII with fibrin as substrate and cofactor, Biochemistry 31 (1992) 423–429.
[50] B. Shenkman, Y. Einav, T. Livnat, I. Budnik, U. Martinowitz, In vitro evaluation of clot quality and stability in a model of severe thrombocytopenia: effect of fibrinogen, factor XIII and thrombin-activatable fibrinolysis inhibitor, Blood Transfus 12 (2014) 78–84.
[51] G.L. Reed, G.R. Matsueda, E. Haber, Fibrin-fibrin and alpha 2-antiplasmin-fibrin cross-linking by platelet factor XIII increases the resistance of platelet clots to fibrinolysis, Trans. Assoc. Am. Phys. 104 (1991) 21–28.
[52] G.L. Reed, G.R. Matsueda, E. Haber, Platelet factor XIII increases the fibrinolytic resistance of platelet-rich clots by accelerating the crosslinking of alpha 2-antiplasmin to fibrin, Thromb. Haemost. 68 (1992) 315–320.
[53] C.W. Francis, V.J. Marder, Rapid formation of large molecular weight α-polymers in cross-linked fibrin induced by high Factor XIII concentrations: role of platelet Factor XIII, J. Clin. Invest. 80 (1987) 1459–1465.
[54] F.D. Rubens, D.W. Perry, M.W.C. Hatton, P.D. Bishop, M.A. Packham, R.L. Kinlough-Rathbone, Platelet accumulation on fibrin-coated polyethylene: role of platelet activation and factor XIII, Thromb. Haemost. 73 (1995) 850–856.
[55] Z. Hevessy, G. Haramura, Z. Boda, M. Udvardy, L. Muszbek, Promotion of the crosslinking of fibrin and α2-antiplasmin by platelets, Thromb. Haemost. 75 (1996) 161–167.
[56] V. Schroeder, H.P. Kohler, New developments in the area of factor XIII, J. Thromb. Haemost. 11 (2013) 234–244.
[57] G. Dickneite, H. Herwald, W. Korte, Y. Allanore, C.P. Denton, M.M. Cerinic, Coagulation factor XIII: a multifunctional transglutaminase with clinical potential in a range of conditions, Thromb. Haemost. 113 (2015) 686–697.
[58] A. Ichinose, Factor XIII is a key molecule at the intersection of coagulation and fibrinolysis as well as inflammation and infection control, Int. J. Hematol. 95 (2012) 362–370.
[59] A.S. Wolberg, F.R. Rosendaal, J.I. Weitz, I.H. Jaffer, G. Agnelli, T. Baglin, N. MacKman, Venous thrombosis, Nat. Rev. Dis. Prim. 1 (2015) 15006.
[60] S. Kattula, J.R. Byrnes, S.M. Martin, L.A. Holle, B.C. Cooley, M.J. Flick, A.S. Wolberg, Factor XIII in plasma, but not in platelets, mediates red blood cell retention in clots and venous thrombus size in mice, Blood Adv. 2 (2018) 25–35.
[61] J.R. Byrnes, A.S. Wolberg, Newly-Recognized roles of factor XIII in thrombosis, Semin. Thromb. Hemost. 42 (2016) 445–454.
[62] L. Lóránd, A.J. Gray, K. Brown, R.B. Credo, C.G. Curtis, R.A. Domanik, P. Stenberg, Dissociation of the subunit structure of fibrin stabilizing factor during activation of the zymogen, Biochem. Biophys. Res. Commun. 56 (1974) 914–922.

[63] D. Lukacova, E. Haber, G.R. Matsueda, G.L. Reed, Inhibition of factor XIII activation by an anti-peptide monoclonal antibody, Biochemistry 30 (1991) 10164–10170.
[64] G.L. Reed, A.K. Houng, The contribution of activated factor XIII to fibrinolytic resistance in experimental pulmonary embolism, Circulation 99 (1999) 299–304.
[65] G.L. Reed, Immunoinhibitors of Factor XIII, US Patent (1995) US005470957A.
[66] O.V. Mitkevich, J.H. Sobel, J.R. Shainoff, T.N. Vlasik, G.F. Kalantarov, I.N. Trakht, Z.A. Streltsova, G.P. Samokhin, Monoclonal antibody directed to a fibrinogen Aα #529-539 epitope inhibits α-chain crosslinking by transglutaminases, Blood Coagul. Fibrinolysis 7 (1996) 85–92.
[67] O.V. Mitkevich, J.R. Shainoff, P.M. DiBello, V.C. Yee, D.C. Teller, G.B. Smejkal, P.D. Bishopi, I.S. Kolotushkina, K. Fickenscher, G.P. Samokhin, Coagulation factor XIIIa undergoes a conformational change evoked by glutamine substrate, J. Biol. Chem. 273 (1998) 14387–14391.
[68] L. Lóránd, N.G. Rule, H.H. Ong, R. Furlanetto, A. Jacobsen, J. Downey, N. Öner, J. Bruner-Lóránd, Amine specificity in transpeptidation. Inhibition of fibrin cross-linking, Biochemistry 7 (1968) 1214–1223.
[69] K.F. Freund, S.L. Gaul, K.P. Doshi, D.A. Claremon, D.C. Remy, J.J. Baldwin, P.A. Friedman, A.M. Stern, A novel factor XIIIa inhibitor enhances clot lysis rates, Fibrinolysis 2 (1988) 67.
[70] K.F. Freund, K.P. Doshi, S.L. Gaul, A.M. Stern, D.A. Claremon, D.C. Remy, J.J. Baldwin, S.M. Pitzenberger, Transglutaminase inhibition by 2-[(2-oxopropyl) thio]imidazolium derivatives: mechanism of factor XIIIa inactivation, Biochemistry 33 (1994) 10109–10119.
[71] E.M. Leidy, A.M. Stern, P.A. Friedman, L.R. Bush, Enhanced thrombolysis by a factor XIIIa inhibitor in a rabbit model of femoral artery thrombosis, Thromb. Res. 59 (1990) 15–26.
[72] C. Barsigian, A.M. Stern, J. Martinez, Tissue (type II) transglutaminase covalently incorporates itself, fibrinogen, or fibronectin into high molecular weight complexes on the extracellular surface of isolated hepatocytes. Use of 2-[(2-oxopropyl) thio]imidazolium derivatives as cellular transg, J. Biol. Chem. 266 (1991) 22501–22509.
[73] R.J. Shebuski, G.R. Sitko, D.A. Claremon, J.J. Baldwin, D.C. Remy, A.M. Stern, Inhibition of factor XIIIa in a canine model of coronary thrombosis: effect on reperfusion and acute reocclusion after recombinant tissue-type plasminogen activator, Blood 75 (1990) 1455–1459.
[74] A.A. Tymiak, J.G. Tuttle, S.D. Kimball, T. Wang, V.G. Lee, A Simple and rapid screen for inhibitors of factor XIIIa, J. Antibiot. (Tokyo) 46 (1993) 204–206.
[75] C.A. Avery, R.J. Pease, K. Smith, M. Boothby, H.M. Buckley, P.J. Grant, C.W.G. Fishwick, (±) cis-bisamido epoxides: a novel series of potent FXIII-A inhibitors, Eur. J. Med. Chem. 98 (2015) 49–53.
[76] H. Kogen, T. Kiho, K. Tago, S. Miyamoto, T. Fujioka, N. Otsuka, K. Suzuki-Konagai, T. Ogita, Alutacenoic acids A and B, rare naturally occurring cyclopropenone derivatives isolated from fungi: potent non-peptide factor XIIIa inhibitors, J. Am. Chem. Soc. 122 (2000) 1842–1843.
[77] Y. Iwata, K. Tago, T. Kiho, H. Kogen, T. Fujioka, N. Otsuka, K. Suzuki-Konagai, T. Ogita, S. Miyamoto, Conformational analysis and docking study of potent factor XIIIa inhibitors having a cyclopropenone ring, J. Mol. Graph. Model. 18 (2000) 591–599.
[78] R.A. Al-Horani, R. Karuturi, M. Lee, D.K. Afosah, U.R. Desai, Allosteric inhibition of factor XIIIa. non-saccharide glycosaminoglycan mimetics, but not glycosaminoglycans, exhibit promising inhibition profile, PloS One 11 (2016) 1–20.
[79] G. Reinhardt, α-Halogenmethyl carbonyl compounds as very potent inhibitors of factor XIIIa in vitro, Ann. N. Y. Acad. Sci. 370 (1981) 836–842.
[80] M.V. Catani, F. Bernassola, A. Rossi, G. Melino, Inhibition of clotting factor XIII activity by nitric oxide, Biochem. Biophys. Res. Commun. 249 (1998) 275–278.
[81] A. Heil, J. Weber, C. Büchold, R. Pasternack, M. Hils, Differences in the inhibition of coagulation factor XIII-A from animal species revealed by Michael Acceptor- and thioimidazol based blockers, Thromb. Res. 131 (2013) 214–222.
[82] R. Pasternack, C. Büchold, R. Jähnig, C. Pelzer, M. Sommer, A. Heil, P. Florian, G. Nowak, U. Gerlach, M. Hils, Novel inhibitor ZED3197 as potential drug candidate in anticoagulation targeting coagulation FXIIIa (F13a), J. Thromb. Haemost. 18 (2020) 191–200.
[83] R. Nussinov, C.J. Tsai, Allostery in disease and in drug discovery, Cell 153 (2013) 293–305.
[84] S. Lu, S. Li, J. Zhang, Harnessing allostery: a novel approach to drug discovery, Med. Res. Rev. 34 (2014) 1242–1285.
[85] G. Kar, O. Keskin, A. Gursoy, R. Nussinov, Allostery and population shift in drug discovery, Curr. Opin. Pharmacol. 10 (2010) 715–722.
[86] M. Merdanovic, T. Mönig, M. Ehrmann, M. Kaiser, Diversity of allosteric regulation in proteases, ACS Chem. Biol. 8 (2013) 19–26.
[87] N. Pozzi, A.D. Vogt, D.W. Gohara, E. Di Cera, Conformational selection in trypsin-like proteases, Curr. Opin. Struct. Biol. 22 (2012) 421–431.
[88] D.W. Gohara, E. Di Cera, Allostery in trypsin-like proteases suggests new therapeutic strategies, Trends Biotechnol. 29 (2011) 577–585.
[89] P. Hauske, C. Ottmann, M. Meltzer, M. Ehrmann, M. Kaiser, Allosteric regulation of proteases, ChemBioChem 9 (2008) 2920–2928.
[90] M.J. Flick, X.L. Du, D.P. Witte, M. Jirousková, D.A. Soloviev, S.J. Busuttil, E.F. Plow, J.L. Degen, Leukocyte engagement of fibrin(ogen) via the integrin receptor αMβ2/Mac-1 is critical for host inflammatory response in vivo, J. Clin. Invest. 113 (2004) 1596–1606.
[91] P. Lauer, H.J. Metzner, G. Zettlmeißl, M. Li, A.G. Smith, R. Lathe, G. Dickneite, Targeted inactivation of the mouse locus encoding coagulation factor XIII-A: hemostatic abnormalities in mutant mice and characterization of the coagulation deficit, Thromb. Haemost. 88 (2002) 967–974.
[92] M. Janning, K. Holstein, B. Spath, C. Schnabel, P. Bannas, C. Bokemeyer, F. Langer, Relevant bleeding diathesis due to acquired factor XIII deficiency, Hämostaseologie 33 (2013) 50–54.
[93] L. Muszbek, Z. Bereczky, Z. Bagoly, I. Komáromi, É. Katona, Factor XIII: a coagulation factor with multiple plasmatic and cellular functions, Physiol. Rev. 91 (2011) 931–972.
[94] M.H. Abdel Aziz, P.S. Sidhu, A. Liang, J.Y. Kim, P.D. Mosier, Q. Zhou, D.H. Farrell, U.R. Desai, Designing allosteric regulators of thrombin. Monosulfated benzofuran dimers selectively interact with Arg173 of exosite 2 to induce inhibition, J. Med. Chem. 55 (2012) 6888–6897.
[95] P.S. Sidhu, M.H. Abdel Aziz, A. Sarkar, A.Y. Mehta, Q. Zhou, U.R. Desai, Designing allosteric regulators of thrombin. Exosite 2 features multiple subsites that can be targeted by sulfated small molecules for inducing inhibition, J. Med. Chem. 56 (2013) 5059–5070.
[96] Z. Wang, R.J. Collighan, K. Pytel, D.L. Rathbone, X. Li, M. Griffin, Characterization of heparin-binding site of tissue transglutaminase: its importance in cell surface targeting, matrix deposition, and cell signaling, J. Biol. Chem. 287 (2012) 13063–13083.
[97] R.A. Al-Horani, R. Karuturi, D.T. White, U.R. Desai, Plasmin regulation through allosteric, sulfated, small molecules, Molecules 20 (2015) 608–624.
[98] R.A. Al-Horani, U.R. Desai, Designing allosteric inhibitors of factor XIa. Lessons from the interactions of sulfated pentagalloylglucopyranosides, J. Med. Chem. 57 (2014) 4805–4818.
[99] R.A. Al-Horani, A. Liang, U.R. Desai, Designing nonsaccharide, allosteric activators of antithrombin for accelerated inhibition of factor Xa, J. Med. Chem. 54 (2011) 6125–6138.
[100] H. Lortat-Jacob, I. Burhan, A. Scarpellini, A. Thomas, A. Imberty, R.R. Vivès, T. Johnson, A. Gutierrez, E.A.M. Verderio, Transglutaminase-2 interaction with heparin: identification of a heparin binding site that regulates cell adhesion to fibronectin-transglutaminase-2 matrix, J. Biol. Chem. 287 (2012) 18005–18017.
[101] S. Finney, L. Seale, R.T. Sawyer, R.B. Wallis, Tridegin, a new peptidic inhibitor of factor XIIIa, from the blood-sucking leech Haementeria ghilianii, Biochem. J. 324 (1997) 797–805.
[102] W. Linxweiler, C. Burger, O. Pöschke, U. Hofmann, A. Wolf, Glucose-Dehydrogenase Fusionsproteine und ihre Verwendung in Expressionssystemen, International Patent, 2000 WO 00/49039 A2.
[103] R.T. Sawyer, R.B. Wallis, L. Seale, S. Finney, Inhibitors of fibrin cross-linking and/or transglutaminases, US Patent (2000) US006025330A.
[104] H. Giersiefen, J. Stöckel, T. Pamp, M. Ohlmann, Modifizierte Tridegine, ihre Herstellung und Verwendung als Transglutaminase-Inhibitoren, European Patent (2002) EP1458866B1.
[105] M. Böhm, T. Kühl, K. Hardes, R. Coch, C. Arkona, B. Schlott, T. Steinmetzer, D. Imhof, Synthesis and functional characterization of tridegin and its analogues: inhibitors and substrates of factor XIIIa, ChemMedChem 7 (2012) 326–333.
[106] M. Böhm, C.A. Bäuml, K. Hardes, T. Steinmetzer, D. Roeser, Y. Schaub, M.E. Than, A. Biswas, D. Imhof, Novel insights into structure and function of factor XIIIa-inhibitor tridegin, J. Med. Chem. 57 (2014) 10355–10365.
[107] C.A. Bäuml, T. Schmitz, A.A. Paul George, M. Sudarsanam, K. Hardes, T. Steinmetzer, L.A. Holle, A.S. Wolberg, B. Pötzsch, J. Oldenburg, A. Biswas, D. Imhof, Coagulation factor XIIIa inhibitor tridegin: on the role of disulfide bonds for folding, stability, and function, J. Med. Chem. 62 (2019) 3513–3523.
[108] I. Lindemann, J. Böttcher, K. Oertel, J. Weber, M. Hils, R. Pasternack, U. Linne, A. Heine, G. Klebe, Inhibitors of transglutaminase 2: a therapeutic option in celiac disease, XXth Int. Symp. Med. Chem. Drugs Futur. 33 (2007) 2747.
[109] S. Schaertl, M. Prime, J. Wityak, C. Dominguez, I. Muñoz-Sanjuan, R.E. Pacifici, S. Courtney, A. Scheel, D. Macdonald, A profiling platform for the characterization of transglutaminase 2 (TG2) inhibitors, J. Biomol. Screen 15 (2010) 478–487.
[110] B.A. Fox, V.C. Yee, L.C. Pedersen, I. Le Trong, P.D. Bishop, R.E. Stenkamp, D.C. Teller, Identification of the calcium binding site and a novel ytterbium site in blood coagulation factor XIII by X-ray crystallography, J. Biol. Chem. 274 (1999) 4917–4923.
[111] A. Electricwala, R. Hartwell, M.D. Scawen, T. Atkinson, The complete amino acid sequence of a hirudin variant from the leech Hirudinaria manillensis, J. Protein Chem. 12 (1993) 365–370.
[112] S. Jin Hong, K. Won Kang, Purification of granulin-like polypeptide from the blood-sucking leech, Hirudo nipponia, Protein Expr. Purif. 16 (1999) 340–346.
[113] J. Dodt, H.P. Müller, U. Seemüller, J.Y. Chang, The complete amino acid sequence of hirudin, a thrombin specific inhibitor. Application of colour carboxymethylation, FEBS Lett. 165 (1984) 180–184.
[114] J.L. Krstenansky, T.J. Owen, M.T. Yates, S.J.T. Mao, The C-terminal binding domain of hirullin P18: antithrombin activity and comparison to hirudin peptides, FEBS Lett. 269 (1990) 425–429.
[115] J.L. Richardson, Crystal structure of the human alpha-thrombin-haemadin complex: an exosite II-binding inhibitor, EMBO J. 19 (2000) 5650–5660.
[116] M. Salzet, V. Chopin, J.L. Baert, I. Matias, J. Malecha, Theromin, a novel leech thrombin inhibitor, J. Biol. Chem. 275 (2000) 30774–30780.
[117] C. Dunwiddie, N.A. Thornberry, H.G. Bull, M. Sardana, P.A. Friedman, J.W. Jacobs, E. Simpson, Antistasin, a leech-derived inhibitor of factor Xa. Kinetic analysis of enzyme inhibition and identification of the reactive site, J. Biol. Chem. 264 (1989) 16694–16699.
[118] C.T. Dunwiddie, L. Waxman, G.P. Vlasuk, P.A. Friedman, Purification and characterization of inhibitors of blood coagulation factor Xa from hematophagous organisms, Methods Enzymol. 223 (1993) 291–312.
[119] U. Rester, W. Bode, C.A.M. Sampaio, E.A. Auerswald, A.P.Y. Lopes, Cloning, purification, crystallization and preliminary X-ray diffraction analysis of the antistasin-type inhibitor ghilanten (domain I) from Haementeria ghilianii in complex with porcine β-trypsin, Acta Crystallogr. Sect. D Biol. Crystallogr. 57 (2001)

1038–1041.
[120] V. Chopin, M. Salzet, J.L. Baert, F. Vandenbulcke, P.E. Sautiere, J.P. Kerckaert, J. Malecha, Therostasin, a novel clotting factor Xa inhibitor from the rhynchobdellid leech, Theromyzon tessulatum, J. Biol. Chem. 275 (2000) 32701–32707.
[121] A.M. Krezel, G. Wagner, J. Seymour-Ulmer, R.A. Lazarus, Structure of the RGD protein decorsin: conserved motif and distinct function in leech proteins that affect blood clotting, Science 264 (1994) 1944–1947.
[122] P. Mazur, W.J. Henzel, J.L. Seymour, R.A. Lazarus, Ornatins: potent glycoprotein IIb-IIIa antagonists and platelet aggregation inhibitors from the leech Placobdella ornata, Eur. J. Biochem. 202 (1991) 1073–1082.
[123] C. Söllner, R. Mentele, C. Eckerskorn, H. Fritz, C.P. Sommerhoff, Isolation and characterization of hirustasin, an antistasin-type serine-proteinase inhibitor from the medical leech Hirudo medicinalis, Eur. J. Biochem. 219 (1994) 937–943.
[124] D.R. Kim, K.W. Kang, Amino acid sequence of piguamerin, an antistasin-type protease inhibitor from the blood sucking leech Hirudo nipponia, Eur. J. Biochem. 254 (1998) 692–697.
[125] H. Il Jung, S. Il Kim, K.S. Ha, C.O. Joe, K.W. Kang, Isolation and characterization of guamerin, a new human leukocyte elastase inhibitor from Hirudo nipponia, J. Biol. Chem. 270 (1995) 13879–13884.
[126] H. Kim, T.T.T. Chu, D.Y. Kim, D.R. Kim, C.M.T. Nguyen, J. Choi, J.R. Lee, M.J. Hahn, K.K. Kim, The crystal structure of guamerin in complex with chymotrypsin and the development of an elastase-specific inhibitor, J. Mol. Biol. 376 (2008) 184–192.
[127] L.L. Zavalova, I.P. Baskova, S.A. Lukyanov, A.V. Sass, E.V. Snezhkov, S.B. Akopov, I.I. Artamonova, V.S. Archipova, V.A. Nesmeyanov, D.G. Kozlov, S.V. Benevolensky, V.I. Kiseleva, A.M. Poverenny, E.D. Sverdlov, Destabilase from the medicinal leech is a representative of a novel family of lysozymes, BBA - Protein Struct. Mol. Enzymol. 1478 (2000) 69–77.
[128] L.L. Zavalova, E.V. Kuzina, N.B. Levina, I.P. Baskova, Monomerization of fragment DD by destabilase from the medicinal leech does not alter the N-terminal sequence of the γ-chain, Thromb. Res. 71 (1993) 241–244.
[129] E. Fink, H. Rehm, C. Gippner, W. Bode, M. Eulitz, W. Machleidt, H. Fritz, The primary structure of Bdellin B-3 from the leech Hirudo medicinalis, Biol. Chem. 367 (1986) 1235–1242.
[130] F.J. Roters, E. Zebe, Protease inhibitors in the alimentary tract of the medicinal leech Hirudo medicinalis: in vivo and in vitro studies, J. Comp. Physiol. B. 162 (1992) 85–92.
[131] D. Reverter, J. Vendrell, F. Canals, J. Horstmann, F.X. Avilés, H. Fritz, C.P. Sommerhoff, A carboxypeptidase inhibitor from the medical leech Hirudo medicinalis: isolation, sequence analysis, cDNA cloning, recombinant expression, and characterization, J. Biol. Chem. 273 (1998) 32927–32933.
[132] J.L. Arolas, V. Castillo, S. Bronsoms, F.X. Aviles, S. Ventura, Designing out disulfide bonds of leech carboxypeptidase inhibitor: implications for its folding, stability and function, J. Mol. Biol. 392 (2009) 529–546.
[133] T.C. White, M.A. Berny, D.K. Robinson, H. Yin, W.F. DeGrado, S.R. Hanson, O.J.T. McCarty, The leech product saratin is a potent inhibitor of platelet integrin α2β1 and von Willebrand factor binding to collagen, FEBS J. 274 (2007) 1481–1491.
[134] W. Gronwald, J. Bomke, T. Maurer, B. Domogalla, F. Huber, F. Schumann, W. Kremer, F. Fink, T. Rysiok, M. Frech, H.R. Kalbitzer, Structure of the leech protein saratin and characterization of its binding to collagen, J. Mol. Biol. 381 (2008) 913–927.
[135] F. Faria, I.D.L.M. Junqueira-De-Azevedo, P.L. Ho, M.U. Sampaio, A.M. Chudzinski-Tavassi, Gene expression in the salivary complexes from Haementeria depressa leech through the generation of expressed sequence tags, Gene 349 (2005) 173–185.
[136] E. Fuller, B.R. Green, P. Catlin, O. Buczek, J.S. Nielsen, B.M. Olivera, G. Bulaj, Oxidative folding of conotoxins sharing an identical disulfide bridging framework, FEBS J. 272 (2005) 1727–1738.
[137] A.A. Tietze, D. Tietze, O. Ohlenschläger, E. Leipold, F. Ullrich, T. Kühl, A. Mischo, G. Buntkowsky, M. Görlach, S.H. Heinemann, D. Imhof, Structurally diverse μ-conotoxin PIIIA isomers block sodium channel $Na_v1.4$, Angew. Chem. Int. Ed. 51 (2012) 4058–4061.
[138] J.Y. Chang, Diverse pathways of oxidative folding of disulfide proteins: underlying causes and folding models, Biochemistry 50 (2011) 3414–3431.
[139] A.A. Paul George, P. Heimer, A. Maaß, J. Hamaekers, M. Hofmann-Apitius, A. Biswas, D. Imhof, Insights into the folding of disulfide-rich μ-conotoxins, ACS Omega 3 (2018) 12330–12340.
[140] A.M. Steiner, G. Bulaj, Optimization of oxidative folding methods for cysteine-rich peptides: a study of conotoxins containing three disulfide bridges, J. Pept. Sci. 17 (2011) 1–7.
[141] P. Heimer, A.A. Tietze, C.A. Bäuml, A. Resemann, F.J. Mayer, D. Suckau, O. Ohlenschläger, D. Tietze, D. Imhof, Conformational μ-conotoxin PIIIA isomers revisited: impact of cysteine pairing on disulfide-bond assignment and structure elucidation, Anal. Chem. 90 (2018) 3321–3327.
[142] Q. Zhu, S. Liang, L. Martin, S. Gasparini, A. Ménez, C. Vita, Role of disulfide bonds in folding and activity of leiurotoxin I: just two disulfides suffice, Biochemistry 41 (2002) 11488–11494.
[143] T.S. Han, M.M. Zhang, A. Walewska, P. Gruszczynski, C.R. Robertson, T.E. Cheatham, D. Yoshikami, B.M. Olivera, G. Bulaj, Structurally minimized μ-conotoxin analogues as sodium channel blockers: implications for designing conopeptide-based therapeutics, ChemMedChem 4 (2009) 406–414.
[144] J.L. Arolas, V. Castillo, S. Bronsoms, F.X. Aviles, S. Ventura, Designing out disulfide bonds of leech carboxypeptidase inhibitor: implications for its folding, stability and function, J. Mol. Biol. 392 (2009) 529–546.
[145] R. Yu, V.A.L. Seymour, G. Berecki, X. Jia, M. Akcan, D.J. Adams, Q. Kaas, D.J. Craik, Less is more: design of a highly stable disulfide-deleted mutant of analgesic cyclic α-conotoxin Vc1.1, Sci. Rep. 5 (2015) 13264.
[146] P. Han, K. Wang, X. Dai, Y. Cao, S. Liu, H. Jiang, C. Fan, W. Wu, J. Chen, The role of individual disulfide bonds of μ-conotoxin GIIIA in the inhibition of $Na_v1.4$, Mar. Drugs 14 (2016) 213.
[147] M. Böhm, Structure-activity-relationship studies on the factor XIIIa inhibitor tridegin, PhD Thesis, University of Bonn, 2015, p. 89.

4.1.3 Summary

The presented review summarizes the current state of FXIII inhibitor research.[27] It highlights the potential advantages of an appropriate FXIII inhibitor with respect to conventionally used inhibitors that directly or indirectly inhibit thrombin and subsequently inhibit fibrin formation. The individual FXIII(a) inhibitors are first divided into three classes: 1) inhibitors influencing the mechanism of FXIII-activation, 2) inhibitors that serve as co-substrates and thus prevent fibrin cross-linking and 3) molecules that block the active site of FXIIIa through a direct interaction. The third class is the most promising for the development of new FXIII(a) inhibitors.[27]

A further distinction is made between small molecules and peptidic inhibitors of FXIIIa. Despite their advantages in regard to their good inhibitory potential against FXIIIa, small molecule inhibitors such as cerulenin and alutacenoic acid A and B[180,322] are currently not further developed. The main reasons for this are their low selectivity towards other transglutaminases and their short half-lives in plasma.[180,322] Consequently, the focus of FXIII inhibitor design is currently laid on allosteric and peptide-based compounds, such as the allosteric inhibitor NSGM 13 and the peptidic inhibitors tridegin and ZED3197.[17,319,320]

The analysis of all known FXIII(a) inhibitors revealed that tridegin is very promising for the inhibitor development against FXIIIa. This is mainly attributed to its high potency and selectivity against FXIIIa.[11,12] A further advantage is that extensive studies have already been conducted with tridegin, providing a good basis for further investigations.[11,12,27,324] However, a clear drawback of tridegin is its complex synthesis.[12,13] For this reason, disulfide-deficient variants with better synthesizability were prepared. The synthesis, analytical characterizations as well as the functional analyses of the 2-disulfide-bonded tridegin analogs were part of the present thesis and will be described in detail in the next chapter.

4.2 Chapter II - Coagulation factor XIIIa inhibitor tridegin: On the role of disulfide bonds for folding, stability and function

Authors*

Charlotte A. Bäuml*, Thomas Schmitz*, Ajay Abisheck Paul George, Monica Sudarsanam, Kornelia Hardes, Torsten Steinmetzer, Lori A. Holle, Alisa S. Wolberg, Bernd Pötzsch, Johannes Oldenburg, Arijit Biswas, and Diana Imhof

This article was published in:
Journal of Medicinal Chemistry **2019**, 62, 3513-3523.
DOI: 10.1021/acs.jmedchem.8b01982

Preamble

To fulfil the regulations concerning a cumulative thesis at the Faculty of Mathematics and Natural Sciences at the University of Bonn, this chapter was written based on the publication "Coagulation factor XIIIa inhibitor tridegin: On the role of disulfide bonds for folding, stability and function" and is not presented in its original form, since the described publication has already been used in the dissertation of Dr. Ajay Abisheck Paul George. The latter was significantly involved in the computer-based methods in this work, whereas the experimental part was mainly performed by me. This chapter describes the major work on the 2-disulfide-bonded tridegin analogs that were investigated in more detail in order to optimize the lead structure tridegin. In this regard, the chapter describes the results of the syntheses as well as various structural and functional studies of the different disulfide-deficient analogs. Structurally, the chapter is organized into a brief introduction to this topic, the results section, with all the crucial results related to this dissertation, and a final summary. The methodology section of the publication discussed within this chapter is not rewritten as a part of this thesis. For a detailed description of the applied methods, I refer to the publication.

***Contribution**

TS and CAB contributed equally. The study has been designed by AB and DI. TS performed synthesis and analysis of the peptides. TS, CAB, KH, and TSt performed and analyzed the enzymatic activity assay. LAH and ASW designed, conducted, and analyzed the turbidity and whole blood contraction assays. MS, AAPG, and AB carried out the computational studies. Data analysis and interpretation was carried out by all authors. The manuscript was written through contributions of all authors. All authors have given approval to the final version of the manuscript.

4.2.1 Introduction

Cysteine-rich peptides occur in many organisms, as discussed in section 2.1, and exhibit a wide variety of biological functions.[2] These peptides are characterized by a large number of disulfide bonds with a distinct connectivity, which are crucial for the structure, stability, and biological activity. Several disulfide-bonded peptides, such as hirudin[358] and some conotoxins[359,360] exhibit high therapeutic potential for various diseases. Despite their therapeutic value, there is a major drawback to these peptides: each disulfide bond increases the synthetic complexity. Consequently, each additional disulfide bond negatively affected the yield due to the increased number of reaction and purification steps. As extensively discussed in the previous chapter, one of the most promising FXIIIa inhibitor drug candidates is the disulfide-bonded 66mer peptide tridegin from *H. ghilianii*.[11,12] However, the major obstacle hindering its therapeutic applicability is its synthesis. Considering that tridegin is capable of forming 3 disulfide bonds, synthesis of a single 3-disulfide-bonded tridegin isomer using Fmoc-based protecting group strategy is very tedious and resulted in only very low yields.[13] In an attempt to increase the synthetic yield, the peptide sequence was shortened and linear versions of tridegin (without disulfide bonds) were synthesized. However, all of these modifications resulted in a loss of activity towards FXIIIa.[324]

In this chapter a different strategy for the improvement of the tridegin synthesis is investigated. Disulfide-deficient variants that simplify the synthesis based on a reduced number of disulfide bonds were selectively synthesized.[17] It was anticipated that this approach would preserve activity as shown in other disulfide-deficient approaches.[7–10,53] For this purpose, the disulfide bond between Cys19 and Cys25, which appeared in all three discovered 3-disulfide-bonded isomers in the self-folding experiment of Böhm *et al.*[12], was omitted from tridegin[17]. Consequently, the three 2-disulfide-bonded tridegin variants without the disulfide bond between Cys19-Cys25, were used to investigate the influence of this disulfide bond for the peptide structures and the inhibitory potential towards FXIIIa. In addition, computer-based studies were conducted to gain insights into the structure-activity relationships.[17]

This chapter evaluates whether it is possible to improve the lead structure tridegin by following the disulfide-deficient approach. In this context, the three different 2-disulfide-bonded tridegin variants were prepared using Fmoc-based protecting group strategy and were structurally and functionally characterized by experimental and computational studies (Figure 12).[17]

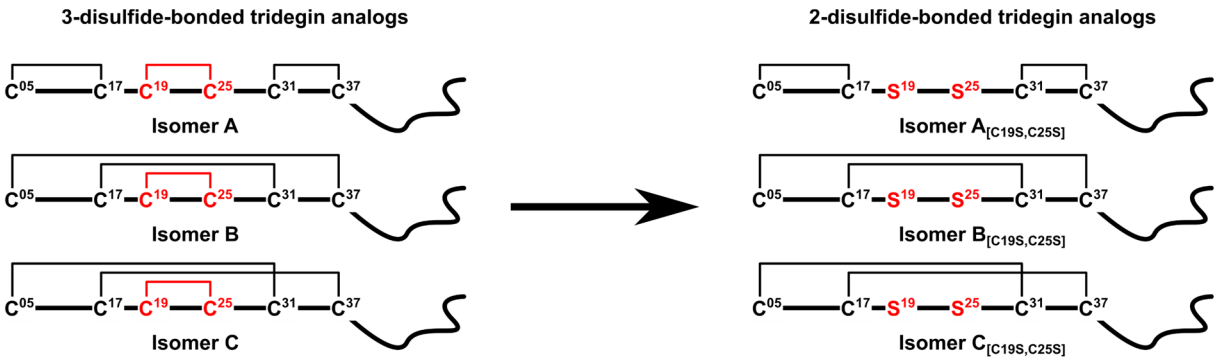

Figure 12: Disulfide bond connectivity of the 3-disulfide-bonded and the derived 2-disulfide-bonded variants synthesized and analyzed in this study.[17]

4.2.2 Results and discussion

Synthesis of the 2-disulfide-bonded tridegin variants

As stated above, based on the isomers A-C from the self-folding experiment, the three disulfide-deficient analogs $A_{[C19S,C25S]}$, $B_{[C19S,C25S]}$, and $C_{[C19S,C25S]}$ were synthesized using a Fmoc-based solid-phase peptide synthesis followed by selective oxidation of the disulfide bonds in solution (Figure 13). For this, acetamidomethyl (Acm) and trityl (Trt) protecting groups were used as orthogonal protecting groups for the selective oxidation of each disulfide bond. The cysteines that should form a disulfide bond were equipped with the same protecting group. In addition, to avoid formation of the third disulfide bond, the cysteines at positions 19 and 25 were replaced by serines.[17]

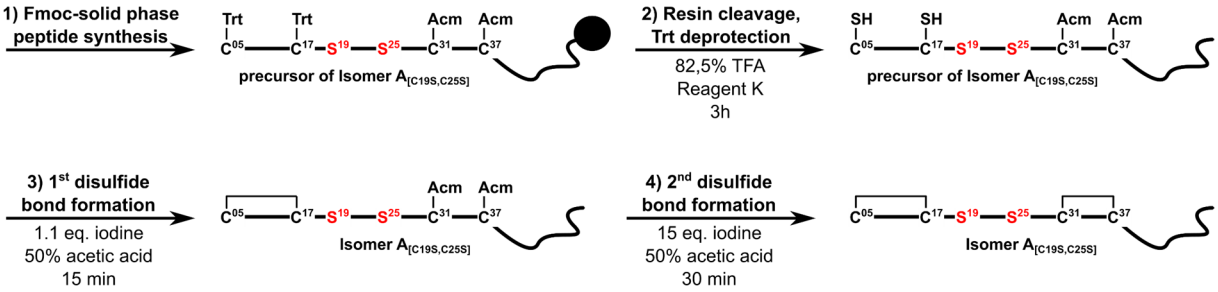

Figure 13: Synthesis strategy of the 2-disulfide-bonded tridegin variants. As representative, the strategy of isomer $A_{[C19S,C25S]}$ is shown.[17]

This resulted in the following pattern on the resin after SPPS: Cys05(Trt), Cys17(Trt), Ser19, Ser25, Cys31(Acm), Cys37(Acm) for $A_{[C19S,C25S]}$, Cys05(Trt), Cys17(Acm), Ser19, Ser25, Cys31(Acm), Cys37(Trt) for $B_{[C19S,C25S]}$, and Cys05(Trt), Cys17(Acm), Ser19, Ser25, Cys31(Trt), Cys37(Acm) for $C_{[C19S,C25S]}$ (Figure 13, 1).[17] The removal of the two protecting groups, as well as the oxidations of the individual disulfide bonds, was carried out sequentially in solution. The thiol functions of the Trt-protected cysteines were already exposed upon cleavage of the peptide chain from the resin due to the acidic conditions (Figure 13, 2). The subsequent stepwise oxidation was then conducted via a one-pot reaction. The peptides were dissolved at a concentration of 0.05 mM to avoid intermolecular reactions, while addition of a small excess of iodine (1.1 eq.) initialized the first oxidation (Figure 13, 3). Thereby, the cysteines, which were already unprotected, formed the first disulfide bond. After complete oxidation of the first disulfide bond, the addition of 13.9 eq. iodine led to the deprotection of the Acm-protected cysteines and the formation of the second disulfide bond (Figure 13, 4).[17,361] The reaction was terminated by two different approaches: 1) by the addition of an excess of ascorbic acid or 2) by the removal of iodine by extraction. The comparison of the two termination variants revealed that more by-products occur during the termination with ascorbic acid. These by-products could be a result of iodination or oxidation of other side chains, such as methionine, which may have been triggered by remaining iodine in the reaction solution after ascorbic acid termination and lyophilization.[17,47] The oxidation strategy, in which the one-pot reaction was aborted by iodine extraction, proved to be more promising, which was also evident in the yields after final purification by RP-HPLC. In this case, starting from the precursor material used in the one-pot reaction, yields of 33% for isomer $B_{[C19S,C25S]}$ with bridging Cys05-Cys37, Cys17-Cys31, 14% for isomer $A_{[C19S,C25S]}$ (Cys05-Cys17, Cys31-Cys37) and 19% for isomer $C_{[C19S,C25S]}$ (Cys05-Cys31, Cys17-Cys37) could be achieved (Figure 14A).[17] Comparatively, the yields of the peptides obtained via ascorbic acid termination and the

selectively synthesized 3-disulfide-bonded isomers (chapter III) were all below 10%.[13,17] This demonstrates the improved synthesizability of the isomers via this strategy with isomer $B_{[C19S,C25S]}$ showing the best synthesis results with a yield of 33%.[17]

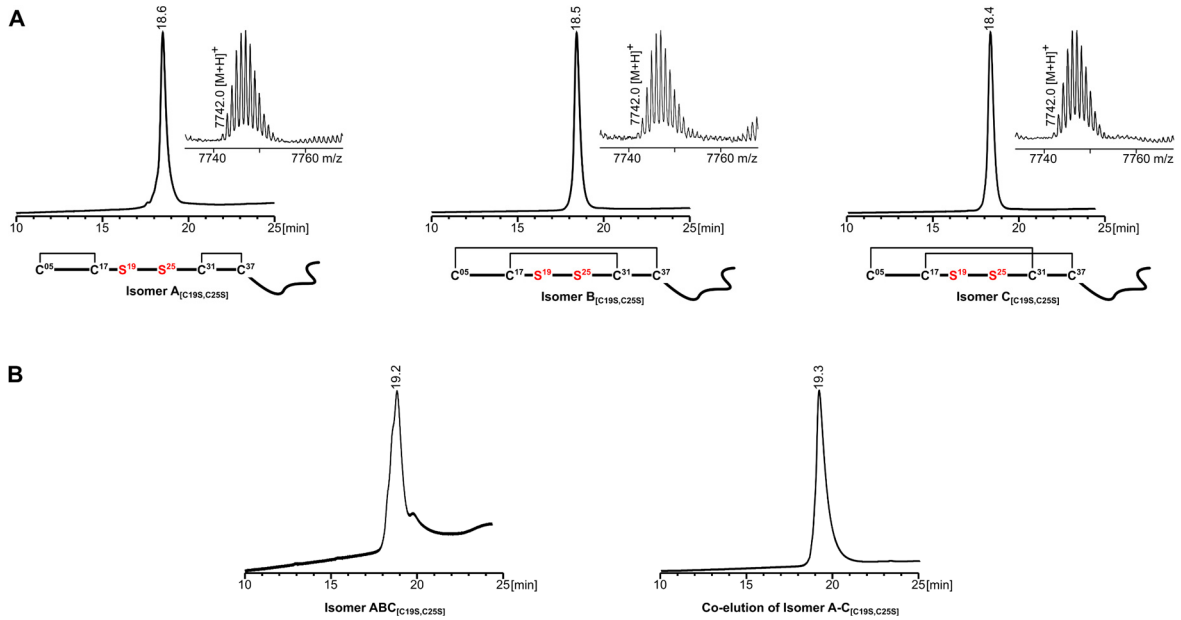

Figure 14: **A**: HPLC profiles of the purified tridegin analogs **$A_{[C19S,C25S]}$-$C_{[C19S,C25S]}$** as well as the corresponding MALDI-TOF mass spectra. **B**: RP-HPLC profile of the mixture **$ABC_{[C19S,C25S]}$** from the self-folding approach as well as RP-HPLC co-elution profile of the purified tridegin analogs **$A_{[C19S,C25S]}$-$C_{[C19S,C25S]}$** in an equimolar mixture. The RP-HPLC elution was performed using a gradient of 20-50% eluent B (0.1% TFA in MeCN; eluent A: 0.1% TFA in H_2O) in 30 min.[17]

In addition to the selective syntheses of the individual isomers, a mixture of disulfide-deficient isomers ($ABC_{[C19S,C25S]}$) was also prepared via a self-folding experiment.[17] The same procedure was followed as previously done in the self-folding experiment of the 3-disulfide-bonded tridegin analogs.[12] As a modification, Cys19 and Cys25 were replaced by serines and no isopropanol was added to the system during buffer oxidation due to the good solubility of the peptide precursor in water.[17] The analysis of the self-folding experiment by HPLC resulted in only one peak, which does not necessarily imply that only one isomer was generated (Figure 14B). Indeed, the self-folding experiment of Böhm *et al.*[12] as well as other studies of µ-PIIIA isomers[6] demonstrated that one peak in the HPLC can also comprise more than one isomer as result of similar physicochemical properties. In this context, an elution profile of an equimolar mixture of the three 2-disulfide-bonded tridegin variants $A_{[C19S,C25S]}$-$C_{[C19S,C25S]}$ was also investigated on an analytical RP-HPLC (Figure 14B). Thereby, the mixture yielded a single peak at a retention time of 19.3 min. This indicates that the isomers have similar physicochemical properties and, consequently, that more than one of these isomers may be present in the mixture of the self-folding experiment ($ABC_{[C19S,C25S]}$). For this reason, the mixture $ABC_{[C19S,C25S]}$ and also the selectively prepared isomers $A_{[C19S,C25S]}$-$C_{[C19S,C25S]}$ were examined for their disulfide bond connectivities.[17]

Analysis of the disulfide bond connectivities

The disulfide bond connectivities were elucidated by MS/MS analysis of a chymotryptic digest, as already applied by Böhm *et al*.[12] The confirmation of the disulfide bond connectivities of the isomers $A_{[C19S,C25S]}$-$C_{[C19S,C25S]}$ was performed by analyzing the digest of the fully oxidized products as well as the linear precursors. The linear precursors confirmed the correct position of the Acm-protecting groups upon LC-ESI-MS/MS sequencing. In addition, digestion of the oxidized samples identified fragments by LC-ESI-MS and -MS/MS that were linked by the expected disulfide bonds of the isomers. Moreover, by reducing these fragments (2 fragments linked via a disulfide bond) with Dithiothreitol (DTT), the mass of the bridged fragments could no longer be detected in LC-ESI-MS, whereas the masses of the two individual fragments appeared. As example for isomer $B_{[C19S,C25S]}$, the disulfide bonds Cys05-Cys37 and Cys17-Cys31 could be identified thereby confirming the disulfide bond connectivity (Figure 15).[17] Thus, the disulfide bond connectivity of the three isomers $A_{[C19S,C25S]}$-$C_{[C19S,C25S]}$ was verified.

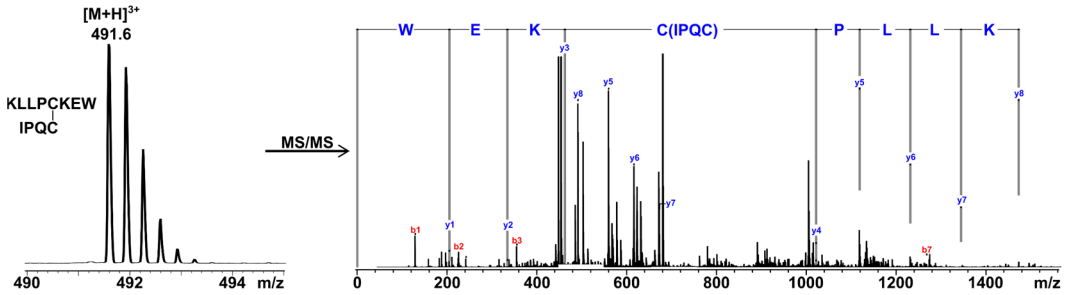

Figure 15: Analysis of the disulfide bond Cys05-Cys37 of isomer $B_{[C19S,C25S]}$. The MS and MS/MS analysis of the disulfide-bonded fragment KLLPCKEW-IPQC confirm the disulfide bond between Cys05 and Cys37.[17]

In addition, all three isomers $A_{[C19S,C25S]}$-$C_{[C19S,C25S]}$ were identified via specific disulfide-bonded fragments within the mixture $ABC_{[C19S,C25S]}$ of the self-folding experiment.[17]

Fluorogenic FXIIIa activity assay

Subsequently, the question whether the disulfide bond between Cys19 and Cys25 is significant for the activity of the tridegin variants was investigated. Therefore, the inhibitory potential of the isomers $A_{[C19S,C25S]}$-$C_{[C19S,C25S]}$ as well as of $ABC_{[C19S,C25S]}$ towards FXIIIa was analyzed using the fluorogenic FXIIIa assay that has been already applied for other tridegin variants.[12,17] As controls, the mixture of isomers A-C from the self-folding experiment (ABC, very active positive control[12]) as well as a linear tridegin variant (all-Ser, less active positive control[12]) in which all cysteines were mutated to serines were used.[12,17] Within the measurements, all disulfide-deficient variants exhibit stable inhibition towards FXIIIa, with IC_{50} values of 0.55 ± 0.05 µM (n=4) for isomer $A_{[C19S,C25S]}$ (Figure 16A), 0.50 ± 0.05 µM (n=3) for isomer $B_{[C19S,C25S]}$ (Figure 16B), 0.48 ± 0.06 µM (n=4) for isomer $C_{[C19S,C25S]}$ (Figure 16C), and 0.51 ± 0.02 µM (n=2) for $ABC_{[C19S,C25S]}$ (Figure 16D). In comparison with ABC (0.45 ± 0.03 µM (n=3)) and All-Ser (0.72 ± 0.05 µM (n=4), it was demonstrated that all disulfide-deficient tridegin variants yielded only in a minor loss of activity with respect to ABC (Figure 16E).[17] Accordingly, these results indicate that the disulfide bond between Cys19 and Cys25 does not exert a significant impact on the activity towards FXIIIa, and therefore should preferably be omitted in future tridegin variants due to the improved synthesizability.[17]

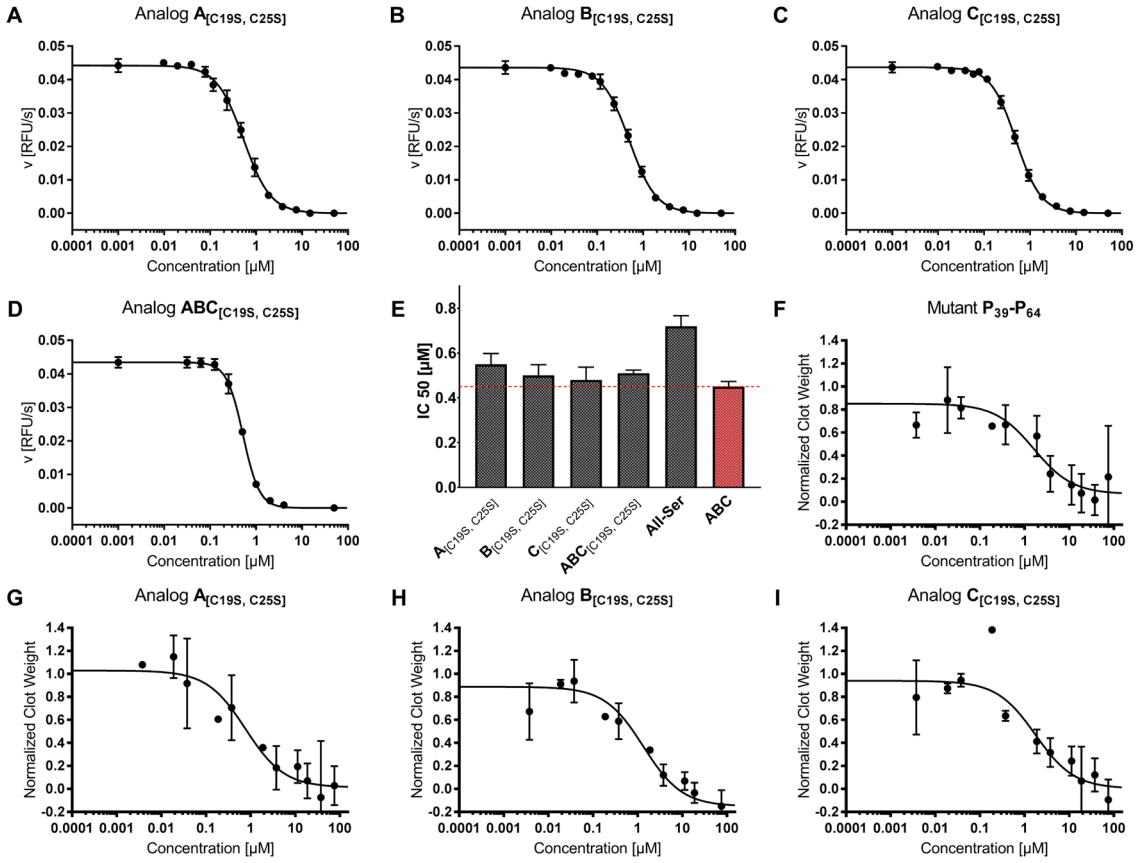

Figure 16: Activity assays of the different disulfide-bonded tridegin variants. **A-E** show the results from the fluorogenic FXIIIa activity assay, whereas **F-I** show the IC_{50} plots of the whole blood clot contraction assay. **A**: IC_{50} plot of isomer $A_{[C19S,C25S]}$; **B**: IC_{50} plot of isomer $B_{[C19S,C25S]}$ **C**: IC_{50} plot of isomer $C_{[C19S,C25S]}$; **D**: IC_{50} plot of isomer $ABC_{[C19S,C25S]}$; **E**: bar chart with the averaged IC_{50} values in comparison to the controls All-Ser and ABC (dashed red line: IC_{50} value of ABC). **F**: IC_{50} plot of isomer [P_{38}-P_{64}]; **G**: IC_{50} plot of isomer $A_{[C19S,C25S]}$; **H**: IC_{50} plot of isomer $B_{[C19S,C25S]}$; **I**: IC_{50} plot of isomer $C_{[C19S,C25S]}$.[17]

Whole blood clot contraction assay

In addition to the FXIIIa activity studies, the isomers $A_{[C19S,C25S]}$-$C_{[C19S,C25S]}$ were assayed for their inhibitory potential against FXIIIa in whole (human) blood samples in the group of Prof. Dr. Alisa Wolberg (Figure 16F-I).[17] Due to the high amount of substance required for these studies, the truncated tridegin fragment P_{39}-P_{64}[324], which was examined in previous studies, was used as a control.[324] The assay relies on the fact that active FXIIIa exerts a critical influence on red blood cell retention in contracted whole blood clots.[123,135] Thereby, FXIIIa contributes crucially to the size of the whole blood clot. However, if FXIIIa is inhibited, fewer red blood cells are deposited in the whole blood clot, which can subsequently be determined with the individual clot weights.[123] The addition of the individual tridegin variants $A_{[C19S,C25S]}$-$C_{[C19S,C25S]}$ and P_{39}-P_{64} resulted in a clot weight reduction with IC_{50} values of 0.7 ± 0.4 µM for $A_{[C19S,C25S]}$ (Figure 16G), 1.1 ± 0.1 µM for $B_{[C19S,C25S]}$ (Figure 16H), 2.3 ± 2.2 µM for $C_{[C19S,C25S]}$ (Figure16I), and 2.2 ± 2.0 µM for P_{39}-P_{64} (Figure 16F) (n=3).[17] Accordingly, all peptides revealed an effect on red blood cell retention in whole blood clots, which is why it could be proved that the isomers also exert an inhibitory potential towards FXIIIa in human blood.[17] To further exclude the possibility that these FXIIIa inhibitors do not interact with other blood coagulation factors, the processes of secondary haemostasis (on which FXIIIa has no influence) were analyzed by a turbidity assay.[17] This revealed no effects of the individual

variants on fibrin formation kinetics or final clot turbidity in plasma. This indicates that the weight loss of whole blood clots was caused exclusively by the interaction of the tridegin variants with FXIIIa.[17]

Molecular dynamics simulations and docking studies

Since the computer-based studies were part of the dissertation of Dr. Ajay Abisheck Paul George, I will mainly focus on the results and the comparison with the experimentally determined data rather than on the methodology of the studies herein. The detailed information can be found in the publication Bäuml, Schmitz *et al*.[17] As already described, the isomers did not show any differences within the activity studies, which is surprising since usually different disulfide bond connectivities lead to distinct conformations, which in turn ought to show dissimilar activities.[6,54] By using computer-based molecular dynamics (MD) and docking studies, it should be investigated why the isomers display similar activities. Due to the lack of NMR or X-ray crystallography structures, the individual tridegin variants were calculated using existing theoretically determined structures of the isomers A-C.[12] In each case, two variants were calculated in which, on the one hand, the bond between Cys19 and Cys25 was kept open *in silico* (Figure 17A) and, on the other hand, the Cys was mutated by Ser as done in the experimentally synthesized isomers (Figure 17B).[17] The comparison of the obtained variants with the initial structures of the 3-disulfide-bonded tridegin isomers[12] showed that the removal of the disulfide bond Cys19-Cys25 does not significantly affect the structural integrity of the disulfide-bonded N-terminal region (1-37). Exclusively the conformation of the C-terminal region (38-66) is significantly changed to some extent by the loss of the disulfide bond, which is more due to the high flexibility of the C-terminal part and less to the loss of the disulfide bond. This implies overall that the removal of the disulfide bond Cys19-Cys25 does not promote unfolding or structural disruption of the peptides, for which reason the peptides demonstrate little loss of activity towards FXIIIa.[17]

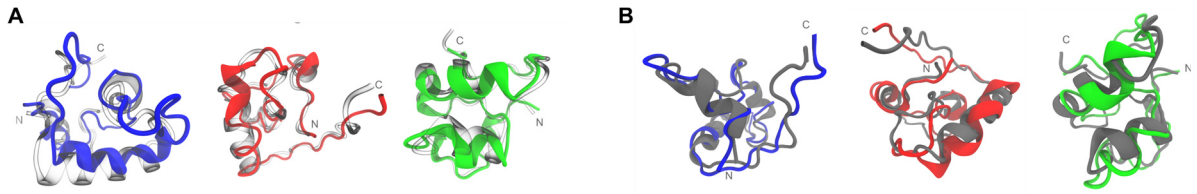

Figure 17: Simulated structures of different 2-disulfide-bonded tridegin variants. **A**: Simulated structures of isomer A (blue), B (red) and C (green) with *in silico* removal of the disulfide bond Cys19-Cys25 superimposed on their respective starting structures (transparent). **B**: Simulated structures of $A_{[C19S,C25S]}$ (blue), $B_{[C19S,C25S]}$ (red), and $C_{[C19S,C25S]}$ (green) superimposed on their respective parent 3-disulfide bonded isomers A-C (grey cartoons).[12] All simulated structures presented here refer to the energy-minimized structures of the final snapshot in the 300 ns MD simulation.[17]

The subsequent docking studies on which the MD simulated structures of the 3- and 2-disulfide-bonded tridegin variants were docked to FXIIIa° (PDB ID: 4KTY[148]) revealed that all best dock conformations bound in the same FXIIIa region as isomers A and B described in earlier studies (Figure 18).[12] Even isomer $C_{[C19S,C25S]}$ interacts with FXIIIa at the same site, located near the catalytically active Cys314 of FXIIIa, although the 3-disulfide-bonded isomer C investigated earlier docked far away from the active site.[12] In summary, it was shown for the isomers $A_{[C19S,C25S]}$-$C_{[C19S,C25S]}$, that multiple conformations of the three isomers bind nonspecifically near the active site of FXIIIa and thereby probably block the active site for

substrates in a similar manner. In this context, it was assumed that the isomers $A_{[C19S,C25S]}$-$C_{[C19S,C25S]}$ do not directly interact with the amino acid residues of FXIIIa that are important for the activity. Consequently, the docking studies provided the visual explanations for the experimentally obtained result, demonstrating that all three isomers $A_{[C19S,C25S]}$-$C_{[C19S,C25S]}$ possess similar inhibitory activities.[17]

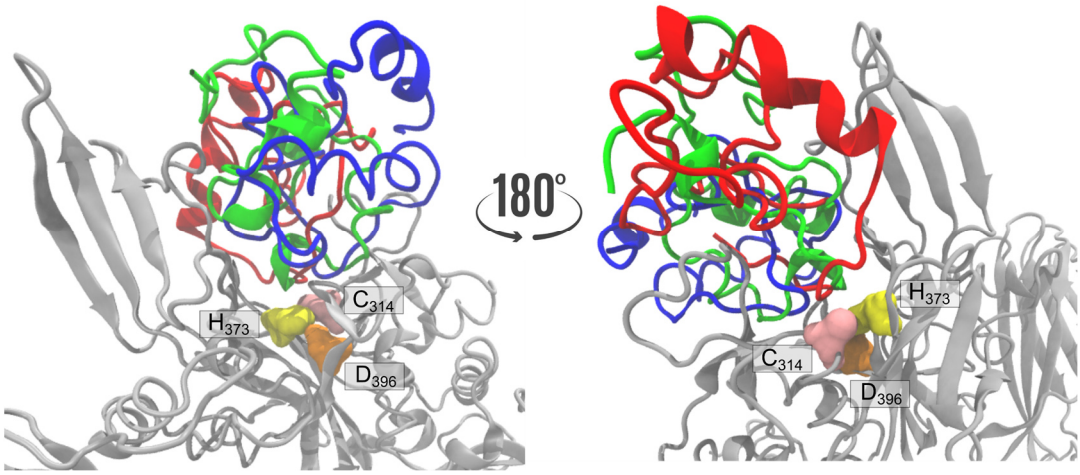

Figure 18: Docking of all the different 2-disulfide bonded tridegin variants on the crystal structure of FXIIIa° (PDB ID: 4KTY[148]). Two 180° rotated orientations of the docked poses of isomer $A_{[C19S,C25S]}$ (blue), $B_{[C19S,C25S]}$ (red) and $C_{[C19S,C25S]}$ (green) on FXIIIa° are shown. The isomers docked in close proximity to the catalytic triad of FXIIIa, Cys314 (pink), His373 (yellow), and Asp396 (orange).[17]

4.2.3 Summary

In summary, this study analyzed the impact of the disulfide bond Cys19-Cys25 for the inhibitory potential of tridegin towards FXIIIa. For this purpose, different 2-disulfide-bonded tridegin variants ($A_{[C19S,C25S]}$-$C_{[C19S,C25S]}$, $ABC_{[C19S,C25S]}$) were prepared and investigated via a fluorogenic activity assay and a whole blood clot contraction assay.[17] In both assays, a similar inhibitory potential of all three isomers $A_{[C19S,C25S]}$-$C_{[C19S,C25S]}$ towards FXIIIa was observed. In addition, the isomers $A_{[C19S,C25S]}$-$C_{[C19S,C25S]}$ as well as $ABC_{[C19S,C25S]}$ showed no loss of activity in the fluorogenic activity assay compared to the 3-disulfide-bonded mixture ABC.[12,17] This indicates that the disulfide bond Cys19-Cys25 appears to have little impact on the inhibitory potential towards FXIIIa.[17] In addition, the disulfide bond connectivity of the remaining disulfide bonds also seems not to be crucial for the activity. This could be explained by the fact that the N-terminal part containing the disulfide bonds mediates the binding of tridegin to FXIIIa and the C-terminal fragment is exclusively responsible for the inhibitory action of tridegin.[12] Moreover, due to the preserved activity of the disulfide-deficient isomer $A_{[C19S,C25S]}$-$C_{[C19S,C25S]}$ and the simplified synthesis, the presented tridegin variants could serve in future as useful tools for research on FXIIIa or as lead structures for the development of new anticoagulants. In this context, isomer $B_{[C19S,C25S]}$ should be mentioned as the most promising isomer, as it exhibits similar activities to all other isomers towards FXIIIa and simultaneously provided the best synthesis results.[17]

The study already demonstrated the high potential of the disulfide-deficient tridegin variants.[17] The improved synthesizability enables more studies in the following, which will be described in more detail in chapters III and IV.[13,18] However, what was missing at this time was the individual comparison with the 3-disulfide-bonded tridegin isomers. In Chapter III, the synthesis of 5 3-disulfide-bonded tridegin variants is described, where 3 of the 5 isomers were isomers A-C obtained from the self-folding experiment. As a consequence, this study allowed the direct comparison of the selectively synthesized 2- and 3-disulfide-bonded tridegin variants for the first time.[13] Furthermore, the study presented in this chapter was complemented by specificity studies towards another transglutaminase, TGase 2.[13]

4.3 Chapter III - Distinct 3-disulfide-bonded isomers of tridegin differentially inhibit coagulation factor XIIIa: The influence of structural stability on bioactivity

Authors*

Charlotte A. Bäuml, Ajay Abisheck Paul George, Thomas Schmitz, Paul Sommerfeld, Markus Pietsch, Lars Podsiadlowski, Torsten Steinmetzer, Arijit Biswas, and Diana Imhof

This article was published in:
European Journal of Medicinal Chemistry **2020**, 201, 112474.
DOI: 10.1016/j.ejmech.2020.112472

4.3.1 Introduction

The results of the 2-disulfide-bonded isomers (see section 4.3.2) were very promising and demonstrated only a slight loss of activity compared to the mixture ABC obtained from a self-folding experiment.[17] However, since the individual 3-disulfide-bonded tridegin isomers could not be separated from each other,[12] direct comparison of the 2-disulfide-bonded tridegin isomers with their corresponding 3-disulfide-bonded variants has not been performed yet. This chapter III describes the individual synthesis, analytical and functional characterizations of the three 3-disulfide-bonded isomers A, B and C as well as two additional isomers D and E.[13] Their activities towards FXIIIa were compared with the 2-disulfide-bonded isomers (chapter II). To investigate the specificity of the tridegin variants in comparison to other transglutaminases, the inhibitory potential towards TGase 2 was analyzed. Therefore, one 2- ($ABC_{[C19S,C25S]}$) and one 3-disulfide-bonded tridegin (isomer B) variant were tested as representatives. Furthermore, genome sequencing of *H. ghilianii* was conducted in a renewed attempt to fully confirm the native primary amino acid sequence of tridegin. Along with the experimental studies, computer-based studies were also performed to derive structure-activity relationships. To accomplish that, docking studies with FXIIIa and the individual 3-disulfide-bonded isomers were conducted to explain the results from the activity studies.[13]

***Contributions:**

The study has been designed by AB and DI. CAB performed synthesis and analysis of the peptides. AAPG and AB carried out the computational studies. CAB, TS, and TSt performed and analyzed the FXIIIa isopeptidase activity assay. PS and MP performed and analyzed the FXIIIa and TGase 2 transamidase activity assays. LP and CAB identified tridegin in genomic DNA of *H. ghilianii*. AB and DI analyzed and interpreted all data. The manuscript was written through contributions of all authors. All authors have given approval to the final version of the manuscript.

4.3.2 Article

On the following pages, the article is printed in its published form with permission of Elsevier Masson SAS, Amsterdam, Netherlands.

European Journal of Medicinal Chemistry 201 (2020) 112474

Contents lists available at ScienceDirect

European Journal of Medicinal Chemistry

journal homepage: http://www.elsevier.com/locate/ejmech

Research paper

Distinct 3-disulfide-bonded isomers of tridegin differentially inhibit coagulation factor XIIIa: The influence of structural stability on bioactivity

Charlotte A. Bäuml [a], Ajay Abisheck Paul George [a], Thomas Schmitz [a], Paul Sommerfeld [b], Markus Pietsch [b], Lars Podsiadlowski [c], Torsten Steinmetzer [d], Arijit Biswas [e], Diana Imhof [a, *]

[a] Pharmaceutical Biochemistry and Bioanalytics, Pharmaceutical Institute, University of Bonn, An der Immenburg 4, D-53121, Bonn, Germany
[b] Institute II of Pharmacology, Center of Pharmacology, Medical Faculty, University of Cologne, Gleueler Str. 24, D-50931, Cologne, Germany
[c] Center for Molecular Biodiversity Research (ZMB), Zoological Research Museum Alexander Koenig (ZFMK), Adenauerallee 160, D-53113, Bonn, Germany
[d] Institute of Pharmaceutical Chemistry, Philipps University of Marburg, Marbacher Weg 6, D-35032, Marburg, Germany
[e] Institute of Experimental Hematology and Transfusion Medicine, University Hospital Bonn, Sigmund-Freud-Str. 25, D-53127, Bonn, Germany

ARTICLE INFO

Article history:
Received 6 March 2020
Received in revised form
14 May 2020
Accepted 15 May 2020
Available online 23 May 2020

Keywords:
Coagulation factor XIIIa
Transglutaminase
Peptide inhibitor
Disulfide bridge
Protein folding
Cysteine-rich

ABSTRACT

Tridegin is a 66mer cysteine-rich coagulation factor XIIIa (FXIIIa) inhibitor from the giant amazon leech *Haementeria ghilianii* of yet unknown disulfide connectivity. This study covers the structural and functional characterization of five different 3-disulfide-bonded tridegin isomers. In addition to three previously identified isomers, one isomer containing the inhibitory cystine knot (ICK, *knottin*) motif, and one isomer with the leech antihemostatic protein (LAP) motif were synthesized in a regioselective manner. A fluorogenic enzyme activity assay revealed a positive correlation between the constriction of conformational flexibility in the N-terminal part of the peptide and the inhibitory potential towards FXIIIa with clear differences between the isomers. This observation was supported by molecular dynamics (MD) simulations and subsequent molecular docking studies. The presented results provide detailed structure-activity relationship studies of different tridegin disulfide isomers towards FXIIIa and reveal insights into the possibly existing native linkage compared to non-native disulfide tridegin species.

1. Introduction

As the leading cause of death worldwide, cardiovascular diseases (CVDs) account for 17.9 million deaths per year (31%) [1]. The underlying pathology of CVDs including ischemic heart disease, ischemic stroke, and venous thromboembolism is the formation of a thrombus following events of blood coagulation [2]. The very last step of this complex clotting system – the cross-linking of fibrin to a stable crosslinked fibrin clot – is achieved by the activated blood coagulation factor XIIIa (FXIIIa) [3].

Unlike all other enzymatically active blood coagulation factors, which are serine proteases, FXIIIa is a transglutaminase that crosslinks glutamine and lysine residues of proteins via isopeptide bonds [3]. Furthermore, FXIIIa plays a crucial role in wound healing and is linked to a plethora of different physiological processes like angiogenesis, bone biology [4], immunological processes [5,6], energy metabolism [7], and pregnancy [8]. FXIII occurs in two different forms: The cellular FXIII (cFXIII) is composed of an A_2 homodimer, whereas an A_2B_2 hetero-tetramer constitutes the plasma FXIII (pFXIII) [3]. pFXIII is expressed as zymogen and proteolytically activated by thrombin leading to the release of an activation peptide [3,9]. Upon cleavage, the FXIII-A subunits undergo structural changes, detach from the FXIII-B subunits, and dissociate into monomers [10–14]. The FXIII-B subunits have regulatory and carrier functions [15–18], whereas the FXIII-A subunits harbor the catalytic triad consisting of Cys314, His373, and Asp396 [19]. Calcium binding to FXIII also plays an important role for FXIII activation as well as its structure and function [10,14].

Several studies have demonstrated the importance of FXIII in the formation and stability of blood clots and hence in the onset of venous thrombosis [20–24]. On the one hand, timely activation of

* Corresponding author.
E-mail address: dimhof@uni-bonn.de (D. Imhof).

https://doi.org/10.1016/j.ejmech.2020.112474
0223-5234/

Abbreviations

APBS	Adaptive Poisson-Boltzmann Solver
Acm	acetamidomethyl
CVD	cardiovascular disease
DMC	*N*,*N*-dimethylcasein
DMF	dimethylformamide
DMSO	dimethyl sulfoxide
DTT	dithiothreitol
ESI	electrospray ionization
FXIII	blood coagulation factor XIII
FXIIIa	activated FXIII
GPU	graphical processing unit
H. depressa	*Haementeria depressa*
H. ghilianii	*Haementeria ghilianii*
HPLC	high performance liquid chromatography
MALDI	matrix-assisted laser desorption/ionization
MD	molecular dynamics
MEP	molecular electrostatic potential
MOPS	4-morpholino-propanesulfonic acid
MS	mass spectrometry
Rg	radius of gyration
R-I-Cad	rhodamine B-isonipectoyl-cadaverine
RMSD	root-mean square deviation
RMSF	per-residue root mean square fluctuation
SASA	solvent-accessible surface area
*t*Bu	*tert*-butyl
tris	tris(hydroxymethyl)aminomethane
Trt	trityl

FXIII seems to play a critical role in red blood cell retention and thus in thrombus size during thrombus formation [25]. On the other hand, FXIII-mediated crosslinking of fibrin increases clot rigidity and stability rendering the clot less susceptible to fibrinolysis [26]. Furthermore, Byrnes *et al.* demonstrated the FXIII-B subunit-dependent acceleration of zymogen FXIII-A_2B_2 activation by binding of fibrinogen gamma-chain residues 390 to 396 to FXIII-A_2B_2 [27].

While the therapeutic potential of targeting FXIIIa is clearly evident, drugs inhibiting FXIIIa are yet to be developed [24]. A major challenge in FXIIIa drug design is the close relation of FXIII to tissue transglutaminase 2 (TGase2). TGase2 is a ubiquitously expressed enzyme involved in many different physiological processes like migration, differentiation, and cell death [28]. Hence, to reduce the risk of extensive side effects, selective activity of an inhibitor towards FXIIIa is highly desirable. Several non-peptidic [29–32] as well as peptide-derived [33–35] FXIIIa inhibitors have been studied so far. Recently, the peptidomimetic FXIIIa inhibitor ZED3197 showed promising results in *in vitro* and *in vivo* studies [36]. In addition, sulfated glucosaminoglycans (GAG) and non-saccharide GAG mimetics (NSGM) have been studied as potential allosteric FXIIIa inhibitors by Al-Horani and co-workers [37]. Nonetheless, most of these FXIIIa inhibitors do not distinguish well between FXIII and TGase2 (or other transglutaminases like TGase6) or show rather short half-lives in *in vivo* models [31,32,36–40].

Tridegin is a 66mer oligopeptide naturally produced by the giant amazon leech *Haementeria ghilianii* (*H. ghilianii*). Tridegin was first isolated and characterized in 1997 and inhibits FXIIIa with great potency, whereas it is described to affect guinea pig tissue transglutaminase to a much lower extent [41]. Previous work by our group started to elucidate structure-function relationships of this peptide using chemically modified tridegin variants as well as biochemical and computational tools [42,43]. The interaction site of tridegin with FXIIIa was narrowed down to a C-terminal sequence around Gln52 (Q52) [42]. Furthermore, a moderate influence of the three disulfide bonds located within the N-terminal region on the peptide's inhibitory activity was suggested [43]. Tridegin is composed of two functionally different segments: The C-terminal part (residues 38-66) is responsible for inhibitory action at the catalytic triad of FXIIIa, whereas the N-terminal fragment (residues 1-37) is essential for peptide stability and contributes to the binding affinity to the target enzyme [42,43]. In addition, we could demonstrate that the synthetically produced tridegin obtained from a self-folding approach consists of three different 3-disulfide-bonded isomers (out of 15 theoretically possible isomers). Since structural information of tridegin from NMR or X-ray analysis is still missing due to the complexity and flexibility of the molecule, the three structures were modeled and subjected to molecular docking studies with the known FXIIIa structure [19,43]. These studies suggested different inhibitory activities of the individual isomers, although they share a common property, namely the middle disulfide bond C19–C25 [43]. The consequent analysis of all possible 2-disulfide-bonded isomers (globular, ribbon, and bead structure) lacking the middle disulfide bond demonstrated its role in folding, stability, and function of tridegin. At the same time, the synthesis of active tridegin variants could be enormously facilitated and accelerated [44].

In contrast, the separation of the three aforementioned 3-disulfide-bonded tridegin isomers could not be achieved by conventional HPLC methods so far, which hampers the further strategic approach to drug development based on the native lead [43]. Hence, experimental data on the inhibitory potential of the individual isomers are still missing. In an attempt to fill this gap in tridegin-related research, our present study focuses on the complex regioselective synthesis and subsequent functional and structural analysis of five different 3-disulfide-bonded tridegin isomers. Earlier studies on 3-disulfide-bonded conotoxin peptide isomers revealed that a different disulfide connectivity within the same sequence leads to deviating activity towards the respective biological target [45–49]. Moreover, a systematic targeted synthesis of all possible fifteen 3-disulfide-bonded isomers of a cysteine-rich peptide has been proven to be highly challenging [50]. At the same time, it was found that not all of the possible isomers possess a considerable biological activity [49]. In particular, all variants possessing a disulfide bond at either terminus showed an increased flexibility (independent of the two other bonds) and, in turn, less bioactivity [49,50]. As a consequence of the observed deviating activity of different disulfide isomers, and due to the much higher complexity of the synthesis of a 66mer multiply-bridged peptide, only five out of the fifteen possible disulfide isomers were selected for regioselective synthesis in the present study. In addition to the three previously identified tridegin isomers, i.e. isomers **A**-**C** (Fig. 1), the inhibitory cysteine-knot-motif (ICK, *knottin*) carrying isomer **D** as well as an isomer possessing the connectivity of the leech antihemostatic protein (LAP) [51,52] motif (isomer **E**) – known from e.g. hirudin – were produced. These isomers were analyzed (chemically and biologically) as supposedly rigid (**D**) and flexible (**E**) folds, respectively (Fig. 1). Molecular dynamics (MD) simulations and docking studies of complexes with FXIIIa were performed to complement the experimental data of the five isomers and to derive more detailed structure-activity relationships for an in-depth analysis of tridegin action on FXIIIa. In addition, the latter

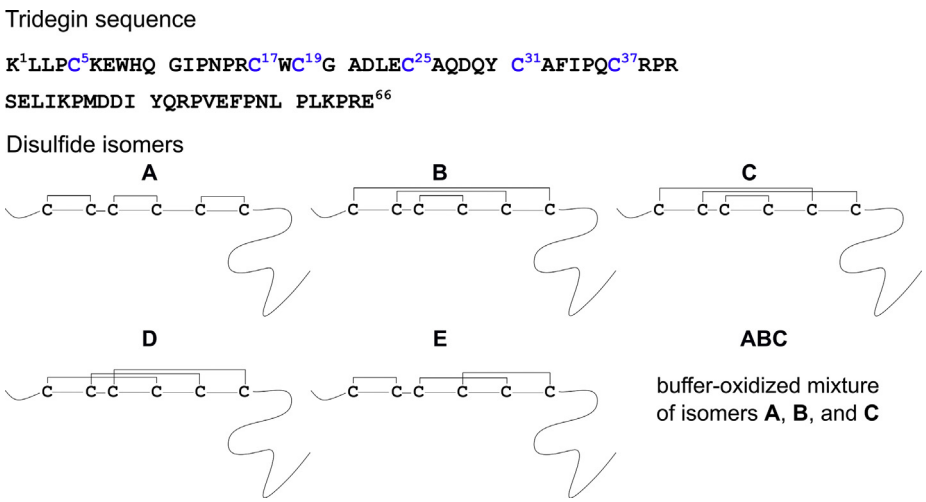

Fig. 1. Tridegin amino acid sequence (cysteines are marked in blue) and schematic disulfide connectivities of synthesized disulfide isomers **A**-**E**. **ABC** was characterized in previous studies [43,44]. (For interpretation of the references to color in this figure legend, the reader is referred to the Web version of this article.)

investigations shall support future drug development based on this native leech-derived compound.

2. Results and discussion

2.1. Design and synthesis of peptides

Five different 3-disulfide-bonded tridegin isomers (**A**-**E**, Fig. 1) were synthesized by regioselective solid-phase peptide synthesis (SPPS) and subsequent stepwise oxidation in solution. The previously produced and characterized mixture of isomers A, B, and C (**ABC**) [42,43] as well as the commercially available recombinant tridegin (Zedira®, **Z**) were used as references in the performed activity assays. In comparison to the synthetically produced variants, tridegin **Z** carries an additional methionine at the N-terminus as well as a hexahistidine tag at its C-terminus.

Targeted synthesis of peptides with three or more disulfide bonds is a time-consuming, expensive, and challenging procedure [50]. Different protecting group strategies can be applied depending on the peptide sequence and the complexity of the synthesis [53–56]. Isomers **A**-**E** were synthesized via a protecting-group strategy using trityl (Trt), acetamidomethyl (Acm), and *tert*-butyl (*t*Bu) protecting groups for the respective cysteine pairs (Fig. 2). Linear precursors were assembled on a polymer resin by means of Fmoc SPPS and subjected to stepwise oxidation in solution. The first and second disulfide bond were both selectively formed in a one-pot reaction with increasing amounts of iodine [44,57]. Quenching of iodine by addition of ascorbic acid [50] led to solubility issues of the product in the following third oxidation step. This problem was circumvented by iodine extraction using cyclohexane. The oxidation progress of each isomer was monitored by HPLC and MALDI-TOF MS. Fully oxidized isomers **A**-**E** were obtained in acceptable yields (5–9% of purified linear precursor) and high purity (>95%) after RP HPLC purification (Table S1, Fig. S1).

In earlier studies, the separation of tridegin isomers **A**, **B**, and **C** from the mixture (**ABC**) of the self-folding oxidation approach was not feasible with the available chromatographic methods [43]. Consequently, in the present study a coelution experiment with the synthesized isomers **A**, **B**, and **C** was performed in order to confirm this observation. Similar analyses have been performed earlier with the 15 isomers of μ-conotoxin PIIIA as well as three 2-disulfide-bonded tridegin analogues [44,50]. The equimolar mixture of isomers **A**, **B**, and **C** eluted in form of a single HPLC peak (Fig. S2). A small shoulder before the peak was observed. This shoulder, however, was not sufficient to ensure a clear chromatographic separation of the three disulfide isomers. Hence, the three tridegin isomers **A**, **B**, and **C** have very similar physicochemical properties and are another example for the fact that a combination of different analysis methods (e.g., NMR and MS/MS analysis) is necessary for the unequivocal identification of distinct isomers of a multiply disulfide-bridged peptide.

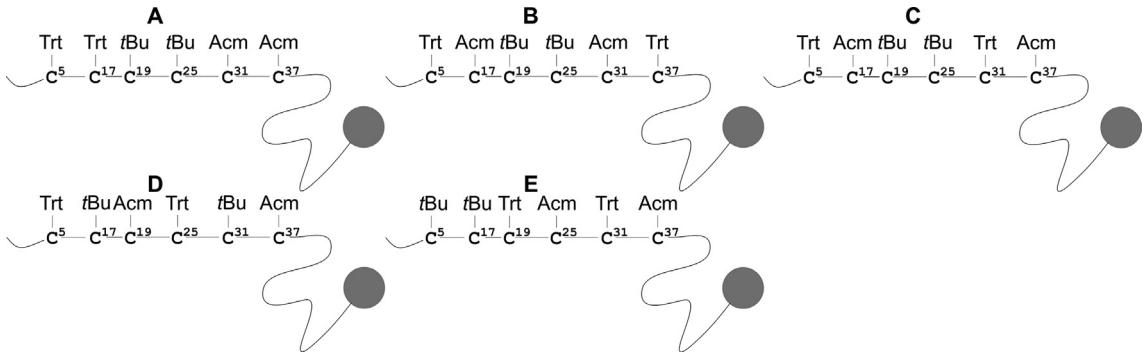

Fig. 2. Schematic representation of the protecting group strategy used for the synthesis of isomers **A**-**E**. Trt: trityl, *t*Bu: *tert*-butyl, Acm: acetamidomethyl.

2.2. Analysis of disulfide connectivities in isomers A-E and tridegin Z

The desired disulfide connectivities of isomers **A**-**E** were analyzed by employing proteolytic digest by a chymotrypsin/trypsin mixture and subsequent mass spectrometric analysis before and after reduction of the fragments (Fig. S3) following an earlier described protocol [43]. Using this approach, all disulfide bonds were confirmed (Table S2).

Besides, the disulfide connectivity of tridegin **Z** was analyzed using the same approach. Herein, it was taken into consideration that the recombinant tridegin **Z** carries an additional methionine at the N-terminus as well as a hexahistidine tag at the C-terminus of the peptide in comparison to the synthetically produced tridegin variants. The acquired data pointed to the probable existence of isomers 1–4, which correspond to the synthesized isomers **A**-**D**, as well as isomer 10 (disulfide connectivity C1–C4, C2–C3, C5–C6) (Table S3, green). Six further isomers displayed an MS sequence coverage of 100%. Due to their lower MS/MS sequence coverage (<25%), which at the same time did not include sequence parts in the N-terminal peptide segment (residues 1–37), the probability of their actual appearance was ranked as intermediate (Table S3, yellow). The remaining four isomers showed MS sequence coverages below 100% and were therefore classified as unlikely (Table S3, red). Consequently, recombinant tridegin **Z** seems to represent a mixture of at least five (high probability) to eleven (high and moderate probabilities) disulfide isomers.

2.3. Isopeptidase enzyme activity assay

Previous work disclosed the role of the N-terminal (residues 1–37, three disulfide bonds) and the C-terminal part (residues 38–66, flexible region) of tridegin as well as the general influence of the disulfide bonds on the inhibitory activity of the peptide [42,43]. In addition, the function of the middle disulfide bond C19–C25 (common in isomers **A**-**C**) with regards to folding, stability, and activity of tridegin was investigated recently [44]. The present study, however, focuses on the impact of different disulfide linkages in selected 3-disulfide-bonded tridegin isomers on their functional and structural properties. The commercially available recombinant tridegin (Zedira®, **Z**) and the previously characterized isomer mixture **ABC** [42–44] were used as references.

IC_{50} values were determined in a previously described fluorogenic assay based on the isopeptidase activity of FXIIIa [43,44]. In this fluorogenic system, the tridegin isomer mixture **ABC** was shown to inhibit FXIIIa with IC_{50} values between 0.30 and 0.45 μM in earlier studies [43,44]. The tested tridegin variants inhibited FXIIIa in an IC_{50} range from 0.45 to 0.95 μM. Tridegin isomers **A**, **B**, **C**, **D**, and **E** displayed IC_{50} values of 0.82 ± 0.05 μM, 0.69 ± 0.04 μM, 0.59 ± 0.04 μM, 0.64 ± 0.06 μM, and 0.83 ± 0.06 μM, respectively (Fig. 3A, Tables S4 and S5). Tridegin **Z** and **ABC** inhibited FXIIIa with IC_{50} values of 0.93 ± 0.11 μM and 0.45 ± 0.03 μM. Thus, the IC_{50} values of the produced isomers did not differ greatly, which was expected due to the fact that disulfide-deficient tridegin (**All-Ser**) also showed an inhibitory effect on FXIIIa [43,44]. Among the five tested isomers, isomer **C** (C5–C31, C17–C37, C19–C25) exhibited the lowest IC_{50} value. Isomers **D** (C5–C25, C17–C31, C19–C37) and **B** (C5–C37, C17–C31, C19–C25) inhibited FXIIIa with slightly higher, but comparable, IC_{50} values. Interestingly, isomers **A** (C5–C17, C19–C25, C31–C37) and **E** (C5–C17, C19–C31, C25–C37), which – due to their disulfide connectivities – have a potentially more flexible N-terminal part than isomers **B**, **C**, and **D** (Fig. 1) showed less activity. These observations point to a possible positive correlation between a conformationally constrained N-terminal tridegin segment and tridegin's overall inhibitory potential. The isomer mixture **ABC** displayed the highest inhibitory potential of all tested tridegin variants, even compared to the most active isomer **C**. In this regard, it is possible that interactions between the isomers **A**, **B**, and **C** or dimerization and oligomerization during the oxidation and/or processing procedures render the compound mixture more active than its individual components. However, if comparing the IC_{50} values of the isomers and the mixtures (0.45–0.95 μM), the differences (1.3- to 2.1-fold) are not dramatic and, thus, should not be overinterpreted.

In order to be able to compare the generated IC_{50} values with the former results of the 2-disulfide-bonded tridegin analogues ($\mathbf{A}_{[C19S,C25S]}$, $\mathbf{B}_{[C19S,C25S]}$, $\mathbf{C}_{[C19S,C25S]}$, $\mathbf{ABC}_{[C19S,C25S]}$) [44], the data obtained therein were normalized using two tridegin variants ($\mathbf{C}_{[C19S,C25S]}$ and **Z**), which had been measured in both studies (Table S4). Remarkably, the trend in inhibitory activity found for the 3-disulfide-bonded isomers (**A**<**B**<**C**) was previously also observed in the respective 2-disulfide-bonded analogues (Fig. 3A), but therein, the differences seem to be less pronounced [44]. Furthermore, the analogue mixture $\mathbf{ABC}_{[C19S,C25S]}$ also seems to be more active than its individual components. This finding supports the hypothesis of the above-mentioned interaction of the components with one another leading to a slightly more favorable inhibition of the enzyme.

Tridegin **Z** inhibited FXIIIa with an IC_{50} value of 0.93 ± 0.11 μM, which is comparable to the inhibitory potential of the **All-Ser** mutant (Fig. 3A, Tables S4 and S5). The sequence differences of tridegin **Z** in comparison to the synthetic tridegin variants (additional methionine at N-terminus and hexahistidine tag at C-terminus, as mentioned above) could account for its comparably low inhibitory potential. Second, the disulfide connectivity analysis of tridegin **Z** pointed towards a mixture of five to eleven different disulfide isomers (five with a high probability and six with a moderate probability) (Table S3). Therefore, the presence of less active isomers that are not present in the mixture of synthetic tridegin might also render tridegin **Z** less active. Third, it should be noted that HPLC and MS analyses of recombinant tridegin **Z** point to the existence of possible side products (Fig. S1) that might also lower the overall activity of the tested substance. Eventually, since former studies already demonstrated different inhibitory potentials of recombinantly and synthetically obtained tridegin [43], the recombinant production of tridegin **Z** may account in part for its reduced activity.

The progress curves in the presence of the different inhibitors were monitored over a period of 30 min. Tridegin isomers **A**-**E** displayed a nearly constant FXIIIa inhibition, whereas the progress curves for tridegin **Z** revealed a more pronounced decrease of inhibitory efficacy with time (Fig. S4). This possibly substrate-like behavior has previously been observed for N-terminally truncated tridegin variants [42,43]. The more pronounced reduction of inhibitory activity over time in tridegin **Z** might be attributed to its C-terminal hexahistidine tag as this is its essential sequential difference in comparison to isomers **A**-**E**.

2.4. Transamidase enzyme activity assay

As the mentioned fluorogenic assay only monitors the isopeptidase activity of FXIIIa, an additional fluorescence anisotropy enzyme activity assay was performed to confirm the inhibitors' effect on FXIIIa transamidase activity [58]. Tridegin analogue mixture $\mathbf{ABC}_{[C19S,C25S]}$, which had been synthesized and characterized in a previous study [44], was tested in this assay system and displayed an IC_{50} value of 2.16 ± 0.21 μM, thus validating the inhibitory potential of the 2-disulfide-bonded tridegin analogues (Fig. 3B).

Due to the fact that the discrimination between FXIIIa and

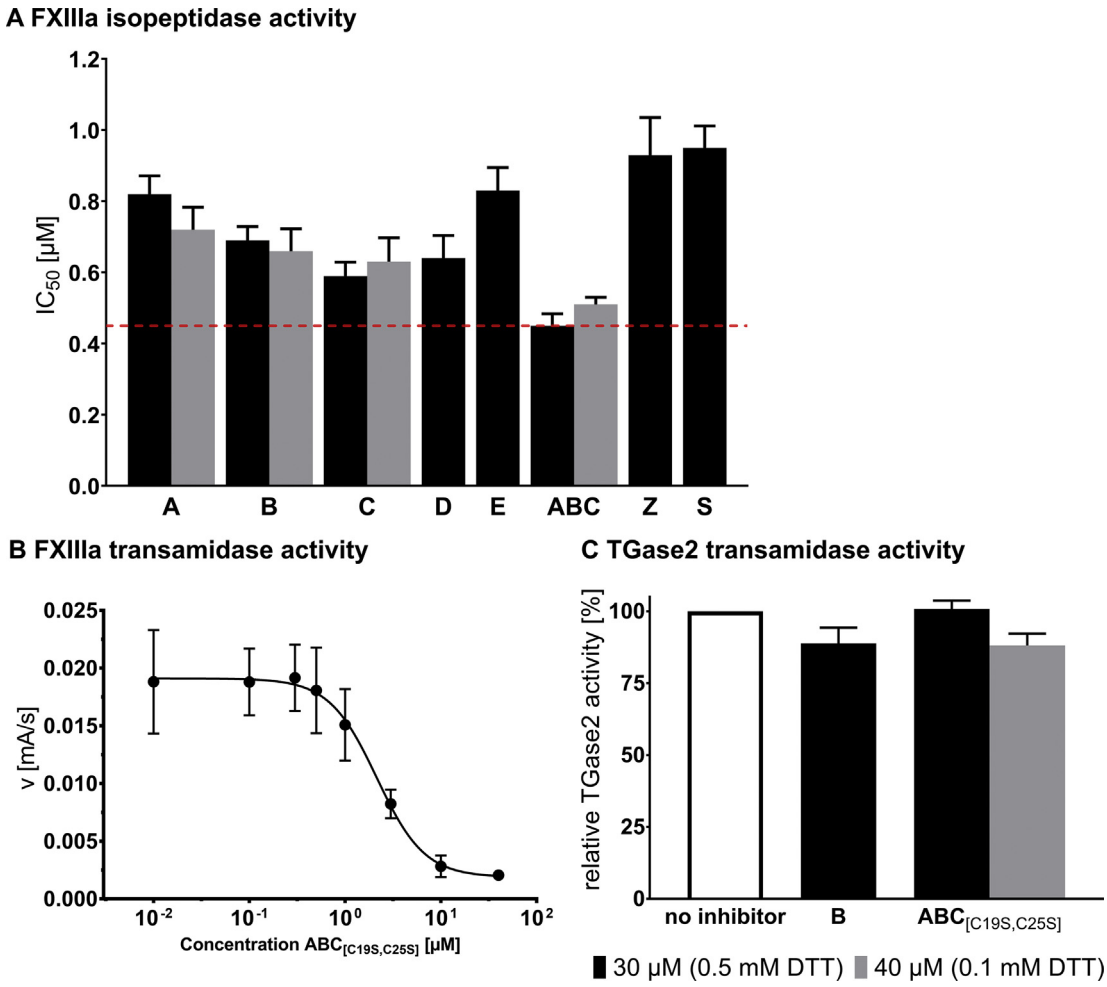

Fig. 3. Tridegin variants in enzymatic assays for FXIIIa and TGase2. A: bar chart comparison of determined IC_{50} values from FXIIIa isopeptidase activity assay with normalized values from Bäuml *et al.* 2019 [44]. Black: IC_{50} values of 3-disulfide-bonded tridegins **A**, **B**, **C**, **D**, **E**, **ABC**, and **Z** as well as mutant **All-Ser** (**S**). Grey: Corresponding 2-disulfide-bonded analogues $\mathbf{A}_{[C19S,C25S]}$, $\mathbf{B}_{[C19S,C25S]}$, $\mathbf{C}_{[C19S,C25S]}$, and $\mathbf{ABC}_{[C19S,C25S]}$ (normalized values from Bäuml *et al.* 2019 [44]). Dashed red line indicates IC_{50} value of previously characterized **ABC** [43] (0.45 µM) as reference. B: IC_{50} determination of $\mathbf{ABC}_{[C19S,C25S]}$ in a FXIIIa transamidase activity assay (0.1 mM DTT). C: relative TGase2 enzyme activity (%) in presence of **B** and $\mathbf{ABC}_{[C19S,C25S]}$. Black: 30 µM inhibitor, 0.5 mM DTT; grey: 40 µM inhibitor, 0.1 mM DTT. Error bars depict standard deviation. (For interpretation of the references to color in this figure legend, the reader is referred to the Web version of this article.)

TGase2 is often discussed as problematic for FXIIIa inhibitors, the effect of the 3-disulfide-bonded isomers, exemplified with compound **B**, and the 2-disulfide-bonded mixture $\mathbf{ABC}_{[C19S,C25S]}$ on TGase2 was explored as well. In a similar fluorescence anisotropy enzyme activity assay with TGase2 [58,59], neither of the two samples showed a marked effect on TGase2 activity at concentrations of 10 and 30 µM (Fig. 3C, Table S6). As the TGase2 activity was routinely performed in the presence of the reducing agent DTT (0.5 mM), the assay was repeated with a lower DTT concentration (0.1 mM), which was also used in the above-mentioned FXIIIa fluorescence anisotropy assay, in order not to interfere with the present disulfide connectivity of the tridegin variants. At a concentration of 40 µM, $\mathbf{ABC}_{[C19S,C25S]}$ reduced the TGase2 activity only by 12%. In consequence, the 2-disulfide-bonded tridegin analogues are potent and specific FXIIIa inhibitors (Fig. 3C).

2.5. Computational analysis of conformational dynamics and interaction with FXIIIa

The main goal of the *in silico* component of this study was to investigate and understand the interaction of the five tridegin isomers (**A-E**) with FXIIIa at a molecular level (Fig. 4). Each of the five isomers (**A-E**) was subjected to explicit-solvent all-atom MD simulations at 300 K for 1000 ns and from the simulations, the backbone root-mean square deviation (RMSD), per-residue root mean square fluctuation (RMSF), radius of gyration of the isomer (Rg), solvent-accessible surface area (SASA) [60], per-residue solvent accessible surface area ($SASA_{res}$), and an estimate of the solvation free energy (ΔG_{solv}) [61] derived from the SASA calculations, were computed and plotted (Table S7, Figs. S5–S11). Our simulations revealed that the RMSD, Rg, and SASA measures equilibrated around their mean values (Table S7). The mean ΔG_{solv} values [61], used to discriminate between thermodynamically favorable conformations and unfavorable ones, were the lowest for isomers **A**, **B** and **C** (-10.8 ± 3.0 kJ/mol, -7.7 ± 3.1 kJ/mol and -6.1 ± 3.8 kJ/mol) rationalizing their occurrence and identification in the buffer-oxidation mixture (**ABC**) over other possible isomers. In order to select the most populated yet structurally diverse conformations from this 10000-structure ensemble, the Gromos clustering method [62] was applied to the MD trajectory using a 2 Å backbone RMSD cut-off to determine cluster membership. This reduced the number of structures to be analyzed to a lower number than 10000. The centroids of the top five clusters were chosen as candidates for docking simulations on FXIIIa. The backbone RMSD computed

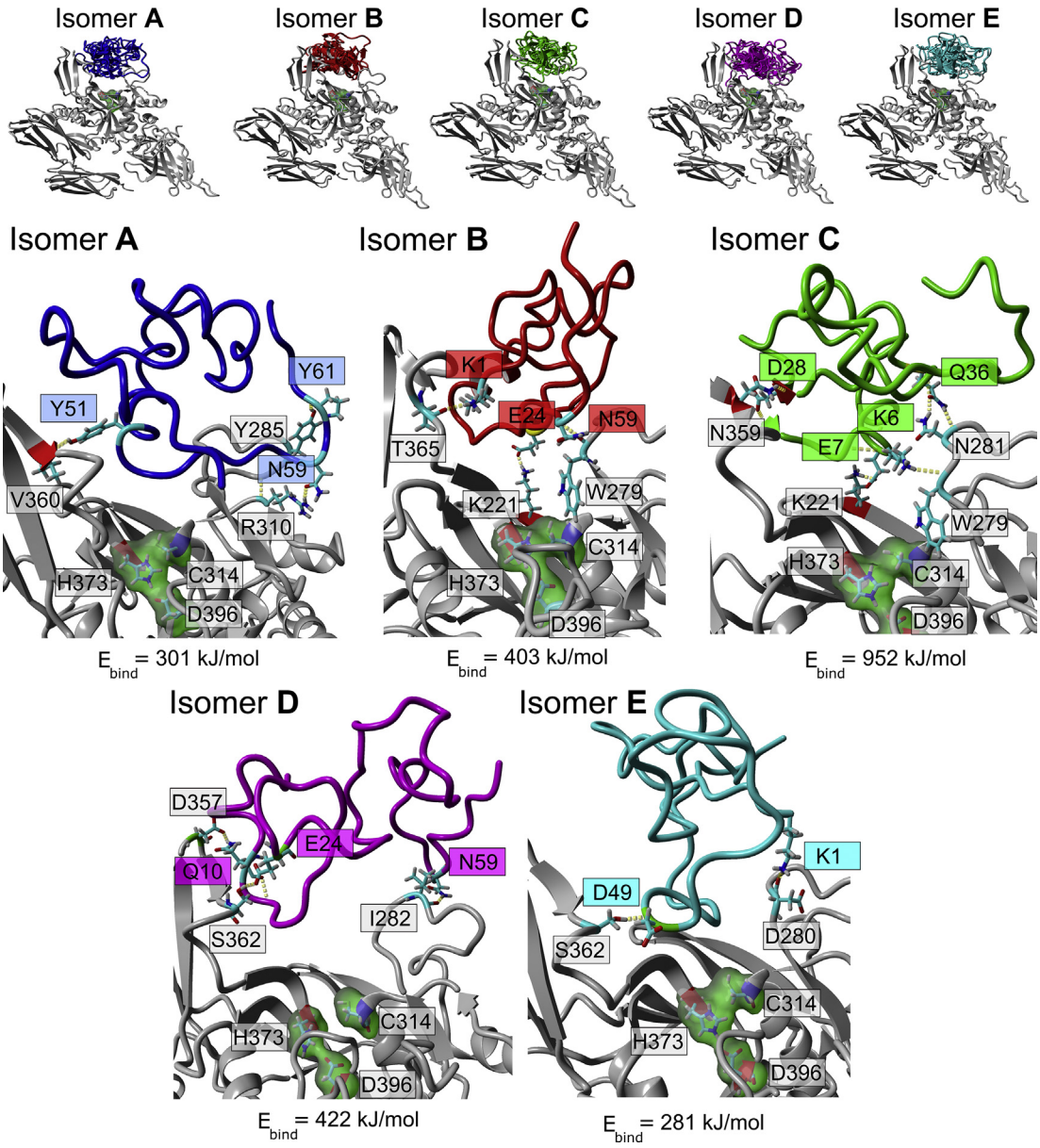

Fig. 4. Computational analysis of the interaction of tridegin isomers **A**-**E** with FXIIIa. Above: five top ranked conformations of the tridegin isomers **A** (blue ribbons), **B** (red ribbons), **C** (green ribbons), **D** (magenta ribbons) and **E** (cyan ribbons) docked on the structure of FXIIIa (grey ribbon; the residues of the catalytic triad are shown in surface representation). Below: zoom-in of best ranked respective isomer-FXIIIa complexes. Residues of the isomer forming H-bonded interactions (yellow-dotted lines) with residues in FXIIIa are shown as sticks and are labeled with rectangular panels color-coordinated to the isomer structure. The active site residues of FXIIIa (C314, H373 and D396) are shown as sticks enclosed by their molecular surfaces (green translucent surface) and labeled to show their proximity to the docked poses of the isomers. The binding energy of the complex (E_{bind}) is indicated within the panel.

among the five chosen structures for each isomer varied between ~4.5 Å and ~5.5 Å indicating reasonable structural diversity (Table S8). Superimposition of these structures revealed a better alignment of the disulfide-bonded N-terminal region (residues 1–37) as opposed to the flexible C-terminal region, as expected (Fig. S12). Each of the five structures of the isomers was docked on a MD-equilibrated structure of FXIIIa obtained from recent work by Singh *et al.* [63] A structural alignment done via MUSTANG [64] revealed that the crystal structure of FXIIIa (PDB: 4KTY) [19] and the MD-derived structure from the Singh *et al.* [63] study (used in the current work) had an RMSD of only 1.50 Å over 577 aligned residues between the two structures (Fig. S13). Each of the five structures chosen for the respective isomer was subject to molecular docking simulations using the Vina [65] algorithm embedded in YASARA Structure (version 19.7.17) [66]. Similar to earlier work [44], the 'ensemble docking' [67] approach was used (see Experimental Section for details). Interestingly, the top-scored docked poses for each of the five structures for every isomer bound to FXIIIa at the same location right above the active site catalytic triad residues (C314, H373, and D396) as shown in Fig. 4. From these poses, the isomer-FXIIIa complex with the best Vina ranking was subjected to a 500 ps refinement simulation in YASARA using the YAMBER force field [68] followed by an explicit 5 ns long MD simulation of the complex from which estimates of binding energies were determined. From analyses on these simulation trajectories, we were able to shed further light on the possible mechanism of inhibition and the subtle differences in inhibitory activities found experimentally between the different isomers (**A-**

E). From molecular electrostatic potentials (MEP) calculated between FXIIIa and the interacting isomers, it was evident that the predominant driver to the isomer-FXIIIa- association was electrostatic interaction. The structure of FXIIIa had an overall MEP ranging between −43 kJ/mol and −48 kJ/mol which could be considered as strongly negative relative to the overall MEPs of the bound isomers whose values ranged between −3 kJ/mol and −6 kJ/mol (Table S9). Therefore, the relative electrostatic interaction between the strongly negative FXIIIa and the isomers with relatively positive potentials formed the basis of the isomer-FXIIIa association. A closer analysis of the interaction interfaces between the isomers and FXIIIa revealed that each isomer presents different parts of its surface to participate in electrostatic interactions (Fig. S14A). Between the isomers **A**, **B**, and **C** a mild overlap in residues in the C-terminal segment was observed. Interestingly, isomer **C** presents three sequence patches of almost the same length (9–14 residues) spaced roughly equidistantly from each other. This could mean that almost all parts of this isomer are involved in electrostatic contacts resulting in an interaction that is relatively more stable than that of the other isomers (Fig. S14A). Similarly, isomer **C** also has the maximum number of interatomic contacts with residues from FXIIIa (Fig. S14B). While the number of isomer-FXIIIa contacts is comparable among isomers **A**, **B**, and **D**, it is the lowest for isomer **E**. At a more granular level, the number of hydrogen bonds formed between the isomer and FXIIIa could contribute to the subtle differences observed in FXIIIa inhibition . We therefore computed hydrogen bonds that persisted for at least 80% of the simulation for each isomer-FXIIIa complex. Accordingly, isomer **C** forms four hydrogen bonds with FXIIIa indicating the possibility of better inhibitory potential over isomers **A, B**, and **D** that formed three hydrogen bonds with FXIIIa and isomer E with only two hydrogen bonds that persisted for 80% of the simulation (Fig. 4). The relative electrostatic surface exposure, the number of isomer-FXIIIa contacts, and the number of hydrogen bonds could all holistically contribute towards the experimentally observed inhibitory activity in a corollary fashion. This hypothesis is supported by the binding energies computed from the simulations as seen in Fig. 4.

Our computational results provide an explanation for the inhibitory activity of all the isomers experimentally quantified by the IC_{50} values because all the isomers are found to bind close to the active site of FXIIIa as shown in Fig. 4. In each case the binding is further stabilized by hydrogen bonds between the isomer and channel residues (Fig. 4). Most notably, the isomer **C** with the highest measured inhibitory activity from the fluorogenic enzyme activity assay also has the highest E_{bind} value of 952 kJ/mol (Fig. 4) making it clear that lower concentrations of this isomer can induce enzyme inhibition. The rest of the E_{bind} values also follow the same trend of progression with the IC_{50} values thereby indicating that the computational approaches used herein provide a clear basis to the experimentally observed activity of the five tridegin isomers (**A-E**).

2.6. Identification of the gene encoding tridegin in Haementeria ghilianii

The tridegin amino acid sequence, which was first identified by Finney *et al*. in 1997, contained a couple of ambiguities [41]. Due to the lack of access to native material, our research group relied on a sequence alignment with a tridegin homologue in *Haementeria depressa* (*H. depressa*) to complete the peptide sequence [42]. Since the postulated inhibitory potential of tridegin from the initial report was never reached again in later studies and as our present research analyzes the impact of cysteine residues at positions which were questionable in the initial study, a verification of the used sequence was overdue. We finally gained access to native material, i.e. dissected salivary glands, of *Haementeria ghilianii*, isolated and sequenced genomic DNA, and identified the potential gene encoding tridegin. The obtained data confirm 62 of 66 positions (94%) of the postulated tridegin sequence (Fig. 5). All cysteine residues, all ambiguous positions from Finney *et al*. [41], as well as the supposedly essential residues for inhibitory activity in tridegin's N-terminal segment (Ile50, Gln52, Leu62) [42] were verified. Since further studies employing more sophisticated methods are ongoing, the detailed procedure and genomic analysis will be reported elsewhere.

3. Conclusion

The present study elucidates the impact of different disulfide connectivities on structure and function of the leech-derived cysteine-rich FXIIIa inhibitor tridegin. A previous study identified three different 3-disulfide-bonded isomers after synthesis via a self-folding approach in buffer [43]. As these isomers could not be separated by means of available chromatographic methods so far, a targeted synthesis using an orthogonal protecting group strategy was required in order to analyze the functional properties of the three isomers. Consequently, these disulfide isomers (**A-C**), which all share the disulfide bridge C19–C25, were synthesized in a selective manner and characterized. In addition, two further isomers (**D** and **E**) containing the *knottin* (ICK) fold and the disulfide connectivity known from the LAP motif, respectively, were included based on other disulfide-rich peptides such as conotoxins (ICK) and hirudin (LAP).

In vitro and *in silico* analyses of the five disulfide isomers reveal that the inhibitory activity of a given isomer is, among other things, a collateral function of the disulfide connectivity of the isomer. To this end, we observe that isomers **B**, **C**, and **D,** that harbor multiple overlapping disulfide bonds, adopt conformations that present more favorable surfaces of the isomers to FXIIIa (Fig. 4). This results in a greater extent of isomer-FXIIIa interactions and the concomitant inhibitory activity (Fig. 3) compared to isomers **A** and **E** that harbor ≤ 1 overlapping disulfide-bonded configurations. A similar link between conformation and function has been found earlier for the μ-conotoxin PIIIA [49,50]. Notably, the *knottin* fold (isomer **D**), inhibits FXIIIa with a similar potency as the most active isomer (**C**). The comparatively low inhibitory potential of the isomer harboring the LAP motif (isomer **E**) is yet another indication [43] that tridegin cannot be compared with hirudin.

Besides, the disulfide connectivity of differently produced tridegin variants (synthetic and recombinant) has been clarified revealing the existence of even more disulfide isomers in the recombinant product compared to the self-folding approach.

Future studies, however, should focus on applications of 2-disulfide-bonded tridegin analogues, since their synthesis is tremendously less laborious and less cost-intensive while – at the same time – preserving their inhibitory potential compared to the 3-disulfide-bonded counterparts [44].

Eventually, the native tridegin amino acid sequence, which has been unclear in certain positions since 1997 [41], has been confirmed by genome sequencing of DNA isolated from the giant amazon leech *H. ghilianii*. The generated genomic data, which will be published elsewhere shortly, enable future phylogenetic studies and bring about a large basis for the exploration of the leech's genome for further pharmaceutically active compounds.

4. Experimental Section

4.1. Materials

Fmoc-amino acids were purchased from Orpegen Peptide

```
1  KLLPCKEXHQ GIPNPRCXCG ADLEXAQDQY CAFIPQC/ERPR SELIKPMDDI YQRPVC/EFPNL PLKPRC/E
2  KLLPCKEWHQ GIPNPRCWCG ADLECAQDQY CAFIPQ C RPR SELIKPMDDI YQRPV E FPNL PLKPR E
3    LPCKEWHQ GIPNPRCWCG ADLECAQDQY CAFIPQ C RP  SELIKPMDDI YQRPV E FPNL PLKPR
```

Fig. 5. Verification of the tridegin sequence in native genomic DNA from *H. ghilianii*. 1: original tridegin sequence determined by Finney *et al.* [41] Ambiguous amino acid positions are marked in red. 2: used sequence based on an alignment with a homological sequence from *H. depressa* in Böhm *et al.* 2012 [42]. Previously equivocal residues are marked in bold letters. 3: identified tridegin sequence in genomic DNA from *H. ghilianii*. Verified positions which are important for the inhibitory potential of tridegin are marked in green.

Chemicals (Heidelberg, Germany) and Novabiochem (Schwalbach, Germany). HBTU and resins for solid-phase peptide synthesis were purchased from IRIS Biotech (Marktredwitz, Germany). Further chemicals employed in peptide synthesis, including reagent-grade *N*-methylmorpholine, piperidine, trifluoroacetic acid (TFA), *N*,*N*-dimethylformamide (DMF), and dimethyl sulfoxide (DMSO), were obtained from Sigma-Aldrich Chemie GmbH (Munich, Germany), Alfa Aesar (Karlsruhe, Germany), Abcr GmbH (Karlsruhe, Germany), VWR International (Darmstadt, Germany), and FLUKA Chemika (Seelze, Germany). Solvents (acetonitrile, water, methanol, cyclohexane, diethyl ether) and chemicals (iodine, acetic acid) used for peptide purification and oxidation were purchased from VWR International (Darmstadt, Germany) and Fisher Scientific (Schwer-te, Germany). Buffer components ($CaCl_2$, HCl, MOPS, NaCl, Na_2HPO_4, NaH_2PO_4, NaOH, Tris, Tris-HCl) were obtained from Carl Roth GmbH + Co. KG (Karlsruhe, Deutschland) and VWR International (Darmstadt, Germany). Tridegin **Z** (T087), TGase2 (T022), and FXIIIa (T070) were acquired from Zedira GmbH (Darmstadt, Germany). Additional components used in enzymatic assays (DMSO and *N*,*N*-dimethylcasein, DMC) were bought from Sigma-Aldrich Chemie GmbH (Munich, Germany). Fibrogammin P was a kind gift from CSL Behring (Marburg, Germany).

4.2. Peptide synthesis and purification

The linear precursors of the five tridegin isomers were synthesized by automated standard Fmoc solid-phase peptide synthesis using an EPS 221 peptide synthesizer from Intavis Bioanalytical Instruments (Cologne, Germany) as described earlier [42]. An Fmoc Rink-Amide MBHA resin with a loading capacity of 0.53 mmol/g was used as polymeric support. Side chains of trifunctional amino acids were protected as follows: Arg(Pbf), Asn(Trt), Asp(O*t*Bu), Cys(Acm), Cys(Trt), Cys(*t*Bu), Gln(Trt), Glu(O*t*Bu), His(Trt), Lys(Boc), Ser(*t*Bu), Trp(Boc), Tyr(*t*Bu). Peptide cleavage from the resin and deprotection of protected side chains except for Cys(Acm) and Cys(*t*Bu) were carried out in a reagent K/TFA mixture (82.5% TFA, 5% H_2O, 5% phenol, 5% thioanisole, 2.5% ethanedithiol) as previously described [42].

The crude product (yields: 33–76%) was purified via semi-preparative RP HPLC using a Shimadzu LC-8A instrument (Duisburg, Essen) equipped with a Knauer Eurospher column (C18, 250 × 32 mm, 5 μm particle size, 100 Å pore size). A gradient elution system of 0.1% TFA in water (eluent A) and 0.1% TFA in acetonitrile/water (90:10) was employed. Elution was carried out with an increase of eluent B from 10 to 60% over 120 min at a flow rate of 10 mL/min. Peak detection was achieved at λ = 220 nm. The collected fractions were lyophilized and stored at −20 °C.

The purity of the linear peptides (yields: 17–26%) was >95%, which was assessed by analytical RP HPLC on a Shimadzu LC-10AT equipped with a Vydac 218 TP column (C18, 250 × 4.6 mm, 5 μm particle size, 300 Å pore size). The gradient elution system contained 0.1% TFA in water (eluent A) and 0.1% TFA in acetonitrile (eluent B). Peptide elution was achieved with an increase of eluent B from 20 to 60% over 40 min at 1 mL/min. Peptides were detected at λ = 220 nm.

4.3. Oxidation of the linear precursors

The regioselective synthesis of the five 3-disulfide-bridged isomers was accomplished via a protecting group strategy using Cys(Trt), Cys(Acm), and Cys(*t*Bu) for the respective cysteine pairs. The formation of the first two bridges was carried out in an iodine-catalyzed one-pot reaction essentially as described recently [44]. The linear precursors were dissolved in 50% AcOH (0.05 mM, 1 eq.). 1.1 eq. of iodine (0.1 M in MeOH) was added to the solution and the reaction was stirred for 5 min at RT. After 5 min, the formation of the first disulfide bridge was complete and additional 13.9 eq. of iodine (0.1 M in MeOH) was added to the reaction solution. The solution was stirred for 15 (**A**, **B**, **C**, **E**) or 30 min (**D**) at RT and the reaction was stopped by iodine extraction (3-4x) in cyclohexane. The product was lyophilized and subsequently used for the next synthesis step without further purification.

The cleavage of the *t*Bu protecting group as well as the formation of the third disulfide bond was carried out in TFA/DMSO/anisole based on previous descriptions [69]. The lyophilized peptide powder was dissolved in TFA/DMSO/anisole (97:2.9:0.1) and stirred for 30 min at RT. The solution was then concentrated on a rotary evaporator followed by gently coating and rubbing with diethyl ether (3x). The residual solution was diluted in H_2O, freeze-dried, and stored at −20 °C.

The oxidized products were purified using a semi-preparative RP HPLC system (Shimadzu LC-8A, Duisburg, Germany) equipped with a Vydac 218TP1022 column (C18, 250 × 22 mm, 5 μm particle size, 100 Å pore size). The gradient elution system consisted of 0.1% TFA in water (eluent A) and 0.1% TFA in acetonitrile/water (90:10) (eluent B). The elution was realized by an increase of eluent B from 10 to 60% over 120 min at a flow rate of 10 mL/min. The peptides were detected at λ = 220 nm. The purity of the collected fractions (>95%) was determined by analytical RP HPLC on a Shimadzu LC-20AD device equipped with a Vydac column (218TP24 or 208TP24, C18 or C8, 250 × 4.6 mm, 5 μm particle size, 300 Å pore size). Peptide elution was carried out via a gradient of 20–60% eluent B (0.1% TFA in acetonitrile) over eluent A (0.1% TFA in water) in 40 min at a flow rate of 1 mL/min. Peptide elution was monitored at λ = 220 nm. Analyzed fractions with similar elution properties were combined. Based on the deployed linear precursors, yields of purified oxidized peptides ranged between 5 and 9% (Table S1). The purified products were lyophilized and stored at −20 °C.

4.4. Peptide characterization

Peptide characterization was achieved by means of analytical HPLC (see above), mass spectrometry, and amino acid analysis.

The peptide concentration as well as the amino acid composition was analyzed using an LC 3000 system from Eppendorf-Biotronik (Hamburg, Germany). Peptide hydrolysis was carried out in 6 N HCl at 110 °C in sealed tubes for 24 h. Subsequently, the hydrolyzed peptides were dried in a vacuum concentrator and redissolved. The respective amino acid concentrations were determined by comparison with an amino acid standard solution (Laborservice Onken, Gründau, Germany).

Peptide masses were determined using matrix-assisted laser

desorption/ionization (MALDI) and electrospray ionization (ESI) mass spectrometry. MALDI mass spectra were produced on an autoflex III smartbeam, an autoflex II and an UltrafleXtreme instrument (all Bruker Daltonics, Bremen, Germany). A micrOTOF-Q III device (Bruker Daltonics, Bremen, Germany) was used to measure ESI mass spectra.

4.5. Determination of disulfide connectivity

The disulfide connectivity of isomers **A**-**E** and tridegin variant **Z** was determined as described recently [43,44].

4.6. Enzyme activity assays

FXIIIa and TGase2 enzyme activity was measured using different systems. The comparison of the inhibitory potential of different tridegin variants towards FXIIIa was performed in a FXIIIa isopeptidase activity assay using the fluorogenic substrate H-Tyr(3-NO_2)-Glu(NH-$(CH_2)_4$-NH-Abz)-Val-Lys-Val-Ile-NH_2 as described previously [43].

The fluorescence anisotropy-based TGase2 enzyme activity assay was in principle carried out as described earlier [58]. The reaction mixture (total volume 100 μL) contained 5 μg/mL human TGase2 (T022, Zedira, Darmstadt, Germany), 0.81 μM rhodamine B-isonipectoyl-cadaverine (R-I-Cad), 30 μM N,*N*-dimethylcasein (DMC), 0.5 mM DTT, and 5% DMSO. The inhibitor concentration in the preliminary and main experiment of the first measurement was 10 μM and 30 μM, respectively. The peptide inhibitors were prepared in a stock solution (250 μM in H_2O). The assay buffer consisted of 100 mM MOPS, 3 mM $CaCl_2$, and 0.05 mM EDTA-Na_2 (pH 8.0). The enzyme buffer in the first measurement contained 100 mM MOPS, 3 mM $CaCl_2$, 10 mM dithiothreitol (DTT), and 20% (v/v) glycerol (pH 8.0). In the preliminary experiments, the enzyme activity was monitored with and without a 30 min pre-incubation (30 °C in the plate reader) of tridegin variant, substrate, and TGase2 by means of the Multi-Mode Microplate Reader Synergy 2 (BioTek, USA; Gen5 Software Version 1.11.5). The reaction was started by addition of DMC (with pre-incubation) or by addition of TGase2 (without pre-incubation). The enzyme activity was followed over a period of 15–30 min at 30 °C (λex = 540 nm, λem = 620 nm) and analyzed over the first 10 min (linear range) by linear regression (GraphPad Prism Version 6.01, GraphPad Software, La Jolla, CA, USA). In the main experiment of the first measurement, the pre-incubation was omitted and the reaction was started by addition of TGase2.

In a second measurement, the DTT concentration in the assay was decreased from 0.5 mM to 0.1 mM in order to diminish the possibility of a disulfide bridge reduction in tridegin. This was achieved by lowering the DTT concentration of the enzyme buffer from 10 mM to 2 mM. The peptide stock solution was prepared in assay buffer instead of H_2O. The inhibitor concentration was 40 μM and the reaction was started after a 30 min pre-incubation (TGase2, R-I-Cad, inhibitor) by the addition of DMC. Apart from these modifications, the reaction conditions were consistent with those in the first measurement (see above).

The FXIIIa transamidase activity assay conditions were consistent with those of the described second measurement of the TGase2 assay. Instead of TGase2, FXIIIa (final concentration 5 μg/mL, T070, Zedira, Darmstadt) was used. The final DTT concentration was 0.1 mM. The enzyme reaction was started after a 30 min pre-incubation (R-I-Cad, FXIIIa, inhibitor) at 30 °C by the addition of DMC. The enzyme activity was monitored in three duplicate measurements with eight different inhibitor concentrations (0.01–40 μM) and analyzed by linear regression. The IC_{50} was subsequently determined by nonlinear regression (GraphPad Prism Version 6.01, GraphPad Software, La Jolla, CA, USA) [58].

4.7. Molecular modeling of tridegin isomers D and E

The structures of tridegin isomers **D** and **E** were determined by molecular modeling using a threading approach as described previously for isomers **A**, **B**, and **C** [43]. The threaded structures were finalized in YASARA version 16 [68].

4.8. Molecular dynamics simulations of tridegin isomers A-E

All-atom molecular dynamics (MD) simulations of the tridegin isomers **A-E** were conducted using the GROMACS simulation suite (version 2018) [70–72]. As all of the tridegin isomers (**A-E**) lack experimentally resolved structures, computationally derived structure models of the isomers from the present study and an earlier report [43] were used as starting coordinates in all the *in silico* analyses done in the current work. Performance improvements in the form of efficient usage of graphical processing units (GPUs) introduced in the 2018 version of GROMACS [73] enabled the simulation of individual isomers (**A-E**) in solution for 1000 ns. Barring this increase in simulation time, the rest of the simulation setup was essentially identical to what was described in our earlier work using tridegin isomers **A-C** [44]. Conformational analysis of the MD trajectories thus obtained, were done via tools available within the GROMACS package. This included the backbone root-mean square deviation (RMSD), the per-residue root mean square fluctuation (RMSF), the radius of gyration (Rg) of all protein atoms, the solvent-accessible surface area (SASA) of the protein, the per-residue contribution to the SASA ($SASA_{res}$) and an estimate of the solvation free energy (ΔG_{solv}) derived from the SASA. The SASA and $SASA_{res}$ computations were done via the double cubic lattice method [60], using a default water molecule probe radius of 1.4 Å. The ΔG_{solv} estimates plotted as a function of simulation time were done using the method implemented by Eisenberg *et al.* [61] that takes into account the solvation energies per exposed surface area obtained from the SASA computation. The 10000 frames written to disk from each simulation were further clustered by the Gromos clustering algorithm using a 2 Å backbone RMSD cut-off [62]. The centroids of the top five clusters from each simulation were used as inputs to the molecular docking simulations. All simulations were conducted at 300 K using the AMBER99SB-ILDN force field [74].

4.9. Molecular docking simulations of tridegin isomers A-E on FXIIIa

Molecular docking simulations of the tridegin isomers **A-E** on FXIIIa were conducted using the Vina [65] docking algorithm shipped with the YASARA (version 19.9.17) molecular modeling suite [75]. Similar to earlier work [44], the ensemble docking [67] method was used wherein the receptor (FXIIIa), was modeled as a 20-member-ensemble comprising of 20 high-scoring side-chain conformations generated at 300 K, to which the isomers (**A-E)** were docked 400 times on each of the ensemble member resulting in 8000 runs per simulation. The structure of FXIIIa used as the receptor in the docking simulations was obtained in a pre-equilibrated state from the MD trajectory of the crystal structure of FXIIIa (PDB: 4KTY [19]) in monomeric form as produced by Singh *et al.* [63] Two distinct modes of docking simulations, distinguished by the docking search space used (based on the size of the simulation cell drawn) were conducted. First, a 20 Å simulation cell around all atoms of the FXIIIa structure was drawn in order to find all regions on the protein with which the tridegin isomers can interact. Based on the consensus from the Vina docking scores obtained from this exercise, the simulation cell was restricted to 20 Å around the Cα atom of the H373 residue of FXIIIa, which is the

central residue of the catalytic triad (C314, H373, D396) that forms the active site of FXIIIa. The top five scoring complexes as determined by Vina were individually subjected to a MD-based refinement procedure for 500 ps using the protocol implemented by the *md_refine.mcr* macro embedded in YASARA [66,68]. The lowest energy isomer-FXIIIa complex produced from the refinement simulations of each isomer was further subjected to explicit all-atom MD simulations for 5 ns using the *md_run.mcr* macro in YASARA [66]. Care was taken that all parameters including force field, temperature, pressure, and cut-off schemes were maintained identical to the GROMACS simulations (in line with previous work that used the GROMACS-YASARA combination for MD [49]). The Adaptive Poisson-Boltzmann Solver (APBS) program embedded in YASARA was used to calculate the binding energy (E_{bind}) of the tridegin isomer's association with FXIIIa from this 5 ns post-docking-refinement MD simulation. The complex with the highest E_{bind} is considered and presented as the best binding mode/conformation of the isomer. Given that the isomer-FXIIIa complex systems comprise of over ~250000 atoms, a longer time scale was not feasible. From this 5 ns equilibration trajectory the Poisson-Boltzmann binding energy [76] (E_{bind}) to qualitatively describe the isomer-FXIIIa interaction was computed and the complex with the highest E_{bind} value was considered as the most probable binding mode/conformation of the isomer. It is emphasized that the energies computed are purely arbitrary measures to quantify the isomer-FXIIIa interaction and cannot be compared with experimentally determined binding energies. Finally, the APBS program was also used to calculate the molecular electrostatic potential (MEP) of the FXIIIa structure as well the docked poses of isomers **A-E** on the surface of FXIIIa.

Author contributions

The study has been designed by AB and DI. CAB performed synthesis and analysis of the peptides. AAPG and AB carried out the computational studies. CAB, TSc, and TSt performed and analyzed the FXIIIa isopeptidase activity assay. PS and MP performed and analyzed the FXIIIa and TGase2 transamidase activity assays. LP and CAB identified tridegin in genomic DNA of *H. ghilianii*. AB and DI analyzed and interpreted all data. The manuscript was written through contributions of all authors. All authors have given approval to the final version of the manuscript.

Funding sources

The Bruker micrOTOF-Q instrument (to D.I.) and the Bruker ultrafleXtreme TOF/TOF instrument (to M. Engeser) were funded by the University of Bonn, the Ministry of Innovation, Science and Research of North-Rhine Westfalia, and the DFG. This study was financially supported by the German Foundation of Heart Research and by the University of Bonn within university science program HSPII (to D.I.).

Declaration of competing interest

The authors declare that they have no known competing financial interests or personal relationships that could have appeared to influence the work reported in this paper.

Acknowledgment

Financial support by the German Foundation of Heart Research to D.I. is gratefully acknowledged. We are thankful to M. Sylvester (Core Facility Mass Spectrometry, Institute of Biochemistry and Molecular Biology, University of Bonn, Germany) and M. Engeser (Department of Mass Spectrometry, Institute of Chemistry, University of Bonn, Germany) for access to the MALDI-MS instruments. Factor XIIIa for the transamidase activity assay was a generous gift from R. Löser (Helmholtz-Zentrum Dresden-Rossendorf, Institute of Radiopharmaceutical Cancer Research, Dresden, Germany).

Appendix A. Supplementary data

Supplementary data to this article can be found online at https://doi.org/10.1016/j.ejmech.2020.112474.

References

[1] World Health Organization, Global Health Estimates 2016: Deaths by Cause, Age, Sex, by Country and by Region. 2000-2016, Genf, 2018.
[2] S. Mendis, P. Puska, B. Norrving, Global Atlas on Cardiovascular Disease Prevention and Control, WHO, Genf, 2011.
[3] L. Muszbek, Z. Bereczky, Z. Bagoly, I. Komáromi, É. Katona, Factor XIII: a coagulation factor with multiple plasmatic and cellular functions, Physiol. Rev. 91 (2011) 931–972, https://doi.org/10.1152/physrev.00016.2010.
[4] A. Mousa, C. Cui, A. Song, V.D. Myneni, H. Sun, J.J. Li, M. Murshed, G. Melino, M.T. Kaartinen, Transglutaminases factor XIII-A and TG2 regulate resorption, adipogenesis and plasma fibronectin homeostasis in bone and bone marrow, Cell Death Differ. 24 (2017) 844–854, https://doi.org/10.1038/cdd.2017.21.
[5] N.J. Shubin, V.A. Glukhova, M. Clauson, P. Truong, M. Abrink, G. Pejler, N.J. White, G.H. Deutsch, S.R. Reeves, T. Vaisar, R.G. James, A.M. Piliponsky, Proteome analysis of mast cell releasates reveals a role for chymase in the regulation of coagulation factor XIIIA levels via proteolytic degradation, J. Allergy Clin. Immunol. 139 (2017) 323–334, https://doi.org/10.1016/j.jaci.2016.03.051.
[6] H. Raghu, C. Cruz, C.L. Rewerts, M.D. Frederick, S. Thornton, E.S. Mullins, J.G. Schoenecker, J.L. Degen, M.J. Flick, Transglutaminase factor XIII promotes arthritis through mechanisms linked to inflammation and bone erosion, Blood 125 (2015) 427–437, https://doi.org/10.1182/blood-2014-08-594754.
[7] V.D. Myneni, A. Mousa, M.T. Kaartinen, Factor XIII-A transglutaminase deficient mice show signs of metabolically healthy obesity on high fat diet, Sci. Rep. 6 (2016) 35574, https://doi.org/10.1038/srep35574.
[8] L.A.T. Sharief, R.A. Kadir, Congenital factor XIII deficiency in women: a systematic review of literature, Haemophilia 19 (2013) e349–e357, https://doi.org/10.1111/hae.12259.
[9] V. Schroeder, H.P. Kohler, Factor XIII: structure and function, Semin. Thromb. Hemost. 42 (2016) 422–428, https://doi.org/10.1055/s-0036-1571341.
[10] S. Gupta, A. Biswas, M.S. Akhter, C. Krettler, C. Reinhart, J. Dodt, A. Reuter, H. Philippou, V. Ivaskevicius, J. Oldenburg, Revisiting the mechanism of coagulation factor XIII activation and regulation from a structure/functional perspective, Sci. Rep. 6 (2016) 30105, https://doi.org/10.1038/srep30105.
[11] B.A. Anokhin, V. Stribinskis, W.L. Dean, M.C. Maurer, Activation of factor XIII is accompanied by a change in oligomerization state, FEBS J. 284 (2017) 3849–3861, https://doi.org/10.1111/febs.14272.
[12] B.A. Anokhin, W.L. Dean, K.A. Smith, M.J. Flick, R.A.S. Ariëns, H. Philippou, M.C. Maurer, Proteolytic and nonproteolytic activation mechanisms result in conformationally and functionally different forms of coagulation factor XIII A, FEBS J. (2019) 452–464, https://doi.org/10.1111/febs.15040.
[13] A.D. Protopopova, A. Ramirez, D.V. Klinov, R.I. Litvinov, J.W. Weisel, Factor XIII topology: organization of B subunits and changes with activation studied with single-molecule atomic force microscopy, J. Thromb. Haemost. 17 (2019) 737–748, https://doi.org/10.1111/jth.14412.
[14] S. Singh, J. Dodt, P. Volkers, E. Hethershaw, H. Philippou, V. Ivaskevicius, D. Imhof, J. Oldenburg, A. Biswas, Structure functional insights into calcium binding during the activation of coagulation factor XIII A, Sci. Rep. 9 (2019) 11324, https://doi.org/10.1038/s41598-019-47815-z.
[15] V. Schroeder, H.P. Kohler, New developments in the area of factor XIII, J. Thromb. Haemost. 11 (2013) 234–244, https://doi.org/10.1111/jth.12074.
[16] M. Souri, T. Osaki, A. Ichinose, The non-catalytic B subunit of coagulation factor XIII accelerates fibrin cross-linking, J. Biol. Chem. 290 (2015) 12027–12039, https://doi.org/10.1074/jbc.M114.608570.
[17] S. Singh, M.S. Akhter, J. Dodt, A. Sharma, S. Kaniyappan, H. Yadegari, V. Ivaskevicius, J. Oldenburg, A. Biswas, Disruption of structural disulfides of coagulation FXIII-B subunit; functional implications for a rare bleeding disorder, Int. J. Mol. Sci. 20 (2019) 1956, https://doi.org/10.3390/ijms20081956.
[18] S. Singh, M.S. Akhter, J. Dodt, P. Volkers, A. Reuter, C. Reinhart, C. Krettler, J. Oldenburg, A. Biswas, Identification of potential novel interacting partners for coagulation factor XIII B (FXIII-B) subunit, a protein associated with a rare bleeding disorder, Int. J. Mol. Sci. 20 (2019) 2682, https://doi.org/10.3390/ijms20112682.
[19] M. Stieler, J. Weber, M. Hils, P. Kolb, A. Heine, C. Büchold, R. Pasternack, G. Klebe, Structure of active coagulation factor XIII triggered by calcium binding: basis for the design of next-generation anticoagulants, Angew. Chem. Int. Ed. 52 (2013) 11930–11934, https://doi.org/10.1002/anie.201305133.
[20] A. Undas, R.A.S. Ariëns, Fibrin clot structure and function: a role in the pathophysiology of arterial and venous thromboembolic diseases,

Arterioscler. Thromb. Vasc. Biol. 31 (2011) e88–e99, https://doi.org/10.1161/ATVBAHA.111.230631.
[21] R.A.S. Ariëns, Fibrin(ogen) and thrombotic disease, J. Thromb. Haemost. 11 (2013) 294–305, https://doi.org/10.1111/jth.12229.
[22] K.I. Bridge, H. Philippou, R.A.S. Ariëns, Clot properties and cardiovascular disease, Thromb. Haemost. 112 (2014) 901–908, https://doi.org/10.1160/TH14-02-0184.
[23] J.R. Byrnes, A.S. Wolberg, Newly-recognized roles of factor XIII in thrombosis, Semin. Thromb. Hemost. 42 (2016) 445–454, https://doi.org/10.1055/s-0036-1571343.
[24] A.S. Wolberg, Fibrinogen and factor XIII: newly recognized roles in venous thrombus formation and composition, Curr. Opin. Hematol. 25 (2018) 358–364, https://doi.org/10.1097/MOH.0000000000000445.
[25] M.M. Aleman, J.R. Byrnes, J.-G. Wang, R. Tran, W.A. Lam, J. Di Paola, N. Mackman, J.L. Degen, M.J. Flick, A.S. Wolberg, Factor XIII activity mediates red blood cell retention in venous thrombi, J. Clin. Invest. 124 (2014) 3590–3600, https://doi.org/10.1172/JCI75386.
[26] C. Duval, P. Allan, S.D.A. Connell, V.C. Ridger, H. Philippou, R.A.S. Ariëns, Roles of fibrin α- and γ-chain specific cross-linking by FXIIIa in fibrin structure and function, Thromb. Haemost. 111 (2014) 842–850, https://doi.org/10.1160/TH13-10-0855.
[27] J.R. Byrnes, C. Wilson, A.M. Boutelle, C.B. Brandner, M.J. Flick, H. Philippou, A.S. Wolberg, The interaction between fibrinogen and zymogen FXIII-A2B2 is mediated by fibrinogen residues γ390-396 and the FXIII-B subunits, Blood 128 (2016) 1969–1979, https://doi.org/10.1182/blood-2016-04-712323.
[28] S. Gundemir, G. Colak, J. Tucholski, G.V.W. Johnson, Transglutaminase 2: a molecular Swiss army knife, Biochim. Biophys. Acta - Mol. Cell Res. 1823 (2012) 406–419, https://doi.org/10.1016/j.bbamcr.2011.09.012.
[29] K.F. Freund, K.P. Doshi, S.L. Gaul, D.A. Claremon, D.C. Remy, J.J. Baldwin, S.M. Pitzenberger, A.M. Stern, Transglutaminase inhibition by 2-[(2-oxopropyl)thio]imidazolium derivatives: mechanism of factor XIIIa inactivation, Biochemistry 33 (1994) 10109–10119, https://doi.org/10.1021/bi00199a039.
[30] A.A. Tymiak, J.G. Tuttle, S.D. Kimball, T. Wang, V.G. Lee, A simple and rapid screen for inhibitors of factor XIIIa, J. Antibiot. (Tokyo) 46 (1993) 204–206, https://doi.org/10.7164/antibiotics.46.204.
[31] H. Kogen, T. Kiho, K. Tago, S. Miyamoto, T. Fujioka, N. Otsuka, K. Suzuki-Konagai, T. Ogita, Alutacenoic acids A and B, rare naturally occurring cyclopropenone derivatives isolated from fungi: potent non-peptide factor XIIIa inhibitors, J. Am. Chem. Soc. 122 (2000) 1842–1843, https://doi.org/10.1021/ja992355s.
[32] C.A. Avery, R.J. Pease, K. Smith, M. Boothby, H.M. Buckley, P.J. Grant, C.W.G. Fishwick, (±) cis-bisamido epoxides: a novel series of potent FXIII-A inhibitors, Eur. J. Med. Chem. 98 (2015) 49–53, https://doi.org/10.1016/j.ejmech.2015.05.019.
[33] T.M. Sabo, P.B. Brasher, M.C. Maurer, Perturbations in factor XIII resulting from activation and inhibition examined by solution based methods and detected by MALDI-TOF MS, Biochemistry 46 (2007) 10089–10101, https://doi.org/10.1021/bi700579z.
[34] K. Hardes, M.Z. Hammamy, T. Steinmetzer, Synthesis and characterization of novel fluorogenic substrates of coagulation factor XIII-A, Anal. Biochem. 442 (2013) 223–230, https://doi.org/10.1016/j.ab.2013.07.043.
[35] A. Heil, J. Weber, C. Büchold, R. Pasternack, M. Hils, Differences in the inhibition of coagulation factor XIII-A from animal species revealed by Michael Acceptor- and thioimidazol based blockers, Thromb. Res. 131 (2013) e214–e222, https://doi.org/10.1016/j.thromres.2013.02.008.
[36] R. Pasternack, C. Büchold, R. Jähnig, C. Pelzer, M. Sommer, A. Heil, P. Florian, G. Nowak, U. Gerlach, M. Hils, Novel inhibitor ZED3197 as potential drug candidate in anticoagulation targeting coagulation FXIIIa (F13a), J. Thromb. Haemost. 18 (2020) 191–200, https://doi.org/10.1111/jth.14646.
[37] R.A. Al-Horani, R. Karuturi, M. Lee, D.K. Afosah, U.R. Desai, Allosteric inhibition of factor xiiia. non-saccharide glycosaminoglycan mimetics, but not glycosaminoglycans, exhibit promising inhibition profile, PLoS One 11 (2016) e0160189, https://doi.org/10.1371/journal.pone.0160189.
[38] R.J. Shebuski, G.R. Sitko, D.A. Claremon, J.J. Baldwin, D.C. Remy, A.M. Stern, Inhibition of factor XIIIa in a canine model of coronary thrombosis: effect on reperfusion and acute reocclusion after recombinant tissue-type plasminogen activator, Blood 75 (1990) 1455–1459, https://doi.org/10.1182/blood.V75.7.1455.1455.
[39] C. Barsigian, A.M. Stern, J. Martinez, Tissue (type II) transglutaminase covalently incorporates itself, fibrinogen, or fibronectin into high molecular weight complexes on the extracellular surface of isolated hepatocytes, J. Biol. Chem. 266 (1991) 22501–22509.
[40] M.E. Prime, O.A. Andersen, J.J. Barker, M.A. Brooks, R.K.Y. Cheng, I. Toogood-Johnson, S.M. Courtney, F.A. Brookfield, C.J. Yarnold, R.W. Marston, P.D. Johnson, S.F. Johnsen, J.J. Palfrey, D. Vaidya, S. Erfan, O. Ichihara, B. Felicetti, S. Palan, A. Pedret-Dunn, S. Schaertl, I. Sternberger, A. Ebneth, A. Scheel, D. Winkler, L. Toledo-Sherman, M. Beconi, D. Macdonald, I. Muñoz-Sanjuan, C. Dominguez, J. Wityak, Discovery and structure-activity relationship of potent and selective covalent inhibitors of transglutaminase 2 for Huntington's disease, J. Med. Chem. 55 (2012) 1021–1046, https://doi.org/10.1021/jm201310y.
[41] S. Finney, L. Seale, R.T. Sawyer, R.B. Wallis, Tridegin, a new peptidic inhibitor of factor XIIIa, from the blood-sucking leech Haementeria ghilianii, Biochem. J. 324 (1997) 797–805, https://doi.org/10.1042/bj3240797.
[42] M. Böhm, T. Kühl, K. Hardes, R. Coch, C. Arkona, B. Schlott, T. Steinmetzer, D. Imhof, Synthesis and functional characterization of tridegin and its analogues: inhibitors and substrates of factor XIIIa, ChemMedChem 7 (2012) 326–333, https://doi.org/10.1002/cmdc.201100405.
[43] M. Böhm, C.A. Bäuml, K. Hardes, T. Steinmetzer, D. Roeser, Y. Schaub, M.E. Than, A. Biswas, D. Imhof, Novel insights into structure and function of factor XIIIa-inhibitor tridegin, J. Med. Chem. 57 (2014) 10355–10365, https://doi.org/10.1021/jm501058g.
[44] C.A. Bäuml, T. Schmitz, A.A. Paul George, M. Sudarsanam, K. Hardes, T. Steinmetzer, L.A. Holle, A.S. Wolberg, B. Pötzsch, J. Oldenburg, A. Biswas, D. Imhof, Coagulation factor XIIIa inhibitor tridegin: on the role of disulfide bonds for folding, stability, and function, J. Med. Chem. 62 (2019) 3513–3523, https://doi.org/10.1021/acs.jmedchem.8b01982.
[45] A.A. Tietze, D. Tietze, O. Ohlenschläger, E. Leipold, F. Ullrich, T. Kühl, A. Mischo, G. Buntkowsky, M. Görlach, S.H. Heinemann, D. Imhof, Structurally diverse μ-conotoxin PIIIA isomers block sodium channel $Na_V1.4$, Angew. Chem. Int. Ed. 51 (2012) 4058–4061, https://doi.org/10.1002/anie.201107011.
[46] K.K. Khoo, K. Gupta, B.R. Green, M.-M. Zhang, M. Watkins, B.M. Olivera, P. Balaram, D. Yoshikami, G. Bulaj, R.S. Norton, Distinct disulfide isomers of μ-conotoxins KIIIA and KIIIB block voltage-gated sodium channels, Biochemistry 51 (2012) 9826–9835, https://doi.org/10.1021/bi301256s.
[47] B.B. Carstens, G. Berecki, J.T. Daniel, H.S. Lee, K.A. V Jackson, H.S. Tae, M. Sadeghi, J. Castro, T. O'Donnell, A. Deiteren, S.M. Brierley, D.J. Craik, D.J. Adams, R.J. Clark, Structure-activity studies of cysteine-rich α-conotoxins that inhibit high-voltage-activated calcium channels via $GABA_B$ receptor activation reveal a minimal functional motif, Angew. Chem. Int. Ed. 55 (2016) 4692–4696, https://doi.org/10.1002/anie.201600297.
[48] Z.V.F. Wright, S. McCarthy, R. Dickman, F.E. Reyes, S. Sanchez-Martinez, A. Cryar, I. Kilford, A. Hall, A.K. Takle, M. Topf, T. Gonen, K. Thalassinos, A.B. Tabor, The role of disulfide bond replacements in analogues of the tarantula toxin ProTx-II and their effects on inhibition of the voltage-gated sodium ion channel $Na_v1.7$, J. Am. Chem. Soc. 139 (2017) 13063–13075, https://doi.org/10.1021/jacs.7b06506.
[49] A.A. Paul George, P. Heimer, E. Leipold, T. Schmitz, D. Kaufmann, D. Tietze, S.H. Heinemann, D. Imhof, Effect of conformational diversity on the bioactivity of μ-conotoxin PIIIA disulfide isomers, Mar. Drugs 17 (2019) 390, https://doi.org/10.3390/md17070390.
[50] P. Heimer, A.A. Tietze, C.A. Bäuml, A. Resemann, F.J. Mayer, D. Suckau, O. Ohlenschläger, D. Tietze, D. Imhof, Conformational μ-conotoxin PIIIA isomers revisited: impact of cysteine pairing on disulfide-bond assignment and structure elucidation, Anal. Chem. 90 (2018) 3321–3327, https://doi.org/10.1021/acs.analchem.7b04854.
[51] A.M. Krezel, G. Wagner, J. Seymour-Ulmer, R.A. Lazarus, Structure of the RGD protein decorsin: conserved motif and distinct function in leech proteins that affect blood clotting, Science 264 (1994) 1944–1947, https://doi.org/10.1126/science.8009227.
[52] J.L. Richardson, B. Kröge, W. Hoeffken, J.E. Sadler, P. Pereira, R. Huber, W. Bode, P. Fuentes-Prior, Crystal structure of the human alpha-thrombin-haemadin complex: an exosite II-binding inhibitor, EMBO J. 19 (2000) 5650–5660, https://doi.org/10.1093/emboj/19.21.5650.
[53] K. Akaji, Y. Kiso, Synthesis of cystine peptides, in: Synthesis of Peptides and Peptidomimetics, Georg Thieme Verlag, Stuttgart, 2004, pp. 101–177.
[54] L. Moroder, H.-J. Musiol, M. Götz, C. Renner, Synthesis of single- and multiple-stranded cystine-rich peptides, Biopolymers 80 (2005) 85–97, https://doi.org/10.1002/bip.20174.
[55] Y. Hidaka, Overview of the regulation of disulfide bond formation in peptide and protein folding, Curr. Protoc. Protein Sci. 76 (2014) 28.6.1–28.6.6, https://doi.org/10.1002/0471140864.ps2806s76.
[56] S. Shimamoto, H. Katayama, M. Okumura, Y. Hidaka, Chemical methods and approaches to the regioselective formation of multiple disulfide bonds, Curr. Protoc. Protein Sci. 76 (2014) 28.8.1–28.8.28, https://doi.org/10.1002/0471140864.ps2808s76.
[57] M. Mochizuki, S. Tsuda, K. Tanimura, Y. Nishiuchi, Regioselective formation of multiple disulfide bonds with the aid of postsynthetic S-tritylation, Org. Lett. 17 (2015) 2202–2205, https://doi.org/10.1021/acs.orglett.5b00786.
[58] C. Hauser, R. Wodtke, R. Löser, M. Pietsch, A fluorescence anisotropy-based assay for determining the activity of tissue transglutaminase, Amino Acids 49 (2017) 567–583, https://doi.org/10.1007/s00726-016-2192-5.
[59] R. Wodtke, C. Hauser, G. Ruiz-Gómez, E. Jäckel, D. Bauer, M. Lohse, A. Wong, J. Pufe, F.-A. Ludwig, S. Fischer, S. Hauser, D. Greif, M.T. Pisabarro, J. Pietzsch, M. Pietsch, R. Löser, N^{ε}-Acryloyllysine piperazides as irreversible inhibitors of transglutaminase 2: synthesis, structure-activity relationships, and pharmacokinetic profiling, J. Med. Chem. 61 (2018) 4528–4560, https://doi.org/10.1021/acs.jmedchem.8b00286.
[60] F. Eisenhaber, P. Lijnzaad, P. Argos, C. Sander, M. Scharf, The double cubic lattice method: efficient approaches to numerical integration of surface area and volume and volume to dot surface contouring of molecular assemblies, J. Comput. Chem. 16 (1995) 273–284, https://doi.org/10.1002/jcc.540160303.
[61] D. Eisenberg, A.D. McLachlan, Solvation energy in protein folding and stability, Nature 319 (1986) 199–203, https://doi.org/10.1038/319199a0.
[62] X. Daura, K. Gademann, B. Jaun, D. Seebach, W.F. van Gunsteren, A.E. Mark, Peptide folding: when simulation meets experiment, Angew. Chem. Int. Ed. 38 (1999) 236–240, https://doi.org/10.1002/(sici)1521-3773(19990115)38:1/2<236::aid-anie236>3.3.co;2-d.
[63] S. Singh, A. Nazabal, S. Kaniyappan, J.-L. Pellequer, A.S. Wolberg, D. Imhof,

J. Oldenburg, A. Biswas, The plasma factor XIII heterotetrameric complex structure: unexpected unequal pairing within a symmetric complex, Biomolecules 9 (2019) 765, https://doi.org/10.3390/biom9120765.
[64] A.S. Konagurthu, J.C. Whisstock, P.J. Stuckey, A.M. Lesk, MUSTANG: a multiple structural alignment algorithm, Proteins 64 (2006) 559–574, https://doi.org/10.1002/prot.20921.
[65] O. Trott, A.J. Olson, AutoDock Vina: improving the speed and accuracy of docking with a new scoring function, efficient optimization, and multithreading, J. Comput. Chem. 31 (2010) 455–461, https://doi.org/10.1002/jcc.21334.
[66] E. Krieger, G. Vriend, New ways to boost molecular dynamics simulations, J. Comput. Chem. 36 (2015) 996–1007, https://doi.org/10.1002/jcc.23899.
[67] E.M. Novoa, L.R. de Pouplana, X. Barril, M. Orozco, Ensemble docking from homology models, J. Chem. Theor. Comput. 6 (2010) 2547–2557, https://doi.org/10.1021/ct100246y.
[68] E. Krieger, T. Darden, S.B. Nabuurs, A. Finkelstein, G. Vriend, Making optimal use of empirical energy functions: force-field parameterization in crystal space, Proteins 57 (2004) 678–683, https://doi.org/10.1002/prot.20251.
[69] A. Cuthbertson, B. Indrevoll, A method for the one-pot regioselective formation of the two disulfide bonds of α-conotoxin SI, Tetrahedron Lett. 41 (2000) 3661–3663, https://doi.org/10.1016/S0040-4039(00)00437-8.
[70] M.J. Abraham, T. Murtola, R. Schulz, S. Páll, J.C. Smith, B. Hess, E. Lindahl, GROMACS: high performance molecular simulations through multi-level parallelism from laptops to supercomputers, SoftwareX 1–2 (2015) 19–25, https://doi.org/10.1016/j.softx.2015.06.001.
[71] D. van der Spoel, E. Lindahl, B. Hess, G. Groenhof, A.E. Mark, H.J.C. Berendsen, GROMACS: fast, flexible, and free, J. Comput. Chem. 26 (2005) 1701–1718, https://doi.org/10.1002/jcc.20291.
[72] H.J.C. Berendsen, D. van der Spoel, R. van Drunen, GROMACS: a message-passing parallel molecular dynamics implementation, Comput. Phys. Commun. 91 (1995) 43–56, https://doi.org/10.1016/0010-4655(95)00042-E.
[73] C. Kutzner, S. Páll, M. Fechner, A. Esztermann, B.L. de Groot, H. Grubmüller, More bang for your buck: improved use of GPU nodes for GROMACS 2018, J. Comput. Chem. 40 (2019) 2418–2431, https://doi.org/10.1002/jcc.26011.
[74] K. Lindorff-Larsen, S. Piana, K. Palmo, P. Maragakis, J.L. Klepeis, R.O. Dror, D.E. Shaw, Improved side-chain torsion potentials for the Amber ff99SB protein force field, Proteins 78 (2010) 1950–1958, https://doi.org/10.1002/prot.22711.
[75] E. Krieger, G. Vriend, YASARA View – molecular graphics for all devices – from smartphones to workstations, Bioinformatics 30 (2014) 2981–2982, https://doi.org/10.1093/bioinformatics/btu426.
[76] N.A. Baker, Poisson-Boltzmann methods for biomolecular electrostatics, Methods Enzymol. 383 (2004) 94–118, https://doi.org/10.1016/S0076-6879(04)83005-2.

4.3.3 Summary

This chapter summarizes the synthesis of 5 3-disufide-bonded tridegin isomers (A-E) selectively prepared via Fmoc-based protecting group strategy as well as the elucidation of their disulfide bond connectivity.[13] As expected, markedly lower synthesis yields were obtained compared to the 2-disulfide-bonded tridegin variants (see chapter II) reflecting the higher synthesis effort.[13,17] Subsequent activity studies towards FXIIIa, evidenced that the individual 2- and 3-disulfide bonded isomers all exhibited similar inhibitory potentials with similar IC_{50} values.[13,17] A trend in regard to inhibitory potential from isomer C with the highest inhibitory potential through isomers D and B to isomers A and E with the lowest potential was observed, both in *in vitro* activity assays as well as the computer-based studies. It was suggested that the number of overlapping disulfide bonds in the N-terminal part of the peptides, which are more abundant in isomers B, C, and D, enhance the interaction to FXIIIa and thus increase the inhibitory potential.[13] Furthermore, it was observed that the 2-disulfide-bonded $ABC_{[C19S,C25S]}$ and the 3-disulfide-bonded isomer B showed only low inhibitory potentials towards TGase 2, indicating a high specificity for FXIIIa. In addition to the comparative studies, the amino acid sequence of tridegin was confirmed via sequencing of genomic DNA from *H. ghilianii*.[13]

This chapter provides strong evidence for the applicability of the 2-disulfide-bonded tridegin variants described in chapter II.[17] It was shown, that high activity and specificity is pertained together with a drastically improved synthesizability.[13,17] On the basis of these facts, the focus of future lead structure optimization should lie on the less complex, 2-disulfide-bonded tridegin variants. In order to gain deeper insights into structure-activity-relationships and thus supporting lead optimization, the structure of one tridegin variant, isomer $B_{[C19S,C25S]}$, is analyzed in the following chapter IV. Therefore, the structure was elucidated by a combination of NMR and MD simulations and used for further docking studies on FXIIIa.[18]

4.4 Chapter IV - NMR-based structural characterization of a 2-disulfide-bonded analogue of the FXIIIa inhibitor tridegin: New insights into structure-activity relationships

Authors*

Thomas Schmitz, Ajay Abisheck Paul George, Britta Nubbemeyer, Charlotte A. Bäuml, Torsten Steinmetzer, Oliver Ohlenschläger, Arijit Biswas, and Diana Imhof

This article was published in:
International Journal of Molecular Sciences **2020**, 22, 880.
DOI: 10.3390/ijms22020880

4.4.1 Introduction

In chapter II and III, disulfide-deficient tridegin isomers emerged as ideal lead structures for the design of peptidic FXIIIa inhibitors.[13,17] So far, molecular docking experiments of the individual tridegin variants (also for the 2-disulfide-bonded tridegin variants, chapter II) on FXIIIa have been conducted with theoretically calculated tridegin structures.[12,13,17] This chapter IV investigates the structure of the disulfide deficient tridegin variant $B_{[C19S,C25S]}$ using 2D-NMR spectroscopy. Due to overlap in the signals of the full-length 66mer peptide, a direct signal assignment from the 2D-NMR spectra is not possible. Therefore, the tridegin variant $B_{[C19S,C25S]}$ was divided into two parts which were individually subjected to NMR and used for structure elucidation.[18] The first fragment consisted of the rigid N-terminal fragment (1-37) containing all disulfide bonds (Cys05-Cys37, Cys17-Cys31), while the second fragment consisted of the flexible C-terminal part (38-66).[12,17,18] The experimentally determined structures were subsequently linked and the final structure of isomer $B_{[C19S,C25S]}$ was calculated using molecular dynamics simulation. In addition to the structural analyses of the two fragments, the N-terminal fragment was examined for its inhibitory potential towards FXIIIa.[18] For the C-terminal fragment, this has already been performed in previous studies.[12]

The established structure was used to derive new insights into the structure-activity relationship of this peptide by molecular docking experiments to a modified version of the crystal structure of FXIIIa° (PDB ID: 4KTY[148]).

***Contributions:**

The study has been designed by DI with support of TS. TS performed synthesis as well as functional and structural analysis of the peptides. BN performed the MS measurements and TSt provided his expertise regarding the FXIIIa activity assay. TS and CAB performed the FXIIIa activity assay. TS and OO analyzed the NMR spectra and calculated the peptide structures. AAPG and AB carried out the computational studies. Data analysis and interpretation was carried out by all authors. The manuscript was written through contributions of all authors. All authors have given approval to the final version of the manuscript.

4.4.2 Article

On the following pages, the article is printed in its published form.

International Journal of
Molecular Sciences

MDPI

Article

NMR-Based Structural Characterization of a Two-Disulfide-Bonded Analogue of the FXIIIa Inhibitor Tridegin: New Insights into Structure–Activity Relationships

Thomas Schmitz [1], Ajay Abisheck Paul George [1,2], Britta Nubbemeyer [1], Charlotte A. Bäuml [1], Torsten Steinmetzer [3], Oliver Ohlenschläger [4], Arijit Biswas [5] and Diana Imhof [1,*]

1 Pharmaceutical Biochemistry and Bioanalytics, Pharmaceutical Institute, University of Bonn, An der Immenburg 4, D-53121 Bonn, Germany; t.schmitz@uni-bonn.de (T.S.); Ajay.PaulGeorge@BioSolveIT.de (A.A.P.G.); Britta.Nubbemeyer@uni-bonn.de (B.N.); charlotte.baeuml@uni-bonn.de (C.A.B.)
2 BioSolveIT GmbH, An der Ziegelei 79, D-53757 Sankt Augustin, Germany
3 Institute of Pharmaceutical Chemistry, Philipps University of Marburg, Marbacher Weg 6, 35032 Marburg, Germany; torsten.steinmetzer@staff.uni-marburg.de
4 Leibniz Institute on Aging—Fritz-Lipmann-Institute, Beutenbergstr. 11, D-07745 Jena, Germany; Oliver.Ohlenschlaeger@leibniz-fli.de
5 Institute of Experimental Hematology and Transfusion Medicine, University Hospital Bonn, Sigmund-Freud-Str. 25, D-53127 Bonn, Germany; arijit.biswas@ukbonn.de
* Correspondence: dimhof@uni-bonn.de; Tel.: +49-(0)228-735-254

Abstract: The saliva of blood-sucking leeches contains a plethora of anticoagulant substances. One of these compounds derived from *Haementeria ghilianii*, the 66mer three-disulfide-bonded peptide tridegin, specifically inhibits the blood coagulation factor FXIIIa. Tridegin represents a potential tool for antithrombotic and thrombolytic therapy. We recently synthesized two-disulfide-bonded tridegin variants, which retained their inhibitory potential. For further lead optimization, however, structure information is required. We thus analyzed the structure of a two-disulfide-bonded tridegin isomer by solution 2D NMR spectroscopy in a combinatory approach with subsequent MD simulations. The isomer was studied using two fragments, i.e., the disulfide-bonded N-terminal (Lys1–Cys37) and the flexible C-terminal part (Arg38–Glu66), which allowed for a simplified, label-free NMR-structure elucidation of the 66mer peptide. The structural information was subsequently used in molecular modeling and docking studies to provide insights into the structure–activity relationships. The present study will prospectively support the development of anticoagulant-therapy-relevant compounds targeting FXIIIa.

Keywords: coagulation factor XIIIa; transglutaminase; coagulation cascade; tridegin; peptide inhibitor; cysteine-rich; disulfide bonds; NMR spectroscopy; structure analysis

Citation: Schmitz, T.; Paul George, A.A.; Nubbemeyer, B.; Bäuml, C.A.; Steinmetzer, T.; Ohlenschläger, O.; Biswas, A.; Imhof, D. NMR-Based Structural Characterization of a Two-Disulfide-Bonded Analogue of the FXIIIa Inhibitor Tridegin: New Insights into Structure–Activity Relationships. *Int. J. Mol. Sci.* **2021**, *22*, 880. https://doi.org/10.3390/ijms22020880

Received: 23 December 2020
Accepted: 12 January 2021
Published: 17 January 2021

1. Introduction

Leeches, such as the medical leech *Hirudo medicinalis*, have been used as a biomedical tool from ancient times up to the present day. They were mainly used to remove blood, which should help to detoxify the patient [1]. Because of these bloodsucking properties and the intent to avoid clot formation during blood intake, the leeches' saliva contains a variety of anticoagulants that can be used for the control and treatment of hemostasis. Over 20 different compounds with antithrombotic activity have already been isolated from the salivary glands of various leeches, showing a direct or indirect influence on the blood coagulation cascade [2,3]. One of these compounds is the well-known thrombin inhibitor hirudin, which is isolated from the leech *Hirudo medicinalis* [4,5]. Based on this natural compound, anticoagulants such as bivalirudine and argatroban have already been successfully developed for the treatment of cardiovascular and thromboembolic diseases [6–8]. However, anticoagulants that directly or indirectly inhibit thrombin frequently increase the risk

of undesired bleeding, making them unsuitable for many therapeutic applications [9,10]. Since thrombin catalyzes the penultimate step of the blood coagulation cascade—the formation of fibrin polymers starting from fibrinogen—an influence on any of the previously required coagulation factors always indirectly affects thrombin [11]. Therefore, one way to achieve a thrombin-independent impact on the blood coagulation cascade is the inhibition/activation of the final step, the crosslinking of the fibrin polymers catalyzed by FXIIIa [12,13].

FXIIIa is a transglutaminase that forms isopeptide bonds within the fibrin polymer by linking a glutamine side chain and a lysine side chain, providing increased blood clot stability. In this regard, the isopeptide bond formation is catalyzed by a catalytic triad composed of Cys314, His373, and Asp396 and a catalytic dyad (His342, Glu401) located in the active side of FXIIIa [12,14–16]. Inhibiting this factor leads to unstable blood clots that are smaller in size and can be easily dissolved by fibrinolysis [17–20]. Consequently, FXIIIa serves as an interesting target for the development of anticoagulants in order to circumvent the problem of undesired bleeding. So far, several small-molecule inhibitors such as cerulenin and alutacenoic acid A have been investigated for their inhibitory potential against FXIIIa [21–24]. However, many of these small-molecule inhibitors possess a low selectivity and/or half-life in plasma. Thus, the development of these inhibitors has not been pursued further. Nowadays, the main focus is directed toward peptidic and allosteric FXIIIa inhibitors, such as the peptidomimetic inhibitor ZED3197 and glucosaminoglycan-derived inhibitors, e.g., NSGM 13 (non-saccharide glucosaminoglycan mimetics), introduced by Al-Horani et al. [23–26]. Furthermore, the peptidic inhibitor tridegin, a 66mer peptide, first isolated from the giant Amazon leech *Haementeria ghilianii* in 1997, has been investigated for its high inhibitory potential against FXIIIa [23,27]. Tridegin belongs to the class of cysteine-rich peptides due to its 6 cysteines within the amino acid sequence. The natural disulfide bond connectivity of tridegin could not be elucidated so far [28–31], which is due to the fact that a peptide with 6 cysteines has the ability to form 15 different three-disulfide-bonded isomers. So far, final conclusions have not been drawn concerning the folding of tridegin to the bioactive conformation and whether it is folded in a BPTI-like (Bovine pancreatic trypsin inhibitor) fashion, according to which one isomer is preferentially formed, or in a hirudin-like manner, where a maximum of 15 possible three-disulfide-bonded isomers are formed [32,33]. A folding experiment performed by Böhm et al. in 2014 provided first hints regarding the preferentially formed disulfide-bonded isomers of tridegin [30]. Therein, three of the 15 possible three-disulfide-bonded isomers were identified, which all shared the disulfide bond between Cys19–Cys25 and possessed similar activities toward FXIIIa [28,30]. In addition to the three-disulfide-bonded tridegin isomers, several variants lacking the disulfide bond between Cys19–Cys25 were synthesized in a following approach in order to determine the significance of this bond for their inhibitory potential against FXIIIa [29]. The results revealed that the activity against FXIIIa was not lost, despite the missing disulfide bond. Due to the unchanged activity and the improved synthetic outcome, the two-disulfide-bonded tridegin analogues, in particular the isomer $B_{[C19S,C25S]}$ with the disulfide bonds Cys5–Cys37 and Cys17–Cys31, are used as a lead structure for further research on tridegin and its influence on FXIIIa [29].

The aim of the current study is to gain further insight into tridegin's structure, folding, and interaction with FXIIIa. In order to obtain a more precise understanding of the mode of action against FXIIIa, a structure of the tridegin isomer $B_{[C19S,C25S]}$ was determined by a combination of NMR (nuclear magnetic resonance) spectroscopy and molecular dynamics (MD) simulation studies. This two-disulfide-bonded isomer, $B_{[C19S,C25S]}$, was subsequently applied for molecular docking studies on FXIIIa. The information received from this study was used to refine structure–activity relationships of the tridegin–FXIIIa interaction. Our results may pave the way for further investigations on FXIIIa as well as the optimization/development of lead structures for antithrombotic and thrombolytic therapy.

2. Results and Discussion

2.1. Peptide Synthesis and Characterization

To elucidate the structure of the two-disulfide-bonded isomer $B_{[C19S,C25S]}$ (Figure 1a) [29], two segments derived from the peptide sequence were synthesized for NMR measurements. The reason for dividing the tridegin isomer into an N-terminal and a C-terminal part was the size of the 66mer peptide and the high number of proline residues within the sequence, which complicate the assignment of the NMR signals and hamper structure calculation. Therefore, a C-terminal fragment (amino acids 38–66) already described by Böhm et al. [31] and a new N-terminal fragment (amino acids 1–37) with the disulfide bonds Cys5–Cys37 and Cys17–Cys31 were produced (Supplementary Table S1, Supplementary Figure S1). For the synthesis of the latter fragment, a solid-phase peptide synthesis using the Fmoc-strategy with acetamidomethyl (Acm)- and trityl (Trt) -protecting groups (Cys5, Cys37 and Cys17, Cys31, respectively) and a subsequent stepwise oxidation in solution was conducted, similar to the strategy used for the earlier described two-disulfide-bonded tridegin analogues [29]. The stepwise oxidation process was performed in a one-pot reaction with iodine (oxidizing agent), whereby the former Trt-protected cysteines, were deprotected during the cleavage of the peptide from the solid support and initially linked, followed by the cleavage of the Acm-protected cysteines (Figure 1b). The selective disulfide bond formation during the synthesis of the two disulfide bonds was controlled by increasing the amount of iodine as described previously [29] and by adjusting the acetic acid concentration. For the disulfide bond formation of the cysteines formerly protected by Trt, the first oxidation was performed in 100% acetic acid, whereas the deprotection of the Acm-protected cysteines and the formation of the second disulfide bond was completed in 70% acetic acid. Due to the higher acid concentration in the first oxidation, the acid-stable Acm-protected cysteines are additionally prevented from unwanted cleavage, thus ensuring the stepwise formation of the disulfide bonds [34]. To confirm the correct disulfide bond connectivity, the N-terminal fragment was digested using chymotrypsin, and the resulting fragments were analyzed subsequently by MS/MS as earlier described [29]. Several disulfide-bonded fragments representative for the disulfide bonds Cys5–Cys37 and Cys17–Cys31 were detected, confirming the correct disulfide bond connectivity of the N-terminal fragment (Figure 1c, Supplementary Table S2).

In addition, activity studies of the N-terminal fragment on FXIIIa were performed using the established FXIIIa isopeptidase activity assay [28–30]. As already observed in the case of a three-disulfide-bonded N-terminal fragment of tridegin [30], no inhibitory potential against FXIIIa was found. However, as described earlier, it is expected that the N-terminal fragment enhances the binding between tridegin and FXIIIa. In contrast, the C-terminal fragment exhibits inhibitory activity toward FXIIIa [30].

2.2. Structure Elucidation by NMR Spectroscopy

The structure of isomer $B_{[C19S,C25S]}$ [29] was determined by combining the two structures of the peptide fragments. First, these structures were elucidated by natural abundance 2D NMR spectroscopy, recording TOCSY (total correlation spectroscopy), NOESY (nuclear Overhauser enhancement spectroscopy), COSY (correlated spectroscopy), and ^{13}C-HSQC (heteronuclear single quantum coherence) spectra and calculated by Cyana [35] based on the distance and dihedral angle restraints. Within the signal assignment of the NMR spectra, the spectral resolution of the 2D NMR spectra (TOCSY and NOESY) at a magnetic field of 16.4 T allowed a clear resonance assignment for both peptide fragments (Figure 2, Supplementary Table S3).

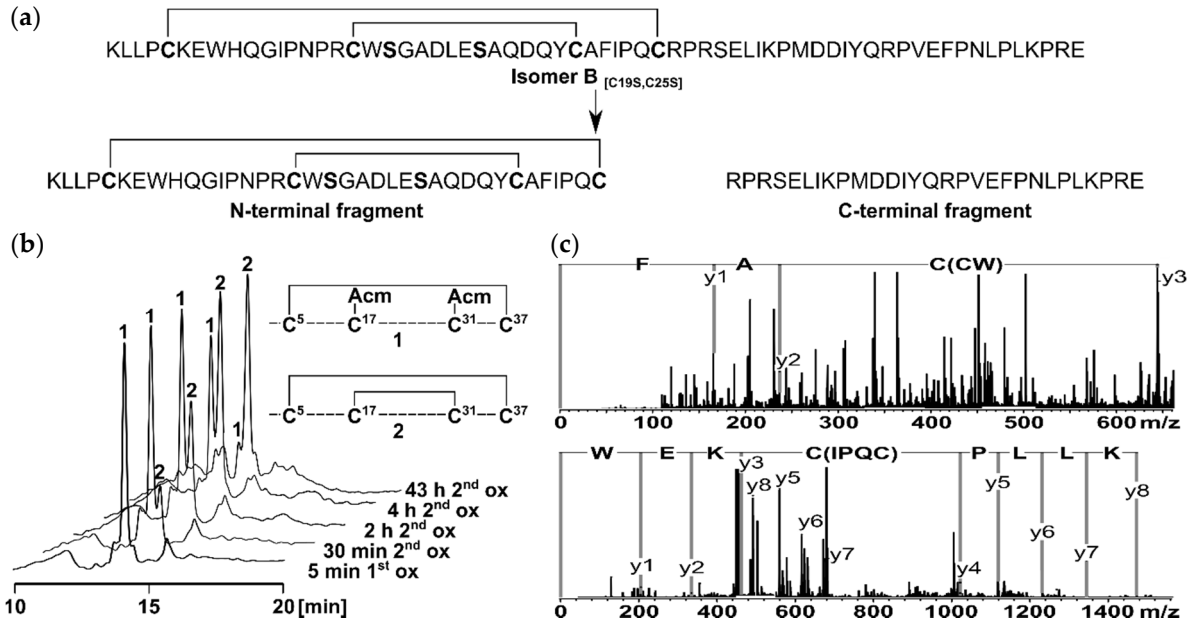

Figure 1. (**a**) Derivation of the two fragments from the two-disulfide-bonded tridegin isomer $B_{[C19S,C25S]}$ [29]. The N-terminal fragment consists of amino acid 1–37 and contains the disulfide bonds Cys5–Cys37 and Cys17–Cys31. The C-terminal fragment is composed of amino acids 38–66 without a cysteine residue; (**b**) HPLC elution profiles of the stepwise oxidation strategy applied for the synthesis of the N-terminal fragment. During the first oxidation (1.1 eq. iodine, 100% AcOH) the first disulfide bond between Cys5 and Cys37 was formed (1). Subsequently the second disulfide bond between Cys17 and Cys31 was built (2) by increasing the amount of iodine (15 eq.) and adjusting the concentration of AcOH (70%); (**c**) MS/MS analysis of the N-terminal fragment after digestion with chymotrypsin. The disulfide bond connectivity was confirmed by the characteristic MS/MS fragments C(CW) AF and KLLP C(IPQC) KEW.

The TOCSY, COSY, and HSQC spectra of the C-terminal fragment showed a high resolution and well-separated signals, which could be easily associated with the individual spin systems of the 29 amino acids. A subsequent "sequential walk" within the H_N–H_α region of the NOESY and TOCSY spectra (Figure 2a) resulted in a sequence-specific assignment of the signals, despite the difficulty of the occurrence of six prolines. Proline residues lead to an interruption of the sequential walk due to the lack of H_N. The assignments within the NOESY spectrum were used to solve the solution structures of the C-terminal fragment via Cyana [35]. The NOESY spectrum already revealed few correlations between amino acids that were separated by more than two amino acids within the sequence. This resulted in a very small number of distance restraints for the structure calculation, which was reflected in a flexible structure of the C-terminal fragment (Figure 3, Supplementary Table S4) with a backbone root mean square deviation (RMSD) of 8.54 ± 2.83 Å.

The NMR spectra of the N-terminal fragment contained more signals due to the higher number of amino acids (37 amino acids), which were successfully attributed to the amino acid positions by assigning the amino acid spin system and subsequent sequential walk within the H_N–H_α range (Figure 2b), as it was already performed for the C-terminal fragment. The two disulfide bonds as well as possible secondary structure elements within the N-terminal fragment result in a more rigid structure compared to the C-terminal fragment, enabling NOESY correlations between distant amino acids within the peptide sequence. In this context, NOESY correlations between the amino acids Trp8–Gln36, Pro15–Phe33, Cys17–Phe33, Arg16–Tyr30, Trp18–Cys31, and Ser19–Tyr30 confirmed the disulfide bond connectivity Cys5–Cys37 and Cys17–Cys31 of the N-terminal fragment, which was already verified by the aforementioned MS/MS analysis of the chymotryptic digest. The numerous NOESY correlations led to a higher set of distance restraints, which, in addition to the dihedral angle restraints, were included in the calculation of the structure via Cyana [35]. In contrast to the C-terminal fragment, three secondary structure elements

stabilized by the disulfide bonds Cys5–Cys37 and Cys17–Cys31 were identified within the N-terminal fragment (RMSD of residues 5–37: 1.20 ± 0.39 Å), e.g., one helix (Glu24–Tyr30) and two β-turns (His9–Ile12, Trp18–Ala21) (Figure 3, Supplementary Table S4). Especially the fact that the two secondary structure elements in the region Trp18–Tyr30 result in a close proximity of the serine residues at position 19 and 25 is remarkable. This may indicate that the disulfide bond between Cys19–Cys25, which occurs in the three-disulfide-bonded tridegin isomers [30], is formed as a consequence of the secondary structure elements. Regarding this, it may be concluded that during the folding process, this bond is only established after the formation of the secondary structure elements.

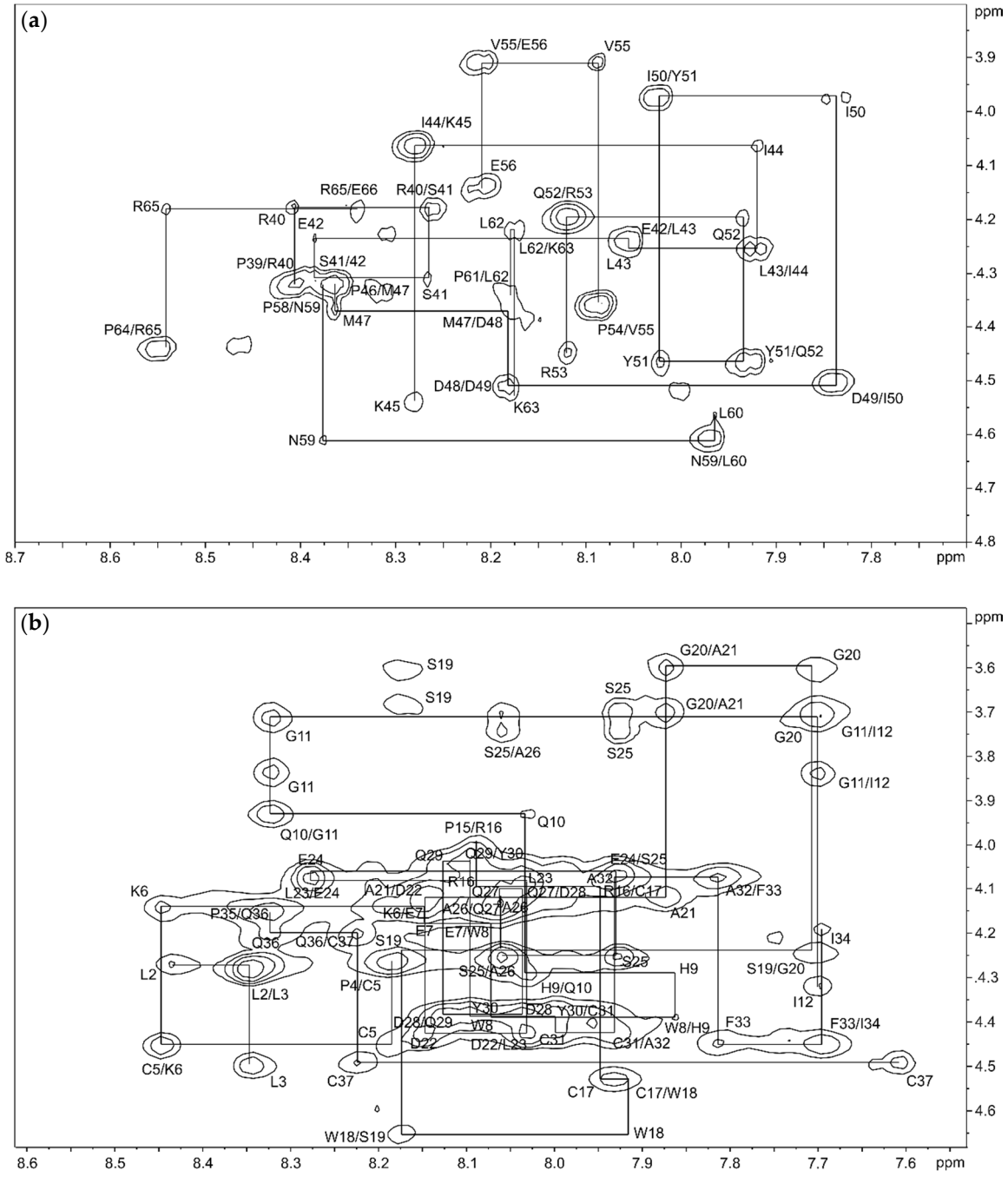

Figure 2. Backbone H_N–H_α region of the 150 ms NOESY (nuclear Overhauser enhancement spectroscopy) spectrum of the C-terminal fragment (**a**) and the N-terminal fragment (**b**) in 95% H_2O/5% D_2O with backbone connectivities labeled.

Figure 3. NMR structure of the rigid N-terminal fragment (**left**) and the flexible C-terminal fragment (**right**) presented as ensembles of the 10 structures with the lowest energies. grey: flexible C-terminal fragment; yellow: disulfide bonds Cys5–Cys37 and Cys17–Cys31; blue: helix; green: β-turns.

To determine the isomer $B_{[C19S,C25S]}$ structure [29], the distance and dihedral angle restraints of the N- and the C-terminal fragments were combined and the complete structure ensemble (100 structures, Figure 4) of the tridegin variant was calculated using Cyana [35]. Thereby, the determined secondary structure elements of the N-terminal fragment as well as the flexibility of the C-terminal fragment were preserved. The possibility of the C-terminal fragment (residue 38–66) to undergo large conformational changes was characterized by an RMSD of 14.14 ± 2.76 Å for the combined isomer $B_{[C19S,C25S]}$ structure [29] with reference to the lowest energy structure (Figure 4a). Additionally, within the structure ensemble of isomer $B_{[C19S,C25S]}$ [29] a massive proportion of this observed variation (12.15 ± 3.27 Å) resulted from the flexible C-terminal fragment (residues 38–66) while the N-terminal fragment alone (residues 1–37) had a backbone RMSD of 3.77 ± 1.42 Å. However, since the calculated structure ensemble of isomer $B_{[C19S,C25S]}$ [29] is only a combination of the independently resolved NMR structures of the N- and C-terminal fragment, the structures were further investigated via molecular dynamics simulations.

2.3. MD-Based Analysis of Isomer $B_{[C19S,C25S]}$

For the investigation of the aforementioned isomer $B_{[C19S,C25S]}$ structure [29], the model with the lowest energy from the 100-member NMR ensemble of the calculated isomer $B_{[C19S,C25S]}$ structures [29] was subjected to a 300-ns-long all-atom molecular dynamics. The prime motivation behind this effort was to produce a solvent-equilibrated ensemble of the isomer $B_{[C19S,C25S]}$ structure [29], which was originally produced by combining the independently resolved fragments (N-terminal and C-terminal fragments, as described above) determined by NMR spectroscopy. Additionally, the final structure from this MD simulation was also used as an input for molecular docking experiments on the crystal structure of FXIIIa (PDB ID: 4KTY) [16].

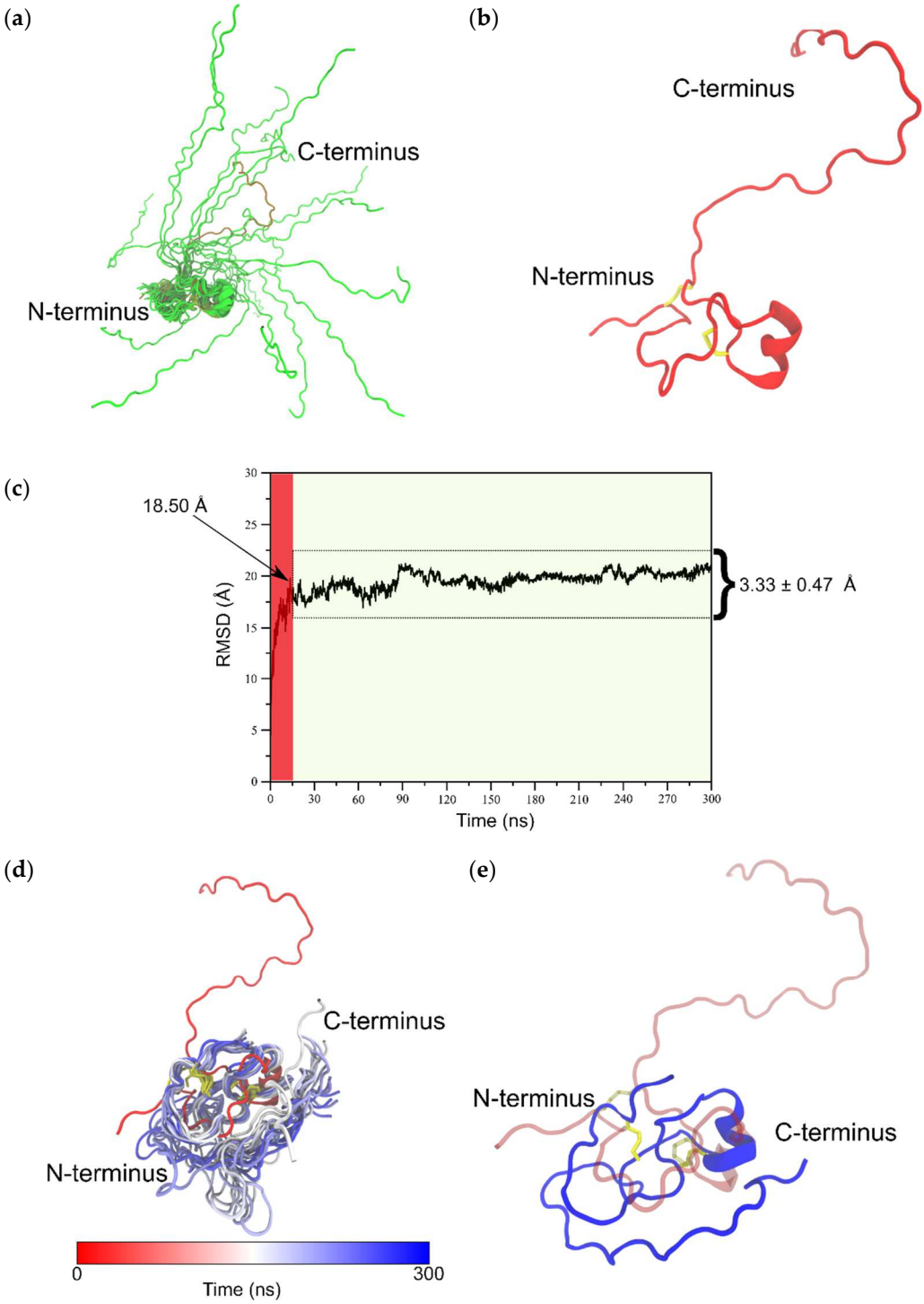

Figure 4. (**a**) Figure depicts 20 structures (green cartoons) from the 100-member NMR ensemble of full-length isomer $B_{[C19S,C25S]}$ [29] aligned on the N-terminal residues (1–37). The lowest energy model 1 is shown as red cartoons. (**b**) The lowest energy model from the NMR ensemble of isomer $B_{[C19S,C25S]}$ [29] used as input in the 300 ns molecular dynamics (MD) simulation. (**c**) Backbone root mean square deviation (RMSD) trace from the 300 ns MD simulation of isomer $B_{[C19S,C25S]}$ [29] with respect to its starting structure. The initial 15 ns of this simulation is considered as the equilibration phase (shaded red) and the remainder of the simulation (shaded green) is considered the production phase of the simulation. (**d**) Figure presents 20 equidistant structures from between 150 and 300 ns of the simulation as an ensemble (white to blue gradient cartoons) with the starting structure (red cartoon) shown as an indicator of the extent of structural change especially at the C-terminal (residues 38–66). (**e**) The final snapshot of the 300 ns MD simulation (blue cartoon) shown along with the starting structure (red transparent cartoon).

As already discussed in Section 2.2, analyses conducted of the NMR ensemble of the combined (N-terminal and C-terminal fragments) isomer $B_{[C19S,C25S]}$ structure [29] (Figure 4a) strongly indicated that the elongated C-terminal segment could potentially undergo large conformational changes upon further equilibration to attain its fully folded conformation. It was therefore clear that, prior to molecular docking experiments, MD-based refinement of this structure was necessary. To this end, a 300-ns-long all-atom MD simulation was performed on the NMR structure with the lowest energy (Figure 4b), and the resulting trajectory was analyzed for structural changes over the course of the simulation. A large conformational rearrangement marked by an 18.50 Å change in backbone RMSD was observed within the first 15 ns of the 300 ns simulation (Figure 4c). This was characterized by a rapid collapse of the flexible C-terminal fragment (residues 38–66) around the disulfide-bonded N-terminal segment (residues 1–37). Remarkably, after this initial dramatic change, the remainder of the simulation saw the structure steadily equilibrate deviating only by an average of 3.33 ± 0.47 Å with respect to the structure at 15 ns. The large deviation between the NMR starting structure and the final simulation structure can clearly be explained due to the fact that, in the NMR structure, the N- and C-terminal segments were resolved as separate entities and were combined as a final step to create the full-length isomer $B_{[C19S,C25S]}$ structure [29]. We believe that our simulation captures the full extent of conformational changes the structure would have undergone if the N-terminal and C-terminal segments could possibly have been resolved as a single entity via NMR spectroscopy and that the structures obtained from any part of the trajectory after the initial 15 ns would surely fall within the low-energy conformations of isomer $B_{[C19S,C25S]}$ [29] in its physiological environment. To further confirm this, we show that the conformational ensemble for the entire structure produced via the MD simulation (containing 2850 snapshots) has an RMSD of 3.33 ± 0.47 Å, which is comparable to the RMSD (3.77 ± 1.42 Å) of the 100-member NMR ensemble of the N-terminal segment of isomer $B_{[C19S,C25S]}$ [29]. We also note that the α-helical motif seen in the NMR starting structure (Glu24–Tyr30) was consistently found through the production phase of the MD simulation. The final snapshot of this 300 ns simulation was used as an input structure for subsequent molecular docking simulations. A video of this MD simulation is provided as supplementary content. Structural alignments of the final snapshot of the simulation with a previously computationally modeled version of the same peptide [29] using the MUSTANG algorithm [36] revealed that although the general fold was preserved, the NMR-based model (current study) varied from the earlier computational model (Figure 5b–d) [29]. This is understandable based on the fact that the earlier model was produced by mutating its three-disulfide-bonded counterpart, which again had its origins in computational modeling. Interestingly though, the parts of the C-terminal segment, seemed to align well against each other (Figure 5b–d). The current produced model has the clear advantage that its origin is from NMR spectroscopy. As a means to confirm that this MD-derived structure from the 300 ns simulation was reproducible, a second, independent 1000-ns-long simulation was conducted. The equilibrated structures from this longer simulation aligned well with the structure produced by the 300 ns simulation in this study (Supplementary Figure S2).

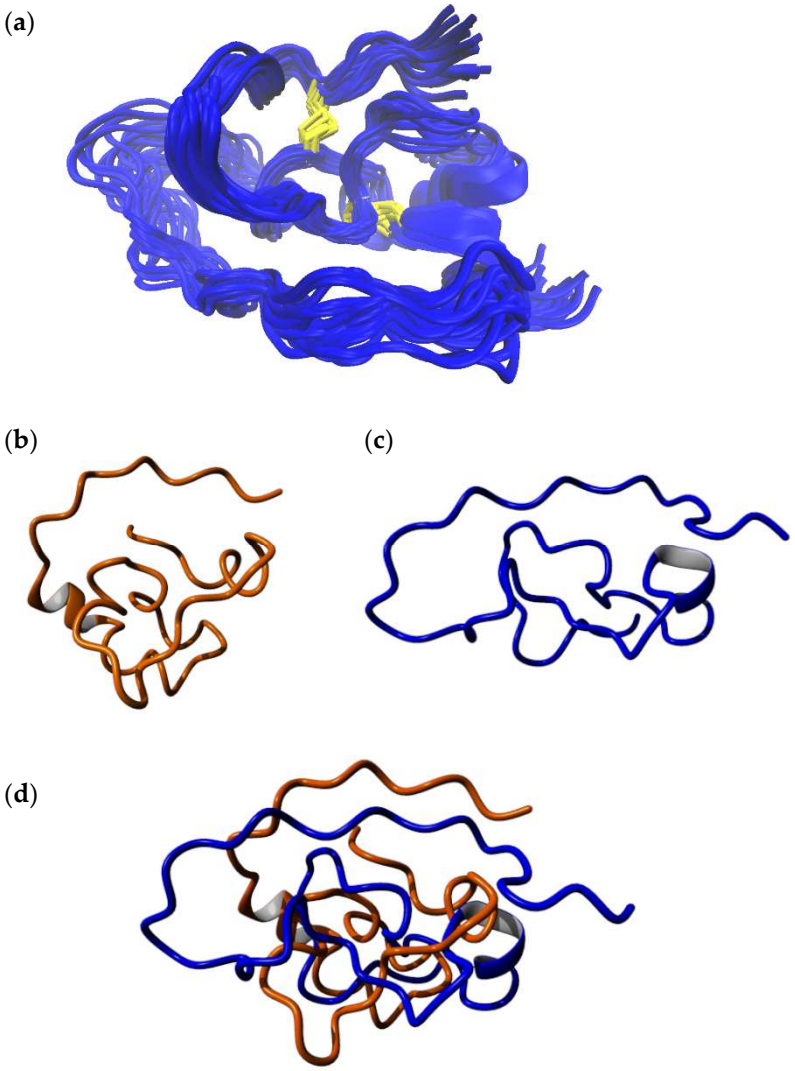

Figure 5. (**a**) The final 20 snapshots of the 300 ns MD simulation of the full-length model of isomer $B_{[C19S,C25S]}$ [29]. (**b**) Computationally derived structure of the same peptide analogue from an earlier study [29]. (**c**) Final snapshot from the 300 ns simulation from the current study. (**d**) Structural alignment of the final structure from the 300 ns MD simulation from the current study (blue) with the computationally derived structure of the same peptide (orange) from an earlier study [29]. The alignment indicates that the two models essentially have varying structures while the underlying fold is preserved. The computationally derived structure from earlier work has a more compact fold owing to the fact that it was created based on its three-disulfide-bonded parent, where residues Cys19 and Cys25 were linked by a disulfide bond. A fair alignment between the trailing end of the C-terminal segment is observed. The alignment was carried out using the MUSTANG algorithm [36].

2.4. Molecular Docking of Full-Length Tridegin Variant on FXIIIa

Docking of the full-length model of isomer $B_{[C19S,C25S]}$ [29] (derived from the final 300 ns simulation snapshot) (Figure 5a) onto FXIIIa resulted in one pose amongst the top-ten docking poses that satisfies the inhibitory characteristic of tridegin (i.e., it binds next to the catalytic site) (Supplementary Figure S3). All remaining docks cluster around the β-barrel domain of FXIIIa, which is located significantly far from the FXIIIa catalytic site, and are therefore irrelevant to our analysis. On an atomic/residual level, the important docking pose of isomer $B_{[C19S,C25S]}$ [29] shows the C-terminal region (residues 53–60) participating in several non-covalent interactions in and around the catalytic site (Figure 6, Supplementary Table S5–S7). The original non-proteolytically activated crystal structure from Stieler et al. [16] presents a hydrophobic tunnel at the active site formed by the

aromatic interactions between the Trp279 and Trp370 residues of FXIIIa (Figure 6). The two ends of this tunnel serve as the entry points for the FXIIIa substrates, lysine and glutamine, through which they reach the catalytic Cys314 at the bottom of the cavity that the tunnel is formed on top of. The original non-proteolytically activated crystal structure of FXIIIa (PDB ID: 4KTY [16]) was stabilized using the FXIIIa inhibitor ZED1301, which irreversible bound to the catalytic Cys314, thereby occupying the hydrophobic tunnel and preventing access for competitive substrate [16]. The mode of inhibition for the full-length model of isomer $B_{[C19S,C25S]}$ [29] is very similar to that of ZED1301 since residues from the C-terminal region not only participate in hydrophobic interactions with FXIIIa residues that would form the hydrophobic tunnel, but some tridegin residues such as Arg53 and Phe57 also stabilize the C-terminal region by interacting with the critical Trp279 and Trp370 FXIIIa residues (Supplementary Figure S4, Supplementary Table S5–S7). Therefore, the C-terminal region appears to competitively occupy the substrate-entry hydrophobic tunnel, thereby preventing substrate access to the catalytic Cys314 similar to ZED1301. An improvement compared to the inhibitor ZED1301 might be that the model structure of isomer $B_{[C19S,C25S]}$ [29] also potentially blocks the catalytic dyad of FXIIIa (His342, Glu401) which is responsible for incorporating the substrate lysine into the hydrophobic tunnel. This is suspected since the inhibitor ZED1301 does not reach the catalytic dyad, whereas the tridegin analogue rests on the residues His342 and Glu401. In addition to the ZED1301 comparison, the docking results of the NMR-based model structure was aligned to a previously reported docking with the computationally modeled version of the same peptide (Supplementary Figure S5) [29]. In this regard, both dockings showed a similar binding into the hydrophobic tunnel of FXIIIa, despite the overall structural variations between the two (Figure 5b–d). However, there is one significant difference between the two complexes, which is the orientation of the C-terminal part within the hydrophobic pocket. While the NMR-based structure guide through the hydrophobic tunnel showed that the C-terminus of the peptide is on the Q-site (site of the tunnel where glutamine normally binds) of FXIIIa, the C-terminus of the previously reported structure [29] was observed on the K-site (site where lysine binds) close to the catalytic dyad. The differences in the orientation can be attributed to two main things: (a) firstly the differences in the N-terminal structure (residue 1–37) in both isomer $B_{[C19S,C25S]}$ models [29], whose role in this interaction is to orient the C-terminal region within the FXIIIa hydrophobic pocket, and (b) methodological differences in the implementation of docking between the current and previous study. The similarity in binding location though further underlines the importance of the C-terminal fragment in binding and subsequent inhibition of FXIIIa.

Although the Arg16 residue from the tridegin isomer $B_{[C19S,C25S]}$ N-terminal part [29] of the NMR-based model also appears to interact with FXIIIa in this docking pose, the effect of the N-terminal region (residue 1–37) might only be complimentary. The interaction may only play a role in the initial establishment of contact between isomer $B_{[C19S,C25S]}$ [29] and FXIIIa but is unlikely to play any role in the subsequent inhibition. This was confirmed by a docking were only the N-terminal fragment was docked to FXIIIa. Similar to isomer $B_{[C19S,C25S]}$ [29], when we dock only the NMR-based N-terminal fragment structure of the tridegin analogue on FXIIIa, one docking pose amongst top-ten docked close to the catalytic site. However, unlike the full-length isomer $B_{[C19S,C25S]}$ [29] model, the N-terminal fragment structure binds only superficially on top of the catalytic site (Supplementary Figure S6). In this docking pose, neither the hydrophobic tunnel nor any hydrophobic access is disrupted, which is also a hint for the reduced influence of the N-terminal part on the inhibition to FXIIIa.

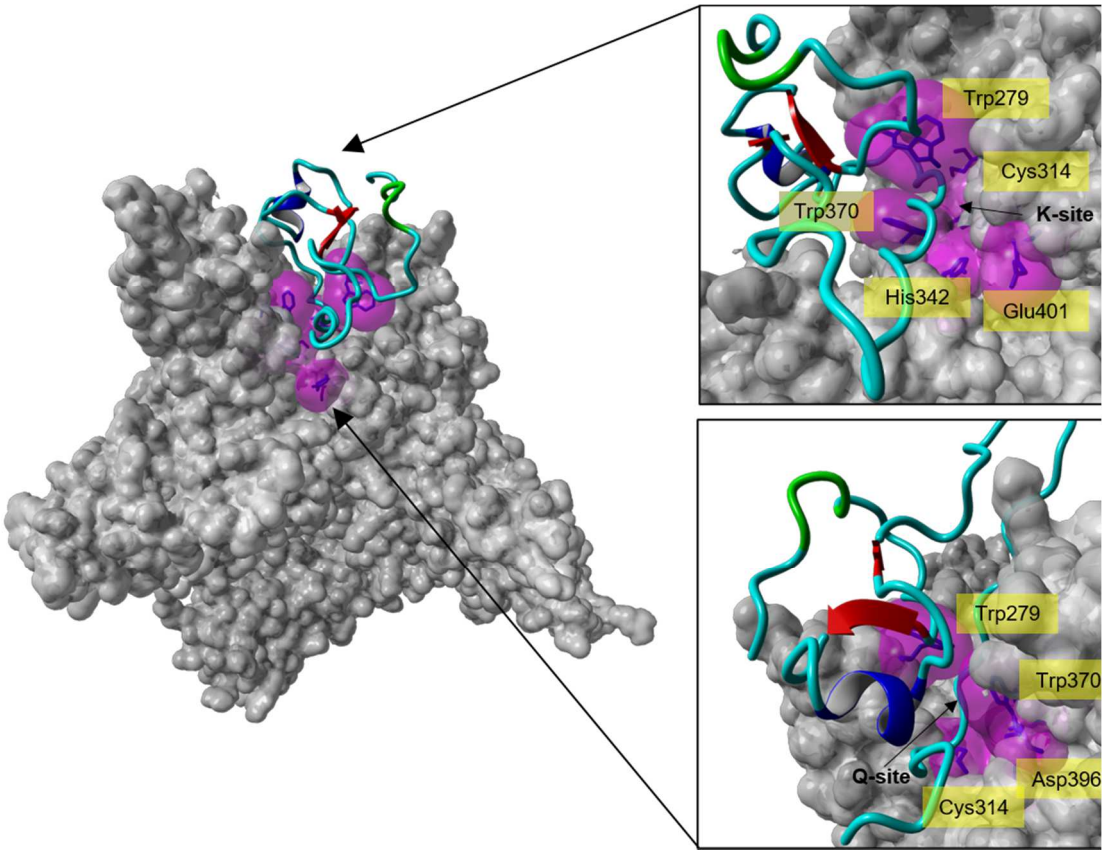

Figure 6. Molecular docking analysis of the interaction of isomer $B_{[C19S,C25S]}$ [29] with the catalytic site of FXIIIa. **Left**: Crystal structure of the calcium-activated FXIIIa-monomer (PDB ID: 4KTY [16], grey surface) docked with one of the top-ten-ranked conformations of isomer $B_{[C19S,C25S]}$ [29] (cyan ribbon), which interacts with the catalytic site of FXIIIa. **Right**: Zoom-in from different directions (lysine access site (**top**, K-site) and glutamine access site (**bottom**, Q-site)) of the FXIIIa active site interacting with isomer $B_{[C19S,C25S]}$ [29]. The active site residues of FXIIIa (Cys314, His373, Asp396, Trp279, and Trp370) are shown as blue sticks enclosed by their molecular surfaces (violet translucent surface).

3. Materials and Methods

3.1. Materials

Fmoc-amino acids were purchased from Orpegen Peptide Chemicals (Heidelberg, Germany) and Novabiochem (Schwalbach, Germany). HBTU, resins, and further chemicals for solid-phase peptide synthesis, including reagent-grade N-methylmorpholine, piperidine, trifluoroacetic acid (TFA), and N,N-dimethylformamide (DMF) were purchased from IRIS Biotech (Marktredwitz, Germany), Sigma-Aldrich Chemie GmbH (Munich, Germany), Alfa Aesar (Karlsruhe, Germany), Abcr GmbH (Karlsruhe, Germany), VWR International (Darmstadt, Germany), and FLUKA Chemika (Seelze, Germany). Solvents (acetonitrile, water, methanol, ethyl acetate, diethyl ether) and chemicals (iodine, acetic acid) used for peptide purification and oxidation were obtained from VWR International (Darmstadt, Germany) and Fisher Scientific (Schwerte, Germany).

3.2. Peptide Synthesis and Purification

The synthesis of the linear peptide precursors according to an automated standard Fmoc SPPS protocol using a ResPep SL peptide synthesizer from Intavis Bioanalytical Instruments GmbH (Cologne, Germany) as well as the subsequent peptide cleavage from the resin and the purification step via RP-HPLC were carried out as previously described [29].

The purity of the linear peptides was >95%, which was assessed by analytical RP-HPLC on a Shimadzu LC-20AD system equipped with a Vydac 218TP column (C18, 250 × 4.6 mm, 5 µm particle size, 300 Å pore size). The gradient elution system contained

0.1% TFA in water (eluent A) and 0.1% TFA in acetonitrile (eluent B). Peptide elution was achieved with a gradient of 20% to 50% eluent B in 30 min and a flow rate of 1 mL/min. The peptides were detected at λ = 220 nm.

3.3. Selective Oxidation of the N-Terminal Fragment

The selective oxidation of the two-disulfide-bonded N-terminal peptide Lys1–Cys37 proceeded in a one-pot reaction slightly modified to the already described protocol [29]. In brief, the linear precursors (1 eq.) were dissolved in 100% acetic acid to yield a final concentration of 0.05 mM. The oxidation of the first disulfide bond with 1.1 eq. iodine (0.1 M in methanol) was stirred at room temperature and under argon atmosphere. After 15 min, 13.9 eq. iodine (0.1 M in methanol) and water was added to the reaction mixture in order to decrease the acetic acid concentration to 70%. The reaction was stirred for a further 43 h (second oxidation). The oxidation reaction was stopped by the removal of iodine by extraction with the same volume of ethyl acetate (three times). The peptide-containing aqueous solutions were combined, freeze-dried, and purified via RP-HPLC.

3.4. Peptide Characterization and Determination of Disulfide Connectivity

Peptide characterization was achieved by means of analytical RP-HPLC (see above for the linear precursor), mass spectrometry, and amino acid analysis.

The peptide concentration as well as the amino acid composition were analyzed using an LC 3000 system from Eppendorf-Biotronik (Hamburg, Germany). Peptide hydrolysis was carried out in 6 N HCl at 110 °C in sealed tubes for 24 h. Subsequently, the hydrolyzed peptides were dried in a vacuum concentrator and redissolved. The respective amino acid concentrations were determined by comparison with an amino acid standard solution (Laborservice Onken, Gründau, Germany).

Peptide masses were determined using matrix-assisted laser desorption/ionization (MALDI) mass spectrometry. As matrix 2,5-dihydroxyacetophenone (2,5-DHAP) was used according to the manufacture's guideline (Bruker Daltonics, Bremen, Germany). MALDI mass spectra were produced on an UltrafleXtreme instrument (Bruker Daltonics, Bremen, Germany).

The disulfide connectivity of the N-terminal fragment was determined as described recently [29,30]. Therefore, a micrOTOF-Q III device (Bruker Daltonics, Bremen, Germany) was used to measure electrospray ionization (ESI) mass and tandem-mass spectra.

3.5. Enzyme Activity Assay

The inhibitory potential of the N-terminal tridegin fragment toward FXIIIa was performed in an FXIIIa isopeptidase activity assay using the fluorogenic substrate H-Tyr(3-NO_2)-Glu(NH-$(CH_2)_4$-NH-Abz)-Val-Lys-Val-Ile-NH_2 as described previously [30].

3.6. NMR Spectroscopy and Structure Prediction

The natural abundance NMR experiments for the ^{1}H, ^{15}N, and ^{13}C chemical shift assignments were performed at 293 K in 50 mM sodium phosphate pH 6.3 (95% H_2O/5% D_2O) on a Bruker Avance III HD 700 MHz Cryo spectrometer. The peptides were measured at a concentration of 3 mM, and the backbone as well as the side chain atoms were assigned via a combination of 2D [^{1}H, ^{1}H]-TOCSY, [^{1}H, ^{1}H]-NOESY, [^{1}H, ^{1}H]-COSY, and [^{1}H, ^{13}C]-HSQC spectra using water suppression. The spectra were processed with TOP SPIN 4.0.6 (Bruker) and analyzed using CcpNmr Analysis (Collaborative Computing Project for NMR). Distance constraints were extracted form [^{1}H,^{1}H]-NOESY spectra acquired with a mixing time of 150 ms and a recycle delay of 1.5 s. Upper-limit-distance constraints were calibrated according to their intensities in the NOESY spectra. To calculate the structure of the fragments based on the chemical shift data the program Cyana [35] was used. Cyana [35] was also used to calculate a hypothetical structure of the full-length tridegin analogue out of the combined distance and dihedral restraints from the NMR experiments of the N-

and C-terminal fragments. The 100 structures with the lowest energies were selected to represent the NMR-solution structures.

3.7. Molecular Dynamics (MD) Simulations

Molecular dynamics (MD) simulations in this study were carried out using the Gromacs 2018 package [37,38]. The first model of the 100-member NMR ensemble of the full-length model of isomer $B_{[C19S,C25S]}$ [29] was used as the starting structure of the 300-ns-long simulation. The peptide was placed in the center of a cubic simulation cell, with the edges of the cube separated by at least 12 Å from all atoms of the peptide. The peptide was solvated using the TIP3P water model [39] with additional Na+ and Cl− counter ions added to achieve a physiological salt concentration of 0.9%, while maintaining a zero net charge on the entire system. The solvated system was subjected to 5000 steps of steepest-descents energy minimization with the Amber-ff14sb [40] force field, which was used to describe atomic motions for all parts of the simulation. The energy-minimized system was first subjected to a temperature equilibration in the NVT (constant number of atoms, volume, temperature) ensemble for 2 ns, with temperature maintained by the velocity-rescaled variant of the Berendsen thermostat at 300 K [41]. Subsequently a 2 ns simulation to equilibrate the pressure of the system at 1 atm was conducted in the NPT (constant number of atoms, pressure, temperature) ensemble aided by the Parrinello–Rahman barostat [42,43]. During both the temperature and pressure equilibration runs, all heavy atoms were position-restrained by the LINCS algorithm [44]. The production run was conducted for 300 ns using a 2 fs timestep. Long-range interactions were cutoff at 10 Å, and the electrostatics were described by the particle-mesh Ewald method [45,46]. Periodic boundary conditions were employed in the simulations, the effects of which were adjusted prior to conducting analyses on the trajectory. Trajectory analysis, namely the backbone root mean square deviation (RMSD) computation was conducted in VMD 1.9.3. [47], which was also used in the creation of molecular graphics. Snapshots were written at a 100 ps interval to disc, resulting in a total of 3000 snapshots collected for analysis, from this simulation.

3.8. Blind Docking Studies on the FXIIIa Crystall Structure (PDB ID: 4KTY)

The full-length model of isomer $B_{[C19S,C25S]}$ [29] was used for docking onto the modified and simulation-equilibrated crystal structure of FXIIIa originally derived from the source PDB ID: 4KTY [16]. The PDB structure used as a receptor for docking was a simulation-averaged structure of the non-proteolytically activated FXIIIa, which had been modified, i.e., missing regions/loop filled, all heteroatoms/water molecules removed, and subjected to classical molecular dynamic simulation. The details of this simulation have been reported earlier [15]. The full-length model obtained as the final snapshot of the 300 ns MD simulation (described in Section 3.7) was used as the ligand for the docking simulation. Docking was performed on the Hdock server (http://hdock.phys.hust.edu.cn/) in a blind fashion and under the default conditions of the server [48]. The Hdock server is based on a hybrid algorithm of template-based modeling and ab initio free docking and is currently ranked favorably amongst the topmost automated docking servers in the recent CASP (critical assessment of protein structure prediction) competitions [49]. Only the top-ten docking poses generated by the server were closely inspected. The docking pose that strongly agreed with the experimental data was subjected to a docking refinement protocol on the Haddock 2.2 webserver (https://milou.science.uu.nl/services/HADDOCK2.2/haddockserver-refinement.html) that allows for flexible refinement in explicit solvent of the docked complex [50]. The model with the best Haddock score from the output clusters generated out of the refinement protocol was finally inspected in terms of interatomic interactions on the protein interaction calculator webserver (http://pic.mbu.iisc.ernet.in/) [51]. Similarly docking was also performed with the energetically minimum NMR structure of the well-defined N-terminal fragment as the ligand and the above-described FXIIIa structure as the receptor.

4. Conclusions

In summary, we have experimentally determined for the first time, the structure of a two-disulfide-bonded tridegin variant. This structure contained a flexible C-terminal segment and a more rigid N-terminal part which showed distinct secondary structure elements besides being stabilized by the two disulfide bonds Cys5–Cys37 and Cys17–Cys31. The cysteine-rich N-terminal fragment also shows that the two serine residues Ser19 and Ser25, which are substituted by the cysteines Cys19 and Cys25 in the three-disulfide-bonded tridegin isomers, were in close proximity to a helix and a β-turn secondary structure element, which suggests that the secondary structure elements are responsible for the formation of this specific disulfide bond. Therefore, it can be assumed for the disulfide bond Cys19–Cys25 in the three-disulfide-bonded tridegin isomer that it is generated after the formation of the secondary structure elements within the folding process. With regard to the structure–activity relationships, it can be assumed that the low structural influence of the disulfide bond results in an already experimentally described comparable binding behavior and inhibitory potential to FXIIIa for the three-disulfide-bonded isomer B [28] and the two-disulfide-bonded isomer $B_{[C19S,C25S]}$ [29].

The full-length structure of isomer $B_{[C19S,C25S]}$ [29] generated from the NMR-based results of the N-terminal and C-terminal fragment was subsequently refined by MD simulations and used for molecular docking to FXIIIa. Thereby, it could be demonstrated that the isomer $B_{[C19S,C25S]}$ [29] binds in close proximity to the active site resulting in a blockage of the catalytic Cys314 for substrates as described earlier [29]. The isomer $B_{[C19S,C25S]}$ [29], especially the C-terminal region, penetrates into the hydrophobic tunnel where the active site of FXIIIa is located and competitively inhibits the transglutaminase functionality of FXIIIa by blocking the catalytic triad and catalytic dyad. The interaction with the hydrophobic tunnel of FXIIIa demonstrates how important the flexible C-terminal region is for the inhibition mode of isomer $B_{[C19S,C25S]}$ [29] and that the rigid N-terminal segment only plays a minor role for the inhibition by enhancing the binding to FXIIIa.

In conclusion, the deeper insight into the structure–activity relationships of the FXIIIa inhibitor tridegin from the docking studies will prospectively support the future development of anticoagulant-therapy-relevant compounds targeting FXIIIa.

Supplementary Materials: The following are available online at https://www.mdpi.com/1422-0067/22/2/880/s1.

Author Contributions: The study has been designed by D.I., T.S. (Thomas Schmitz) performed synthesis as well as functional and structural analysis of the peptides. B.N. performed the MS measurements and T.S. (Torsten Steinmetzer) provided his expertise regarding the FXIIIa activity assay. T.S. (Thomas Schmitz) and C.A.B. performed the FXIIIa activity assay. T.S. (Thomas Schmitz) and O.O. analyzed the NMR spectra and calculated the peptide structures. A.A.P.G. and A.B. carried out the computational studies. Data analysis and interpretation was carried out by all authors. The manuscript was written through contributions of all authors. All authors have given approval to the final version of the manuscript. All authors have read and agreed to the published version of the manuscript.

Funding: The Bruker ultrafleXtreme TOF/TOF instrument (to M. Engeser) and the Bruker Avance III HD 700 MHz Cryo spectrometer (to S. Nozinovic) were funded by the University of Bonn, the Ministry of Innovation, Science, and Research of North-Rhine Westfalia and the DFG. This study was financially supported by the German Foundation of Heart Research and by the University of Bonn within university science program HSPII (to D.I.).

Institutional Review Board Statement: Not applicable.

Informed Consent Statement: Not applicable.

Data Availability Statement: The data presented in this study are available on request from the corresponding author.

Acknowledgments: We are grateful to D. Menche and S. Nozinovic (University of Bonn) as well as R. Hartmann and D. Willbold (FZ Jülich) for measuring the 2D NMR spectra of the peptides on their instruments. This work was supported by the German Foundation of Heart Research to D.I., which is gratefully acknowledged. The FLI (Fritz-Lipmann-Institute) is member of the Leibniz Association (WGL) and financially supported by the Federal Government of Germany and the State of Thuringia (to O.O.).

Conflicts of Interest: The authors declare no competing financial interest.

Abbreviations

Acm	Acetamidomethyl
AcOH	Acetic acid
Arg	Arginine
Asp	Aspartic acid
BPTI	Bovine pancreatic trypsin inhibitor
CASP	critical assessment of protein structure prediction
COSY	Correlated spectroscopy
Cys	Cysteine
2,5-DHAP	2,5-Dihydroxyacetophenone
DMF	Dimethylformamide
ESI	Electrospray ionization
Fmoc	Fluorenylmethoxycarbonyl
FXIII	Blood coagulation factor XIII
FXIIIa	Activated blood coagulation factor XIII
Glu	Glutamic acid
HBTU	2-(1H-Benzotriazol-1-yl)-1,1,3,3-tetramethyluronium hexafluorophosphate
HSQC	Heteronuclear single quantum coherence
His	Histidine
Ile	Isoleucine
Lys	Lysine
MALDI	Matrix-assisted laser desorption/ionization
MD	Molecular dynamics
MS	Mass spectrometry
MS/MS	Tandem mass spectrometry
NMR	Nuclear magnetic resonance
NOESY	Nuclear Overhauser enhancement spectroscopy
NPT	constant number of atoms, pressure, temperature
NSGM	Non-saccharide glucosaminoglycan mimetics
NVT	constant number of atoms, volume, temperature
Phe	Phenylalanine
Pro	Proline
RMSD	Root mean square deviation
RP-HPLC	Reversed-phase high-performance liquid chromatography
Ser	Serine
SPPS	Solid phase peptide synthesis
TFA	Trifluoroacetic acid
TOCSY	Total correlation spectroscopy
Trt	Trityl
Trp	Tryptophane
Tyr	Tyrosine
VMD	Visual molecular dynamics

References

1. Whitaker, I.S.; Rao, J.; Izadi, D.; Butler, P.E. Historical Article: Hirudo medicinalis: Ancient origins of, and trends in the use of medicinal leeches throughout history. *Br. J. Oral Maxillofac. Surg.* **2004**, *42*, 133–137. [CrossRef]
2. Kvist, S.; Manzano-Marín, A.; de Carle, D.; Trontelj, P.; Siddall, M.E. Draft genome of the European medicinal leech Hirudo medicinalis (Annelida, Clitellata, Hirudiniformes) with emphasis on anticoagulants. *Sci. Rep.* **2020**, *10*, 9885. [CrossRef] [PubMed]

3. Salzet, M. Anticoagulants and inhibitors of platelet aggregation derived from leeches. *FEBS Lett.* **2001**, *492*, 187–192. [CrossRef]
4. Greinacher, A.; Warkentin, T.E. The direct thrombin inhibitor hirudin. *Thromb. Haemost.* **2008**, *99*, 819–829. [CrossRef]
5. Markwardt, F. Hirudin as alternative anticoagulant—A historical review. *Semin. Thromb. Hemost.* **2002**, *28*, 405–414. [CrossRef]
6. Callas, D.D.; Hoppensteadt, D.; Fareed, J. Comparative studies on the anticoagulant and protease generation inhibitory actions of newly developed site-directed thrombin inhibitory drugs. Efegatran, argatroban, hirulog, and hirudin. *Semin. Thromb. Hemost.* **1995**, *21*, 177–183. [CrossRef]
7. Arsenault, K.A.; Hirsh, J.; Whitlock, R.P.; Eikelboom, J.W. Direct thrombin inhibitors in cardiovascular disease. *Nat. Rev. Cardiol.* **2012**, *9*, 402–414. [CrossRef]
8. Lee, C.J.; Ansell, J.E. Direct thrombin inhibitors. *Br. J. Clin. Pharmacol.* **2011**, *72*, 581–592. [CrossRef]
9. Griffin, J.H. Blood coagulation. The thrombin paradox. *Nature* **1995**, *378*, 337–338. [CrossRef]
10. Shaw, C.M.; O'Hanlon, D.M.; McEntee, G.P. Venous thrombosis. *Am. J. Surg.* **2003**, *186*, 167–168. [CrossRef]
11. Lane, D.A.; Philippou, H.; Huntington, J.A. Directing thrombin. *Blood* **2005**, *106*, 2605–2612. [CrossRef] [PubMed]
12. Muszbek, L.; Bereczky, Z.; Bagoly, Z.; Komáromi, I.; Katona, É. Factor XIII: A coagulation factor with multiple plasmatic and cellular functions. *Physiol. Rev.* **2011**, *91*, 931–972. [CrossRef] [PubMed]
13. Weisel, J.W.; Litvinov, R.I. Fibrin Formation, Structure and Properties. *Subcell. Biochem.* **2017**, *82*, 405–456. [CrossRef] [PubMed]
14. Gupta, S.; Biswas, A.; Akhter, M.S.; Krettler, C.; Reinhart, C.; Dodt, J.; Reuter, A.; Philippou, H.; Ivaskevicius, V.; Oldenburg, J. Revisiting the mechanism of coagulation factor XIII activation and regulation from a structure/functional perspective. *Sci. Rep.* **2016**, *6*, 30105. [CrossRef] [PubMed]
15. Singh, S.; Nazabal, A.; Kaniyappan, S.; Pellequer, J.-L.; Wolberg, A.S.; Imhof, D.; Oldenburg, J.; Biswas, A. The Plasma Factor XIII Heterotetrameric Complex Structure: Unexpected Unequal Pairing within a Symmetric Complex. *Biomolecules* **2019**, *9*, 765. [CrossRef]
16. Stieler, M.; Weber, J.; Hils, M.; Kolb, P.; Heine, A.; Büchold, C.; Pasternack, R.; Klebe, G. Structure of active coagulation factor XIII triggered by calcium binding: Basis for the design of next-generation anticoagulants. *Angew. Chem. Int. Ed. Engl.* **2013**, *52*, 11930–11934. [CrossRef]
17. Aleman, M.M.; Byrnes, J.R.; Wang, J.-G.; Tran, R.; Lam, W.A.; Di Paola, J.; Mackman, N.; Degen, J.L.; Flick, M.J.; Wolberg, A.S. Factor XIII activity mediates red blood cell retention in venous thrombi. *J. Clin. Investig.* **2014**, *124*, 3590–3600. [CrossRef]
18. Byrnes, J.R.; Wolberg, A.S. Newly-Recognized Roles of Factor XIII in Thrombosis. *Semin. Thromb. Hemost.* **2016**, *42*, 445–454. [CrossRef]
19. Duval, C.; Allan, P.; Connell, S.D.A.; Ridger, V.C.; Philippou, H.; Ariëns, R.A.S. Roles of fibrin α- and γ-chain specific cross-linking by FXIIIa in fibrin structure and function. *Thromb. Haemost.* **2014**, *111*, 842–850. [CrossRef]
20. Wolberg, A.S. Fibrinogen and factor XIII: Newly recognized roles in venous thrombus formation and composition. *Curr. Opin. Hematol.* **2018**, *25*, 358–364. [CrossRef]
21. Avery, C.A.; Pease, R.J.; Smith, K.; Boothby, M.; Buckley, H.M.; Grant, P.J.; Fishwick, C.W.G. (±) cis-Bisamido epoxides: A novel series of potent FXIII-A inhibitors. *Eur. J. Med. Chem.* **2015**, *98*, 49–53. [CrossRef] [PubMed]
22. Iwata, Y.; Tago, K.; Kiho, T.; Kogen, H.; Fujioka, T.; Otsuka, N.; Suzuki-Konagai, K.; Ogita, T.; Miyamoto, S. Conformational analysis and docking study of potent factor XIIIa inhibitors having a cyclopropenone ring. *J. Mol. Graph. Model.* **2000**, *18*, 591–599. [CrossRef]
23. Schmitz, T.; Bäuml, C.A.; Imhof, D. Inhibitors of blood coagulation factor XIII. *Anal. Biochem.* **2020**, *605*, 113708. [CrossRef] [PubMed]
24. Al-Horani, R.A.; Kar, S. Factor XIIIa inhibitors as potential novel drugs for venous thromboembolism. *Eur. J. Med. Chem.* **2020**, *200*, 112442. [CrossRef] [PubMed]
25. Pasternack, R.; Büchold, C.; Jähnig, R.; Pelzer, C.; Sommer, M.; Heil, A.; Florian, P.; Nowak, G.; Gerlach, U.; Hils, M. Novel inhibitor ZED3197 as potential drug candidate in anticoagulation targeting coagulation FXIIIa (F13a). *J. Thromb. Haemost.* **2020**, *18*, 191–200. [CrossRef]
26. Al-Horani, R.A.; Karuturi, R.; Lee, M.; Afosah, D.K.; Desai, U.R. Allosteric Inhibition of Factor XIIIa. Non-Saccharide Glycosaminoglycan Mimetics, but Not Glycosaminoglycans, Exhibit Promising Inhibition Profile. *PLoS ONE* **2016**, *11*, e0160189. [CrossRef]
27. Finney, S.; Seale, L.; Sawyer, R.T.; Wallis, R.B. Tridegin, a new peptidic inhibitor of factor XIIIa, from the blood-sucking leech Haementeria ghilianii. *Biochem. J.* **1997**, *324 Pt 3*, 797–805. [CrossRef]
28. Bäuml, C.A.; Paul George, A.A.; Schmitz, T.; Sommerfeld, P.; Pietsch, M.; Podsiadlowski, L.; Steinmetzer, T.; Biswas, A.; Imhof, D. Distinct 3-disulfide-bonded isomers of tridegin differentially inhibit coagulation factor XIIIa: The influence of structural stability on bioactivity. *Eur. J. Med. Chem.* **2020**, *201*, 112474. [CrossRef]
29. Bäuml, C.A.; Schmitz, T.; Paul George, A.A.; Sudarsanam, M.; Hardes, K.; Steinmetzer, T.; Holle, L.A.; Wolberg, A.S.; Pötzsch, B.; Oldenburg, J.; et al. Coagulation Factor XIIIa Inhibitor Tridegin: On the Role of Disulfide Bonds for Folding, Stability, and Function. *J. Med. Chem.* **2019**, *62*, 3513–3523. [CrossRef]
30. Böhm, M.; Bäuml, C.A.; Hardes, K.; Steinmetzer, T.; Roeser, D.; Schaub, Y.; Than, M.E.; Biswas, A.; Imhof, D. Novel insights into structure and function of factor XIIIa-inhibitor tridegin. *J. Med. Chem.* **2014**, *57*, 10355–10365. [CrossRef]

31. Böhm, M.; Kühl, T.; Hardes, K.; Coch, R.; Arkona, C.; Schlott, B.; Steinmetzer, T.; Imhof, D. Synthesis and functional characterization of tridegin and its analogues: Inhibitors and substrates of factor XIIIa. *ChemMedChem* **2012**, *7*, 326–333. [CrossRef] [PubMed]
32. Chang, J.-Y. Diverse pathways of oxidative folding of disulfide proteins: Underlying causes and folding models. *Biochemistry* **2011**, *50*, 3414–3431. [CrossRef] [PubMed]
33. Paul George, A.A.; Heimer, P.; Maaß, A.; Hamaekers, J.; Hofmann-Apitius, M.; Biswas, A.; Imhof, D. Insights into the Folding of Disulfide-Rich μ-Conotoxins. *ACS Omega* **2018**, *3*, 12330–12340. [CrossRef] [PubMed]
34. Liu, H.; Boudreau, M.A.; Zheng, J.; Whittal, R.M.; Austin, P.; Roskelley, C.D.; Roberge, M.; Andersen, R.J.; Vederas, J.C. Chemical synthesis and biological activity of the neopetrosiamides and their analogues: Revision of disulfide bond connectivity. *J. Am. Chem. Soc.* **2010**, *132*, 1486–1487. [CrossRef]
35. Günther, P.; Buchner, L. Combined automated NOE assignment and structure calculation with CYANA. *J. Biomol. NMR* **2015**, *62*, 453–471. [CrossRef]
36. Konagurthu, A.S.; Whisstock, J.C.; Stuckey, P.J.; Lesk, A.M. MUSTANG: A multiple structural alignment algorithm. *Proteins* **2006**, *64*, 559–574. [CrossRef]
37. Abraham, M.J.; Murtola, T.; Schulz, R.; Páll, S.; Smith, J.C.; Hess, B.; Lindahl, E. GROMACS: High performance molecular simulations through multi-level parallelism from laptops to supercomputers. *SoftwareX* **2015**, *1*, 19–25. [CrossRef]
38. Van der Spoel, D.; Lindahl, E.; Hess, B.; Groenhof, G.; Mark, A.E.; Berendsen, H.J.C. GROMACS: Fast, flexible, and free. *J. Comput. Chem.* **2005**, *26*, 1701–1718. [CrossRef]
39. Jorgensen, W.L.; Chandrasekhar, J.; Madura, J.D.; Impey, R.W.; Klein, M.L. Comparison of simple potential functions for simulating liquid water. *J. Chem. Phys.* **1983**, *79*, 926–935. [CrossRef]
40. Maier, J.A.; Martinez, C.; Kasavajhala, K.; Wickstrom, L.; Hauser, K.E.; Simmerling, C. ff14SB: Improving the Accuracy of Protein Side Chain and Backbone Parameters from ff99SB. *J. Chem. Theory Comput.* **2015**, *11*, 3696–3713. [CrossRef]
41. Bussi, G.; Donadio, D.; Parrinello, M. Canonical sampling through velocity rescaling. *J. Chem. Phys.* **2007**, *126*, 14101. [CrossRef] [PubMed]
42. Parrinello, M.; Rahman, A. Polymorphic transitions in single crystals: A new molecular dynamics method. *J. Appl. Phys.* **1981**, *52*, 7182–7190. [CrossRef]
43. Nosé, S.; Klein, M.L. Constant pressure molecular dynamics for molecular systems. *Mol. Phys.* **1983**, *50*, 1055–1076. [CrossRef]
44. Hess, B.; Bekker, H.; Berendsen, H.J.C.; Fraaije, J.G.E.M. LINCS: A linear constraint solver for molecular simulations. *J. Comput. Chem.* **1997**, *18*, 1463–1472. [CrossRef]
45. Darden, T.; York, D.; Pedersen, L. Particle mesh Ewald: An N log(N) method for Ewald sums in large systems. *J. Chem. Phys.* **1993**, *98*, 10089–10092. [CrossRef]
46. Essmann, U.; Perera, L.; Berkowitz, M.L.; Darden, T.; Lee, H.; Pedersen, L.G. A smooth particle mesh Ewald method. *J. Chem. Phys.* **1995**, *103*, 8577–8593. [CrossRef]
47. Humphrey, W.; Dalke, A.; Schulten, K. VMD: Visual molecular dynamics. *J. Mol. Graph.* **1996**, *14*, 33–38. [CrossRef]
48. Yan, Y.; Tao, H.; He, J.; Huang, S.-Y. The HDOCK server for integrated protein-protein docking. *Nat. Protoc.* **2020**, *15*, 1829–1852. [CrossRef]
49. Moult, J.; Fidelis, K.; Kryshtafovych, A.; Schwede, T.; Tramontano, A. Critical assessment of methods of protein structure prediction (CASP)–round x. *Proteins* **2014**, *82* (Suppl. 2), 1–6. [CrossRef]
50. Van Zundert, G.C.P.; Rodrigues, J.P.G.L.M.; Trellet, M.; Schmitz, C.; Kastritis, P.L.; Karaca, E.; Melquiond, A.S.J.; van Dijk, M.; de Vries, S.J.; Bonvin, A.M.J.J. The HADDOCK2.2 Web Server: User-Friendly Integrative Modeling of Biomolecular Complexes. *J. Mol. Biol.* **2016**, *428*, 720–725. [CrossRef]
51. Tina, K.G.; Bhadra, R.; Srinivasan, N. PIC: Protein Interactions Calculator. *Nucleic Acids Res.* **2007**, *35*, W473–W476. [CrossRef] [PubMed]

4.4.3 Summary

In this chapter, the structure of the 2-disulfide-bonded tridegin variant $B_{[C19S,C25S]}$ was elucidated experimentally via 2D-NMR spectroscopy and subsequent molecular modeling.[18] Therefore, the N- and C-terminal fragments of isomer $B_{[C19S,C25S]}$ were separately synthesized and analytically characterized. The disulfide bond connectivity (Cys05-Cys37, Cys17-Cys31) of the N-terminal fragment could be confirmed via the analysis of an enzymatic digest.[18] As expected from former studies[12], the N-terminal fragment displayed no inhibitory potential towards FXIIIa.[18] Subsequent evaluation of the NMR spectra of the two fragments and structural calculations revealed a highly flexible structure for the C-terminal fragment and a rigid structure for the N-terminal fragment. The N-terminal fragment was stabilized by the two disulfide bonds and three structural elements, i.e., two β-turns and a helix. By linking these two fragments using Cyana and following structure optimization using a molecular dynamics simulation, a representative structure of the isomer $B_{[C19S,C25S]}$ was successfully determined.[18] This tridegin variant was investigated for its structure-activity relationship using computer-based docking studies with a modified variant of the FXIIIa° crystal structure (PDB ID: 4KTY[148]). The docking studies confirmed the binding of tridegin close to the active site of FXIIIa and its resulting sterical blockage.[17,18] Furthermore, it was found that the C-terminal part of the tridegin variant enters the hydrophobic tunnel surrounding the active site of FXIIIa and thus competitively blocks the active site for substrates. In turn, the N-terminal portion plays a minor role in inhibition and is required exclusively for binding to FXIIIa, which was also confirmed by the docking study with the NMR-based structure of the N-terminal fragment.[18]

This chapter IV complements the described studies of the 2-disulfide bonded tridegin variants.[13,17,18] The insights into the structure-activity relationships will allow a more directed optimization of the lead structure for future medical applications. For example, in this context, it might be possible to increase the proteolytic stability of the peptide by incorporating D-amino acids without disturbing the crucial contacts of the tridegin variant to FXIIIa. The present work (chapters II-IV) contributes substantially to FXIIIa research and provides a further step towards the pharmacological targeting of FXIIIa.

NMR-based structure elucidation showed once again how complex and laborious the analytics of disulfide-bonded peptides can be. This method is not always efficient to distinguish disulfide-bonded isomers because, in addition to the complex data analysis, it cannot be said with certainty that a distinction of the isomers is possible in the end.[329] As mentioned above, the classical methods such as HPLC and MS are also not always sufficient, so that partial reduction or digestion experiments have to be applied for the differentiation of disulfide-bonded isomers.[6,12,17] In order to contribute to the analysis of disulfide-bonded peptides, the applicability of LC-TIMS-MS for the distinguishability of disulfide-bonded isomers was investigated.[19] For this purpose, the µ-PIIIA variants already available in the working group of Prof. Dr. Diana Imhof were examined, since all 15 3-disulfide-bonded isomers and 3 2-disulfide-bonded isomers of these were available and resulting in a broader spectrum for the overall analyses.[6,54] The results of this study are described in chapter V.

4.5 Chapter V - LC-trapped ion mobility spectrometry-TOF MS differentiation of 2- and 3-disulfide-bonded isomers of the μ-conotoxin PIIIA

Authors*

Thomas Schmitz, Stuart Pengelley, Eckhard Belau, Detlev Suckau, and Diana Imhof

This article was published in:

Analytical Chemistry **2020**, 92, 10920-10924.
DOI: 10.1021/acs.analchem.0c02151

4.5.1 Introduction

As shown in chapters I-IV, disulfide-bonded peptides are interesting pharmacological tools that can be further developed for medical applications. In order to achieve this, not only the synthesis of these peptides and their functional analysis is crucial, but also their analytical characterization. In the case of disulfide-bonded peptides, not only the amino acid sequence, but also the disulfide bond connectivity can play a decisive role for the structure and the resulting biological activity.[6,54,360] The work carried out within the research group of Prof. Dr. Diana Imhof has revealed two extreme examples. The tridegin, comprehensively described in chapters I-IV, illustrates that the omission of a disulfide bond does not necessarily lead to a loss of biological activity, and that different disulfide-bonded isomers can have similar activities.[13,17] In contrast, experiments with the μ-conotoxin PIIIA showed that correct disulfide bond pattern can be crucial for the biological activity.[6,54] Especially in these cases, the precise differentiation of disulfide-bonded isomers is indispensable. However, due to similar physicochemical properties, it is sometimes difficult to distinguish different disulfide-bonded isomers of the same cysteine-rich peptide using methods such as HPLC and MS. Studies on μ-PIIIA[6] and tridegin[12,17] have shown that isomers can have identical HPLC retention times and thus cannot be longer distinguished by conventional methods such as HPLC and MS alone. In order to contribute to the analysis of disulfide-bonded peptides and thus provide important insights into structure-activity relationships, the distinguishability of the existing μ-PIIIA variants was analyzed by LC-TIMS-MS.[19]

In this chapter, different disulfide-bonded μ-PIIIA variants[6,54] are used to investigate whether ion mobility, in particular LC-TIMS-MS, as an additional method to HPLC and MS improves the evaluation and discrimination of disulfide-bonded isomers.[19]

***Contributions:**

DI, TS, SP, and DS conceived the presented idea and designed and planned the experimental studies. SP, EB, and TS. performed the TIMS-MS measurements of the peptides. TS, SP, and DI analyzed and interpreted the data. The manuscript was written through contributions of all authors. All authors have given approval to the final version of the manuscript.

4.5.2 Article

On the following pages, the article is printed in its published form with permission of the American Chemical Society, Washington, United States.

analytical chemistry

pubs.acs.org/ac Letter

LC-Trapped Ion Mobility Spectrometry-TOF MS Differentiation of 2- and 3-Disulfide-Bonded Isomers of the μ-Conotoxin PIIIA

Thomas Schmitz, Stuart Pengelley, Eckhard Belau, Detlev Suckau, and Diana Imhof*

Cite This: *Anal. Chem.* 2020, 92, 10920–10924 Read Online

ACCESS | Metrics & More | Article Recommendations | Supporting Information

ABSTRACT: Disulfide bonds within cysteine-rich peptides are important for their stability and biological function. In this respect, the correct disulfide connectivity plays a decisive role. The differentiation of individual disulfide-bonded isomers by traditional high-performance liquid chromatography (HPLC) and mass spectrometry (MS) is limited due to the similarity in physicochemical properties of the isomers sharing the same amino acid sequence. By using trapped ion mobility spectrometry-mass spectrometry (TIMS-MS), several 2- and 3-disulfide-bonded isomers of the μ-conotoxin PIIIA were investigated for their distinguishability by collision cross section (CCS) values and their characteristic mobilogram traces. The isomers could be differentiated by TIMS-MS and also identified in mixing experiments. Thus, TIMS-MS provides a highly valuable and enriching addition to standard HPLC and MS analysis of conformational isomers of disulfide-rich peptides and proteins.

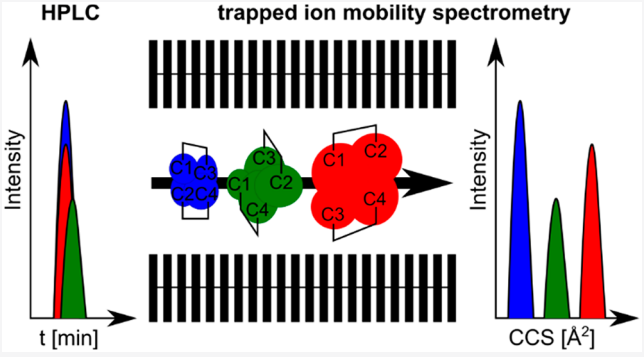

Cysteine-rich peptides, such as defensins,[1] and toxins from scorpions,[2] snakes,[3,4] and cone snails[5−7] play a significant role for many organisms regarding their defense and hunting strategies. These peptides are characterized by their specific intra- or intermolecular disulfide bond network, which is fundamental for folding, stability, and function.[8−11] For the application of such disulfide-rich peptides in biopharmaceutical research, it is important to produce them as highly potent molecules with the correct disulfide connectivity, which is unequivocally associated with their bioactivity.[7,12,13] A peptide sequence containing six cysteine residues can theoretically form 15 different 3-disulfide-bonded isomers, which only differ in their three-dimensional conformation.[14] In this regard, it is crucial to apply suitable analytical methods to study the inherent disulfide connectivity of each isomer and to distinguish these variants with the available standard techniques. The current analytical methods in use for disulfide-rich peptides and the elucidation of their disulfide-bond connectivity are based on high-performance liquid chromatography (HPLC), mass spectrometry (MS),[14−16] X-ray crystallography,[17] and nuclear magnetic resonance (NMR) spectroscopy.[14,18] NMR, X-ray crystallography, and MS/MS sequencing of digested, partially reduced and/or derivatized disulfide-bonded peptides are very time and sample consuming.[14−18] A more general approach simply focuses on the detection and the purity control of such peptides[19,20] without the cumbersome determination of the disulfide connectivity.[7,14,21] In these cases, the correctness of the disulfide connectivity present in the molecule to be examined is assumed on the basis of the retention time (HPLC) and the molar mass (MS).[19,20] This approach, however, cannot provide clear evidence that only one of the disulfide-bonded isomers is present. Several studies have meanwhile demonstrated that different disulfide-bonded isomers showed the same HPLC retention time and, thus, are not distinguishable by standard HPLC and MS.[14,15] An emerging and valuable technique for intact mass protein analysis, i.e., ion mobility-mass spectrometry (IM-MS), has so far not been widely applied to distinguish disulfide-bonded peptide isomers.[22,23] Select IM-MS studies, however, reported that different isomers exhibit varying collision cross section (CCS) values, but there are also examples for disulfide-bonded isomers that cannot be separated due to a low mobility resolution.[24,25] An advancement of IM-MS is the trapped ion mobility spectrometry-mass spectrometry (TIMS-MS), which allows an increased resolution and a better baseline separation.[26,27] This study investigates the applicability of TIMS-MS for the differentiation of several 2- and 3-disulfide-bonded peptide isomers. Exemplarily, different disulfide-bonded variants of the 22 mer

Received: May 19, 2020
Accepted: July 27, 2020
Published: July 27, 2020

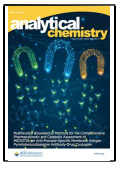

Table 1. Different Disulfide-Bonded PIIIA Variants That Were Analyzed via TIMS-MS[d]

PIIIA variant	Connectivity	Differences related to native Isomer (1)			Monoisotopic mass	$[M+5H]^{5+}$
2[a]	C^4-C^5 - - - C^{11} - - C^{16} - - C^{21}-C^{22}	Cys4-Cys16	Cys5-Cys21	Cys11-Cys22	2603.15[b]	521.63[c]
16[a]	C^4-C^5 - - - S^{11} - - C^{16} - - C^{21}-S^{22}	Cys4-Cys16	Cys5-Cys21	Ser11, Ser22	2573.20[b]	515.64[c]
17[a]	S^4-C^5 - - - C^{11} - - S^{16} - - C^{21}-C^{22}	Ser4, Ser16	Cys5-Cys21	Cys11-Cys22	2573.20[b]	515.64[c]
18[a]	C^4-S^5 - - - C^{11} - - C^{16} - - S^{21}-C^{22}	Cys4-Cys16	Ser5, Ser21	Cys11-Cys22	2573.20[b]	515.64[c]
1[a]	C^4-C^5 - - - C^{11} - - C^{16} - - C^{21}-C^{22}	Cys4-Cys21	Cys5-Cys22	Cys11-Cys16	2603.15[b]	521.63[c]

[a]Numbers of the PIIIA variants are based on Heimer et al.[14] for the 3-disulfide-bonded variants and on Paul George et al.[28] for the 2-disulfide-bonded variants. [b]Theoretical monoisotopic molecular weight [Da]. [c]Measured m/z of the 5-fold protonated PIIIA variant via TIMS-MS. [d]The differences of the PIIIA variants (**1**, **16**–**18**) compared to the naturally occurring isomer (**2**) are marked in red. The numbers attached to the amino acids refer to the position in the sequence ZRL**CC**GFOKS**C**RSRQ**C**KOHR**CC**-NH_2.

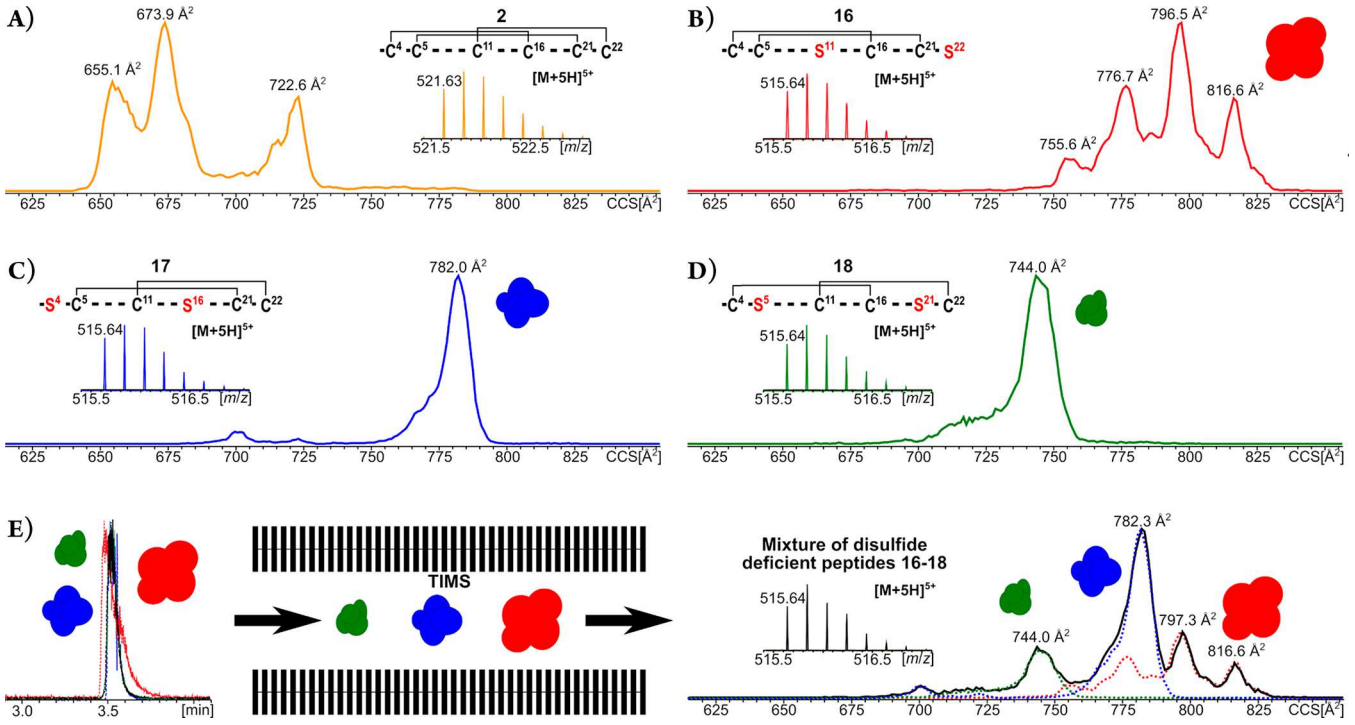

Figure 1. TIMS and MS data of the 5-fold protonated species of the native 3-disulfide-bonded PIIIA isomer (**2**) and the three disulfide-deficient PIIIA variants (**16**–**18**): (A) native isomer **2** (orange); (B) disulfide-deficient variant **16** (red); (C) disulfide-deficient variant **17** (blue); (D) disulfide-deficient variant **18** (green). (E) LC elution (left) and TIMS separation (right) of a mixture of the three disulfide-deficient variants (**16**–**18**, black). The dotted lines within the LC elution profiles and the TIMS mobilograms represent the profiles of the pure variants **16** (red), **17** (blue), and **18** (green).

μ-conotoxin PIIIA from the marine cone snail *Conus purpurascens* were studied and compared in detail.

The μ-conotoxin PIIIA is a potent blocker of the skeletal muscle voltage-gated sodium channel $Na_v1.4$. The natural sequence of the peptide (ZRL**CC**GFOKS**C**RSRQ**C**-KOHR**CC**-NH_2) contains six cysteines capable of forming three disulfide bonds, with the naturally occurring isomer possessing the connectivity Cys4–Cys16, Cys5–Cys21, and Cys11–Cys22 (Table 1, **2**).

The importance of the correct disulfide connectivity on the structure and bioactivity of PIIIA has been demonstrated in recent studies comparing all 15 selectively synthesized disulfide-bonded peptide isomers and, in addition, three disulfide-deficient variants of the native isomer (**2**). Within these studies, the PIIIA variants were characterized by using HPLC, MS/MS, NMR, and computational methods.[7,14,21,28] It was observed that the highly constrained isomer (**2**) has a compact global structure and was the most active isomer with respect to the inhibition of the $Na_v1.4$ channel.[14,28] However, it was also demonstrated with several mixtures of different μ-PIIIA isomers that these cannot be clearly separated and differentiated by HPLC and MS.[14,28] Therefore, analytical methods for the clear differentiation of such disulfide-bonded isomers were pending, and consequently, the applicability of TIMS-MS for the differentiation of μ-PIIIA analogs (Tables 1 and S1) was investigated.

The TIMS-MS measurements of peptides were conducted on a timsTOF Pro instrument coupled to an Elute UHPLC (Bruker Daltonics). The peptides were eluted with an ACQUITY UPLC CSH column (C18, 1.7 μm, 2.1 × 150

https://dx.doi.org/10.1021/acs.analchem.0c02151
Anal. Chem. 2020, 92, 10920−10924

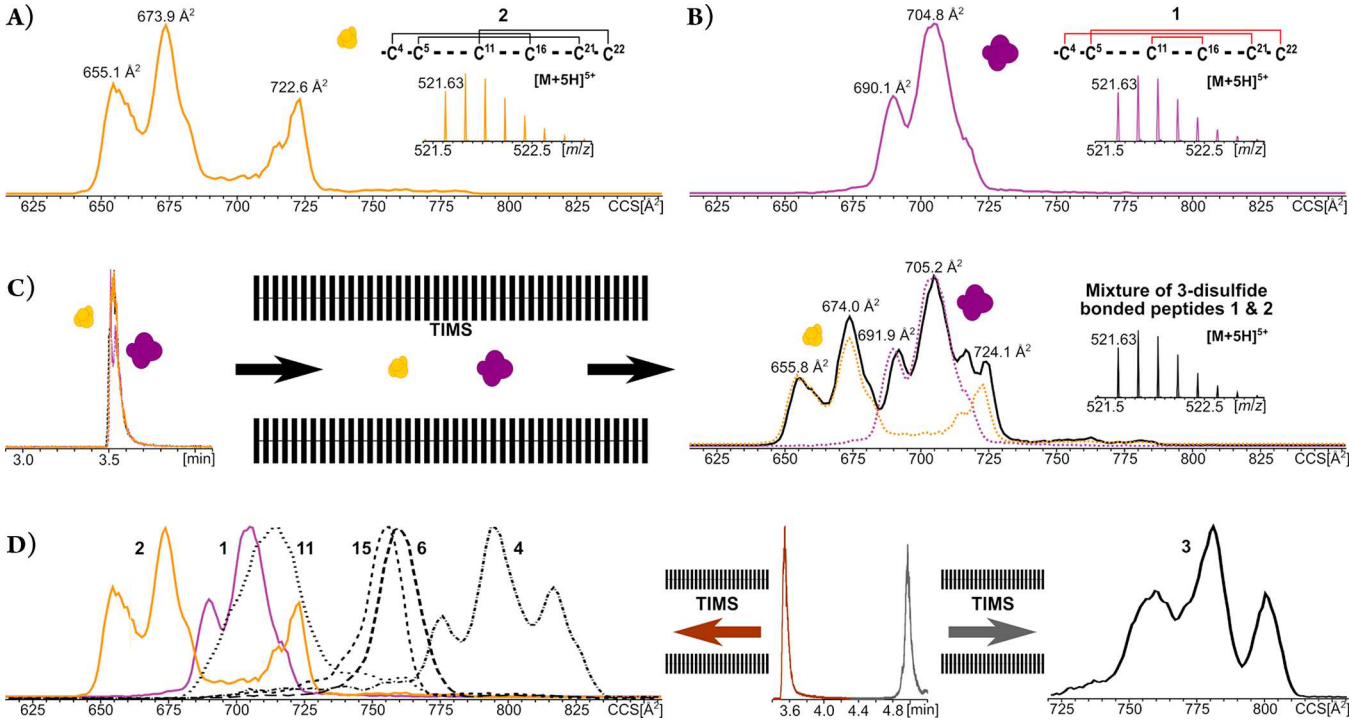

Figure 2. TIMS and MS data of the 5-fold protonated ions of the 3-disulfide-bonded PIIIA isomers **1** and **2**: (A) native isomer **2** (orange); (B) 3-disulfide-bonded isomer **1** (violet). (C) LC elution (left) and TIMS separation (right) of a mixture of the two isomers **1** and **2** (black). The dotted lines represent the individual profiles of the pure isomers **1** (violet) and **2** (orange). (D) Overlapped TIMS and LC elution profiles of the seven 3-disulfide-bonded PIIIA isomers **1**–**4**, **6**, **11**, and **15** (Table S1). All isomers except isomer **3** coelute at 3.5 min (brown peak), and isomer **3** coelutes at 5 min (gray peak). The TIMS profiles of all the isomers except isomer **3** are shown in the overlap (left); the TIMS profile of isomer **3** is on the right.

mm, Waters) with a 5 min gradient. The respective peptides were dissolved in water (+0.1% formic acid) to a concentration of 10 μg/mL. For the mixing experiments, the respective peptides were mixed with an equimolar concentration. The TIMS-MS mobilograms were generated and analyzed with the Compass DataAnalysis software (Bruker Daltonics), and the respective CCS values were calculated. In contrast to drift tube ion mobility spectrometry, ions are pushed through the TIMS mobility analyzer by the drift gas and separated according to their mobility by an electrical field applied in the opposite direction. As a result, bulkier ions with higher CCS values elute earlier (at higher electric field strength) than smaller ions within the TIMS measurements.[29,30]

In Figure 1, the LC-TIMS-MS results of the natural PIIIA isomer **2** were compared with disulfide-deficient, 2-disulfide-bonded analogues **16**–**18**. These analogues varied in the amino acid sequence at two positions where the cysteines were replaced by serines, resulting in the reduction of the number of disulfide bonds in the PIIIA lead.[28] In addition, 3-disulfide-bonded PIIIA isomers, such as peptide **1** (Table 1) coeluting with native peptide **2**, were also examined by LC-TIMS-MS. The CCS values were determined from the highest intensity $[M + 5H]^{5+}$ ions in the mobilograms of all PIIIA isomers, since these peaks correspond to the most populated ion conformation of the PIIIA variants.

The μ-PIIIA isomer **2** (Figure 1A) has a lower CCS value (673.9 Å^2) than the 2-disulfide-bonded variants (**16**–**18**, Figure 1B–D) due to the more compact and rigid structure induced by the third disulfide bond. A parallel analysis of the individual 2-disulfide-bonded peptides (**16**–**18**) illustrates that the ions of peptide **18** (Figure 1D) have a lower CCS value (744.0 Å^2) compared to the ions of the other variants (**16**, 796.5 Å^2; **17**, 782.0 Å^2). This suggests **18** has the most compact structure of the disulfide-deficient peptides (**16**–**18**) and that the disulfide bond between Cys5–Cys21 possibly has the lowest influence on the stability of the native PIIIA isomer **2**. This result is consistent with previous conformational studies using molecular modeling and dynamics simulations of the disulfide-deficient variants.[28] Isomers **16** and **17** are in the high CCS range together, indicating a comparable lower compactness. However, the two peptides (**16**, **17**) can be distinguished very well by the mobilogram fine structure, utilizing the 200 resolving power provided by the TIMS analyzer. Peptide **16** exhibits multiple IMS peaks, whereas peptide **17** showed only one peak (Figure 1B,C). The more complex IMS profile of isomer **16** reveals a higher freedom for conformational changes within the peptide ions, which likely is enabled by a lower degree of conformational fixation by essential disulfide bonds and equilibria resulting from attractive intramolecular interactions, intramolecular charge solvation, and coulomb repulsion as already reported for charge induced unfolding of proteins.[31,32]

Isomers **16**–**18** were pooled prior to LC-TIMS-MS analysis to determine if it is possible to identify the peptides in a mixture (Figure 1E). These data demonstrated that individual, coeluting PIIIA variants can be identified via TIMS within the mixture. Although there is the possibility that a high concentration of one isomer could mask the presence of other isomers, the profiles are clearly distinguishable and should enable the identification and quantification in mixtures, if fitting routines to a profile library are employed.

https://dx.doi.org/10.1021/acs.analchem.0c02151
Anal. Chem. 2020, 92, 10920–10924

The seven 3-disulfide-bonded isomers (**1**−**4**, **6**, **11**, **15**, Tables 1 and S1) were analyzed using LC-TIMS-MS. The respective IMS profiles of the pure peptide samples (**1**−**4**, **6**, **11**, **15**) and the mixture of isomers **1** and **2** were compared with each other. A differentiation of the peptides (**1**−**4**, **6**, **11**, **15**) by LC-TIMS-MS was observed (Figures 2 and S1). Isomer **3** is eluted later than the bulk of the remaining, coeluting isomers (**1**, **2**, **4**, **6**, **11**, **15**), which were solely distinguishable by their different IMS profiles. The naturally occurring isomer (**2**) shows the greatest compactness with the lowest CCS value (673.9 Å^2) of all 3-disulfide-bonded isomers, as previously described by Heimer et al.[14] Isomer **3** displayed a high CCS value (780.9 Å^2) and the highest LC retention time of all 3-disulfide-bonded isomers (Figure 2D). It is also the only isomer in which all three disulfide bonds are disentangled, thus providing a large degree of conformational freedom to expose hydrophobic surfaces to the reversed-phase column material.

In the mobilogram of the mixture of the isomers **1** and **2** (Figure 2C), the contributions of the two isomers were clearly discernible, as was the case with the disulfide-deficient variants (**16**−**18**, Figure 1E). However, this again illustrates that it may remain difficult to identify the isomer composition of a mixture without reference to a profile library. This is clearly heightened, since individual isomers can produce several peaks in the mobilogram due to different conformers for a given charge state. Nevertheless, with the availability of individual high resolution mobilograms of each isomer provided by TIMS, an estimation of mixture composition may be possible even if the isomers are indistinguishable chromatographically and by MS/MS.

The applicability of LC-TIMS-MS for distinguishing multiple disulfide-bonded PIIIA isomers was investigated. Due to the high resolution in the TIMS analyzer, characteristic mobilograms for exemplary isomers were obtained, which suggested that the identification of the individual isomers in a mixture are technically feasible. In addition, the observed order of CCS values are in line with the computer-based and NMR-assisted structural studies of the specific peptides compactness.[14,28] This differentiation of the disulfide-bonded isomers makes TIMS a powerful analytical method for the investigation of these peptides, which are difficult to distinguish by HPLC and MS alone. The study also highlights the potential for isomer composition analysis in a mixture using LC-TIMS-MS. If applied for example in peptide synthesis quality control, LC-TIMS-MS may add information on the isomeric composition, which HPLC or LC-MS alone might miss. The conotoxin isomers in this study highlighted that these disulfide-bonded isomer mixtures can be elucidated if the individual high resolution mobilograms of each isomer in question are known. Next to three disulfide-deficient PIIIA variants, seven out of 15 known 3-disulfide-bonded PIIIA isomers were successfully analyzed using LC-TIMS-MS. It is likely that LC-TIMS-MS is capable of differentiating all 15 possible 3-disulfide-bonded isomers of a specific peptide individually. However, it is still open if that is also possible in a mixture as well.

In summary, this study showed for the first time that LC-TIMS-MS is a valuable addition to the commonly used methods HPLC and MS, as all coeluting PIIIA isomers were clearly distinguished by their characteristic TIMS mobilograms. The method has the potential to be expanded, particularly if mobilogram libraries are utilized in the analysis software.

■ ASSOCIATED CONTENT

Supporting Information

The Supporting Information is available free of charge at https://pubs.acs.org/doi/10.1021/acs.analchem.0c02151.

Table and figure with information on the LC-TIMS-MS measurements of different 3-disulfide-bonded PIIIA isomers (PDF)

■ AUTHOR INFORMATION

Corresponding Author

Diana Imhof − *Pharmaceutical Biochemistry and Bioanalytics, Pharmaceutical Institute, University of Bonn, 53121 Bonn, Germany;* orcid.org/0000-0003-4163-7334; Email: dimhof@uni-bonn.de

Authors

Thomas Schmitz − *Pharmaceutical Biochemistry and Bioanalytics, Pharmaceutical Institute, University of Bonn, 53121 Bonn, Germany*

Stuart Pengelley − *Pharmaceutical Biochemistry and Bioanalytics, Pharmaceutical Institute, University of Bonn, 53121 Bonn, Germany;* orcid.org/0000-0003-2676-8096

Eckhard Belau − *Pharmaceutical Biochemistry and Bioanalytics, Pharmaceutical Institute, University of Bonn, 53121 Bonn, Germany*

Detlev Suckau − *Pharmaceutical Biochemistry and Bioanalytics, Pharmaceutical Institute, University of Bonn, 53121 Bonn, Germany*

Complete contact information is available at: https://pubs.acs.org/10.1021/acs.analchem.0c02151

Author Contributions

D.I., T.S., S.P., and D.S conceived the presented idea and designed and planned the experimental studies. S.P., E.B., and T.S. performed the TIMS-MS measurements of the peptides. T.S, S.P., and D.I. analyzed and interpreted the data. The manuscript was written through contributions of all authors. All authors have given approval to the final version of the manuscript.

Notes

The authors declare no competing financial interest.

■ ACKNOWLEDGMENTS

This study was financially supported partly by the German Heart Foundation and the University of Bonn (to D.I.).

■ REFERENCES

(1) Ganz, T. *Nat. Rev. Immunol.* **2003**, *3*, 710−720.

(2) Sarfo-Poku, C.; Eshun, O.; Lee, K. H. *Toxicon* **2016**, *122*, 109−112.

(3) Almeida, J. R.; Mendes, B.; Lancellotti, M.; Marangoni, S.; Vale, N.; Passos, Ó.; Ramos, M. J.; Fernandes, P. A.; Gomes, P.; Da Silva, S. L. *Eur. J. Med. Chem.* **2018**, *149*, 248−256.

(4) Moga, M. A.; Dimienescu, O. G.; Arvătescu, C. A.; Ifteni, P.; Pleş, L. *Molecules* **2018**, *23*, 692.

(5) Fuller, E.; Green, B. R.; Catlin, P.; Buczek, O.; Nielsen, J. S.; Olivera, B. M.; Bulaj, G. *FEBS J.* **2005**, *272*, 1727−1738.

(6) Jin, A.-H.; Muttenthaler, M.; Dutertre, S.; Himaya, S. W. A.; Kaas, Q.; Craik, D. J.; Lewis, R. J.; Alewood, P. F. *Chem. Rev.* **2019**, *119*, 11510−11549.

(7) Tietze, A. A.; Tietze, D.; Ohlenschläger, O.; Leipold, E.; Ullrich, F.; Kühl, T.; Mischo, A.; Buntkowsky, G.; Görlach, M.; Heinemann, S. H.; et al. *Angew. Chem., Int. Ed.* **2012**, *51*, 4058−4061.

(8) Weissman, J. S.; Kim, P. S. *Science* **1992**, *256*, 112−114.
(9) Wedemeyer, W. J.; Welker, E.; Narayan, M.; Scheraga, H. A. *Biochemistry* **2000**, *39*, 4207−4216.
(10) Cemazar, M.; Zahariev, S.; Lopez, J. J.; Carugo, O.; Jones, J. A.; Hore, P. J.; Pongor, S. *Proc. Natl. Acad. Sci. U. S. A.* **2003**, *100*, 5754−5759.
(11) Bulaj, G.; Buczek, O.; Goodsell, I.; Jimenez, E. C.; Kranski, J.; Nielsen, J. S.; Garrett, J. E.; Olivera, B. M. *Proc. Natl. Acad. Sci. U. S. A.* **2003**, *100*, 14562−14568.
(12) Dutton, J. L.; Bansal, P. S.; Hogg, R. C.; Adams, D. J.; Alewood, P. F.; Craik, D. J. *J. Biol. Chem.* **2002**, *277*, 48849−48857.
(13) Carstens, B. B.; Berecki, G.; Daniel, J. T.; Lee, H. S.; Jackson, K. A. V.; Tae, H.-S.; Sadeghi, M.; Castro, J.; O'Donnell, T.; Deiteren, A.; et al. *Angew. Chem., Int. Ed.* **2016**, *55*, 4692−4696.
(14) Heimer, P.; Tietze, A. A.; Bäuml, C. A.; Resemann, A.; Mayer, F. J.; Suckau, D.; Ohlenschläger, O.; Tietze, D.; Imhof, D. *Anal. Chem.* **2018**, *90*, 3321−3327.
(15) Böhm, M.; Bäuml, C. A.; Hardes, K.; Steinmetzer, T.; Roeser, D.; Schaub, Y.; Than, M. E.; Biswas, A.; Imhof, D. *J. Med. Chem.* **2014**, *57*, 10355−10365.
(16) Xu, H.; Zhang, L.; Freitas, M. A. *J. Proteome Res.* **2008**, *7*, 138−144.
(17) Clarke, J.; Henrick, K.; Fersht, A. R. *J. Mol. Biol.* **1995**, *253*, 493−504.
(18) Mobli, M.; King, G. F. *Toxicon* **2010**, *56*, 849−854.
(19) Wu, Y.; Wu, X.; Yu, J.; Zhu, X.; Zhangsun, D.; Luo, S. *Molecules* **2014**, *19*, 966−979.
(20) Shi, J.; So, L.-Y.; Chen, F.; Liang, J.; Chow, H.-Y.; Wong, K.-Y.; Wan, S.; Jiang, T.; Yu, R. *J. Pept. Sci.* **2018**, *24*, No. e3087.
(21) Heimer, P.; Schmitz, T.; Bäuml, C. A.; Imhof, D. *J. Visualized Exp.* **2018**, e58368.
(22) Kanu, A. B.; Dwivedi, P.; Tam, M.; Matz, L.; Hill, H. H. *J. Mass Spectrom.* **2008**, *43*, 1−22.
(23) Sans, M.; Feider, C. L.; Eberlin, L. S. *Curr. Opin. Chem. Biol.* **2018**, *42*, 138−146.
(24) Delvaux, C.; Massonnet, P.; Kune, C.; Haler, J. R. N.; Upert, G.; Mourier, G.; Gilles, N.; Quinton, L.; de Pauw, E.; Far, J. *Anal. Chem.* **2020**, *92*, 2425−2434.
(25) Massonnet, P.; Haler, J. R. N.; Upert, G.; Degueldre, M.; Morsa, D.; Smargiasso, N.; Mourier, G.; Gilles, N.; Quinton, L.; de Pauw, E. *J. Am. Soc. Mass Spectrom.* **2016**, *27*, 1637−1646.
(26) Dit Fouque, K. J.; Moreno, J.; Hegemann, J. D.; Zirah, S.; Rebuffat, S.; Fernandez-Lima, F. *Anal. Chem.* **2018**, *90*, 5139−5146.
(27) Jeanne Dit Fouque, K.; Bisram, V.; Hegemann, J. D.; Zirah, S.; Rebuffat, S.; Fernandez-Lima, F. *Anal. Bioanal. Chem.* **2019**, *411*, 6287−6296.
(28) Paul George, A. A.; Heimer, P.; Leipold, E.; Schmitz, T.; Kaufmann, D.; Tietze, D.; Heinemann, S. H.; Imhof, D. *Mar. Drugs* **2019**, *17*, 390.
(29) Michelmann, K.; Silveira, J. A.; Ridgeway, M. E.; Park, M. A. *J. Am. Soc. Mass Spectrom.* **2015**, *26*, 14−24.
(30) Silveira, J. A.; Michelmann, K.; Ridgeway, M. E.; Park, M. A. *J. Am. Soc. Mass Spectrom.* **2016**, *27*, 585−595.
(31) Ghosh, D.; Baksi, A.; Mudedla, S. K.; Nag, A.; Ganayee, M. A.; Subramanian, V.; Pradeep, T. *J. Phys. Chem. C* **2017**, *121*, 13335−13344.
(32) Gabelica, V.; Shvartsburg, A. A.; Afonso, C.; Barran, P.; Benesch, J. L. P.; Bleiholder, C.; Bowers, M. T.; Bilbao, A.; Bush, M. F.; Campbell, J. L.; et al. *Mass Spectrom. Rev.* **2019**, *38*, 291−320.

https://dx.doi.org/10.1021/acs.analchem.0c02151
Anal. Chem. 2020, 92, 10920−10924

4.5.3 Summary

In the present chapter, three different 2-disulfide-bonded µ-PIIIA variants[54] and 7 of the 15 possible 3-disulfide-bonded µ-PIIIA isomers[6] were investigated for their distinguishability by LC-TIMS-MS.[19] The 2-disulfide-bonded µ-PIIIA variants demonstrated that, despite the same retention time in the LC and the same molar mass, they could be distinguished by the CCS values of the corresponding ions and identified in mixing experiments. In addition, comparison of the disulfide-deficient variants with the naturally occurring 3-disulfide-bonded µ-PIIIA isomer showed that all three disulfide-deficient variants have larger CCS values, which can be explained due to the lack of a disulfide bond and the resulting higher flexibility.[19,54] The analysis of the CCS values of the 2-disulfide-bonded µ-PIIIA variants also corroborated previous studies[6,54], which reported that the isomer without the disulfide bond Cys5-Cys21 has the most compact structure.[54] Analogous to the 2-disulfide-bonded µ-PIIIA variants, all 7 3-disulfide-bonded isomers could be distinguished from each other by LC-TIMS-MS. In this case, one of the 7 isomers could be distinguished by retention time within LC, whereas the other 6 isomers could be differentiated by their ion mobility spectrometry profiles.[19]

This chapter demonstrates the potential of LC-TIMS-MS to distinguish disulfide-bonded isomers of a cysteine-rich peptide and to identify them in mixtures, which is why LC-TIMS-MS can be considered as a valuable addition to the commonly used methods HPLC and MS.

This study describes a specific application example in the context of disulfide-bonded peptides. The potential of LC-TIMS-MS as an additional method for the discrimination of disulfide-bonded isomers becomes apparent. In the future, this study may be extended to other disulfide-bonded peptides such as tridegin described in chapters I-IV. In addition to distinguishing disulfide-bonded isomers, this method also provides information about the spatial compactness of the compounds analyzed. Thus, this method is additionally valuable for comparing the structural flexibility of different disulfide-bonded isomers.

In summary, the present work provided not only valuable insights into the structure-activity relationships of tridegin with respect to FXIIIa and contributed to the further development of the lead structure, it also allowed the development of methodologies for the analytical characterization of disulfide-bonded peptides.

5 Conclusions

Today, the most common cause of death worldwide are cardiovascular diseases, which can be triggered by a dysregulated haemostasis.[233] Consequently, the development of anticoagulants is of great significance for the research but also for the treatment of the corresponding diseases. An interesting pharmacological target protein in this context is the blood coagulation factor FXIIIa, which, in addition to many functions in physiological processes, also catalyzes the final step of the blood coagulation cascade, the fibrin cross-linking.[192] An interference of this factor would therefore affect the structure and stability of the fibrin clot in a thrombin-independent manner. However, most of the anticoagulants used today, inhibiting the thrombin generation by directly or indirectly influencing the blood coagulation cascade.[120,356] This results in less fibrin formation from fibrinogen and thus reduces the generation of the stabilizing fibrin network.[357] As a consequence, therapies with such drugs often cause bleeding as an undesirable side effect.[120] In this regard, it is anticipated that FXIIIa inhibition minimize side effects by influencing the stabilization of the fibrin network rather than its synthesis. However, the development of such FXIIIa-specific inhibitors has not yet progressed to the point of being readily and routinely used in medical applications.[27]
The present dissertation is an important advancement in this field of research by having investigated the only naturally occurring peptidic FXIIIa inhibitor, tridegin, derived from the giant leech *H. ghilianii*.[11,323] In this work, the focus has been on the importance of disulfide bonds for the structural and functional properties of tridegin. Since previous studies revealed a common disulfide bond between Cys19-Cys25 in all three 3-disulfide bonded tridegin isomers (isomers A-C) identified in a self-folding experiment,[12] a closer examination of this disulfide bond was conducted. Questions on the exact influence of the Cys19-Cys25 disulfide bond on the structure and inhibitory potential against FXIIIa and the possibility to generate tridegin variants by removing this disulfide bond, without loss of activity towards FXIIIa arose. To answer these questions, three 2-disulfide bonded tridegin variants ($A_{[C19S,C25S]}$-$C_{[C19S,C25S]}$), in which the disulfide bond Cys19-Cys25 was eliminated by a cysteine-serine mutation, were prepared in parallel via the disulfide-deficient approach.[17] The experimental outcomes of the synthesis strategies already provided promising results in this regard.[17] Compared to the selective syntheses of the 3-disulfide bonded isomers A-C,[13] the synthesis effort was minimized by 2 instead of 3 oxidation steps.[17] Consequently, the yields of the pure and completely oxidized peptides could be significantly increased (from less than 10% to more than 30% yield).[17] In respect to synthetic yields, the best tridegin variant was isomer $B_{[C19S,C25S]}$ (33% yield), which is therefore currently regarded as lead structure for further development of tridegin and other anticoagulants.[17] The improved yields have already allowed to perform more functional as well as structural studies with these disulfide-deficient variants due to the larger available amounts.[17,18] The functional studies provided the most important insight with regard to the lead structure optimization of tridegin: The peptides showed similar inhibitory potentials towards FXIIIa as the isomers A-C.[13] Accordingly, it was shown that the disulfide bond between Cys19-Cys25 exerts a minor effect on FXIIIa inhibition and that this bond can be omitted to simplify the synthesis. In addition to the experimentally determined data, these results were augmented and confirmed by computer-based molecular modeling and docking studies, wherein it was shown that the disulfide-deficient isomers block the active site of FXIIIa similarly to the 3-disulfide bonded isomers.[17] Consequently, the approach optimized the lead structure tridegin for the development of pharmacologically relevant anticoagulants. Apart from the comparison with the 3-disulfide bonded isomers, the peptides $A_{[C19S,C25S]}$-$C_{[C19S,C25S]}$ were also investigated for their potency and specificity towards FXIIIa via further functional

studies.[13] Based on the mixture $ABC_{[C19S,C25S]}$, it was shown that the analogs have a significantly lower effect on TGase 2, which highlights their specificity towards FXIIIa.[13] Furthermore, the potency and specificity towards FXIIIa could be confirmed in assays using human whole blood. The subsequent step, the investigation of the inhibitory potential towards FXIIIa *in vivo* could also provide first results using mouse models (not yet published). The peptide $B_{[C19S,C25S]}$, which could be synthesized most efficiently, was investigated for its activity against FXIIIa *in vivo*, as well as for its plasma half-life. It was observed that the tridegin variant inhibits FXIIIa in the mouse model but the inhibitory potential against FXIIIa was completely lost after a few minutes. A possible explanation for the rapid loss of the inhibitory potential against FXIIIa *in vivo* could be that the tridegin variant is degraded by proteolytic enzymes. In this process, the peptide chains could be hydrolyzed at specific sites and the structure and thus the function of the tridegin variant is disrupted.

In addition to the functional studies, NMR structure elucidation was also performed for the first time to obtain an experimentally derived structure of a tridegin variant, more precisely the isomer $B_{[C19S,C25S]}$.[18] Due to the difficulty of analyzing a 66mer peptide via NMR, the peptide was first divided into an N- and a C-terminal fragment and these fragments were structurally elucidated via 2D-NMR spectroscopy. A very flexible structure of the C-terminal fragment (AS 38-66) and a rigid structure of the N-terminal fragment (AS 1-37), with different structural elements such as helix and β-turn elements, could be determined. These structures were subsequently linked to yield the isomer $B_{[C19S,C25S]}$, and the full-length structure was optimized using MD simulations. The resulting structure, which still comprised the flexibility of the C-terminal part and the rigidity of the N-terminal fragment, was examined for its structure-activity relationships by molecular docking to the FXIIIa° crystal structure (PDB ID: 4KTY[148]).[18] The docking studies showed that the structure of isomer $B_{[C19S,C25S]}$ not only superficially blocks the active site of FXIIIa but also that the C-terminal part of the tridegin structure enters the hydrophobic tunnel of the active site of FXIIIa and thus competitively inhibits substrate turnover. This highlights the importance of the flexible C-terminal part within tridegin for the inhibitory potential against FXIIIa. The N-terminal part plays only a minor role with respect to the inhibitory mechanism.[18] The retention of the flexible C-terminal fragment in all disulfide-bonded isomers studied in this work, with only the N-terminal part structurally modified via the disulfide bonds, may explain why all isomers exhibit similar activities towards FXIIIa. In addition, the new findings may help to further optimize the lead structure of tridegin in the future, possibly leading to the development of a useful compound for medical applications.

In summary, an improved understanding of tridegin and new insights into its structure-activity relationships regarding FXIIIa were obtained from this work. In addition, only a minor impact of the Cys19-Cys25 disulfide bond on the inhibitory potential towards FXIIIa could be determined, and therefore the tridegin structure could be optimized by reducing the number of disulfide bonds. However, initial *in vivo* studies have shown that the 2-disulfide bonded tridegin variant only exhibited inhibitory potential toward FXIIIa for a very short time in the mouse model. Since only assumptions can be made as to what happens to the peptides in plasma, future studies such as plasma stability of the peptides or plasma protein binding, which can be performed in the context of ADME (absorption, distribution, metabolism, excretion) studies, may provide new insights into this area of concern. If the peptides are considered to be degraded in the blood by proteolytic enzymes, modifications within the peptide sequence could be made in the future to provide higher stability to proteolytic digestion. An example in this context would be the incorporation of D-amino acids within the peptide sequence, although the synthesis of different 66mer peptides with D-amino acids included would be very time-consuming and expensive. In order to pre-select the positions for this purpose, the structure

of isomer $B_{[C19S,C25S]}$ elucidated in this dissertation could be utilized to first perform computer-based mutation studies with D-amino acids. MD simulations and docking studies could then be performed to theoretically determine which mutations have the least effect on the structure, and thus likely the function of the tridegin variant. This selection of peptides could then be studied again for their functionality and stability towards proteolytic degradation in the mouse model.

Disulfide-bonded peptides can be pharmacologically relevant. This is evidenced by the fact that disulfide-bonded peptides are already used as drugs in several diseases.[90,101] In this context, tridegin can also be mentioned, since it can potentially be used as a lead structure for the development of anticoagulants. Furthermore, within the tridegin studies it could be shown that the removal of a disulfide bond does not necessarily lead to a significant loss of activity in disulfide-bonded peptides.[17] However, this is not always the case, as there are disulfide-bonded peptides, such as the μ-conotoxin PIIIA, for which a specific disulfide bond connectivity is essential for their biological activity.[6,54] Especially in these cases, the analytical determination of the disulfide bond connectivity but also the distinguishability of the individual isomers is indispensable. This requires a certain standard of the methods for analytical characterization. With respect to similar physicochemical properties, it is possible that different disulfide-bonded isomers coelute in the HPLC, which is why the usage of conventional HPLC and MS methods is not always sufficient for the differentiation of these isomers.[6,12] Additionally, previous studies within the working group of Prof. Dr. Diana Imhof showed that NMR- but also MS/MS-based techniques can be very time consuming in this regard.[6] Therefore, the present work provides an important contribution for the distinguishability of disulfide-bonded peptides. Using different μ-PIIIA variants, the applicability of LC-TIMS-MS for the differentiation of various disulfide-bonded isomers was analyzed.[19] It was illustrated that the peptides could be distinguished by their TIMS profiles and identified within isomer mixtures.[19] In the future, this promising study can be transfered to other application examples, such as tridegin, yielding into an important advance for the analytical characterization of disulfide-bonded peptides. In addition, the method can give insights into the structural compactness of different isomers and thus into their flexibility.

In the frame of this dissertation, it was possible to optimize the lead structure of tridegin by using disulfide-deficient variants.[13,17,18] The reduction of the synthesis complexity leads to higher amounts of tridegin which could be used for both, functional and structural analyses. The 2-disulfide-bonded tridegin isomers, especially Isomer $B_{[C19S,C25S]}$, can be used as a tool in FXIII research and for medical applications.[13,17,18] Furthermore, the studies of different μ-PIIIA variants demonstrated that LC-TIMS-MS is a valuable complement to HPLC and MS for the differentiation of various disulfide-bonded isomers.[19] Thus, a significant contribution to the analysis of disulfide-bonded peptides was achieved, which can also be applied to distinguish disulfide-bonded tridegin variants in the future.

Abbreviations

All abbreviations for amino acids and corresponding derivatives have been used according to the recommendations of the Nomenclature Committee of IUB (NC-IUB) and the IUPAC-IUB Joint Commission on Biochemical Nomenclature (JCBN). All amino acids and derivatives are in L-configuration unless otherwise stated.

1D	one-dimensional
1Nal	1-naphthylalanine
2D	two-dimensional
3D	three-dimensional
α_2-AP	α_2-antiplasmin
aa	amino acid
Abu	α-aminobutanoic acid
Acm	acetamidomethyl
AcOH	acetic acid
ADME	absorption, distribution, metabolism, excretion
Aib	α-aminoisobutyric acid
BPTI	bovine pancreatic trypsin inhibitor
CCS	collision cross section
cFXIII	cellular FXIII
CID	collision-induced dissociation
COSY	correlated spectroscopy
Cys or C	cysteine
DOTA	1,4,7,10-tetra-azacyclododecane-1,4,7,10-tetraacetic acid
DTT	dithiothreitol
DVT	deep vein thrombosis
ESI	electron spray ionization
FDA	Food and Drug Administration
Fmoc	9-fluorenylmethoxycarbonyl
FpA	fibrinopeptide A
FpB	fibrinopeptide B
FII(a)	(activated) blood coagulation factor II
FV(a)	(activated) blood coagulation factor V
FVIII(a)	(activated) blood coagulation factor VIII
FIX(a)	(activated) blood coagulation factor IX
FX(a)	(activated) blood coagulation factor X
FXI(a)	(activated) blood coagulation factor XI
FXIII(a)	(activated) blood coagulation factor XIII
FXIII-A_2	FXIII homodimer composed of A subunits
FXIII-A°	non-proteolytically activated FXIIIa
FXIII-A_2B_2	FXIII heterotetramer from FXIII-A2 and –B
FXIII-B_2	FXIII homodimer composed of B subunits
GPCR	G protein-coupled receptor

GSH	glutathione, reduced
GSSG	glutathione, oxidized
H. ghilianii	*Haementeria ghilianii*
HPLC	high performance liquid chromatography
HSQC	heteronuclear single quantum coherence
Hyp	hydroxyproline
IC_{50}	half-maximal inhibitory concentration
ISD	in-source decay
IUB	International Union of Biochemistry
IUPAC	International Union of Pure and Applied Chemistry
LC	liquid chromatography
MALDI	matrix-assisted laser desorption ionization
MD	molecular dynamics
MeCN	acetonitrile
MS	mass spectrometry
MS/MS	tandem-mass spectrometry
nAChR	nicotinic acetylcholine receptor
NET	norepinephrine transporter
Nle	norleucine
NMR	nuclear magnetic resonance
NOESY	Nuclear Overhauser enhancement spectroscopy
NSGM	non-saccharide sulfated glucosaminoglycan
Oic	octahydroindole-2-carboxylic acid
-(ol)	C-terminal carboxylic acid function is reduced to alcohol function
PAI-2	plasminogen activator inhibitor 2
PDB	protein data bank
PE	pulmonary embolism
PEG	polyethylene glycol
pFXIII(a)	(activated) plasmatic FXIII
PG	protecting group
Pmt	(4R)-4-[(E)-penta-2,4-dienyl]-4,N-dimethyl-threonine
PSD	post-source decay
RMSD	root mean square deviation
RP-HPLC	reversed phase-HPLC
SPPS	solid-phase peptide synthesis
TAFI	thrombin-activatable fibrinolysis inhibitor
TF	tissue factor
TFA	trifluoro acetic acid
TGase	transglutaminase
Thi	β-2-thienylalanine
Tic	1,2,3,4-tetrahydroisoquinoline-3-carboxylic acid
TIMS	trapped ion mobility spectrometry
TOCSY	total correlation spectroscopy

TOF	time of flight
Trt	trityl, triphenylmethyl
U.S.	United states of America
VGPC	voltage-gated potassium channel
VGSC	voltage-gated sodium channel
WHO	World Health Organization

List of figures

List of tables

References

[1] K. Fosgerau, T. Hoffmann, Peptide therapeutics: current status and future directions. *Drug Discov Today* **2015**, *20*, 122.

[2] C. E. Correnti, M. M. Gewe, C. Mehlin, A. D. Bandaranayake, W. A. Johnsen, P. B. Rupert, M.-Y. Brusniak, M. Clarke, S. E. Burke, W. de van der Schueren et al., Screening, large-scale production and structure-based classification of cystine-dense peptides. *Nat Struct Mol Biol* **2018**, *25*, 270.

[3] M. Góngora-Benítez, J. Tulla-Puche, F. Albericio, Multifaceted roles of disulfide bonds. Peptides as therapeutics. *Chem Rev* **2014**, *114*, 901.

[4] L. Moroder, H.-J. Musiol, M. Götz, C. Renner, Synthesis of single- and multiple-stranded cystine-rich peptides. *Biopolymers* **2005**, *80*, 85.

[5] K. B. Akondi, M. Muttenthaler, S. Dutertre, Q. Kaas, D. J. Craik, R. J. Lewis, P. F. Alewood, Discovery, synthesis, and structure-activity relationships of conotoxins. *Chem Rev* **2014**, *114*, 5815.

[6] P. Heimer, A. A. Tietze, C. A. Bäuml, A. Resemann, F. J. Mayer, D. Suckau, O. Ohlenschläger, D. Tietze, D. Imhof, Conformational μ-Conotoxin PIIIA Isomers Revisited: Impact of Cysteine Pairing on Disulfide-Bond Assignment and Structure Elucidation. *Anal Chem* **2018**, *90*, 3321.

[7] Q. Zhu, S. Liang, L. Martin, S. Gasparini, A. Ménez, C. Vita, Role of disulfide bonds in folding and activity of leiurotoxin I: just two disulfides suffice. *Biochemistry* **2002**, *41*, 11488.

[8] T. S. Han, M.-M. Zhang, A. Walewska, P. Gruszczynski, C. R. Robertson, T. E. Cheatham, D. Yoshikami, B. M. Olivera, G. Bulaj, Structurally minimized mu-conotoxin analogues as sodium channel blockers: implications for designing conopeptide-based therapeutics. *ChemMedChem* **2009**, *4*, 406.

[9] J. L. Arolas, V. Castillo, S. Bronsoms, F. X. Aviles, S. Ventura, Designing out disulfide bonds of leech carboxypeptidase inhibitor: implications for its folding, stability and function. *J Mol Biol* **2009**, *392*, 529.

[10] R. Yu, V. A. L. Seymour, G. Berecki, X. Jia, M. Akcan, D. J. Adams, Q. Kaas, D. J. Craik, Less is More: Design of a Highly Stable Disulfide-Deleted Mutant of Analgesic Cyclic α-Conotoxin Vc1.1. *Sci Rep* **2015**, *5*, 13264.

[11] S. Finney, L. Seale, R. T. Sawyer, R. B. Wallis, Tridegin, a new peptidic inhibitor of factor XIIIa, from the blood-sucking leech Haementeria ghilianii. *Biochem J* **1997**, *324*, 797.

[12] M. Böhm, C. A. Bäuml, K. Hardes, T. Steinmetzer, D. Roeser, Y. Schaub, M. E. Than, A. Biswas, D. Imhof, Novel insights into structure and function of factor XIIIa-inhibitor tridegin. *J Med Chem* **2014**, *57*, 10355.

[13] C. A. Bäuml, A. A. Paul George, T. Schmitz, P. Sommerfeld, M. Pietsch, L. Podsiadlowski, T. Steinmetzer, A. Biswas, D. Imhof, Distinct 3-disulfide-bonded isomers of tridegin differentially inhibit coagulation factor XIIIa: The influence of structural stability on bioactivity. *Eur J Med Chem* **2020**, *201*, 112474.

[14] J. L. Mitchell, N. J. Mutch, Let's cross-link: diverse functions of the promiscuous cellular transglutaminase factor XIII-A. *J Thromb Haemost* **2019**, *17*, 19.

[15] J. R. Byrnes, A. S. Wolberg, Newly-Recognized Roles of Factor XIII in Thrombosis. *Semin Thromb Hemost* **2016**, *42*, 445.

[16] M. Pieters, A. S. Wolberg, Fibrinogen and fibrin: An illustrated review. *Res Pract Thromb Haemost* **2019**, *3*, 161.

[17] C. A. Bäuml, T. Schmitz, A. A. Paul George, M. Sudarsanam, K. Hardes, T. Steinmetzer, L. A. Holle, A. S. Wolberg, B. Pötzsch, J. Oldenburg et al., Coagulation Factor XIIIa Inhibitor Tridegin: On the Role of Disulfide Bonds for Folding, Stability, and Function. *J Med Chem* **2019**, *62*, 3513.

[18] T. Schmitz, A. A. Paul George, B. Nubbemeyer, C. A. Bäuml, T. Steinmetzer, O. Ohlenschläger, A. Biswas, D. Imhof, NMR-Based Structural Characterization of a Two-Disulfide-Bonded Analogue of the FXIIIa Inhibitor Tridegin: New Insights into Structure-Activity Relationships. *Int J Mol Sci* **2021**, *22*, 880.

[19] T. Schmitz, S. Pengelley, E. Belau, D. Suckau, D. Imhof, LC-Trapped Ion Mobility Spectrometry-TOF MS Differentiation of 2- and 3-Disulfide-Bonded Isomers of the μ-Conotoxin PIIIA. *Anal Chem* **2020**, *92*, 10920.

[20] A. Henninot, J. C. Collins, J. M. Nuss, The Current State of Peptide Drug Discovery: Back to the Future? *J Med Chem* **2018**, *61*, 1382.

[21] J. L. Lau, M. K. Dunn, Therapeutic peptides: Historical perspectives, current development trends, and future directions. *Bioorg Med Chem* **2018**, *26*, 2700.

[22] M. W. Pennington, A. Czerwinski, R. S. Norton, Peptide therapeutics from venom: Current status and potential. *Bioorg Med Chem* **2018**, *26*, 2738.

[23] R. J. Mart, R. D. Osborne, M. M. Stevens, R. V. Ulijn, Peptide-based stimuli-responsive biomaterials. *Soft Matter* **2006**, *2*, 822.

[24] T. S. Kang, R. M. Kini, Structural determinants of protein folding. *Cell Mol Life Sci* **2009**, *66*, 2341.

[25] R. J. Lewis, M. L. Garcia, Therapeutic potential of venom peptides. *Nat Rev Drug Discov* **2003**, *2*, 790.

[26] V. Herzig, B. Cristofori-Armstrong, M. R. Israel, S. A. Nixon, I. Vetter, G. F. King, Animal toxins - Nature's evolutionary-refined toolkit for basic research and drug discovery. *Biochem Pharmacol* **2020**, *181*, 114096.

[27] T. Schmitz, C. A. Bäuml, D. Imhof, Inhibitors of blood coagulation factor XIII. *Anal Biochem* **2020**, *605*, 113708.

[28] D. J. Craik, N. L. Daly, J. Mulvenna, M. R. Plan, M. Trabi, Discovery, structure and biological activities of the cyclotides. *Curr Protein Pept Sci* **2004**, *5*, 297.

[29] N. L. Daly, K. J. Rosengren, D. J. Craik, Discovery, structure and biological activities of cyclotides. *Adv Drug Deliv Rev* **2009**, *61*, 918.

[30] N. Sewald, H.-D. Jakubke, Peptides. *Chemistry and Biology*, John Wiley & Sons Incorporated, Weinheim, **2009**.

[31] D. Yang, A. Biragyn, L. W. Kwak, J. J. Oppenheim, Mammalian defensins in immunity: more than just microbicidal. *Trends Immunol* **2002**, *23*, 291.

[32] T. Ganz, Defensins: antimicrobial peptides of innate immunity. *Nat Rev Immunol* **2003**, *3*, 710.

[33] R. I. Lehrer, W. Lu, α-Defensins in human innate immunity. *Immunol Rev* **2012**, *245*, 84.

[34] S. J. Moore, C. L. Leung, J. R. Cochran, Knottins: disulfide-bonded therapeutic and diagnostic peptides. *Drug Discov Today Technol* **2012**, *9*, e1-e70.

[35] A. E. Garcia, J. A. Camarero, Biological activities of natural and engineered cyclotides, a novel molecular scaffold for peptide-based therapeutics. *Curr Mol Pharmacol* **2010**, *3*, 153.

[36] D. C. Ireland, R. J. Clark, N. L. Daly, D. J. Craik, Isolation, sequencing, and structure-activity relationships of cyclotides. *J Nat Prod* **2010**, *73*, 1610.

[37] J. E. Lin, M. Valentino, G. Marszalowicz, M. S. Magee, P. Li, A. E. Snook, B. A. Stoecker, C. Chang, S. A. Waldman, Bacterial heat-stable enterotoxins: translation of pathogenic peptides into novel targeted diagnostics and therapeutics. *Toxins* **2010**, *2*, 2028.

[38] G. F. King, Venoms as a platform for human drugs: translating toxins into therapeutics. *Expert Opin Biol Ther* **2011**, *11*, 1469.

[39] G. F. King, Venoms to drugs. *Venom as a source for the development of human therapeutics*, Royal Society of Chemistry, Cambridge, **2015**.

[40] G. F. King, M. C. Hardy, Spider-venom peptides: structure, pharmacology, and potential for control of insect pests. *Annu Rev Entomol* **2013**, *58*, 475.

[41] A.-H. Jin, M. Muttenthaler, S. Dutertre, S. W. A. Himaya, Q. Kaas, D. J. Craik, R. J. Lewis, P. F. Alewood, Conotoxins: Chemistry and Biology. *Chem Rev* **2019**, *119*, 11510.

[42] R. Halai, D. J. Craik, Conotoxins: natural product drug leads. *Nat. Prod. Rep.* **2009**, *26*, 526.

[43] R. J. Lewis, S. Dutertre, I. Vetter, M. J. Christie, Conus venom peptide pharmacology. *Pharmacol Rev* **2012**, *64*, 259.

[44] A. Greinacher, T. E. Warkentin, The direct thrombin inhibitor hirudin. *Thromb Haemost* **2008**, *99*, 819.

[45] L. Moroder, D. Besse, H. J. Musiol, S. Rudolph-Böhner, F. Siedler, Oxidative folding of cystine-rich peptides vs regioselective cysteine pairing strategies. *Biopolymers* **1996**, *40*, 207.

[46] A. Felix, L. Moroder, C. Toniolo, Houben-Weyl Methods of Organic Chemistry Vol. E 22b, 4th Edition Supplement, Georg Thieme Verlag, Stuttgart, **2004**.

[47] D. Andreu, F. Albericio, N. A. Solé, M. C. Munson, M. Ferrer, G. Barany, Formation of disulfide bonds in synthetic peptides and proteins. *Methods Mol Biol* **1994**, *35*, 91.

[48] T. M. Postma, F. Albericio, Disulfide Formation Strategies in Peptide Synthesis. *Eur. J. Org. Chem.* **2014**, *17*, 3519.

[49] A. Chakraborty, A. Sharma, F. Albericio, B. G. de La Torre, Disulfide-Based Protecting Groups for the Cysteine Side Chain. *Org Lett* **2020**, *22*, 9644.

[50] J.-Y. Chang, Diverse pathways of oxidative folding of disulfide proteins: underlying causes and folding models. *Biochemistry* **2011**, *50*, 3414.

[51] C. B. Anfinsen, Principles that govern the folding of protein chains. *Science* **1973**, *181*, 223.

[52] C. B. Anfinsen, H. A. Scheraga, Experimental and Theoretical Aspects of Protein Folding. *Adv Protein Chem* **1975**, *29*, 205.

[53] P. Xu, Q. Kaas, Y. Wu, X. Zhu, X. Li, P. J. Harvey, D. Zhangsun, D. J. Craik, S. Luo, Structure and Activity Studies of Disulfide-Deficient Analogues of αO-Conotoxin GeXIVA. *J Med Chem* **2020**, *63*, 1564.

[54] A. A. Paul George, P. Heimer, E. Leipold, T. Schmitz, D. Kaufmann, D. Tietze, S. H. Heinemann, D. Imhof, Effect of Conformational Diversity on the Bioactivity of μ-Conotoxin PIIIA Disulfide Isomers. *Mar Drugs* **2019**, *17*.

[55] P. Han, K. Wang, X. Dai, Y. Cao, S. Liu, H. Jiang, C. Fan, W. Wu, J. Chen, The Role of Individual Disulfide Bonds of μ-Conotoxin GIIIA in the Inhibition of NaV1.4. *Mar Drugs* **2016**, *14*.

[56] K. K. Khoo, Z.-P. Feng, B. J. Smith, M.-M. Zhang, D. Yoshikami, B. M. Olivera, G. Bulaj, R. S. Norton, Structure of the analgesic mu-conotoxin KIIIA and effects on the structure and function of disulfide deletion. *Biochemistry* **2009**, *48*, 1210.

[57] L. Di, Strategic approaches to optimizing peptide ADME properties. *AAPS J* **2015**, *17*, 134.

[58] A. A. Kaspar, J. M. Reichert, Future directions for peptide therapeutics development. *Drug Discov Today* **2013**, *18*, 807.

[59] L. K. Buckton, M. N. Rahimi, S. R. McAlpine, Cyclic Peptides as Drugs for Intracellular Targets: The Next Frontier in Peptide Therapeutic Development. *Chemistry* **2020**.

[60] J. K. Klint, S. Senff, N. J. Saez, R. Seshadri, H. Y. Lau, N. S. Bende, E. A. B. Undheim, L. D. Rash, M. Mobli, G. F. King, Production of recombinant disulfide-rich venom peptides for structural and functional analysis via expression in the periplasm of E. coli. *PLoS ONE* **2013**, *8*, e63865.

[61] R. B. Merrifield, Solid Phase Peptide Synthesis. I. The Synthesis of a Tetrapeptide. *J Am Chem Soc* **1963**, *85*, 2149.

[62] P. E. Dawson, S. B. Kent, Synthesis of native proteins by chemical ligation. *Annu Rev Biochem* **2000**, *69*, 923.

[63] Y. Ma, C.-J. Lee, J.-S. Park, Strategies for Optimizing the Production of Proteins and Peptides with Multiple Disulfide Bonds. *Antibiotics* **2020**, *9*, 541.

[64] Y. Ding, J. P. Ting, J. Liu, S. Al-Azzam, P. Pandya, S. Afshar, Impact of non-proteinogenic amino acids in the discovery and development of peptide therapeutics. *Amino Acids* **2020**, *52*, 1207.

[65] F. E. Sin, D. Isenberg, An evaluation of voclosporin for the treatment of lupus nephritis. *Expert Opin Pharmacother* **2018**, *19*, 1613.

[66] B. A. Falls, Y. Zhang, Insights into the Allosteric Mechanism of Setmelanotide (RM-493) as a Potent and First-in-Class Melanocortin-4 Receptor (MC4R) Agonist To Treat Rare Genetic Disorders of Obesity through an in Silico Approach. *ACS Chem Neurosci* **2019**, *10*, 1055.

[67] A. Pfeifer, U. Knigge, J. Mortensen, P. Oturai, A. K. Berthelsen, A. Loft, T. Binderup, P. Rasmussen, D. Elema, T. L. Klausen et al., Clinical PET of neuroendocrine tumors using 64Cu-DOTATATE: first-in-humans study. *J Nucl Med* **2012**, *53*, 1207.

[68] B. G. de La Torre, F. Albericio, Peptide Therapeutics 2.0. *Molecules* **2020**, *25*, 2293.

[69] B. G. de La Torre, F. Albericio, The Pharmaceutical Industry in 2019. An Analysis of FDA Drug Approvals from the Perspective of Molecules. *Molecules* **2020**, *25*, 745.

[70] B. G. de La Torre, F. Albericio, The Pharmaceutical Industry in 2017. An Analysis of FDA Drug Approvals from the Perspective of Molecules. *Molecules* **2018**, *23*, 533.

[71] B. G. de La Torre, F. Albericio, The Pharmaceutical Industry in 2016. An Analysis of FDA Drug Approvals from a Perspective of the Molecule Type. *Molecules* **2017**, *22*, 368.

[72] B. G. de La Torre, F. Albericio, The Pharmaceutical Industry in 2018. An Analysis of FDA Drug Approvals from the Perspective of Molecules. *Molecules* **2019**, *24*, 809.

[73] F. Albericio, H. G. Kruger, Therapeutic peptides. *Future Med Chem* **2012**, *4*, 1527.

[74] S. Dhillon, S. J. Keam, Bremelanotide: First Approval. *Drugs* **2019**, *79*, 1599.

[75] M. M. McNeil, A. F. Nahhas, T. L. Braunberger, I. H. Hamzavi, Afamelanotide in the Treatment of Dermatologic Disease. *Skin Therapy Lett* **2018**, *23*, 6.

[76] T. D. Poeppel, I. Binse, S. Petersenn, H. Lahner, M. Schott, G. Antoch, W. Brandau, A. Bockisch, C. Boy, 68Ga-DOTATOC Versus 68Ga-DOTATATE PET/CT in Functional Imaging of Neuroendocrine Tumors. *J Nucl Med* **2011**, *52*, 1864.

[77] S. Das, T. Al-Toubah, G. El-Haddad, J. Strosberg, 177Lu-DOTATATE for the treatment of gastroenteropancreatic neuroendocrine tumors. *Expert Rev Gastroenterol Hepatol* **2019**, *13*, 1023.

[78] L. B. Knudsen, J. Lau, The Discovery and Development of Liraglutide and Semaglutide. *Front Endocrinol* **2019**, *10*, 155.

[79] S. S. C. Rao, Plecanatide: a new guanylate cyclase agonist for the treatment of chronic idiopathic constipation. *Therap Adv Gastroenterol* **2018**, *11*, 1-14.

[80] G. R. Gabreanu, An update on the diagnosis of growth hormone deficiency. *Discoveries (Craiova)* **2018**, *6*, e82.

[81] C. Friedl, E. Zitt, Role of etelcalcetide in the management of secondary hyperparathyroidism in hemodialysis patients: a review on current data and place in therapy. *Drug Des Devel Ther* **2018**, *12*, 1589.

[82] S. C. Khalique, N. Ferguson, Angiotensin II (Giapreza): A Distinct Mechanism for the Treatment of Vasodilatory Shock. *Cardiol Rev* **2019**, *27*, 167.

[83] S. Gonnelli, C. Caffarelli, Abaloparatide. *Clin Cases Miner Bone Metab* **2016**, *13*, 106.

[84] D. E. Baker, T. L. Levien, Lixisenatide. *Hosp Pharm* **2017**, *52*, 65.

[85] A. T. Nunes, C. M. Annunziata, Proteasome inhibitors: structure and function. *Semin Oncol* **2017**, *44*, 377.

[86] J. A. Messina, V. G. Fowler, G. R. Corey, Oritavancin for acute bacterial skin and skin structure infections. *Expert Opin Pharmacother* **2015**, *16*, 1091.

[87] O. Braide-Moncoeur, N. T. Tran, J. R. Long, Peptide-based synthetic pulmonary surfactant for the treatment of respiratory distress disorders. *Curr Opin Chem Biol* **2016**, *32*, 22.

[88] S. Feng, S. Chang, L. Yan, H. Dong, X. Xu, C. Wang, Y. Liang, K. Liu, Design, synthesis, and activity evaluation of novel erythropoietin mimetic peptides. *Bioorg Med Chem Lett* **2018**, *28*, 3038.

[89] R. W. Busby, A. P. Bryant, W. P. Bartolini, E. A. Cordero, G. Hannig, M. M. Kessler, S. Mahajan-Miklos, C. M. Pierce, R. M. Solinga, L. J. Sun et al., Linaclotide, through activation of guanylate cyclase C, acts locally in the gastrointestinal tract to elicit enhanced intestinal secretion and transit. *Eur J Pharmacol* **2010**, *649*, 328.

[90] P. L. McCormack, Linaclotide: a review of its use in the treatment of irritable bowel syndrome with constipation. *Drugs* **2014**, *74*, 53.

[91] E. D. Deeks, Icatibant. *Drugs* **2010**, *70*, 73.

[92] C. Grunfeld, A. Dritselis, P. Kirkpatrick, Tesamorelin. *Nat Rev Drug Discov* **2011**, *10*, 95.

[93] A. V. Gubskaya, I. J. Khan, L. M. Valenzuela, Y. V. Lisnyak, J. Kohn, Investigating the Release of a Hydrophobic Peptide from Matrices of Biodegradable Polymers: An Integrated Method Approach. *Polymer (Guildf)* **2013**, *54*, 3806.

[94] A. C.-L. Lee, J. L. Harris, K. K. Khanna, J.-H. Hong, A Comprehensive Review on Current Advances in Peptide Drug Development and Design. *Int J Mol Sci* **2019**, *20*, 2383.

[95] A. L. Harvey, Toxins and drug discovery. *Toxicon* **2014**, *92*, 193.

[96] S. Becker, H. Terlau, Toxins from cone snails: properties, applications and biotechnological production. *Appl Microbiol Biotechnol* **2008**, *79*, 1.

[97] B. M. Olivera, W. R. Gray, R. Zeikus, J. M. McIntosh, J. Varga, J. Rivier, V. de Santos, L. J. Cruz, Peptide neurotoxins from fish-hunting cone snails. *Science* **1985**, *230*, 1338.

[98] B. Gao, C. Peng, J. Yang, Y. Yi, J. Zhang, Q. Shi, Cone Snails: A Big Store of Conotoxins for Novel Drug Discovery. *Toxins* **2017**, *9*, 397.

[99] Y. Fu, C. Li, S. Dong, Y. Wu, D. Zhangsun, S. Luo, Discovery Methodology of Novel Conotoxins from Conus Species. *Mar Drugs* **2018**, *16*, 417.

[100] P. Escoubas, G. F. King, Venomics as a drug discovery platform. *Expert Rev Proteomics* **2009**, *6*, 221.

[101] G. P. Miljanich, Ziconotide: neuronal calcium channel blocker for treating severe chronic pain. *Curr Med Chem* **2004**, *11*, 3029.

[102] S. Bajaj, J. Han, Venom-Derived Peptide Modulators of Cation-Selective Channels: Friend, Foe or Frenemy. *Front Pharmacol* **2019**, *10*, 58.

[103] G. Bulaj, M.-M. Zhang, B. R. Green, B. Fiedler, R. T. Layer, S. Wei, J. S. Nielsen, S. J. Low, B. D. Klein, J. D. Wagstaff et al., Synthetic muO-conotoxin MrVIB blocks TTX-resistant sodium channel NaV1.8 and has a long-lasting analgesic activity. *Biochemistry* **2006**, *45*, 7404.

[104] K. P. R. Nilsson, E. S. Lovelace, C. E. Caesar, N. Tynngård, P. F. Alewood, H. M. Johansson, I. A. Sharpe, R. J. Lewis, N. L. Daly, D. J. Craik, Solution structure of chi-conopeptide MrIA, a modulator of the human norepinephrine transporter. *Biopolymers* **2005**, *80*, 815.

[105] R. J. Clark, H. Fischer, S. T. Nevin, D. J. Adams, D. J. Craik, The synthesis, structural characterization, and receptor specificity of the alpha-conotoxin Vc1.1. *J Biol Chem* **2006**, *281*, 23254.

[106] P. Heimer, T. Schmitz, C. A. Bäuml, D. Imhof, Synthesis and Structure Determination of µ-Conotoxin PIIIA Isomers with Different Disulfide Connectivities. *J Vis Exp* **2018**, e58368.

[107] S. Kvist, A. Manzano-Marín, D. de Carle, P. Trontelj, M. E. Siddall, Draft genome of the European medicinal leech Hirudo medicinalis (Annelida, Clitellata, Hirudiniformes) with emphasis on anticoagulants. *Sci Rep* **2020**, *10*, 9885.

[108] V. V. Babenko, O. V. Podgorny, V. A. Manuvera, A. S. Kasianov, A. I. Manolov, E. N. Grafskaia, D. A. Shirokov, A. S. Kurdyumov, D. V. Vinogradov, A. S. Nikitina et al., Draft genome sequences of Hirudo medicinalis and salivary transcriptome of three closely related medicinal leeches. *BMC genomics* **2020**, *21*, 331.

[109] U. Rester, W. Bode, C. A. Sampaio, E. A. Auerswald, A. P. Lopes, Cloning, purification, crystallization and preliminary X-ray diffraction analysis of the antistasin-type inhibitor ghilanten (domain I) from Haementeria ghilianii in complex with porcine beta-trypsin. *Acta Crystallogr D Biol Crystallogr* **2001**, *57*, 1038.

[110] D. R. Kim, K. W. Kang, Amino acid sequence of piguamerin, an antistasin-type protease inhibitor from the blood sucking leech Hirudo nipponia. *Eur J Biochem* **1998**, *254*, 692.

[111] C. Söllner, R. Mentele, C. Eckerskorn, H. Fritz, C. P. Sommerhoff, Isolation and characterization of hirustasin, an antistasin-type serine-proteinase inhibitor from the medical leech Hirudo medicinalis. *Eur J Biochem* **1994**, *219*, 937.

[112] A. M. Krezel, G. Wagner, J. Seymour-Ulmer, R. A. Lazarus, Structure of the RGD protein decorsin: conserved motif and distinct function in leech proteins that affect blood clotting. *Science* **1994**, *264*, 1944.

[113] J. L. Richardson, B. Kröger, W. Hoeffken, J. E. Sadler, P. Pereira, R. Huber, W. Bode, P. Fuentes-Prior, Crystal structure of the human alpha-thrombin-haemadin complex: an exosite II-binding inhibitor. *EMBO J* **2000**, *19*, 5650.

[114] R. de Caterina, The current role of anticoagulants in cardiovascular medicine. *J Cardiovasc Med (Hagerstown)* **2009**, *10*, 595.

[115] World Health Organization, Global Health Estimates 2019: Deaths by Cause, Age, Sex, by Country and by Region. 2000-2019, Genf, **2020**.

[116] F. Markwardt, Untersuchungen ber Hirudin. *Naturwissenschaften* **1955**, *42*, 537.

[117] F. Markwardt, Hirudin as alternative anticoagulant--a historical review. *Semin Thromb Hemost* **2002**, *28*, 405.

[118] D. D. Callas, D. Hoppensteadt, J. Fareed, Comparative studies on the anticoagulant and protease generation inhibitory actions of newly developed site-directed thrombin inhibitory drugs. Efegatran, argatroban, hirulog, and hirudin. *Semin Thromb Hemost* **1995**, *21*, 177.

[119] U. R. Desai, New antithrombin-based anticoagulants. *Med Res Rev* **2004**, *24*, 151.

[120] T. Hanslik, J. Prinseau, The use of vitamin K in patients on anticoagulant therapy: a practical guide. *Am J Cardiovasc Drugs* **2004**, *4*, 43.

[121] A. S. Wolberg, F. R. Rosendaal, J. I. Weitz, I. H. Jaffer, G. Agnelli, T. Baglin, N. Mackman, Venous thrombosis. *Nat Rev Dis Primers* **2015**, *1*, 15006.

[122] S. R. Fraser, N. A. Booth, N. J. Mutch, The antifibrinolytic function of factor XIII is exclusively expressed through α_2-antiplasmin cross-linking. *Blood* **2011**, *117*, 6371.

[123] M. M. Aleman, J. R. Byrnes, J.-G. Wang, R. Tran, W. A. Lam, J. Di Paola, N. Mackman, J. L. Degen, M. J. Flick, A. S. Wolberg, Factor XIII activity mediates red blood cell retention in venous thrombi. *J Clin Invest* **2014**, *124*, 3590.

[124] A. J. Gale, Continuing education course #2: current understanding of hemostasis. *Toxicol Pathol* **2011**, *39*, 273.

[125] M. Hoffman, D. M. Monroe, A cell-based model of hemostasis. *Thromb Haemost* **2001**, *85*, 958.

[126] D. M. Monroe, M. Hoffman, H. R. Roberts, Transmission of a procoagulant signal from tissue factor-bearing cell to platelets. *Blood Coagul Fibrin* **1996**, *7*, 459.

[127] M. Díaz-Ricart, E. Estebanell, M. Lozano, J. Aznar-Salatti, J. G. White, A. Ordinas, G. Escolar, Thrombin facilitates primary platelet adhesion onto vascular surfaces in the absence of plasma adhesive proteins: studies under flow conditions. *Haematologica* **2000**, *85*, 280.

[128] D. A. Lane, H. Philippou, J. A. Huntington, Directing thrombin. *Blood* **2005**, *106*, 2605.

[129] S. Palta, R. Saroa, A. Palta, Overview of the coagulation system. *Indian J Anaesth* **2014**, *58*, 515.

[130] J. A. Oliver, D. M. Monroe, H. R. Roberts, M. Hoffman, Thrombin activates factor XI on activated platelets in the absence of factor XII. *Arterioscler Thromb Vasc Biol* **1999**, *19*, 170.

[131] B. Pötzsch, K. Madlener, Hämostaseologie, Springer-Verlag Berlin Heidelberg, Berlin, Heidelberg, **2010**.

[132] G. Cirino, C. Cicala, M. Bucci, L. Sorrentino, G. Ambrosini, G. DeDominicis, D. C. Altieri, Factor Xa as an interface between coagulation and inflammation. Molecular mimicry of factor Xa association with effector cell protease receptor-1 induces acute inflammation in vivo. *J Clin Invest* **1997**, *99*, 2446.

[133] J. S. Greengard, M. J. Heeb, E. Ersdal, P. N. Walsh, J. H. Griffin, Binding of coagulation factor XI to washed human platelets. *Biochemistry* **1986**, *25*, 3884.

[134] S. Kattula, J. R. Byrnes, S. M. Martin, L. A. Holle, B. C. Cooley, M. J. Flick, A. S. Wolberg, Factor XIII in plasma, but not in platelets, mediates red blood cell retention in clots and venous thrombus size in mice. *Blood Adv* **2018**, *2*, 25.

[135] J. R. Byrnes, C. Duval, Y. Wang, C. E. Hansen, B. Ahn, M. J. Mooberry, M. A. Clark, J. M. Johnsen, S. T. Lord, W. A. Lam et al., Factor XIIIa-dependent retention of red blood cells in clots is mediated by fibrin α-chain crosslinking. *Blood* **2015**, *126*, 1940.

[136] Z. Bagoly, L. Muszbek, Factor XIII: What does it look like? *J Thromb Haemost* **2019**, *17*, 714.

[137] E. W. Davie, K. Fujikawa, W. Kisiel, The coagulation cascade: initiation, maintenance, and regulation. *Biochemistry* **1991**, *30*, 10363.

[138] K. Laki, L. Lóránd, On the Solubility of Fibrin Clots. *Science* **1948**, *108*, 280.

[139] L. Lorand, A study on the solubility of fibrin clots in urea. *Hung Acta Physiol* **1948**, *1*, 192.

[140] L. Lorand, Factor XIII and the clotting of fibrinogen: from basic research to medicine. *J Thromb Haemost* **2005**, *3*, 1337.

[141] L. Muszbek, Z. Bereczky, Z. Bagoly, I. Komáromi, É. Katona, Factor XIII: a coagulation factor with multiple plasmatic and cellular functions. *Physiol Rev* **2011**, *91*, 931.

[142] L. Muszbek, G. Haramura, J. Polgár, Transformation of cellular factor XIII into an active zymogen transglutaminase in thrombin-stimulated platelets. *Thromb Haemost* **1995**, *73*, 702.

[143] S. A. Piercy-Kotb, A. Mousa, H. F. Al-Jallad, V. D. Myneni, F. Chicatun, S. N. Nazhat, M. T. Kaartinen, Factor XIIIA transglutaminase expression and secretion by osteoblasts is regulated by extracellular matrix collagen and the MAP kinase signaling pathway. *J Cell Physiol* **2012**, *227*, 2936.

[144] B. A. Anokhin, W. L. Dean, K. A. Smith, M. J. Flick, R. A. S. Ariëns, H. Philippou, M. C. Maurer, Proteolytic and nonproteolytic activation mechanisms result in conformationally and functionally different forms of coagulation factor XIII A. *FEBS J* **2020**, *287*, 452.

[145] B. A. Anokhin, V. Stribinskis, W. L. Dean, M. C. Maurer, Activation of factor XIII is accompanied by a change in oligomerization state. *FEBS J* **2017**, *284*, 3849.

[146] J. Polgár, V. Hidasi, L. Muszbek, Non-proteolytic activation of cellular protransglutaminase (placenta macrophage factor XIII). *Biochem J* **1990**, *267*, 557.

[147] L. Muszbek, R. A. Ariëns, A. Ichinose, Factor XIII: recommended terms and abbreviations. *J Thromb Haemost* **2007**, *5*, 181.

[148] M. Stieler, J. Weber, M. Hils, P. Kolb, A. Heine, C. Büchold, R. Pasternack, G. Klebe, Structure of active coagulation factor XIII triggered by calcium binding: basis for the design of next-generation anticoagulants. *Angew Chem Int Ed Engl* **2013**, *52*, 11930.

[149] S. Singh, A. Nazabal, S. Kaniyappan, J.-L. Pellequer, A. S. Wolberg, D. Imhof, J. Oldenburg, A. Biswas, The Plasma Factor XIII Heterotetrameric Complex Structure: Unexpected Unequal Pairing within a Symmetric Complex. *Biomolecules* **2019**, *9*, 765.

[150] V. Schroeder, H. P. Kohler, Factor XIII deficiency: an update. *Semin Thromb Hemost* **2013**, *39*, 632.

[151] S. Singh, M. S. Akhter, J. Dodt, A. Sharma, S. Kaniyappan, H. Yadegari, V. Ivaskevicius, J. Oldenburg, A. Biswas, Disruption of Structural Disulfides of Coagulation FXIII-B Subunit; Functional Implications for a Rare Bleeding Disorder. *Int J Mol Sci* **2019**, *20*, 1956.

[152] S. Singh, M. S. Akhter, J. Dodt, P. Volkers, A. Reuter, C. Reinhart, C. Krettler, J. Oldenburg, A. Biswas, Identification of Potential Novel Interacting Partners for Coagulation Factor XIII B (FXIII-B) Subunit, a Protein Associated with a Rare Bleeding Disorder. *Int J Mol Sci* **2019**, *20*, 2682.

[153] C. Skerka, Q. Chen, V. Fremeaux-Bacchi, L. T. Roumenina, Complement factor H related proteins (CFHRs). *Mol Immunol* **2013**, *56*, 170.

[154] M. Souri, S. Koseki-Kuno, N. Takeda, J. L. Degen, A. Ichinose, Administration of factor XIII B subunit increased plasma factor XIII A subunit levels in factor XIII B subunit knock-out mice. *Int J Hematol* **2008**, *87*, 60.

[155] M. Souri, H. Kaetsu, A. Ichinose, Sushi domains in the B subunit of factor XIII responsible for oligomer assembly. *Biochemistry* **2008**, *47*, 8656.

[156] L. Patthy, Detecting homology of distantly related proteins with consensus sequences. *J Mol Biol* **1987**, *198*, 567.

[157] M. S. Akhter, S. Singh, H. Yadegari, V. Ivaskevicius, J. Oldenburg, A. Biswas, Exploring the structural similarity yet functional distinction between coagulation factor XIII-B and complement factor H sushi domains. *J Thromb Thrombolysis* **2019**, *48*, 95.

[158] E. Katona, K. Pénzes, A. Csapó, F. Fazakas, M. L. Udvardy, Z. Bagoly, Z. Z. Orosz, L. Muszbek, Interaction of factor XIII subunits. *Blood* **2014**, *123*, 1757.

[159] V. C. Yee, L. C. Pedersen, I. Le Trong, P. D. Bishop, R. E. Stenkamp, D. C. Teller, Three-dimensional structure of a transglutaminase: human blood coagulation factor XIII. *Proc Natl Acad Sci U S A* **1994**, *91*, 7296.

[160] B. A. Fox, V. C. Yee, L. C. Pedersen, I. Le Trong, P. D. Bishop, R. E. Stenkamp, D. C. Teller, Identification of the calcium binding site and a novel ytterbium site in blood coagulation factor XIII by x-ray crystallography. *J Biol Chem* **1999**, *274*, 4917.

[161] V. C. Yee, L. C. Pedersen, P. D. Bishop, R. E. Stenkamp, D. C. Teller, Structural evidence that the activation peptide is not released upon thrombin cleavage of factor XIII. *Thromb Res* **1995**, *78*, 389.

[162] E. L. Hethershaw, P. J. Adamson, K. A. Smith, W. N. Goldsberry, R. J. Pease, S. E. Radford, P. J. Grant, R. A. S. Ariëns, M. C. Maurer, H. Philippou, The role of β-barrels 1 and 2 in the enzymatic activity of factor XIII A-subunit. *J Thromb Haemost* **2018**, *16*, 1391.

[163] L. Lorand, K. KONISHI, Activation of the fibrin stabilizing factor of plasma by thrombin. *Arch Biochem Biophys* **1964**, *105*, 58.

[164] L. Lorand, Factor XIII: structure, activation, and interactions with fibrinogen and fibrin. *Ann N Y Acad Sci* **2001**, *936*, 291.

[165] C. S. Greenberg, C. C. Miraglia, The effect of fibrin polymers on thrombin-catalyzed plasma factor XIIIa formation. *Blood* **1985**, *66*, 466.

[166] S. D. Lewis, T. J. Janus, L. Lorand, J. A. Shafer, Regulation of formation of factor XIIIa by its fibrin substrates. *Biochemistry* **1985**, *24*, 6772.

[167] K. A. Smith, P. J. Adamson, R. J. Pease, J. M. Brown, A. J. Balmforth, P. A. Cordell, R. A. S. Ariëns, H. Philippou, P. J. Grant, Interactions between factor XIII and the alphaC region of fibrinogen. *Blood* **2011**, *117*, 3460.

[168] G. Dickneite, H. Herwald, W. Korte, Y. Allanore, C. P. Denton, M. Matucci Cerinic, Coagulation factor XIII: a multifunctional transglutaminase with clinical potential in a range of conditions. *Thromb Haemost* **2015**, *113*, 686.

[169] I. Komáromi, Z. Bagoly, L. Muszbek, Factor XIII: novel structural and functional aspects. *J Thromb Haemost* **2011**, *9*, 9.

[170] R. L. Eckert, M. T. Kaartinen, M. Nurminskaya, A. M. Belkin, G. Colak, G. V. W. Johnson, K. Mehta, Transglutaminase regulation of cell function. *Physiol Rev* **2014**, *94*, 383.

[171] H. Thomas, K. Beck, M. Adamczyk, P. Aeschlimann, M. Langley, R. C. Oita, L. Thiebach, M. Hils, D. Aeschlimann, Transglutaminase 6: a protein associated with central nervous system development and motor function. *Amino Acids* **2013**, *44*, 161.

[172] L. Lorand, R. M. Graham, Transglutaminases: crosslinking enzymes with pleiotropic functions. *Nat Rev Mol Cell Biol* **2003**, *4*, 140.

[173] H. Tatsukawa, Y. Furutani, K. Hitomi, S. Kojima, Transglutaminase 2 has opposing roles in the regulation of cellular functions as well as cell growth and death. *Cell Death Dis* **2016**, *7*, e2244.

[174] J. M. Wodzinska, Transglutaminases as targets for pharmacological inhibition. *Mini Rev Med Chem* **2005**, *5*, 279.

[175] A.-M. Sulic, K. Kurppa, T. Rauhavirta, K. Kaukinen, K. Lindfors, Transglutaminase as a therapeutic target for celiac disease. *Expert Opin Ther Targets* **2015**, *19*, 335.

[176] M. Lesort, J. Tucholski, M. L. Miller, G. V. Johnson, Tissue transglutaminase: a possible role in neurodegenerative diseases. *Prog Neurobiol* **2000**, *61*, 439.

[177] L. Huang, A.-M. Xu, W. Liu, Transglutaminase 2 in cancer. *Am J Cancer Res* **2015**, *5*, 2756.

[178] L. Lorand, N. G. Rule, H. H. Ong, R. Furlanetto, A. Jacobsen, J. Downey, N. Oner, J. Bruner-Lorand, Amine specificity in transpeptidation. Inhibition of fibrin cross-linking. *Biochemistry* **1968**, *7*, 1214.

[179] K. F. Freund, K. P. Doshi, S. L. Gaul, D. A. Claremon, D. C. Remy, J. J. Baldwin, S. M. Pitzenberger, A. M. Stern, Transglutaminase inhibition by 2-(2-oxopropyl)thioimidazolium derivatives: mechanism of factor XIIIa inactivation. *Biochemistry* **1994**, *33*, 10109.

[180] C. A. Avery, R. J. Pease, K. Smith, M. Boothby, H. M. Buckley, P. J. Grant, C. W. G. Fishwick, (±) cis-Bisamido epoxides: A novel series of potent FXIII-A inhibitors. *Eur J Med Chem* **2015**, *98*, 49.

[181] S. Singh, J. Dodt, P. Volkers, E. Hethershaw, H. Philippou, V. Ivaskevicius, D. Imhof, J. Oldenburg, A. Biswas, Structure functional insights into calcium binding during the activation of coagulation factor XIII A. *Sci Rep* **2019**, *9*, 11324.

[182] S. Gupta, A. Biswas, M. S. Akhter, C. Krettler, C. Reinhart, J. Dodt, A. Reuter, H. Philippou, V. Ivaskevicius, J. Oldenburg, Revisiting the mechanism of coagulation factor XIII activation and regulation from a structure/functional perspective. *Sci Rep* **2016**, *6*, 30105.

[183] A. D. Protopopova, A. Ramirez, D. V. Klinov, R. I. Litvinov, J. W. Weisel, Factor XIII topology: organization of B subunits and changes with activation studied with single-molecule atomic force microscopy. *J Thromb Haemost* **2019**, *17*, 737.

[184] S. I. Chung, M. S. Lewis, J. E. Folk, Relationships of the catalytic properties of human plasma and platelet transglutaminases (activated blood coagulation factor XIII) to their subunit structures. *J Biol Chem* **1974**, *249*, 940.

[185] T. J. Hornyak, J. A. Shafer, Role of calcium ion in the generation of factor XIII activity. *Biochemistry* **1991**, *30*, 6175.

[186] L. C. Pedersen, V. C. Yee, P. D. Bishop, I. Le Trong, D. C. Teller, R. E. Stenkamp, Transglutaminase factor XIII uses proteinase-like catalytic triad to crosslink macromolecules. *Protein Sci* **1994**, *3*, 1131.

[187] D. M. Pinkas, P. Strop, A. T. Brunger, C. Khosla, Transglutaminase 2 undergoes a large conformational change upon activation. *PLoS Biol* **2007**, *5*, e327.

[188] B. Ahvazi, K. M. Boeshans, W. Idler, U. Baxa, P. M. Steinert, Roles of calcium ions in the activation and activity of the transglutaminase 3 enzyme. *J Biol Chem* **2003**, *278*, 23834.

[189] J. W. Keillor, C. M. Clouthier, K. Y. P. Apperley, A. Akbar, A. Mulani, Acyl transfer mechanisms of tissue transglutaminase. *Bioorg Chem* **2014**, *57*, 186.

[190] M. Griffin, R. Casadio, C. M. Bergamini, Transglutaminases: nature's biological glues. *Biochem J* **2002**, *368*, 377.

[191] S. E. Iismaa, S. Holman, M. A. Wouters, L. Lorand, R. M. Graham, A. Husain, Evolutionary specialization of a tryptophan indole group for transition-state stabilization by eukaryotic transglutaminases. *Proc Natl Acad Sci U S A* **2003**, *100*, 12636.

[192] J. W. Weisel, R. I. Litvinov, Fibrin Formation, Structure and Properties. *Subcell Biochem* **2017**, *82*, 405.

[193] J. Z. Zhang, C. Redman, Fibrinogen assembly and secretion. Role of intrachain disulfide loops. *J Biol Chem* **1996**, *271*, 30083.

[194] R. F. A. Zwaal, H. C. Hemker, Blood coagulation, Elsevier, Amsterdam, New York, New York, NY, U.S.A, **2010**.

[195] R. F. Doolittle, Fibrinogen and fibrin. *Annu Rev Biochem* **1984**, *53*, 195.

[196] A. Zhmurov, A. E. X. Brown, R. I. Litvinov, R. I. Dima, J. W. Weisel, V. Barsegov, Mechanism of fibrin(ogen) forced unfolding. *Structure* **2011**, *19*, 1615.

[197] G. Spraggon, D. Applegate, S. J. Everse, J. Z. Zhang, L. Veerapandian, C. Redman, R. F. Doolittle, G. Grieninger, Crystal structure of a recombinant alphaEC domain from human fibrinogen-420. *Proc Natl Acad Sci U S A* **1998**, *95*, 9099.

[198] J. M. Kollman, L. Pandi, M. R. Sawaya, M. Riley, R. F. Doolittle, Crystal structure of human fibrinogen. *Biochemistry* **2009**, *48*, 3877.

[199] Y. I. Veklich, O. V. Gorkun, L. V. Medved, W. Nieuwenhuizen, J. W. Weisel, Carboxyl-terminal portions of the alpha chains of fibrinogen and fibrin. Localization by electron microscopy and the effects of isolated alpha C fragments on polymerization. *J Biol Chem* **1993**, *268*, 13577.

[200] A. D. Protopopova, N. A. Barinov, E. G. Zavyalova, A. M. Kopylov, V. I. Sergienko, D. V. Klinov, Visualization of fibrinogen αC regions and their arrangement during fibrin network formation by high-resolution AFM. *J Thromb Haemost* **2015**, *13*, 570.

[201] V. C. Yee, K. P. Pratt, H. C. F. Côté, I. Le Trong, D. W. Chung, E. W. Davie, R. E. Stenkamp, D. C. Teller, Crystal structure of a 30 kDa C-terminal fragment from the γ chain of human fibrinogen. *Structure* **1997**, *5*, 125.

[202] G. Spraggon, S. J. Everse, R. F. Doolittle, Crystal structures of fragment D from human fibrinogen and its crosslinked counterpart from fibrin. *Nature* **1997**, *389*, 455.

[203] S. J. Everse, G. Spraggon, L. Veerapandian, M. Riley, R. F. Doolittle, Crystal structure of fragment double-D from human fibrin with two different bound ligands. *Biochemistry* **1998**, *37*, 8637.

[204] S. J. Everse, G. Spraggon, L. Veerapandian, R. F. Doolittle, Conformational changes in fragments D and double-D from human fibrin(ogen) upon binding the peptide ligand Gly-His-Arg-Pro-amide. *Biochemistry* **1999**, *38*, 2941.

[205] B. Ly, H. C. Godal, Denaturation of Fibrinogen, the Protective Effect of Calcium. *Pathophysiol Haemos Thromb* **1972**, *1*, 204.

[206] T. M. Odrljin, B. J. Rybarczyk, C. W. Francis, S. O. Lawrence, M. Hamaguchi, P. J. Simpson-Haidaris, Calcium modulates plasmin cleavage of the fibrinogen D fragment γ chain N-terminus: mapping of monoclonal antibody J88B to a plasmin sensitive domain of the γ chain. *Biochimica et Biophysica Acta (BBA) - Protein Structure and Molecular Enzymology* **1996**, *1298*, 69.

[207] S. O. Brennan, R. L. Davis, M. W. Mosesson, I. Hernandez, R. Lowen, S. J. Alexander, Congenital hypodysfibrinogenaemia (Fibrinogen Des Moines) due to a gamma320Asp deletion at the Ca2+ binding site. *Thromb Haemost* **2007**, *98*, 467.

[208] B. G. Langer, J. W. Weisel, P. A. Dinauer, C. Nagaswami, W. R. Bell, Deglycosylation of fibrinogen accelerates polymerization and increases lateral aggregation of fibrin fibers. *J Biol Chem* **1988**, *263*, 15056.

[209] C. V. Dang, C. K. Shin, W. R. Bell, C. Nagaswami, J. W. Weisel, Fibrinogen sialic acid residues are low affinity calcium-binding sites that influence fibrin assembly. *J Biol Chem* **1989**, *264*, 15104.

[210] S. O. Brennan, Variation of fibrinogen oligosaccharide structure in the acute phase response: Possible haemorrhagic implications. *BBA Clin* **2015**, *3*, 221.

[211] J. R. Byrnes, C. Wilson, A. M. Boutelle, C. B. Brandner, M. J. Flick, H. Philippou, A. S. Wolberg, The interaction between fibrinogen and zymogen FXIII-A2B2 is mediated by fibrinogen residues γ390-396 and the FXIII-B subunits. *Blood* **2016**, *128*, 1969.

[212] M. A. Rosenfeld, V. B. Leonova, A. N. Shchegolikhin, A. V. Bychkova, E. A. Kostanova, M. I. Biryukova, Covalent structure of single-stranded fibrin oligomers cross-linked by FXIIIa. *Biochem Biophys Res Commun* **2015**, *461*, 408.

[213] C. Duval, P. Allan, S. D. A. Connell, V. C. Ridger, H. Philippou, R. A. S. Ariëns, Roles of fibrin α- and γ-chain specific cross-linking by FXIIIa in fibrin structure and function. *Thromb Haemost* **2014**, *111*, 842.

[214] K. F. Standeven, A. M. Carter, P. J. Grant, J. W. Weisel, I. Chernysh, L. Masova, S. T. Lord, R. A. S. Ariëns, Functional analysis of fibrin {gamma}-chain cross-linking by activated factor XIII: determination of a cross-linking pattern that maximizes clot stiffness. *Blood* **2007**, *110*, 902.

[215] Y. V. Matsuka, L. V. Medved, M. M. Migliorini, K. C. Ingham, Factor XIIIa-catalyzed cross-linking of recombinant alpha C fragments of human fibrinogen. *Biochemistry* **1996**, *35*, 5810.

[216] J.-P. Collet, J. L. Moen, Y. I. Veklich, O. V. Gorkun, S. T. Lord, G. Montalescot, J. W. Weisel, The alphaC domains of fibrinogen affect the structure of the fibrin clot, its physical properties, and its susceptibility to fibrinolysis. *Blood* **2005**, *106*, 3824.

[217] D. C. Rijken, S. Abdul, J. J. M. C. Malfliet, F. W. G. Leebeek, S. Uitte de Willige, Compaction of fibrin clots reveals the antifibrinolytic effect of factor XIII. *J Thromb Haemost* **2016**, *14*, 1453.

[218] C. C. Helms, R. A. S. Ariëns, S. Uitte de Willige, K. F. Standeven, M. Guthold, α-α Cross-links increase fibrin fiber elasticity and stiffness. *Biophys J* **2012**, *102*, 168.

[219] I. N. Chernysh, C. Nagaswami, P. K. Purohit, J. W. Weisel, Fibrin clots are equilibrium polymers that can be remodeled without proteolytic digestion. *Sci Rep* **2012**, *2*, 879.

[220] Y. Sakata, N. Aoki, Cross-linking of alpha 2-plasmin inhibitor to fibrin by fibrin-stabilizing factor. *J Clin Invest* **1980**, *65*, 290.

[221] H. Ritchie, L. A. Robbie, S. Kinghorn, R. Exley, N. A. Booth, Monocyte plasminogen activator inhibitor 2 (PAI-2) inhibits u-PA-mediated fibrin clot lysis and is cross-linked to fibrin. *Thromb Haemost* **1999**, *81*, 96.

[222] Z. Valnickova, J. J. Enghild, Human procarboxypeptidase U, or thrombin-activable fibrinolysis inhibitor, is a substrate for transglutaminases. Evidence for transglutaminase-catalyzed cross-linking to fibrin. *J Biol Chem* **1998**, *273*, 27220.

[223] J. Cho, D. F. Mosher, Enhancement of thrombogenesis by plasma fibronectin cross-linked to fibrin and assembled in platelet thrombi. *Blood* **2006**, *107*, 3555.

[224] E. A. Ryan, L. F. Mockros, A. M. Stern, L. Lorand, Influence of a Natural and a Synthetic Inhibitor of Factor XIIIa on Fibrin Clot Rheology. *Biophys J* **1999**, *77*, 2827.

[225] E. L. Hethershaw, A. L. La Cilia Corte, C. Duval, M. Ali, P. J. Grant, R. A. S. Ariëns, H. Philippou, The effect of blood coagulation factor XIII on fibrin clot structure and fibrinolysis. *J Thromb Haemost* **2014**, *12*, 197.

[226] W. Liu, C. R. Carlisle, E. A. Sparks, M. Guthold, The mechanical properties of single fibrin fibers. *J Thromb Haemost* **2010**, *8*, 1030.

[227] G. L. Reed, G. R. Matsueda, E. Haber, Fibrin-fibrin and alpha 2-antiplasmin-fibrin cross-linking by platelet factor XIII increases the resistance of platelet clots to fibrinolysis. *Trans Assoc Am Physicians* **1991**, *104*, 21.

[228] G. L. Reed, G. R. Matsueda, E. Haber, Platelet factor XIII increases the fibrinolytic resistance of platelet-rich clots by accelerating the crosslinking of alpha 2-antiplasmin to fibrin. *Thromb Haemost* **1992**, *68*, 315.

[229] C. W. Francis, V. J. Marder, Rapid formation of large molecular weight alpha-polymers in cross-linked fibrin induced by high factor XIII concentrations. Role of platelet factor XIII. *J Clin Invest* **1987**, *80*, 1459.

[230] F. D. Rubens, D. W. Perry, M. W. Hatton, P. D. Bishop, M. A. Packham, R. L. Kinlough-Rathbone, Platelet accumulation on fibrin-coated polyethylene: role of platelet activation and factor XIII. *Thromb Haemost* **1995**, *73*, 850.

[231] Z. Hevessy, G. Haramura, Z. Boda, M. Udvardy, L. Muszbek, Promotion of the crosslinking of fibrin and alpha 2-antiplasmin by platelets. *Thromb Haemost* **1996**, *75*, 161.

[232] V. Tutwiler, R. I. Litvinov, A. P. Lozhkin, A. D. Peshkova, T. Lebedeva, F. I. Ataullakhanov, K. L. Spiller, D. B. Cines, J. W. Weisel, Kinetics and mechanics of clot contraction are governed by the molecular and cellular composition of the blood. *Blood* **2016**, *127*, 149.

[233] A. S. Wolberg, Fibrinogen and factor XIII: newly recognized roles in venous thrombus formation and composition. *Curr Opin Hematol* **2018**, *25*, 358.

[234] I. Cohen, J. M. Gerrard, J. G. White, Ultrastructure of clots during isometric contraction. *J Cell Biol* **1982**, *93*, 775.

[235] K. Kasahara, M. Kaneda, T. Miki, K. Iida, N. Sekino-Suzuki, I. Kawashima, H. Suzuki, M. Shimonaka, M. Arai, Y. Ohno-Iwashita et al., Clot retraction is mediated by factor XIII-dependent fibrin-αIIbβ3-myosin axis in platelet sphingomyelin-rich membrane rafts. *Blood* **2013**, *122*, 3340.

[236] K. Serrano, D. V. Devine, Intracellular factor XIII crosslinks platelet cytoskeletal elements upon platelet activation. *Thromb Haemost* **2002**, *88*, 315.

[237] E. Katona, B. Nagy, J. Kappelmayer, G. Baktai, L. Kovács, T. Márialigeti, B. Dezso, L. Muszbek, Factor XIII in bronchoalveolar lavage fluid from children with chronic bronchoalveolar inflammation. *J Thromb Haemost* **2005**, *3*, 1407.

[238] S. Esnault, E. A. Kelly, R. L. Sorkness, M. D. Evans, W. W. Busse, N. N. Jarjour, Airway factor XIII associates with type 2 inflammation and airway obstruction in asthmatic patients. *J Allergy Clin Immunol* **2016**, *137*, 767-73.e6.

[239] Z. Z. Orosz, E. Katona, A. Facskó, A. Berta, L. Muszbek, A highly sensitive chemiluminescence immunoassay for the measurement of coagulation factor XIII subunits and their complex in tears. *J Immunol Methods* **2010**, *353*, 87.

[240] Z. Z. Orosz, É. Katona, A. Facskó, L. Módis, L. Muszbek, A. Berta, Factor XIII subunits in human tears; their highly elevated levels following penetrating keratoplasty. *Clin Chim Acta* **2011**, *412*, 271.

[241] K. Sugitani, K. Ogai, K. Hitomi, K. Nakamura-Yonehara, T. Shintani, M. Noda, Y. Koriyama, H. Tanii, T. Matsukawa, S. Kato, A distinct effect of transient and sustained upregulation of cellular factor XIII in the goldfish retina and optic nerve on optic nerve regeneration. *Neurochem Int* **2012**, *61*, 423.

[242] K. Sugitani, K. Ogai, H. Muto, K. Onodera, A. Matsuoka, T. Sugita, Y. Koriyama, A novel activation mechanism of cellular Factor XIII in zebrafish retina after optic nerve injury. *Biochem Biophys Res Commun* **2019**, *517*, 57.

[243] N. M. Intagliata, J. P. E. Davis, J. Lafond, U. Erdbruegger, C. S. Greenberg, P. G. Northup, S. H. Caldwell, Acute kidney injury is associated with low factor XIII in decompensated cirrhosis. *Dig Liver Dis* **2019**, *51*, 1409.

[244] I. Tsujimoto, K. Moriya, K. Sakai, G. Dickneite, T. Sakai, Critical role of factor XIII in the initial stages of carbon tetrachloride-induced adult liver remodeling. *Am J Pathol* **2011**, *179*, 3011.

[245] A. Inbal, A. Lubetsky, T. Krapp, D. Castel, A. Shaish, G. Dickneitte, L. Modis, L. Muszbek, A. Inbal, Impaired wound healing in factor XIII deficient mice. *Thromb Haemost* **2005**, *94*, 432.

[246] V. R. Richardson, P. Cordell, K. F. Standeven, A. M. Carter, Substrates of Factor XIII-A: roles in thrombosis and wound healing. *Clin Sci* **2013**, *124*, 123.

[247] R. Dardik, J. Loscalzo, A. Inbal, Factor XIII (FXIII) and angiogenesis. *J Thromb Haemost* **2006**, *4*, 19.

[248] L. Paragh, D. Törőcsik, Factor XIII Subunit A in the Skin: Applications in Diagnosis and Treatment. *Biomed Res Int* **2017**, *2017*, 3571861.

[249] M. Nahrendorf, E. Aikawa, J.-L. Figueiredo, L. Stangenberg, S. W. van den Borne, W. M. Blankesteijn, D. E. Sosnovik, F. A. Jaffer, C.-H. Tung, R. Weissleder, Transglutaminase activity in acute infarcts predicts healing outcome and left ventricular

remodelling: implications for FXIII therapy and antithrombin use in myocardial infarction. *Eur Heart J* **2008**, *29*, 445.

[250] D. Gemmati, G. Zeri, E. Orioli, R. Mari, S. Moratelli, M. Vigliano, J. Marchesini, M. E. Grossi, A. Pecoraro, A. Cuneo et al., Factor XIII-A dynamics in acute myocardial infarction: a novel prognostic biomarker? *Thromb Haemost* **2015**, *114*, 123.

[251] M. Nahrendorf, K. Hu, S. Frantz, F. A. Jaffer, C.-H. Tung, K.-H. Hiller, S. Voll, P. Nordbeck, D. Sosnovik, S. Gattenlöhner et al., Factor XIII deficiency causes cardiac rupture, impairs wound healing, and aggravates cardiac remodeling in mice with myocardial infarction. *Circulation* **2006**, *113*, 1196.

[252] D. Gemmati, M. Vigliano, F. Burini, R. Mari, H. H. A. El Mohsein, F. Parmeggiani, M. L. Serino, Coagulation Factor XIIIA (F13A1): Novel Perspectives in Treatment and Pharmacogenetics. *Curr Pharm Des* **2016**, *22*, 1449.

[253] A. Inbal, L. Muszbek, Coagulation factor deficiencies and pregnancy loss. *Semin Thromb Hemost* **2003**, *29*, 171.

[254] M. Al-Khabori, A. Pathare, M. Menegatti, F. Peyvandi, Recombinant factor XIII A-subunit in a patient with factor XIII deficiency and recurrent pregnancy loss. *J Thromb Haemost* **2018**, *16*, 1052.

[255] L. A. T. Sharief, R. A. Kadir, Congenital factor XIII deficiency in women: a systematic review of literature. *Haemophilia* **2013**, *19*, e349-57.

[256] S. Bouttefroy, S. Meunier, V. Milien, M. Boucekine, P. Chamouni, D. Desprez, A. Harroche, A. Hochart, M. F. Thiercelin-Legrand, B. Wibaut et al., Congenital factor XIII deficiency: comprehensive overview of the FranceCoag cohort. *Br J Haematol* **2020**, *188*, 317.

[257] T. Asahina, T. Kobayashi, Y. Okada, J. Goto, T. Terao, Maternal blood coagulation factor XIII is associated with the development of cytotrophoblastic shell. *Placenta* **2000**, *21*, 388.

[258] A. Ichinose, T. Asahina, T. Kobayashi, Congenital blood coagulation factor XIII deficiency and perinatal management. *Curr Drug Targets* **2005**, *6*, 541.

[259] G. Cohen, R. Hadas, R. Stefania, A. Pagoto, S. Ben-Dor, F. Kohen, D. Longo, M. Elbaz, N. Dekel, E. Gershon et al., Magnetic Resonance Imaging Reveals Distinct Roles for Tissue Transglutaminase and Factor XIII in Maternal Angiogenesis During Early Mouse Pregnancy. *Arterioscler Thromb Vasc Biol* **2019**, *39*, 1602.

[260] Z. Bagoly, E. Katona, L. Muszbek, Factor XIII and inflammatory cells. *Thromb Res* **2012**, *129*, 77.

[261] B. Hoppe, Fibrinogen and factor XIII at the intersection of coagulation, fibrinolysis and inflammation. *Thromb Haemost* **2014**, *112*, 649.

[262] T. G. Loof, M. Mörgelin, L. Johansson, S. Oehmcke, A. I. Olin, G. Dickneite, A. Norrby-Teglund, U. Theopold, H. Herwald, Coagulation, an ancestral serine protease cascade, exerts a novel function in early immune defense. *Blood* **2011**, *118*, 2589.

[263] D. Töröcsik, L. Szeles, G. Paragh, Z. Rakosy, H. Bardos, L. Nagy, M. Balazs, A. Inbal, R. Adány, Factor XIII-A is involved in the regulation of gene expression in alternatively activated human macrophages. *Thromb Haemost* **2010**, *104*, 709.

[264] D. Töröcsik, H. Bárdos, L. Nagy, R. Adány, Identification of factor XIII-A as a marker of alternative macrophage activation. *Cell Mol Life Sci* **2005**, *62*, 2132.

[265] M. Kávai, R. Ádány, G. Pásti, P. Surányi, G. Szücs, L. Muszbek, F. Boján, G. Szegedi, Marker profile, enzyme activity, and function of a human myelomonocytic leukemia cell line. *Cell Immunol* **1992**, *139*, 531.

[266] M. Nahrendorf, D. E. Sosnovik, P. Waterman, F. K. Swirski, A. N. Pande, E. Aikawa, J.-L. Figueiredo, M. J. Pittet, R. Weissleder, Dual channel optical tomographic imaging of leukocyte recruitment and protease activity in the healing myocardial infarct. *Circ Res* **2007**, *100*, 1218.

[267] A. Mousa, C. Cui, A. Song, V. D. Myneni, H. Sun, J. J. Li, M. Murshed, G. Melino, M. T. Kaartinen, Transglutaminases factor XIII-A and TG2 regulate resorption, adipogenesis and plasma fibronectin homeostasis in bone and bone marrow. *Cell Death Differ* **2017**, *24*, 844.

[268] H. Sun, M. T. Kaartinen, Transglutaminase activity regulates differentiation, migration and fusion of osteoclasts via affecting actin dynamics. *J Cell Physiol* **2018**, *233*, 7497.

[269] H. F. Al-Jallad, Y. Nakano, J. L. Y. Chen, E. McMillan, C. Lefebvre, M. T. Kaartinen, Transglutaminase activity regulates osteoblast differentiation and matrix mineralization in MC3T3-E1 osteoblast cultures. *Matrix Biol* **2006**, *25*, 135.

[270] C. Cui, S. Wang, V. D. Myneni, K. Hitomi, M. T. Kaartinen, Transglutaminase activity arising from Factor XIIIA is required for stabilization and conversion of plasma fibronectin into matrix in osteoblast cultures. *Bone* **2014**, *59*, 127.

[271] S. Wang, C. Cui, K. Hitomi, M. T. Kaartinen, Detyrosinated Glu-tubulin is a substrate for cellular Factor XIIIA transglutaminase in differentiating osteoblasts. *Amino Acids* **2014**, *46*, 1513.

[272] H. F. Al-Jallad, V. D. Myneni, S. A. Piercy-Kotb, N. Chabot, A. Mulani, J. W. Keillor, M. T. Kaartinen, Plasma membrane factor XIIIA transglutaminase activity regulates osteoblast matrix secretion and deposition by affecting microtubule dynamics. *PLoS ONE* **2011**, *6*, e15893.

[273] H. Raghu, C. Cruz, C. L. Rewerts, M. D. Frederick, S. Thornton, E. S. Mullins, J. G. Schoenecker, J. L. Degen, M. J. Flick, Transglutaminase factor XIII promotes arthritis through mechanisms linked to inflammation and bone erosion. *Blood* **2015**, *125*, 427.

[274] P. A. Cordell, L. M. Newell, K. F. Standeven, P. J. Adamson, K. R. Simpson, K. A. Smith, C. L. Jackson, P. J. Grant, R. J. Pease, Normal Bone Deposition Occurs in Mice Deficient in Factor XIII-A and Transglutaminase 2. *Matrix Biol* **2015**, *43*, 85.

[275] A. Dorgalaleh, J. Rashidpanah, Blood coagulation factor XIII and factor XIII deficiency. *Blood Rev* **2016**, *30*, 461.

[276] A. S. Lawrie, L. Green, I. J. Mackie, R. Liesner, S. J. Machin, F. Peyvandi, Factor XIII--an under diagnosed deficiency--are we using the right assays? *J Thromb Haemost* **2010**, *8*, 2478.

[277] H. P. Kohler, A. Ichinose, R. Seitz, R. A. S. Ariens, L. Muszbek, Diagnosis and classification of factor XIII deficiencies. *J Thromb Haemost* **2011**, *9*, 1404.

[278] M. Karimi, F. Peyvandi, M. Naderi, A. Shapiro, Factor XIII deficiency diagnosis: Challenges and tools. *Int J Hematol* **2018**, *40*, 3.

[279] L. Muszbek, É. Katona, Diagnosis and Management of Congenital and Acquired FXIII Deficiencies. *Semin Thromb Hemost* **2016**, *42*, 429.

[280] A. Biswas, V. Ivaskevicius, A. Thomas, J. Oldenburg, Coagulation factor XIII deficiency. Diagnosis, prevalence and management of inherited and acquired forms. *Hamostaseologie* **2014**, *34*, 160.

[281] A. Ichinose, Hemorrhagic acquired factor XIII (13) deficiency and acquired hemorrhaphilia 13 revisited. *Semin Thromb Hemost* **2011**, *37*, 382.

[282] F. Peyvandi, D. Di Michele, P. H. B. Bolton-Maggs, C. A. Lee, A. Tripodi, A. Srivastava, Classification of rare bleeding disorders (RBDs) based on the association between coagulant factor activity and clinical bleeding severity. *J Thromb Haemost* **2012**, *10*, 1938.

[283] L. Muszbek, K. Pénzes, É. Katona, Auto- and alloantibodies against factor XIII: laboratory diagnosis and clinical consequences. *J Thromb Haemost* **2018**, *16*, 822.

[284] A. Undas, R. A. S. Ariëns, Fibrin clot structure and function: a role in the pathophysiology of arterial and venous thromboembolic diseases. *Arterioscler Thromb Vasc Biol* **2011**, *31*, e88-99.

[285] R. A. S. Ariëns, Fibrin(ogen) and thrombotic disease. *J Thromb Haemost* **2013**, *11*, 294.

[286] K. I. Bridge, H. Philippou, R. A. S. Ariëns, Clot properties and cardiovascular disease. *Thromb Haemost* **2014**, *112*, 901.

[287] R. C. M. Kotzé, R. A. S. Ariëns, Z. de Lange, M. Pieters, CVD risk factors are related to plasma fibrin clot properties independent of total and or γ' fibrinogen concentration. *Thromb Res* **2014**, *134*, 963.

[288] M. Zabczyk, K. Plens, W. Wojtowicz, A. Undas, Prothrombotic Fibrin Clot Phenotype Is Associated With Recurrent Pulmonary Embolism After Discontinuation of Anticoagulant Therapy. *Arterioscler Thromb Vasc Biol* **2017**, *37*, 365.

[289] J. Cieslik, S. Mrozinska, E. Broniatowska, A. Undas, Altered plasma clot properties increase the risk of recurrent deep vein thrombosis: a cohort study. *Blood* **2018**, *131*, 797.

[290] W. Sumaya, L. Wallentin, S. K. James, A. Siegbahn, K. Gabrysch, M. Bertilsson, A. Himmelmann, R. A. Ajjan, R. F. Storey, Fibrin clot properties independently predict adverse clinical outcome following acute coronary syndrome: a PLATO substudy. *Eur Heart J* **2018**, *39*, 1078.

[291] N. Kucher, V. Schroeder, H. P. Kohler, Role of blood coagulation factor XIII in patients with acute pulmonary embolism. Correlation of factor XIII antigen levels with pulmonary occlusion rate, fibrinogen, D-dimer, and clot firmness. *Thromb Haemost* **2003**, *90*, 434.

[292] Z. Bereczky, E. Balogh, E. Katona, I. Czuriga, I. Edes, L. Muszbek, Elevated factor XIII level and the risk of myocardial infarction in women. *Haematologica* **2007**, *92*, 287.

[293] H. Bárdos, P. Molnár, G. Csécsei, R. Adány, Fibrin deposition in primary and metastatic human brain tumours. *Blood Coagul Fibrin* **1996**, *7*, 536.

[294] S. H. Lee, I. B. Suh, E. J. Lee, G. Y. Hur, S. Y. Lee, S. Y. Lee, C. Shin, J. J. Shim, K. H. In, K. H. Kang et al., Relationships of coagulation factor XIII activity with cell-type and stage of non-small cell lung cancer. *Yonsei Med J* **2013**, *54*, 1394.

[295] A. Porrello, P. L. Leslie, E. B. Harrison, B. K. Gorentla, S. Kattula, S. K. Ghosh, S. H. Azam, A. Holtzhausen, Y. L. Chao, M. C. Hayward et al., Factor XIIIA-expressing inflammatory monocytes promote lung squamous cancer through fibrin cross-linking. *Nat Commun* **2018**, *9*, 1988.

[296] R. Invernizzi, P. de Fazio, A. M. Iannone, L. M. Zambelli, M. P. Rastaldi, G. Ippoliti, E. Ascari, Immunocytochemical detection of factor XIII a—subunit in acute leukemia. *Leuk Res* **1992**, *16*, 829.

[297] J. Kappelmayer, A. Simon, E. Katona, A. Szanto, L. Nagy, A. Kiss, C. Kiss, L. Muszbek, Coagulation factor XIII-A. A flow cytometric intracellular marker in the classification of acute myeloid leukemias. *Thromb Haemost* **2005**, *94*, 454.

[298] F. Kiss, A. Simon, L. Csáthy, Z. Hevessy, E. Katona, C. Kiss, J. Kappelmayer, A coagulation factor becomes useful in the study of acute leukemias: studies with blood coagulation factor XIII. *Cytometry* **2008**, *73*, 194.

[299] F. Kiss, Z. Hevessy, A. Veszprémi, E. Katona, C. Kiss, G. Vereb, L. Muszbek, J. N. Kappelmayer, Leukemic lymphoblasts, a novel expression site of coagulation factor XIII subunit A. *Thromb Haemost* **2006**, *96*, 176.

[300] W. G. Jiang, R. Ablin, A. Douglas-Jones, R. E. Mansel, Expression of transglutaminases in human breast cancer and their possible clinical significance. *Oncol Rep* **2003**, *10*, 2039.

[301] X. Wang, E. Wang, J. J. Kavanagh, R. S. Freedman, Ovarian cancer, the coagulation pathway, and inflammation. *J Transl Med* **2005**, *3*, 25.

[302] C. Y. Vossen, M. Hoffmeister, J. C. Chang-Claude, F. R. Rosendaal, H. Brenner, Clotting factor gene polymorphisms and colorectal cancer risk. *J Clin Oncol* **2011**, *29*, 1722.

[303] Y. An, S. Bekesova, N. Edwards, R. Goldman, Peptides in low molecular weight fraction of serum associated with hepatocellular carcinoma. *Dis Markers* **2010**, *29*, 11.

[304] J. Peltier, J.-P. Roperch, S. Audebert, J.-P. Borg, L. Camoin, Activation peptide of the coagulation factor XIII (AP-F13A1) as a new biomarker for the screening of colorectal cancer. *Clin Proteomics* **2018**, *15*, 15.

[305] P. J. Bungay, R. A. Owen, I. C. Coutts, M. Griffin, A role for transglutaminase in glucose-stimulated insulin release from the pancreatic beta-cell. *Biochem J* **1986**, *235*, 269.

[306] P. R. Sharma, A. J. Mackey, E. A. Dejene, J. W. Ramadan, C. D. Langefeld, N. D. Palmer, K. D. Taylor, L. E. Wagenknecht, R. M. Watanabe, S. S. Rich et al., An Islet-Targeted Genome-Wide Association Scan Identifies Novel Genes Implicated in Cytokine-Mediated Islet Stress in Type 2 Diabetes. *Endocrinology* **2015**, *156*, 3147.

[307] V. D. Myneni, K. Hitomi, M. T. Kaartinen, Factor XIII-A transglutaminase acts as a switch between preadipocyte proliferation and differentiation. *Blood* **2014**, *124*, 1344.

[308] V. D. Myneni, A. Mousa, M. T. Kaartinen, Factor XIII-A transglutaminase deficient mice show signs of metabolically healthy obesity on high fat diet. *Sci Rep* **2016**, *6*, 35574.

[309] R. Seitz, F. Leugner, M. Katschinski, A. Immel, M. Kraus, R. Egbring, B. Göke, Ulcerative colitis and Crohn's disease: factor XIII, inflammation and haemostasis. *Digestion* **1994**, *55*, 361.

[310] S. Higaki, K. Nakano, S. Onaka, A. Amano, Y. Tanioka, K. Harada, S. Hashimoto, I. Sakaida, K. Okita, Clinical significance of measuring blood coagulation factor XIIIA

regularly and continuously in patients with Crohn's disease. *J Gastroenterol Hepatol* **2006**, *21*, 1407.

[311] P.-A. Cougard, A. Desjeux, V. Vitton, K. Baumstarck-Barrau, N. Lesavre, J.-C. Grimaud, The usefulness of factor XIII levels in Crohn's disease. *J Crohns Colitis* **2012**, *6*, 660.

[312] S. Sun, M. A. Karsdal, J. H. Mortensen, Y. Luo, J. Kjeldsen, A. Krag, M. D. Jensen, A.-C. Bay-Jensen, T. Manon-Jensen, Serological Assessment of the Quality of Wound Healing Processes in Crohn's Disease. *J Gastrointestin Liver Dis* **2019**, *28*, 175.

[313] W. S. Hur, N. Mazinani, X. J. D. Lu, L. S. Yefet, J. R. Byrnes, L. Ho, J. H. Yeon, S. Filipenko, A. S. Wolberg, W. A. Jefferies et al., Coagulation factor XIIIa cross-links amyloid β into dimers and oligomers and to blood proteins. *J Biol Chem* **2019**, *294*, 390.

[314] A. Durmaz, E. Kumral, B. Durmaz, H. Onay, G. I. Aslan, F. Ozkinay, S. Pehlivan, M. Orman, O. Cogulu, Genetic factors associated with the predisposition to late onset Alzheimer's disease. *Gene* **2019**, *707*, 212.

[315] X. Shi, Y. Ohta, X. Liu, J. Shang, R. Morihara, Y. Nakano, T. Feng, Y. Huang, K. Sato, M. Takemoto et al., Chronic Cerebral Hypoperfusion Activates the Coagulation and Complement Cascades in Alzheimer's Disease Mice. *Neurosci* **2019**, *416*, 126.

[316] M. Stieler, C. Büchold, M. Schmitt, A. Heine, M. Hils, R. Pasternack, G. Klebe, Structure-Based Design of FXIIIa-Blockers: Addressing a Transient Hydrophobic Pocket in the Active Site of FXIIIa. *ChemMedChem* **2020**, *15*, 900.

[317] D. Lukacova, G. R. Matsueda, E. Haber, G. L. Reed, Inhibition of factor XIII activation by an anti-peptide monoclonal antibody. *Biochemistry* **1991**, *30*, 10164.

[318] Y. Iwata, K. Tago, T. Kiho, H. Kogen, T. Fujioka, N. Otsuka, K. Suzuki-Konagai, T. Ogita, S. Miyamoto, Conformational analysis and docking study of potent factor XIIIa inhibitors having a cyclopropenone ring. *J Mol Graph Model* **2000**, *18*, 591.

[319] R. Pasternack, C. Büchold, R. Jähnig, C. Pelzer, M. Sommer, A. Heil, P. Florian, G. Nowak, U. Gerlach, M. Hils, Novel inhibitor ZED3197 as potential drug candidate in anticoagulation targeting coagulation FXIIIa (F13a). *J Thromb Haemost* **2020**, *18*, 191.

[320] R. A. Al-Horani, R. Karuturi, M. Lee, D. K. Afosah, U. R. Desai, Allosteric Inhibition of Factor XIIIa. Non-Saccharide Glycosaminoglycan Mimetics, but Not Glycosaminoglycans, Exhibit Promising Inhibition Profile. *PLoS ONE* **2016**, *11*, e0160189.

[321] A. A. Tymiak, J. G. Tuttle, S. D. Kimball, T. Wang, V. G. Lee, A simple and rapid screen for inhibitors of factor XIIIa. *J Antibiot* **1993**, *46*, 204.

[322] H. Kogen, T. Kiho, K. Tago, S. Miyamoto, T. Fujioka, N. Otsuka, K. Suzuki-Konagai, T. Ogita, Alutacenoic Acids A and B, Rare Naturally Occurring Cyclopropenone Derivatives Isolated from Fungi: Potent Non-Peptide Factor XIIIa Inhibitors. *J Am Chem Soc* **2000**, *122*, 1842.

[323] L. Seale, S. Finney, R. T. Sawyer, R. B. Wallis, Tridegin, a novel peptidic inhibitor of factor XIIIa from the leech, Haementeria ghilianii, enhances fibrinolysis in vitro. *Thromb Haemost* **1997**, *77*, 959.

[324] M. Böhm, T. Kühl, K. Hardes, R. Coch, C. Arkona, B. Schlott, T. Steinmetzer, D. Imhof, Synthesis and functional characterization of tridegin and its analogues: inhibitors and substrates of factor XIIIa. *ChemMedChem* **2012**, *7*, 326.

[325] J. Drenth, Principles of Protein X-Ray Crystallography, Springer, New York, NY, **2007**.

[326] K. Wüthrich, NMR studies of structure and function of biological macromolecules (Nobel Lecture). *J Biomol NMR* **2003**, *27*, 13.

[327] K. Wüthrich, Protein structure determination in solution by NMR spectroscopy. *J Biol Chem* **1990**, *265*, 22059.

[328] R. K. Spencer, J. S. Nowick, A Newcomer's Guide to Peptide Crystallography. *Isr J Chem* **2015**, *55*, 698.

[329] L. Poppe, J. O. Hui, J. Ligutti, J. K. Murray, P. D. Schnier, PADLOC: a powerful tool to assign disulfide bond connectivities in peptides and proteins by NMR spectroscopy. *Anal Chem* **2012**, *84*, 262.

[330] P. Anand, A. Grigoryan, M. H. Bhuiyan, B. Ueberheide, V. Russell, J. Quinoñez, P. Moy, B. T. Chait, S. F. Poget, M. Holford, Sample limited characterization of a novel disulfide-rich venom peptide toxin from terebrid marine snail Terebra variegata. *PLoS ONE* **2014**, *9*, e94122.

[331] T.-Y. Yen, H. Yan, B. A. Macher, Characterizing closely spaced, complex disulfide bond patterns in peptides and proteins by liquid chromatography/electrospray ionization tandem mass spectrometry. *J Mass Spectrom* **2002**, *37*, 15.

[332] K. Vyatkina, S. Wu, L. J. M. Dekker, M. M. VanDuijn, X. Liu, N. Tolić, M. Dvorkin, S. Alexandrova, T. M. Luider, L. Paša-Tolić et al., De Novo Sequencing of Peptides from Top-Down Tandem Mass Spectra. *J Proteome Res* **2015**, *14*, 4450.

[333] K. Vyatkina, L. J. M. Dekker, S. Wu, M. M. VanDuijn, X. Liu, N. Tolić, T. M. Luider, L. Paša-Tolić, De Novo Sequencing of Peptides from High-Resolution Bottom-Up Tandem Mass Spectra using Top-Down Intended Methods. *Proteomics* **2017**, *17*.

[334] J. J. Gorman, T. P. Wallis, J. J. Pitt, Protein disulfide bond determination by mass spectrometry. *Mass Spectrom Rev* **2002**, *21*, 183.

[335] W. R. Gray, Disulfide structures of highly bridged peptides: a new strategy for analysis. *Protein Sci* **1993**, *2*, 1732.

[336] R. Aebersold, M. Mann, Mass spectrometry-based proteomics. *Nature* **2003**, *422*, 198.

[337] A. I. Nesvizhskii, O. Vitek, R. Aebersold, Analysis and validation of proteomic data generated by tandem mass spectrometry. *Nat Methods* **2007**, *4*, 787.

[338] M. Wang, J. J. Carver, V. V. Phelan, L. M. Sanchez, N. Garg, Y. Peng, D. D. Nguyen, J. Watrous, C. A. Kapono, T. Luzzatto-Knaan et al., Sharing and community curation of mass spectrometry data with Global Natural Products Social Molecular Networking. *Nat Biotechnol* **2016**, *34*, 828.

[339] M. Saunders, A. Wishnia, J. G. Kirkwood, The Nuclear Magnetic Resonance Spectrum of Ribonuclease 1. *J Am Chem Soc* **1957**, *79*, 3289.

[340] M. Pellecchia, D. S. Sem, K. Wüthrich, NMR in drug discovery. *Nat Rev Drug Discov* **2002**, *1*, 211.

[341] J. B. Fenn, Electrospray wings for molecular elephants (Nobel lecture). *Angew Chem Int Ed Engl* **2003**, *42*, 3871.

[342] S. Banerjee, S. Mazumdar, Electrospray ionization mass spectrometry: a technique to access the information beyond the molecular weight of the analyte. *Int J Anal Chem* **2012**, *2012*, 282574.

[343] K. Tanaka, The origin of macromolecule ionization by laser irradiation (Nobel lecture). *Angew Chem Int Ed Engl* **2003**, *42*, 3860.

[344] M. S. Goyder, F. Rebeaud, M. E. Pfeifer, F. Kálmán, Strategies in mass spectrometry for the assignment of Cys-Cys disulfide connectivities in proteins. *Expert Rev Proteomics* **2013**, *10*, 489.

[345] J. Echterbille, L. Quinton, N. Gilles, E. de Pauw, Ion mobility mass spectrometry as a potential tool to assign disulfide bonds arrangements in peptides with multiple disulfide bridges. *Anal Chem* **2013**, *85*, 4405.

[346] L. Zhao, R. T. Almaraz, F. Xiang, J. L. Hedrick, A. H. Franz, Gas-phase scrambling of disulfide bonds during matrix-assisted laser desorption/ionization mass spectrometry analysis. *J Am Soc Mass Spectrom* **2009**, *20*, 1603.

[347] R. Jenkins, J. X. Duggan, A.-F. Aubry, J. Zeng, J. W. Lee, L. Cojocaru, D. Dufield, F. Garofolo, S. Kaur, G. A. Schultz et al., Recommendations for validation of LC-MS/MS bioanalytical methods for protein biotherapeutics. *AAPS J* **2015**, *17*, 1.

[348] R. Aebersold, D. R. Goodlett, Mass spectrometry in proteomics. *Chem Rev* **2001**, *101*, 269.

[349] A. B. Kanu, P. Dwivedi, M. Tam, L. Matz, H. H. Hill, Ion mobility-mass spectrometry. *J Mass Spectrom* **2008**, *43*, 1.

[350] M. Sans, C. L. Feider, L. S. Eberlin, Advances in mass spectrometry imaging coupled to ion mobility spectrometry for enhanced imaging of biological tissues. *Curr Opin Chem Biol* **2018**, *42*, 138.

[351] K. J. Dit Fouque, J. Moreno, J. D. Hegemann, S. Zirah, S. Rebuffat, F. Fernandez-Lima, Identification of Lasso Peptide Topologies Using Native Nanoelectrospray Ionization-Trapped Ion Mobility Spectrometry-Mass Spectrometry. *Anal Chem* **2018**, *90*, 5139.

[352] K. J. Dit Fouque, V. Bisram, J. D. Hegemann, S. Zirah, S. Rebuffat, F. Fernandez-Lima, Structural signatures of the class III lasso peptide BI-32169 and the branched-cyclic topoisomers using trapped ion mobility spectrometry-mass spectrometry and tandem mass spectrometry. *Anal Bioanal Chem* **2019**, *411*, 6287.

[353] V. Schnaible, S. Wefing, A. Resemann, D. Suckau, A. Bücker, S. Wolf-Kümmeth, D. Hoffmann, Screening for disulfide bonds in proteins by MALDI in-source decay and LIFT-TOF/TOF-MS. *Anal Chem* **2002**, *74*, 4980.

[354] D. Suckau, A. Resemann, M. Schuerenberg, P. Hufnagel, J. Franzen, A. Holle, A novel MALDI LIFT-TOF/TOF mass spectrometer for proteomics. *Anal Bioanal Chem* **2003**, *376*, 952.

[355] A.-C. Teger-Nilsson, R. Bylund, D. Gustafsson, E. Gyzander, U. Eriksson, In Vitro Effects of Inogatran, a Selective Low Molecular Weight Thrombin Inhibitor. *Thromb Res* **1997**, *85*, 133.

[356] K. A. Arsenault, J. Hirsh, R. P. Whitlock, J. W. Eikelboom, Direct thrombin inhibitors in cardiovascular disease. *Nat Rev Cardiol* **2012**, *9*, 402.

[357] C. J. Lee, J. E. Ansell, Direct thrombin inhibitors. *Br J Clin Pharmacol* **2011**, *72*, 581.

[358] M. G. Grütter, J. P. Priestle, J. Rahuel, H. Grossenbacher, W. Bode, J. Hofsteenge, S. R. Stone, Crystal structure of the thrombin-hirudin complex: a novel mode of serine protease inhibition. *EMBO J* **1990**, *9*, 2361.

[359] E. Fuller, B. R. Green, P. Catlin, O. Buczek, J. S. Nielsen, B. M. Olivera, G. Bulaj, Oxidative folding of conotoxins sharing an identical disulfide bridging framework. *FEBS J* **2005**, *272*, 1727.

[360] A. A. Tietze, D. Tietze, O. Ohlenschläger, E. Leipold, F. Ullrich, T. Kühl, A. Mischo, G. Buntkowsky, M. Görlach, S. H. Heinemann et al., Structurally diverse μ-conotoxin PIIIA isomers block sodium channel NaV 1.4. *Angew Chem Int Ed Engl* **2012**, *51*, 4058.

[361] M. Mochizuki, S. Tsuda, K. Tanimura, Y. Nishiuchi, Regioselective formation of multiple disulfide bonds with the aid of postsynthetic S-tritylation. *Org Lett* **2015**, *17*, 2202.

Acknowledgements

I would like to thank a number of people who have supported and encouraged me during my doctoral studies and without who's this work would not have been possible.

First of all, I would like to express my gratitude to Prof. Dr. Diana Imhof. Thank you very much for the close supervision, your trust and support during my PhD and Master thesis. I am also very grateful for the challenging but interesting topic of disulfide-bonded peptides, especially tridegin, and the experience and knowledge I was able to acquire during the course of the project.

I would like to thank PD Dr. Arijit Biswas for being the second supervisor of this thesis and for the excellent and close collaboration as well as the support for the optimization of the tridegin lead structure.

I would also like to thank Prof. Dr. Matthias Geyer and Prof. Dr. Dirk Menche for their participation in the examination committee of this thesis.

I would like to thank Prof. Dr. Torsten Steinmetzer and his coworkers for their support during the measurements of the isopeptidase activity assays in Marburg. I would like to thank Prof. Dr. Alisa Wolberg and Dr. Lori A. Holle for the great cooperation during the testing of tridegin in human blood and *in vivo* mouse models. I would like to thank Dr. Markus Pietsch and Paul Sommerfeld for testing tridegin in their fluorescence anisotropy-based assays with FXIIIa and TGase 2. With regard to the NMR structure elucidation of the tridegin variant, I would also like to thank Dr. Oliver Ohlenschläger, who always helped me with NMR-specific questions and was a great support for the structure calculation of the tridegin structure using Cyana. I would like to thank Dr. Stuart Pengelley, Dr. Detlef Suckau and Eckhard Belau for the opportunity to study various disulfide-bonded µ-conotoxin PIIIA isomers on their Bruker-TIMS instruments and for their helpfulness in interpreting the results. Finally, I would like to thank Dr. Senada Nozinovic, Prof. Dr. Dieter Willbold and Dr. Rudolf Hartmann for measuring the NMR spectra.

Financial support for the presented research work as well as for conference attendance was provided by several funders. Therefore, I would like to thank the German Foundation for Heart Research for the financial support within the project "Lead structure and tool: development approaches for tridegin analogs as efficient factor XIIIa inhibitors". I would also like to thank the Gesellschaft Deutscher Chemiker (GDCh), the Bonn Graduate Center and my graduate school BIGS DrugS.

To all current and former members of the Imhof group, Ajay, Amelie, Anna, Avirup, Ben, Britta, Charlotte, Marie, Max, Milena, Monica, Pascal, Sabrina, Sam, Simona, Sven, Tobias, Toni and Yomnah, who have accompanied me over the past years, I would like to thank very much. A special thanks goes to the former members of the Folding Force: Ajay, Charlotte and Pascal.

Finally, I would like to thank my family and friends for their support and encouragement. Especially during the last period of my PhD, I could always count on Tristan & Maja, Daniel & Laura, Karl & Julia, Laura & Daniel, as well as my "Eifeler" friends. I would like to thank my parents, sisters, brothers-in-law, nieces and nephews for their kindness and their taking my mind off work from time to time. I would also like to thank my girlfriend's family for their support and their kind welcome into the family.

Dear Britta, it is hard to put into words how wonderful you have been to me over the past years and how much I am already looking forward to the coming times with you. Thank you for everything.

Publications

1. P. Rabe, **T. Schmitz**, J. S. Dickschat. Mechanistic Investigations on Six Bacterial Terpene Cyclases. *Beilstein J. Org. Chem.*, **2016**, 12, 1839-1850.

2. P. Rabe, J. Rinkel, E. Dolja, **T. Schmitz**, B. Nubbemeyer, T. H. Luu, J. S. Dickschat. Mechanistic Investigations of Two Bacterial Diterpene Cyclases: Spiroviolene Synthase and Tsukubadiene Synthase. *Angew. Chem. Int. Ed.*, **2017**, 56, 2776-2779.

3. P. Heimer*, **T. Schmitz***, C. A. Bäuml*, D. Imhof. Synthesis and Structure Determination of µ-Conotoxin PIIIA Isomers with Different Disulfide Connectivities. *J. Vis. Exp.*, **2018**, 140, e58368. (*equal contribution)

4. C. A. Bäuml*, **T. Schmitz***, A. A. Paul George, M. Sudarsanam, K. Hardes, T. Steinmetzer, L. A. Holle, A. S. Wolberg, B. Pötzsch, J. Oldenburg, A. Biswas, D. Imhof. Coagulation Factor XIIIa Inhibitor Tridegin: On the Role of Disulfide Bonds for Folding, Stability, and Function. *J. Med. Chem.*, **2019**, 62, 3513-3523. (*equal contribution)

5. A. A. Paul George, P. Heimer, E. Leipold, **T. Schmitz**, D. Kaufmann, D. Tietze, S. H. Heinemann, D. Imhof. Effect of Conformational Diversity on the Bioactivity of µ-Conotoxin PIIIA Disulfide Isomers. *Mar. Drugs*, **2019**, 17, 390.

6. **T. Schmitz**, S. Pengelley, E. Belau, D. Suckau, D. Imhof. LC-Trapped Ion Mobility Spectrometry-TOF MS Differentiation of 2- and 3-Disulfide-Bonded Isomers of the µ-Conotoxin PIIIA. *Anal. Chem.*, **2020**, 92, 10920-10924.

7. C. A. Bäuml, A. A. Paul George, **T. Schmitz**, P. Sommerfeld, M. Pietsch, T. Steinmetzer, A. Biswas, D. Imhof. Distinct 3-disulfide-bonded isomers of tridegin differentially inhibit coagulation factor XIIIa: The influence of structural stability on bioactivity. *Eur. J. Med. Chem.*, **2020**, 201, 112474.

8. **T. Schmitz***, C. A. Bäuml*, D. Imhof. Inhibitors of blood coagulation factor XIIIa. *Anal. Biochem.*, **2020**, 605, 113708. (*equal contribution)

9. **T. Schmitz**, A. A. Paul George, B. Nubbemeyer, C. A. Bäuml, T. Steinmetzer, O. Ohlenschläger, A. Biswas, D. Imhof. NMR-Based Structural Characterization of a Two-Disulfide-Bonded Analogue of the FXIIIa Inhibitor Tridegin: New Insights into Structure–Activity Relationships. *Int. J. Mol. Sci.*, **2021**, 22, 880.